

Springer-Verlag Berlin Heidelberg GmbH

Walter Borchardt-Ott

Crystallography

Second edition

With 261 Figures



Springer

Dr. WALTER BORCHARDT-OTT
Institute of Mineralogy
University of Münster
Corrensstraße 24
D-48149 Münster
Germany

Translated by:

Dr. ROBERT O. GOULD
Department of Chemistry
The University of Edinburgh
King's Buildings
West Mains Road
GB-Edinburgh EH9 3JJ
Scotland

Title of the original German edition:
Walter Borchardt-Ott
Kristallographie, 5. Auflage (Springer-Lehrbuch)

ISBN 978-3-540-59478-9

Library of Congress Cataloging-in-Publication Data. Borchardt-Ott, Walter, Crystallography. Second edition / Walter Borchardt-Ott. p. cm. Includes bibliographical references. ISBN 978-3-540-59478-9 ISBN 978-3-642-57754-3 (eBook)

DOI 10.1007/978-3-642-57754-3 1. Crystallography. I. Title. QE437.H38 1996 616.9²25075-dc20 for Library of Congress 95-9590 CIP

This work is subject to copyright. All rights reserved, whether the whole or part of the material is concerned, specifically the rights of translation, reprinting, reuse of illustrations, recitation, broadcasting, reproduction on microfilm or in any other way, and storage in data banks. Duplication of this publication or parts thereof is permitted only under the provisions of the German Copyright Law of September 9, 1965, in its current version, and permission for use must always be obtained from Springer-Verlag. Violations are liable for prosecution under the German Copyright Law.

© Springer-Verlag Berlin Heidelberg 1993, 1995
Originally published by Springer-Verlag Berlin Heidelberg New York in 1993, 1995

The use of general descriptive names, registered names, trademarks, etc. in this publication does not imply, even in the absence of a specific statement, that such names are exempt from the relevant protective laws and regulations and therefore free for general use.

Typesetting: Elsner & Behrens GdBR, Oftersheim
32/3136 SPIN 10504014 - Printed on acid-free paper

Dedicated to Sigrid

Preface to the Second English Edition

This second English edition has been required only 1½ years after the first; it appears shortly before the fifth German edition, of which it is a translation. A major change is the expansion and revision of Chapter 4 by new exercises on the use of the stereographic, orthographic and gnomonic projections, and on indexing. Dr. R. O. Gould has again undertaken the translation and has made a thorough revision of the text of the first edition. I am very grateful to him for his efforts. I should also like to thank Dr. Wolfgang Engel of Springer Verlag, Heidelberg, very much for his encouragement and his help during a collaboration of more than a decade.

Münster, Summer 1995

W. BORCHARDT-OTT

Preface to the First English Edition

This book is based on the lectures which I have now been giving for more than 20 years to chemists and other scientists at the Westfälische Wilhelms-Universität, Münster. It is a translation of the fourth German edition, which will also be appearing in 1993.

It has been my intention to introduce the crystallographic approach in a book which is elementary and easy to understand, and I have thus avoided lengthy mathematical treatments. As will be clear from the contents, topics in crystallography have been covered selectively. For example, crystal structure analysis, crystal physics and crystal optics are only touched on, as they do not fit easily into the scheme of the book.

The heart of the book is firmly fixed in geometrical crystallography. It is from the concept of the space lattice that symmetry operations, Bravais lattices, space groups and point groups are all developed. The symmetry of molecules is described, including the resulting non-crystallographic point groups. The treatment of crystal morphology has been brought into line with the approach used by *International Tables for Crystallography*. The relationship between point groups and physical properties is indicated. Examples of space groups in all crystal systems are treated. Much emphasis is placed on the correspondence between point groups and space groups. The section on crystal chemistry will serve as an introduction to the field. Of the various methods of investigation using X-rays, the powder method is described, and an account is given of the reciprocal lattice. At the end of each chapter are included a large number of exercises, and solutions are given for all of them.

The first stimulus to have this book translated was given by Professor P. E. Fielding of the University of New England in Armidale (Australia). The translation was undertaken by Dr. R. O. Gould of the University of Edinburgh. I thank Dr. Gould for his enthusiasm and for the trouble he has taken over the translation. It was particularly beneficial that we were able to consider the text together thoroughly.

X Preface to the First English Edition

Professor E. Koch and Professor W. Fischer, both of the University of Marburg, have discussed each edition of this book with me, and their criticism has been invaluable. I wish to record my thanks to them also.

Münster, Autumn 1993

W. BORCHARDT-OTT

Contents

Introduction	1
1 The Crystalline State	3
Exercises	8
2 The Lattice and Its Properties	9
2.1 Line Lattice	10
2.2 Plane Lattice	10
2.3 Space Lattice	10
2.4 The Designation of Points, Lines, and Planes in a Space Lattice	11
2.4.1 The Lattice Point uvw	11
2.4.2 Lattice Lines $[uvw]$	12
2.4.3 Lattice Planes (hkl)	13
2.5 The Zonal Equation	16
Exercises	19
3 Crystal Structure	21
Exercises	25
4 Morphology	27
4.1 Relationship Between Crystal Structure and Morphology	27
4.2 Fundamentals of Morphology	28
4.3 Crystal Growth	30
4.4 The Stereographic Projection	33
4.5 The Reflecting Goniometer	36
4.6 The Wulff Net	37
4.7 Indexing of a Crystal	41
4.8 The Gnomonic and Orthographic Projections	47
Exercises	49

5	Principles of Symmetry	57
5.1	Rotation Axes	59
5.2	The Mirror Plane	62
5.3	The Inversion Centre	63
5.4	Compound Symmetry Operations	64
5.4.1	Rotoinversion Axes	65
5.4.2	Rotoreflexion Axes	67
	Exercises	70
6	The 14 Bravais Lattices	71
6.1	The Primitive Space Lattices (P-Lattices)	74
6.2	The Symmetry of the Primitive Lattices	89
6.3	The Centred Lattices	97
6.4	The Symmetry of the Centred Lattices	103
	Exercises	105
7	The Seven Crystal Systems	115
8	Point Groups	119
8.1	The 32 Point Groups	119
8.2	Crystal Symmetry	124
8.2.1	Crystal Forms	124
8.3	Molecular Symmetry	143
8.4	Determination of Point Groups	145
8.5	Enantiomorphism	150
8.6	Point Groups and Physical Properties	150
8.6.1	Optical Activity	150
8.6.2	Piezoelectricity	151
8.6.3	Pyroelectricity	152
8.6.4	Molecular Dipole Moments	152
	Exercises	163
9	Space Groups	183
9.1	Glide Planes and Screw Axes	183
9.1.1	Glide Planes	184
9.1.2	Screw Axes	187
9.2	The 230 Space Groups	189
9.3	Properties of Space Groups	191
9.4	International Tables for Crystallography	203
9.5	Space Group and Crystal Structure	205
	Exercises	207
10	The Interrelationship of Point Groups and Space Groups	213
	Exercise	215

11	Fundamentals of Crystal Chemistry	217
11.1	Coordination	218
11.2	Metal Structures	220
11.3	Structures of Noble Gases and Molecules	224
11.4	Ionic Structures	225
11.4.1	Ionic Radii	226
11.4.2	Octahedral Coordination [6]	226
11.4.3	Cubic Coordination [8]	230
11.4.4	Tetrahedral Coordination [4]	231
11.5	Covalent Structures	236
11.6	Isotypes, Solid Solutions and Isomorphism	236
11.7	Polymorphism	239
11.8	Literature on Crystal Structures	244
	Exercises	245
12	Studies of Crystals by X-Ray Diffraction	249
12.1	The Bragg Equation	249
12.2	The Debye-Scherrer Method	250
12.3	The Reciprocal Lattice	254
12.4	The Laue Groups	260
12.5	The Determination of a Crystal Structure	261
	Exercises	264
13	Crystal Defects	265
13.1	Point Defects	266
13.2	Line Defects	267
13.3	Plane Defects	268
14	Appendix	271
14.1	Symbols for Crystallographic Items	271
14.2	Symmetry Elements	272
14.3	Calculation of Interatomic Distances and Angles in Crystal Structures	275
14.4	Crystal Forms	276
15	Solutions to the Exercises	279
	References	301
	Subject Index	303

Inside back cover (Wulff Net)

Introduction

At the heart of crystallography lies an object – the *crystal*. Crystallography is concerned with the laws governing the crystalline state of solid materials, with the arrangement of atoms in crystals, and with their physical and chemical properties, their synthesis and their growth.

Crystals play a role in many subjects, among them mineralogy, inorganic, organic and physical chemistry, physics, metallurgy, materials science, geology, geophysics, biology and medicine. This pervasiveness is perhaps better understood when it is realised how widespread crystals are: virtually all naturally occurring solids, i.e. minerals, are crystalline, including the raw materials for chemistry, e.g. the ores. A mountain crag normally is made up of crystals of different kinds, while an iceberg is made up of many small ice crystals. Virtually all solid inorganic chemicals are crystalline, and many solid organic compounds are made up of crystals, among them benzene, naphthalene, polysaccharides, proteins, vitamins, rubber and nylon. Metals and alloys, ceramics and building materials are all made up of crystals. The inorganic part of teeth and bones is crystalline. Hardening of the arteries and arthritis in humans and animals can be traced to crystal formation. Even many viruses are crystalline.

This enumeration could be continued endlessly, but it is already obvious that practically any material that can be regarded as solid is crystalline.

In many countries, especially in Germany, crystallography is mainly taught as a part of mineralogy, while elsewhere, notably in Britain and North America, it is more often taught as a part of physics or chemistry. In any case, “crystallographers” may be from a wide variety of scientific backgrounds. Most countries have a National Crystallographic Committee representing the International Union of Crystallography, the body which publishes *Acta Crystallographica* and *International Tables for Crystallography*.

1 The Crystalline State

The outward appearance of a crystal is exceptionally variable, but all the variations which occur can be explained in terms of a single fundamental principle. To grasp this, we must first come to terms with the nature of the crystalline state. The following are a few properties that are characteristic of crystals:

- a) Many crystals not only have smooth faces, but, given ideal growth conditions, have regular geometric shapes (see Figs. 1.1–1.4).
- b) If some crystals (e.g. NaCl) are split, the resulting fragments have similar shapes with smooth faces – in the case of NaCl, small cubes. This phenomenon is known as *cleavage*, and is typical only of crystals.

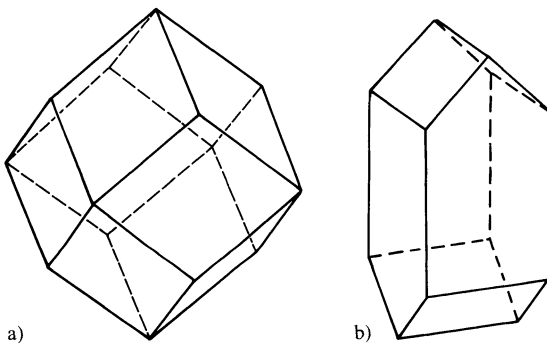


Fig. 1.1 a, b. A garnet crystal with the shape of a rhomb-dodecahedron (a) and a crystal of vitamin B₁₂ (b)

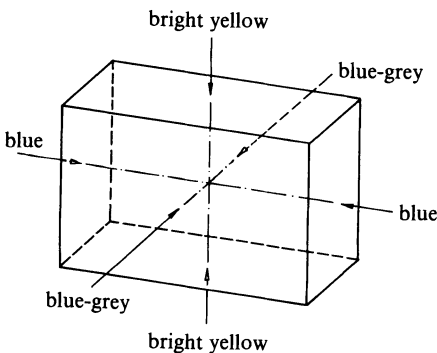


Fig. 1.2. Pleochroism as shown by a crystal of cordierite

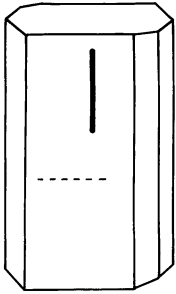


Fig. 1.3. A crystal of kyanite, with a scratch illustrating the anisotropy of its hardness

c) Figure 1.2 shows a corderite crystal and the colours that an observer would see when the crystal is viewed from the given directions. The colours that appear depend on the optical absorption of the crystal in that particular direction. For example, if it absorbs all spectral colours from white light except blue, the crystal will appear blue to the observer. When, as in this case, the absorption differs in the three directions, the crystal is said to exhibit *pleochroism*.

d) When a crystal of kyanite (Al_2OSiO_4) is scratched parallel to its length by a steel needle, a deep indentation will be made in it, while a scratch perpendicular to the crystal length will leave no mark (see Fig.1.3). The *hardness* of this crystal is thus different in the two directions.

e) If one face of a gypsum crystal is covered with a thin layer of wax and a heated metal tip is then applied to that face, the melting front in the wax layer will be ellipsoidal rather than circular (Fig.1.4), showing that the thermal conductivity is greater in direction III than in direction I. *Such behaviour – different values of a physical property in different directions – is called anisotropy*, (see also Fig. 1.5c). If the melting front had been circular, as it is, for example, on

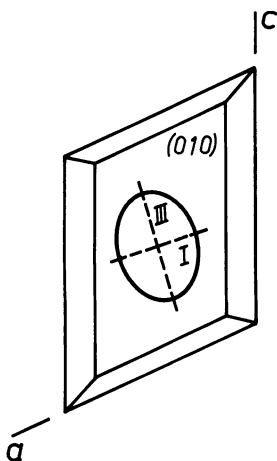
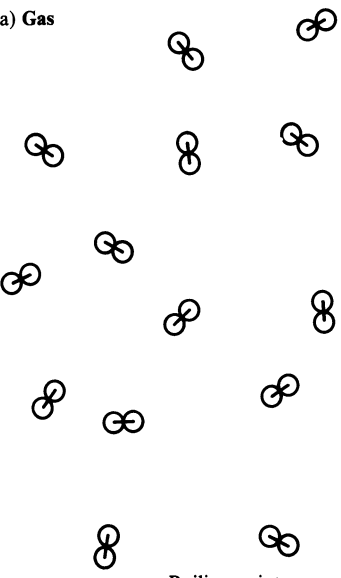
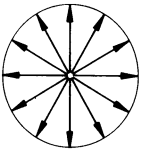
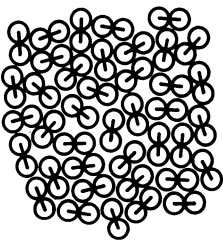
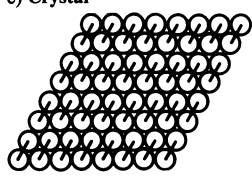
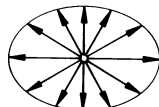


Fig. 1.4. A crystal of gypsum covered with wax showing the melting front. The ellipse is an isotherm, and shows the anisotropy of the thermal conductivity

Representation of the state	Retention of shape	Retention of volume	Distribution of molecules	Physical properties
a) Gas 	No	No	Statistically homogeneous ¹	 Isotropic ²
Boiling point b) Liquid 	Yes	No		
Melting point c) Crystal 	Yes	Yes	Periodically homogeneous ¹	 Anisotropic ³

¹ Equal physical properties in parallel directions \implies

² Equal physical properties in all directions

³ Different physical properties in different directions

Fig. 1.5a-c. Schematic representation of the states of matter. a gas, b liquid, c crystal

a piece of glass, it would imply that the thermal conductivity is the same in all directions. *Such behaviour – the same value of a physical property in all directions – is called isotropy*, (see the right hand side of Fig. 1.5).

Anisotropy of physical properties is normal for crystals. It is, however, not universal, as there are some crystals whose properties are isotropic. The origin of all of the phenomena listed under (a) to (e) lies in the internal structure of crystals. In order to understand this better, let us now consider the various states of aggregation of matter.

All matter, be it gas, liquid or crystal, is composed of atoms, ions or molecules. Matter is thus *discontinuous*. Since, however, the size of the atoms, ions and molecules lies in the Å region ($1 \text{ Å} = 10^{-8} \text{ cm} = 0.1 \text{ nm}$) matter appears to us to be *continuous*. The states of matter may be distinguished in terms of their tendency to retain a characteristic volume and shape. A gas adopts both the volume and the shape of its container, a liquid has constant volume, but adopts the shape of its container, while a crystal retains both its shape and its volume, independent of its container (see Fig. 1.5).

GASES. Figure 1.5a illustrates the arrangement of molecules in a gas at a particular instant in time. The molecules move rapidly through space, and thus have a high kinetic energy. The attractive forces between molecules are comparatively weak, and the corresponding energy of attraction is negligible in comparison to the kinetic energy.

What can be said about the distribution of the molecules at that particular instant? There is certainly no accumulation of molecules in particular locations; there is, in fact, a random distribution. A. Johnsen [21] has illustrated this by a simple analogy (Fig. 1.6a): we scatter 128 lentils over the 64 squares of a chessboard, and observe that in this particular case some squares will have no lentils, some 1, 2, or even 3 – but on average 2. If, instead of single squares we considered blocks of four squares, the number of lentils in the area chosen would fall between 7 and 9, while any similar block of 16 squares would have exactly 32 lentils. Thus, two distinct areas of the same size will tend to contain the same number of lentils, and this tendency will increase as the areas

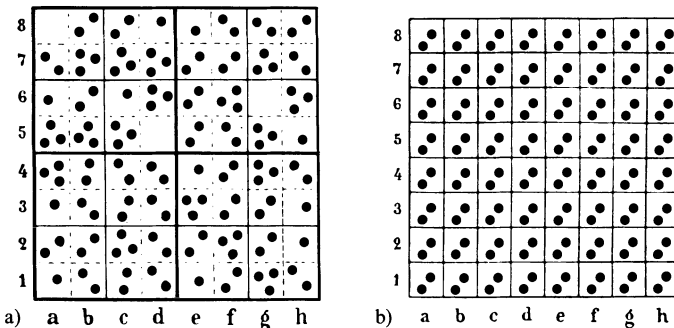


Fig. 1.6a, b. Statistical (a) and periodic (b) homogeneity. Johnsen [21]

considered become larger. This kind of distribution is considered to be *statistically homogeneous*, i.e. it shows the same behaviour in parallel directions, and it may easily be seen that the physical properties of the distribution are isotropic, i.e. are equal in all directions.

LIQUIDS. As the temperature of a gas is lowered, the kinetic energies of the molecules decrease. When the boiling point is reached, the total kinetic energy will be equal to the energy of attraction among the molecules. Further cooling thus converts the gas into a liquid. The attractive forces cause the molecules to “touch” one another. They do not, however, maintain fixed positions, and Fig. 1.5b shows only one of many possible arrangements. The molecules change position continuously. Small regions of order may indeed be found (local ordering), but if a large enough volume is considered, it will also be seen that liquids give a statistically homogeneous arrangement of molecules, and therefore also have isotropic physical properties.

CRYSTALS. When the temperature falls below the freezing point, the kinetic energy becomes so small that the molecules become permanently attached to one another. A three-dimensional framework of attractive interactions forms among the molecules and the array becomes solid – it crystallises. Figure 1.5c shows one possible plane of such a crystal. The movement of molecules in the crystal now consists only of vibrations about a central position. A result of these permanent interactions is that the molecules have become regularly ordered. The distribution of molecules is no longer statistical, but is *periodically homogeneous*; a periodic distribution in three dimensions has been formed (see also Fig. 2.1a).

How can this situation be demonstrated using the chessboard model? (Fig. 1.6b). On each square, there are now precisely two lentils, periodically arranged with respect to one another. The ordering of the lentils parallel to the edges and that along the diagonals are clearly different, and therefore the physical properties in these directions will no longer be the same, but distinguishable – in other words, the crystal has acquired anisotropic properties. This anisotropy is characteristic of the crystalline state.

Definition

A crystal is an anisotropic, homogeneous body consisting of a three-dimensional periodic ordering of atoms, ions or molecules.

All matter tends to crystallise, if the temperature is sufficiently low, since the ordered crystalline phase is the state of lowest energy. There exist, however, materials, such as glass, which never reach this condition. Molten glass is very viscous, and the atoms of which it is made cannot come into a three-dimensional periodic order rapidly enough as the mass cools. Glasses thus have a higher energy content than the corresponding crystals and can best be considered as a frozen, viscous liquid. They are *amorphous* or “form-less” bodies. Such

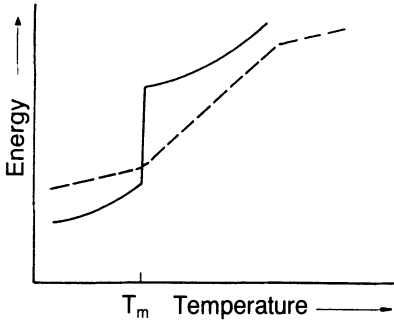


Fig. 1.7. Heating curves for a crystal (—) and a glass (---), T_m is the melting point of the crystal

materials do not produce flat faces or polyhedra since an underlying order is missing.

How then is it possible to distinguish amorphous material from crystals? One possibility is to examine the melting behaviour. As is illustrated in Fig. 1.7, a crystal has a sharp melting point T_m , while amorphous bodies have a region of softening. Another possibility derives from their different properties relative to an incident X-ray beam. The three-dimensional ordering of the atoms in crystals gives rise to sharp interference phenomena, as is further examined in Chapter 12. Amorphous bodies, as they do not have underlying order, produce no such effect.

EXERCISES

Exercise 1.1. Determine the volume of a gas associated with each molecule at normal temperature and pressure.

Exercise 1.2. Determine the packing efficiency of Ne gas ($R_{\text{Ne}} = 1.60 \text{ \AA}$) under normal conditions. The packing efficiency is the ratio of the volume of a neon atom to the volume calculated in example 1.1. For comparison, a copper crystal has a packing efficiency of 74%.

Exercise 1.3. Discuss the use of the term “crystal glass”!

2 The Lattice and Its Properties

A three-dimensional periodic arrangement of atoms, ions or molecules is always present in all crystals. This is particularly obvious for the α -polonium crystal illustrated in Fig. 2.1a. If each atom is represented simply by its centre of gravity, what remains is a *point* or *space lattice* (Fig. 2.1b).

A point or space lattice is a three-dimensional periodic arrangement of points, and it is a pure mathematical concept. The concept of a lattice will now be developed from a lattice point via the line lattice and the plane lattice, finally to the space lattice.

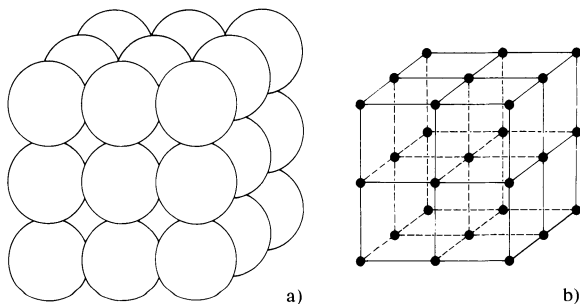


Fig. 2.1 a, b. Three-dimensional periodic arrangement of the atoms in a crystal of α -polonium (a) and the space lattice of the crystal (b)

2.1 Line Lattice

In Fig. 2.2, we may consider moving from the point 0 along the vector \vec{a} to the point 1. By a similar movement of $2\vec{a}$, we will reach point 2, etc. By this movement, one point is brought into coincidence with another, and a *repetition operation* takes place. By means of this operation, called a *lattice translation*, a *line lattice* has been generated. All points which may be brought into coincidence with one another by a lattice translation are called *identical points* or *points equivalent by translation*. $|\vec{a}| = a_0$ is called the *lattice parameter*, and this constant alone completely defines the one-dimensional lattice.

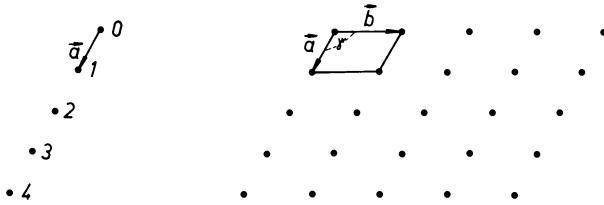


Fig. 2.2

Fig. 2.3

Fig. 2.2. Line lattice with its lattice parameter $|\vec{a}| = a_0$

Fig. 2.3. Plane lattice with the unit mesh defined by the vectors \vec{a} and \vec{b}

2.2 Plane Lattice

If a lattice translation \vec{b} ($\vec{b} \nparallel \vec{a}$) is then allowed to operate on the line lattice in Fig. 2.2, the result is the *plane lattice* or plane net (Fig. 2.3). The vectors \vec{a} and \vec{b} define a *unit mesh*. The entire plane lattice may now be constructed from the knowledge of three lattice parameters, $|\vec{a}| = a_0$, $|\vec{b}| = b_0$ and γ , the included angle. If any point is moved by any arbitrary lattice translation, it will come into coincidence with another point. A plane lattice thus has lattice translations not only parallel to \vec{a} and \vec{b} , but also to any number of combinations of them, i.e. an infinite number of lattice translations.

2.3 Space Lattice

If yet another lattice translation \vec{c} is now introduced in a direction not coplanar with \vec{a} and \vec{b} , its action on the plane lattice in Fig. 2.3 generates the *space lattice* shown in Fig. 2.4. This space lattice can also be produced solely by the operations of three dimensional lattice translations. *In contrast to a finite crystal, a space lattice is infinite.*

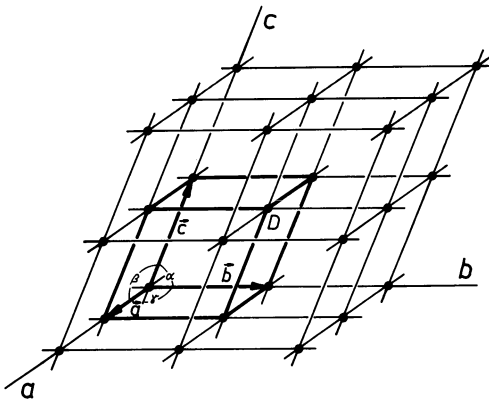


Fig. 2.4. Space lattice with the unit cell defined by the vectors \vec{a} , \vec{b} and \vec{c}

According to the arrangement of the vectors \vec{a} , \vec{b} and \vec{c} , we may introduce an *axial system* with the *crystallographic axes* a , b and c . The vectors \vec{a} , \vec{b} and \vec{c} and their respective crystallographic axes a , b and c are chosen to be *right-handed*. That is, if the right thumb points in the direction of \vec{a} (a) and the index finger is along \vec{b} (b), the middle finger will point in the direction of \vec{c} (c). A lattice, or a crystal described by it, may always be positioned so that \vec{a} (a) points toward the observer, \vec{b} (b) toward the right, and \vec{c} (c) upwards, as is done in Fig. 2.4.

The vectors \vec{a} , \vec{b} and \vec{c} define a *unit cell*, which may alternatively be described by six lattice parameters:

length of lattice translation vectors

interaxial lattice angles

$$|\vec{a}| = a_0$$

$$\vec{a} \wedge \vec{b} = \gamma$$

$$|\vec{b}| = b_0$$

$$\vec{a} \wedge \vec{c} = \beta$$

$$|\vec{c}| = c_0$$

$$\vec{b} \wedge \vec{c} = \alpha$$

Further application of lattice translations to the unit cell will produce the entire space lattice. *The unit cell thus completely defines the entire lattice.*

Every unit cell has eight vertices and six faces. At all vertices there is an identical point. Can all of these points be considered part of the unit cell? The lattice point D in Fig. 2.4 is not only part of the marked-out unit cell, but part of all eight cells which meet at that point. In other words, only one eighth of it may be attributed to the marked unit cell, and since $8 \times \frac{1}{8} = 1$, the unit cell contains only one lattice point. Such unit cells are called simple or *primitive*, and are given the symbol P.

2.4 The Designation of Points, Lines and Planes in a Space Lattice

2.4.1 The Lattice Point uvw

Every lattice point is uniquely defined with respect to the origin of the lattice by the vector $\vec{r} = u\vec{a} + v\vec{b} + w\vec{c}$. The lengths of \vec{a} , \vec{b} and \vec{c} are simply the lattice parameters, so only the coordinates u , v and w require to be specified. They are written as a “triple” uvw . In Fig. 2.5, the vector \vec{r} describes the point 231 (which

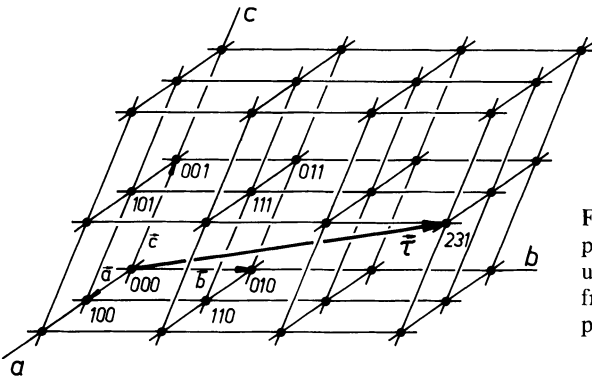


Fig. 2.5. Designation of lattice points using the coordinates uvw that define the vector from the origin to the lattice point uvw , $\vec{r} = u\vec{a} + v\vec{b} + w\vec{c}$

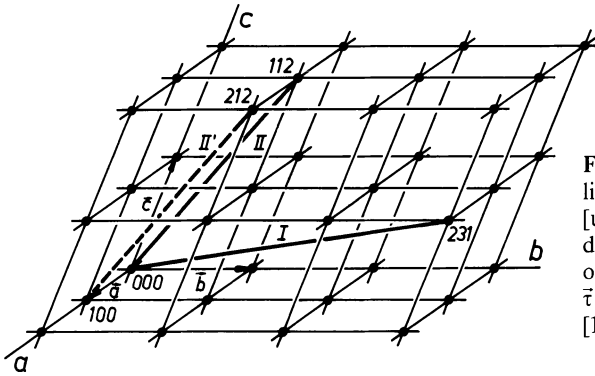


Fig. 2.6. Designation of lattice lines using the coordinates $[uvw]$ (in square brackets) that define the vector from the origin to the given point $\vec{r} = u\vec{a} + v\vec{b} + w\vec{c}$ (I: $[231]$, II: $[112]$)

is read as two-three-one). The coordinates u , v and w normally are integers, but can also have values of integers $+\frac{1}{2}, \frac{1}{3}$ or $\frac{2}{3}$, as is further explained in Chapter 6.4. When they have integral values, the points uvw are the coordinates of the points of a P-lattice. The coordinates of the vertices of a unit cell are given in Fig. 2.5.

2.4.2 Lattice Lines $[uvw]$

A line may be specified mathematically in any coordinate system by two points. The lattice line I in Fig. 2.6 contains the points 000 and 231. Since the lattice line passes through the origin, the other point on its own describes the direction of the line in the lattice, and the coordinates of this point thus define the line. For this purpose, they are placed in square brackets $[231]$, or in general $[uvw]$, to show that they represent the direction of a line.

The lattice line II' passes through the points 100 and 212. Line II is parallel to this line, and passes through the origin as well as the point 112 and consequently both lines may be referred to by the symbol $[112]$.

Note that the triple $[uvw]$ describes not only a lattice line through the origin and the point uvw , but the infinite set of lattice lines which are parallel to it and have the same lattice parameter.

Figure 2.7 shows parallel sets of lattice lines $[110]$, $[120]$ and $[310]$. The repeat distance along the lines increases with u , v , w .

Figure 2.8 shows a projection of a space lattice along c onto the a, b -plane. The lattice line A intersects the points with coordinates 000, 210, 420 and $\bar{2}\bar{1}0$. Note that minus signs are placed above the numbers to which they apply – this applies to all crystallographic triples. Each point on the line has different values uvw , but the ratio $u:v:w$ remains constant. In this case, the smallest triple is

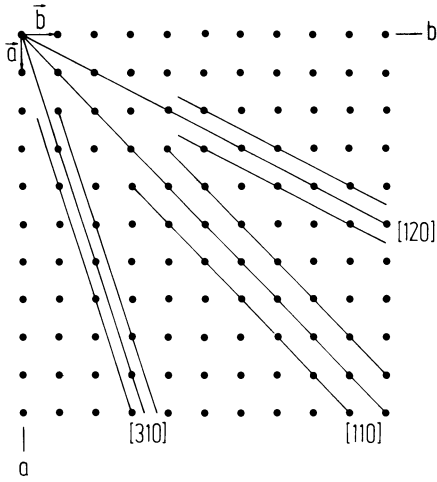


Fig. 2.7. Projection of a lattice onto the a, b-plane showing parallel sets of lattice lines $[100]$, $[120]$ and $[310]$

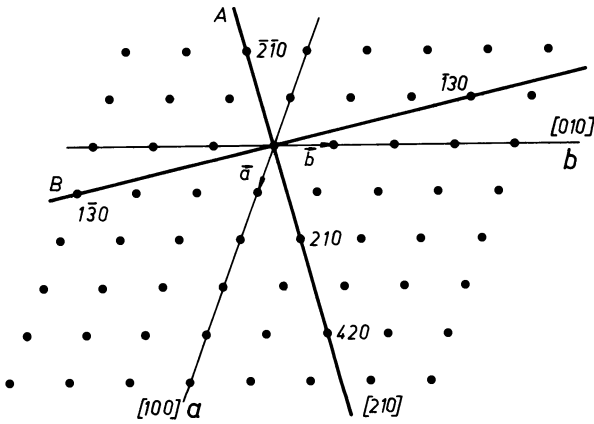


Fig. 2.8. Projection of a space lattice along c onto the a, b-plane. The lattice line A is defined by the triple $[210]$, while B may be given as $[130]$ or $[\bar{1}30]$

used to define the lattice line. Lines parallel to \vec{a} or \vec{b} are thus identified as $[100]$ or $[010]$ respectively, while the line B is given as $[\bar{1}30]$ or $[130]$; note that these two representations define opposite directions for the lattice line.

2.4.3 Lattice Planes (hkl)

Consider a plane in the lattice intersecting the axes a, b and c at the points $m00$, $0n0$ and $00p$. (These coordinates are given as mnp and not uvw to show that the values need not be integral. An example of a lattice plane which does not intersect the axes at lattice points is plane D in Fig. 2.11). The coordinates of the three intercepts completely define the position of a lattice plane (Fig. 2.9). Normally, however, the reciprocals of these coordinates are used rather than the coordinates themselves:

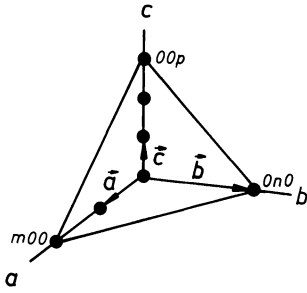


Fig. 2.9. The intercepts on the axes of a lattice plane with the Miller indices (362)

a-axis: $h \sim \frac{1}{m}$

b-axis: $k \sim \frac{1}{n}$

c-axis: $l \sim \frac{1}{p}$

The smallest integral values are chosen for the reciprocal intercepts, and they are then written as a triple (hkl) in round brackets.

Definition

The values (hkl) are called Miller indices, and they are defined as the smallest integral multiples of the reciprocals of the plane intercepts on the axes.

The lattice plane shown in Fig. 2.9 has the intercepts $m|n|p=2|1|3$ the reciprocals of these are $\frac{1}{2}|\frac{1}{1}|\frac{1}{3}$, leading to the Miller indices (362).

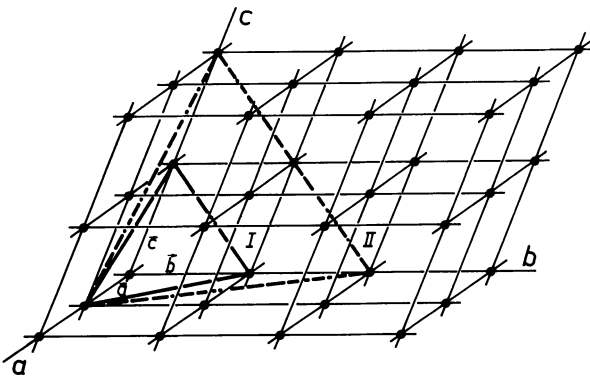


Fig. 2.10. The indexing of lattice planes by Miller indices, the smallest integral multiples of the reciprocals of the intercepts on the axes; I (111), II (211)

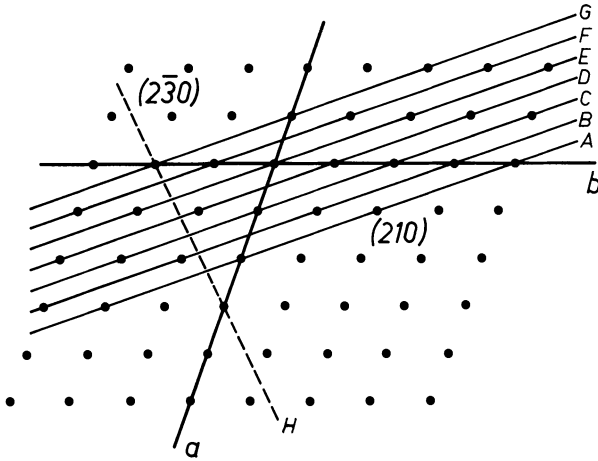


Fig. 2.11. Projection of a space lattice along c onto the a, b -plane. The “lines” A – G are the traces of the lattice planes parallel to c with the Miller indices (210) . The “line” H is the trace of a lattice plane $(2\bar{3}0)$

In the space lattice shown in Fig. 2.10, two lattice planes have been drawn in

	m	n	p	$\frac{1}{m}$	$\frac{1}{n}$	$\frac{1}{p}$	(hkl)
I	1	1	1	1	1	1	(111)
II	1	2	2	1	$\frac{1}{2}$	$\frac{1}{2}$	(211)

In Fig. 2.11, a projection of a lattice is shown together with the lines representing the traces of lattice planes perpendicular to the plane of the paper and parallel to the c -axis. These lattice planes are indexed as follows:

	m	n	p	$\frac{1}{m}$	$\frac{1}{n}$	$\frac{1}{p}$	(hkl)
A	2	4	∞	$\frac{1}{2}$	$\frac{1}{4}$	0	(210)
B	$\frac{3}{2}$	3	∞	$\frac{2}{3}$	$\frac{1}{3}$	0	(210)
C	1	2	∞	1	$\frac{1}{2}$	0	(210)
D	$\frac{1}{2}$	1	∞	2	1	0	(210)
E	–	–	–	–	–	–	–
F	$\frac{1}{2}$	$\bar{1}$	∞	$\bar{2}$	$\bar{1}$	0	$(\bar{2}\bar{1}0)$
G	$\bar{1}$	$\bar{2}$	∞	$\bar{1}$	$\frac{1}{2}$	0	$(\bar{2}\bar{1}0)$
H	3	$\bar{2}$	∞	$\frac{1}{3}$	$\frac{1}{2}$	0	$(2\bar{3}0)$

The lattice planes A to G belong to a set of equally spaced, parallel planes resulting in the same indices. Generally, they are all described by the triple (hkl) , which represents not merely a single lattice plane, but an infinite set of parallel planes. Since the plane E intersects the origin, it cannot be

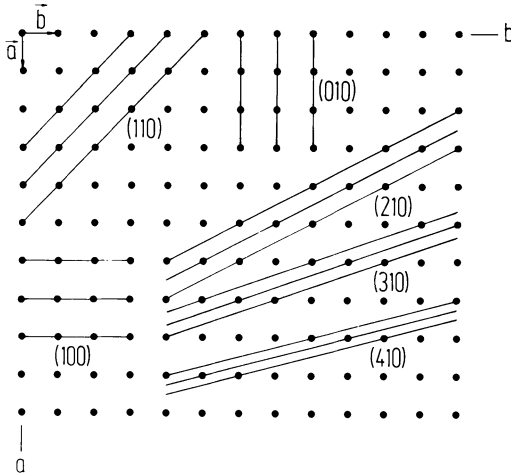


Fig. 2.12. Projection of a lattice onto the a, b-plane, with the projections of six sets of lattice planes

indexed in this position. Note that (210) and $(\bar{2}\bar{1}0)$ define the same parallel set of planes.

Figure 2.12 gives the projection of a lattice onto the a, b-plane. This projection has a square unit cell. The projections of six sets of lattice planes with various indices are also shown. As the indices rise, the spacing between the planes decreases, as does the density of points on each plane.

Planes which are parallel to b and c will thus only have intercepts with a and are indexed as (100). Similarly, (010) intersects only the b-axis, and (001) only c. The line H in Fig. 2.11 is the trace of the plane $(2\bar{3}0)$.

2.5 The Zonal Equation

We may ask what the relationship is between the symbols [uvw] and (hkl) if they represent sets of lines and planes that are parallel to one another. The equation of any plane may be written:

$$\frac{X}{m} + \frac{Y}{n} + \frac{Z}{p} = 1,$$

where X, Y and Z represent the coordinates of points lying on the plane, and m, n and p are the three intercepts of this plane on the crystallographic axes a, b and c (see Sect. 2.4.3). If the substitution is then made $h \sim \frac{1}{m}$, $k \sim \frac{1}{n}$, and $l \sim \frac{1}{p}$, the equation may be written

$$hX + kY + lZ = C,$$

where C is an integer. The equation describes not only a single lattice plane, but a set of parallel lattice planes. For positive h, k and l, giving C a value of +1 describes that plane of the set which lies nearest to the origin in the positive a, b

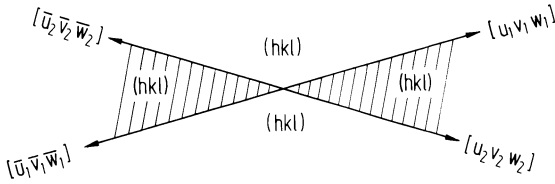


Fig. 2.13. The lattice lines $[u_1v_1w_1]$ and $[u_2v_2w_2]$ define the lattice plane (hkl)

and c directions. Similarly, a value of -1 defines the nearest plane in the negative a , b and c directions from the origin. The plane (hkl) which cuts the origin has the equation:

$$hX + kY + lZ = 0.$$

As an example, the planes D, E and F in Fig. 2.11, are defined by the above equation where $(hkl) = (210)$ and C takes on the values 1, 0 and -1 respectively. For any of these planes, the triple XYZ represents a point on the plane. In particular, on the plane passing through the origin ($C = 0$) this triple XYZ could describe a lattice line – the line connecting the point XYZ to the origin 000 . In this case, we would replace XYZ by uvw giving the relationship:

$$hu + kv + lw = 0.$$

For reasons which will appear later this relationship is called the *zonal equation*.

Applications of the Zonal Equation

a) Two lattice lines $[u_1v_1w_1]$ and $[u_2v_2w_2]$ will describe a lattice plane (hkl) (cf. Fig. 2.13), whose indices may be determined from the double application of the zonal equation:

$$hu_1 + kv_1 + lw_1 = 0$$

$$hu_2 + kv_2 + lw_2 = 0.$$

The solution of these two simultaneous equations for hkl may be expressed in two ways as the ratio of determinants:

$$h : k : l = \begin{vmatrix} v_1w_1 \\ v_2w_2 \end{vmatrix} : \begin{vmatrix} w_1u_1 \\ w_2u_2 \end{vmatrix} : \begin{vmatrix} u_1v_1 \\ u_2v_2 \end{vmatrix} \tag{1}$$

$$\bar{h} : \bar{k} : \bar{l} = \begin{vmatrix} v_2w_2 \\ v_1w_1 \end{vmatrix} : \begin{vmatrix} w_2u_2 \\ w_1u_1 \end{vmatrix} : \begin{vmatrix} u_2v_2 \\ u_1v_1 \end{vmatrix} \tag{2}$$

The lattice plane symbols (hkl) and $(\bar{h}\bar{k}\bar{l})$, however, describe the same set parallel planes.

$$h : k : l = (v_1w_2 - v_2w_1) : (w_1u_2 - w_2u_1) : (u_1v_2 - u_2v_1).$$

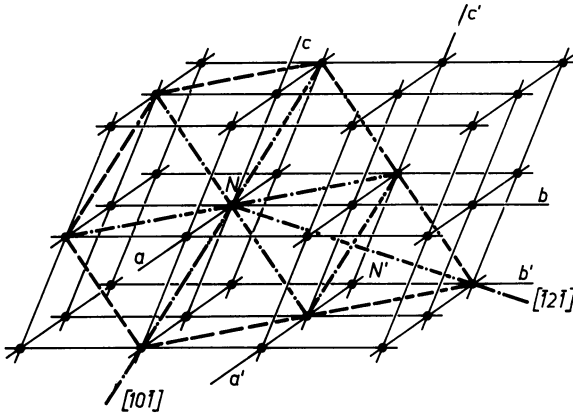


Fig. 2.14. The lattice lines $[10\bar{1}]$ and $[\bar{1}2\bar{1}]$ lie in the lattice plane indicated by the *dashed lines*. Since, however, that plane passes through the origin, it is necessary to consider an alternative origin such as N' in order to assign its indices (111)

The following form is particularly convenient:

$$\begin{array}{c|ccc|c} u_1 & v_1 & w_1 & u_1 & v_1 & w_1 \\ & \times & \times & \times & & \\ u_2 & v_2 & w_2 & u_2 & v_2 & w_2 \\ \hline & (h & k & l) & & \end{array}$$

EXAMPLE. What is the set of lattice planes common to the lines $[10\bar{1}]$ and $[\bar{1}2\bar{1}]$?

$$\begin{array}{c|ccc|c} 1 & 0 & \bar{1} & 1 & 0 & \bar{1} \\ \bar{1} & 2 & \bar{1} & \bar{1} & 2 & \bar{1} \\ \hline & 2 & 2 & 2 & \rightarrow & (111) \end{array}$$

This result can also be obtained geometrically, as in Fig. 2.14. The lattice lines $[10\bar{1}]$ and $[\bar{1}2\bar{1}]$ ($-\cdot-\cdot-\cdot-\cdot-$) lie in the lattice plane ($---$). Other lines lying in the plane are also shown ($-\cdot-\cdot-\cdot-$) in order to make it more obvious. The indicated lattice plane cannot be indexed, as it passes through the origin. The choice of an alternative origin N' makes it possible to index it: $m|n|p=1|1|1 \rightarrow (111)$.

If the determinant is set up in the alternative manner:

$$\begin{array}{c|ccc|c} \bar{1} & 2 & \bar{1} & \bar{1} & 2 & \bar{1} \\ 1 & 0 & \bar{1} & 1 & 0 & \bar{1} \\ \hline & \bar{2} & \bar{2} & \bar{2} & \rightarrow & (\bar{1}\bar{1}\bar{1}). \text{ [see Eq. (2)]} \end{array}$$

(111) and $(\bar{1}\bar{1}\bar{1})$ belong to the same set of parallel lattice planes; in the description of crystal faces (Chap. 4) the symbols (hkl) and $(\bar{h}\bar{k}\bar{l})$ are taken to represent a crystal face and its parallel opposite.

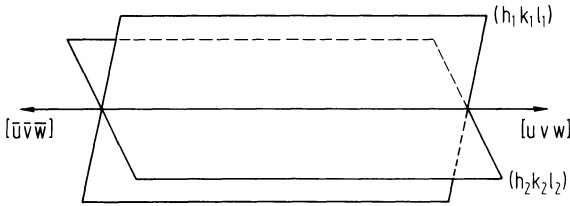


Fig. 2.15. The lattice planes $(h_1 k_1 l_1)$ and $(h_2 k_2 l_2)$ intersect in the lattice line $[uvw]$

b) Two lattice planes $(h_1 k_1 l_1)$ and $(h_2 k_2 l_2)$ intersect in the lattice line $[uvw]$ (see Fig. 2.15), which can be identified by the solution of the equations:

$$h_1 u + k_1 v + l_1 w = 0$$

$$h_2 u + k_2 v + l_2 w = 0.$$

Proceeding in the same method as above leads to the required lattice line $[uvw]$:

h_1	k_1	l_1	h_1	k_1	l_1
	\times	\times	\times		
h_2	k_2	l_2	h_2	k_2	l_2
$[u \quad v \quad w]$					

Note that, as in (a), two solutions are possible: $[uvw]$ and $[\bar{u}\bar{v}\bar{w}]$. In this case, these represent the opposite directions of the same line.

EXAMPLE. Which lattice line is common to the lattice planes (101) and $(\bar{1}12)$?

$\bar{1}$	1	2	$\bar{1}$	1	2
1	0	1	1	0	1
$[1 \quad 3 \quad \bar{1}]$					

If the values of (hkl) are interchanged, the result will be $[\bar{1}\bar{3}1]$.

EXERCISES

- Exercise 2.1.** Make a copy on tracing paper of the lattice points outlining a single unit cell in Fig. 2.5. Lay your tracing on top of a unit cell in the original drawing and satisfy yourself that you can reach any other cell by suitable lattice translations.
- Exercise 2.2.**
- a) Examine the lattice in Fig. 2.16, and give the coordinates of the points P_1, P_2, P_3 and P_4 , the values of $[uvw]$ for the lattice lines that are drawn in.
 - b) On the same diagram, draw in the lines $[2\bar{1}1], [120]$ and $[212]$.
 - c) Determine the lattice planes to which the lines $[131]$ and $[\bar{1}11]$ belong.

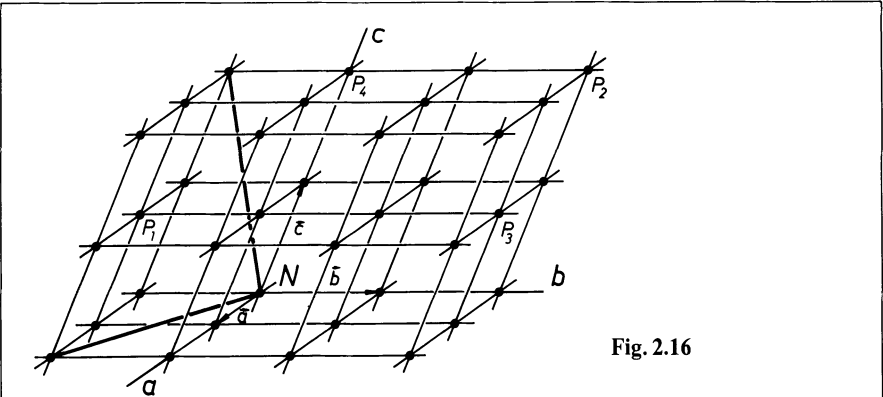


Fig. 2.16

Exercise 2.3. Figure 2.17 is the projection of a lattice along the c-axis onto the a, b-plane. The dark lines labelled I and II are the traces of planes that are parallel to the c-axis.

- Index planes I and II.
- Calculate $[uvw]$ for the line common to the two planes.
- Draw the traces of the planes (320) and $(\bar{1}20)$ on the projection.

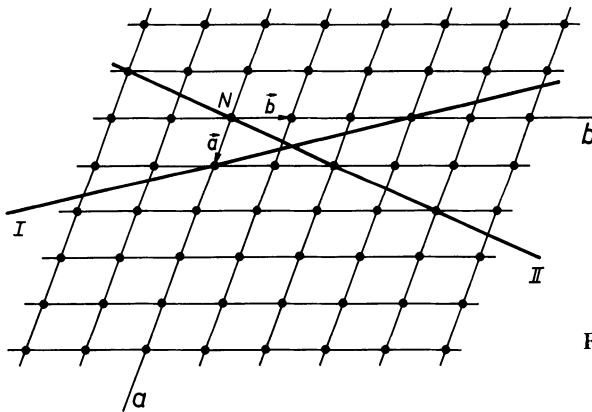


Fig. 2.17

Exercise 2.4. Give (hkl) for a few planes containing the line $[21\bar{1}]$, and give $[uvw]$ for a few lines lying in the plane (121) .

Exercise 2.5. What condition must be fulfilled to make (a) $[100]$ perpendicular to (100) , (b) $[110]$ perpendicular to (110) and (c) $[111]$ perpendicular to (111) ?

Exercise 2.6. What are the relationships between (110) and $(\bar{1}\bar{1}0)$; $(\bar{2}11)$ and $(2\bar{1}\bar{1})$; $[110]$ and $[\bar{1}\bar{1}0]$; $[\bar{2}11]$ and $[2\bar{1}\bar{1}]$?

3 Crystal Structure

In order to progress from a lattice to a crystal, the points of the lattice must be occupied by atoms, ions or molecules. Because the points are all identical, the collections of objects occupying them must also be equal. In general, crystals are not built up so simply as the crystal of α -polonium in Fig. 2.1!

Let us consider the construction of a crystal by means of a hypothetical example. Figure 3.1a shows a **lattice** with a rectangular unit cell projected on the a, b -plane. We now place the molecule ABC in the unit cell of the lattice in such a way that A lies at the origin and B and C within the chosen cell (Fig. 3.1b). The position of B or C with respect to the origin may be described by a vector \vec{r} in terms of the lattice translations \vec{a} , \vec{b} , and \vec{c} :

$$\vec{r} = x\vec{a} + y\vec{b} + z\vec{c} \quad (\text{see Fig. 3.3}).$$

The coordinates are yet another triple: x, y, z , where $0 \leq x, y, z < 1$ for all positions within the unit cell. In our example, the atoms have the following coordinates:

$$\text{A: } 0, 0, 0 \quad \text{B: } x_1, y_1, z_1, \quad \text{C: } x_2, y_2, z_2.$$

This arrangement of atoms within a unit cell is called the **basis**. Lattice translations reproduce the atoms throughout the entire lattice (Fig. 3.1c), or:

lattice + basis = crystal structure.

It follows that not only the A-atoms but also the B- and C-atoms lie on the points of congruent lattices, which differ from one another by the amount indicated in the basis (see Fig. 3.2). Every atom in a crystal structure is repeated throughout the crystal by the same lattice translations.

Thus, the following simple definition of a crystal is possible.

Definition

*Crystals are solid chemical substances with a three-dimensional periodic array of atoms, ions or molecules. This array is called a **crystal structure**.*

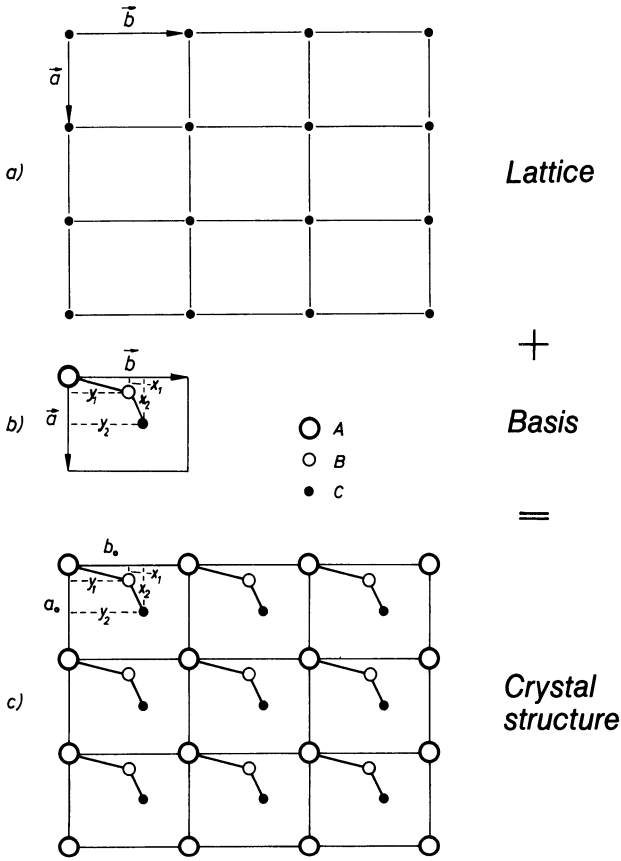


Fig. 3.1 a-c. Interrelationship of the lattice (a), the basis or the arrangement of atoms in the unit cell (b) and the crystal structure (c), all shown as a projection on the a, b-plane

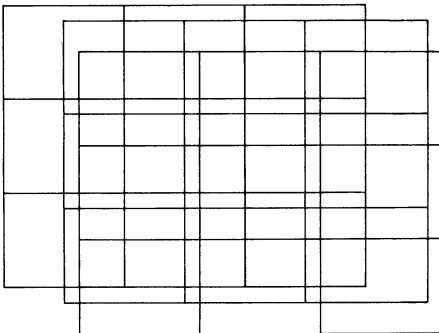


Fig. 3.2. All atoms of the crystal structure shown in Fig. 3.1 lie on the points of congruent lattices

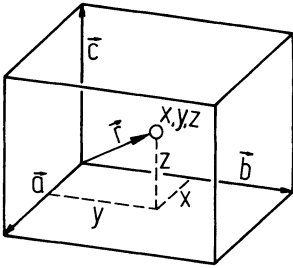


Fig. 3.3. Description of a point in a unit cell by the coordinate-triple x, y, z defining the vector $\vec{r} = x\bar{a} + y\bar{b} + z\bar{c}$

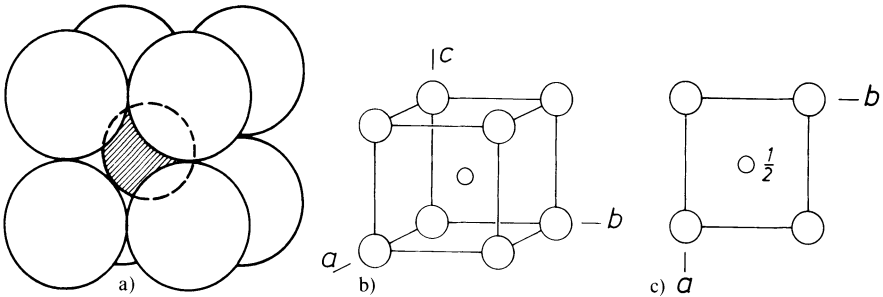


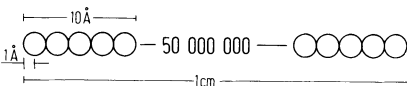
Fig. 3.4a-c. The CsI structure shown in a perspective drawing taking account of the relative sizes of the ions (a), with ions reduced to their centres of gravity (b) and as a parallel projection on (001) (c)

An example of a simple crystal structure is caesium iodide. The unit cell is a cube ($a_0 = b_0 = c_0 = 4.57 \text{ \AA}$, $\alpha = \beta = \gamma = 90^\circ$)¹. The basis is $\text{I}^-: 0, 0, 0$; $\text{Cs}^+: \frac{1}{2}, \frac{1}{2}, \frac{1}{2}$. In Figure 3.4a, a unit cell is shown as a perspective picture, with the relative sizes of the ions indicated. For more complex structures, this method of illustration is less useful, as it prevents the positions of atoms from being clearly seen. Consequently, it is more usual merely to indicate the centres of gravity of the atoms, as in Fig. 3.4b. Figure 3.4c shows the same structure represented as a parallel projection on one cube face.

An important quantity for any structure is Z , the number of chemical formula units per unit cell. For CsI, $Z=1$ as there are only one Cs^+ ion and one I^- ion per cell. Using only structural data, it is thus possible to calculate the density of CsI, since

$$\rho = \frac{m}{V} \text{ g cm}^{-3},$$

¹ The Ångström unit (\AA): $1 \text{ \AA} = 10^{-8} \text{ cm} = 0.1 \text{ nm}$. If a row of spheres with a radius of 1 \AA is made, these will be 50 000 000 of them per centimetre!



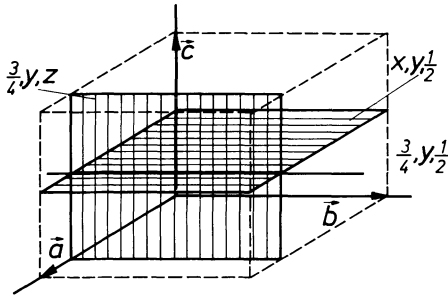


Fig. 3.5. The description of lines and planes in a unit cell by means of coordinates x, y, z

where m is the mass of the atoms in the unit cell and V is the volume of the cell. The mass of one chemical formula is M/N_A , where M is the molar mass and N_A is the Avogadro number, so

$$m = \frac{Z \cdot M}{N_A} \quad \text{and}$$

$$\rho = \frac{Z \cdot M}{N_A \cdot V} \text{ g cm}^{-3}.$$

Thus, taking N_A as $6.023 \times 10^{23} \text{ mol}^{-1}$, for CsI, where $M = 259.81 \text{ g mol}^{-1}$

$$\rho_{\text{CsI}} = \frac{1 \cdot 259.81}{6.023 \cdot 10^{23} \cdot 4.57^3 \cdot 10^{-24}} = 4.52 \text{ g cm}^{-3}.$$

In a structure determination, this operation is carried out in reverse: from the measured density, the number of formula unit per cell is estimated.

Using the values (hkl) and $[uvw]$ we have so far only described the orientations of sets of planes and lines. Consideration of the contents of a unit cell makes it necessary to describe specific planes and lines in the cell. Use of the coordinates x, y, z makes this possible. For example, the coordinates $x, y, \frac{1}{2}$ identify all points in the plane parallel to \vec{a} and \vec{b} which cuts \vec{c} at $\frac{1}{2}$. Figure 3.5 shows the planes $x, y, \frac{1}{2}$ and $\frac{3}{4}, y, z$. The line of intersection may easily be seen to be described by the coordinates $\frac{3}{4}, y, \frac{1}{2}$.

EXERCISES

Exercise 3.1. Cuprite, an oxide of copper, has the

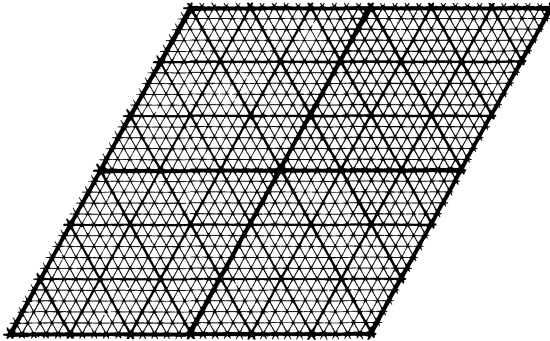
lattice: $a_0 = b_0 = c_0 = 4.27 \text{ \AA}$, $\alpha = \beta = \gamma = 90^\circ$ and the

basis: Cu: $\frac{1}{4}, \frac{1}{4}, \frac{1}{4}$; $\frac{3}{4}, \frac{3}{4}, \frac{1}{4}$; $\frac{3}{4}, \frac{1}{4}, \frac{3}{4}$; $\frac{1}{4}, \frac{3}{4}, \frac{3}{4}$
 O: $0, 0, 0$; $\frac{1}{2}, \frac{1}{2}, \frac{1}{2}$.

- Draw a projection of the structure on $x, y, 0$ (the a, b -plane) and a perspective representation of the structure.
- What is the chemical formula of this compound? What is Z (the number of formula units per unit cell)?
- Calculate the shortest Cu-O distance.
- What is the density of cuprite?

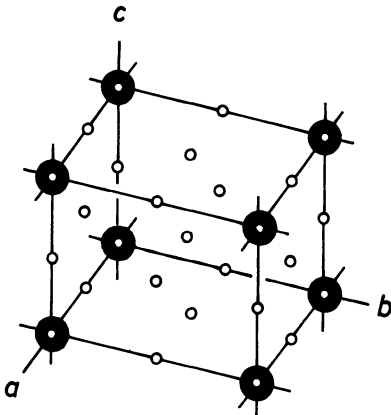
Exercise 3.2. The cell dimensions for a crystal of AlB_2 were determined to be $a_0 = b_0 = 3.00 \text{ \AA}$, $c_0 = 3.24 \text{ \AA}$, $\alpha = \beta = 90^\circ$, $\gamma = 120^\circ$. There is an Al-atom at $0, 0, 0$, and B-atoms at $\frac{1}{3}, \frac{2}{3}, \frac{1}{2}$ and $\frac{2}{3}, \frac{1}{3}, \frac{1}{2}$.

- Draw a projection of four unit cells of this structure on (001) .



- Calculate the shortest Al-B distance.
- Calculate the density of AlB_2 .

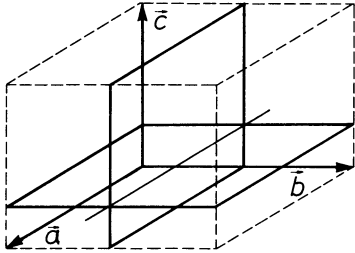
Exercise 3.3. In the accompanying drawing of the unit cell of a lattice, give the coordinates of the points occupied by small circles, which, as we will later learn, represent inversion centres (Chap. 5.3).



Exercise 3.4. Draw the unit cell of a lattice and give the coordinates which describe its “edges”.

Exercise 3.5. For the same unit cell, give the coordinates which describe its “faces”.

Exercise 3.6. Give the coordinates for the planes and lines drawn in the unit cell shown below.



4 Morphology

By the term “morphology”, we refer to the set of faces and edges which enclose a crystal.

4.1 Relationship Between Crystal Structure and Morphology

The abundance of characteristic faces and, at least in ideal circumstances, the regular geometric forms displayed *externally* by crystals result from the fact that *internally*, crystals are built upon a crystal structure. What is, then, the relationship between the crystal structure (the internal structure) and morphology (the external surfaces)? Figure 4.1 shows the crystal structure and the morphology of the mineral galena (PbS). The faces of a crystal are parallel to sets of lattice planes occupied by atoms, while the edges are parallel to lattice lines occupied by atoms. In Fig. 4.1a, these atoms are represented by points. A lattice plane occupied by atoms is not actually flat. This may be seen for the lattice plane (100), (010) or (001) in Fig. 4.1c when the size of the spherical atoms is taken into account, and is even more marked for crystals of molecular com-

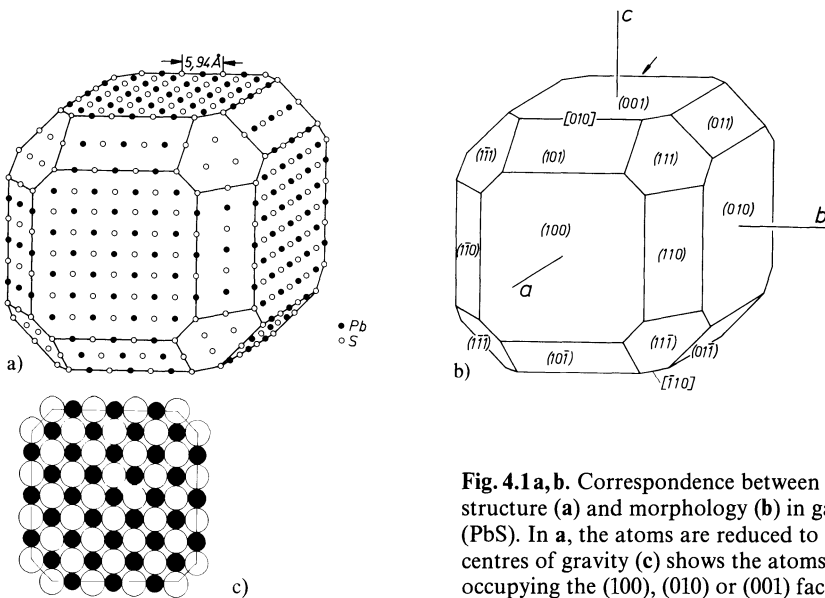


Fig. 4.1 a, b. Correspondence between crystal structure (a) and morphology (b) in galena (PbS). In a, the atoms are reduced to their centres of gravity (c) shows the atoms occupying the (100), (010) or (001) face.

pounds. Atomic radii are very small – of the order of 1 \AA – so crystal faces appear smooth and flat to the eye. A crystal face contains a two-dimensionally periodic array of atoms.

The relationship between crystal structure and morphology may be summarised thus:

- a) *Every crystal face lies parallel to a set of lattice planes; parallel crystal faces correspond to the same set of planes.*
 b) *Every crystal edge is parallel to a set of lattice lines.*

The reverse conclusions must, however, certainly not be drawn, since a crystal will have a very large number of lattice planes and lines, and generally only a few edges and faces.

Furthermore, it should be noted that the shapes in Fig. 4.1 have been drawn to vastly different scales. Suppose the edge of the crystal marked with an arrow is 6 mm in length; then that edge corresponds to some 10^7 lattice translations, since the lattice parameters of galena are all 5.94 \AA .

Since crystal faces lie parallel to lattice planes and crystal edges to lattice lines, Miller indices (hkl) may be used to describe a crystal face, and [uvw] a crystal edge. The morphology of the crystal gives no information about the size of the unit cell, but can in principle give the ratio between one unit cell edge and another. Normally, however, the lattice parameters are known, so the angles between any pair of lattice planes can be calculated and compared with the observed angles between two crystal faces.

The crystal of galena in Fig. 4.1 has been indexed, i.e. the faces have been identified with (hkl). Thus, with the origin chosen suitably inside the crystal, (100) cuts the a-axis and is parallel to b and c; (110) is parallel to c and cuts a and b at the same distance from the origin; (111) cuts a, b and c all at the same distance from the origin.

4.2 Fundamentals of Morphology

Morphology is the study of the external boundary of a crystal, built up of crystal faces and edges. In morphology, the words “form”, “habit” and “zone” have special meanings.

a) **FORM.** The morphology of a crystal is the total collection of faces which characterise a particular crystal. The morphology of the crystals shown in Fig. 4.2 consists of the combination of a hexagonal prism and a “pinacoid”; a pinacoid is a pair of parallel faces which in this case make up the ends of this prism. The prism and the pinacoid are examples of a crystal form, which is further discussed in Chapter 8. In the meantime, we will simply consider *a crystal form as a set of “equal” faces*. It is thus possible to describe the morphology as the set of forms of a crystal.

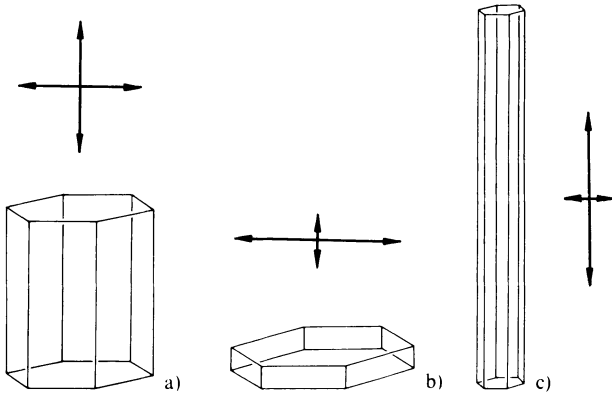


Fig. 4.2a–c. The three basic habits: **a** equant, **b** planar or tabular, **c** prismatic or acicular with the relative rates of growth in different directions shown by *arrows*

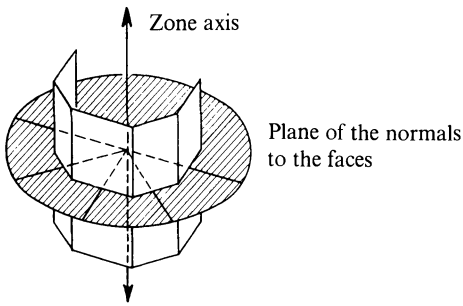


Fig. 4.3. A zone is a set of crystal faces with parallel lines of intersection. The zone axis is perpendicular to the plane of the normals to the intersecting faces, and is thus parallel to their lines of intersection (After [32])

b) HABIT. This term is used to describe the relative sizes of the faces of a crystal. There are three fundamental types of habit: *equant*, *planar or tabular*, and *prismatic or acicular* (needle-shaped). These habits are illustrated in Fig. 4.2 by the relative sizes of the hexagonal prism and the pinacoid.

c) ZONE. The crystals in Figs. 1.1–1.4 show several examples of three or more crystal faces intersecting one another to form parallel edges. *A set of crystal faces whose lines of intersection are parallel is called a zone* (Fig. 4.3). Faces belonging to the same zone are called *tautozonal*. The direction parallel to the lines of intersection is the *zone axis*. Starting from any point inside the crystal, the normals to all the faces in a zone are coplanar, and the zone axis is normal to this plane. Only two faces are required to define a zone.

The galena crystal in Fig. 4.1b shows several zones. For example, the face (100) belongs to the zones $[(101)/10\bar{1}] = [010]$, $[(110)/(1\bar{1}0)] = [001]$, $(111)/(1\bar{1}\bar{1}) = [01\bar{1}]$ and $[(\bar{1}\bar{1}1)/11\bar{1}] = [011]$.

All intersecting faces of a crystal have a zonal relationship with one another. This is evident from consideration of Fig. 4.1b.

The faces or the lattice planes (h_1, k_1, l_1) , (h_2, k_2, l_2) , and (h_3, k_3, l_3) , are tautozonal if and only if

$$\begin{vmatrix} h_1 k_1 l_1 \\ h_2 k_2 l_2 \\ h_3 k_3 l_3 \end{vmatrix} = 0$$

i.e. $h_1 k_2 l_3 + k_1 l_2 h_3 + l_1 h_2 k_3 - h_3 k_2 l_1 - k_3 l_2 h_1 - l_3 h_2 k_1 = 0$.

Do the planes (hkl) belong to the zone [uvw]? The answer depends on whether or not the zonal equation $hu + kv + lw = 0$ is fulfilled. For example, $(\bar{1}\bar{1}2)$ does lie in the zone $[\bar{1}11]$ since $1 \cdot (-1) + (-1) \cdot 1 + 2 \cdot 1 = 0$.

4.3 Crystal Growth

It is easier to understand the morphology of a crystal if the formation and growth of crystals is considered. Crystals grow from, among other things, supersaturated solutions, supercooled melts and vapours. The formation of a crystal may be considered in two steps.

1. NUCLEATION. This is the coming together of a few atoms to form a three-dimensional periodic array – the nucleus – which already shows faces, although it is only a few unit cells in size (see Fig. 4.4a).

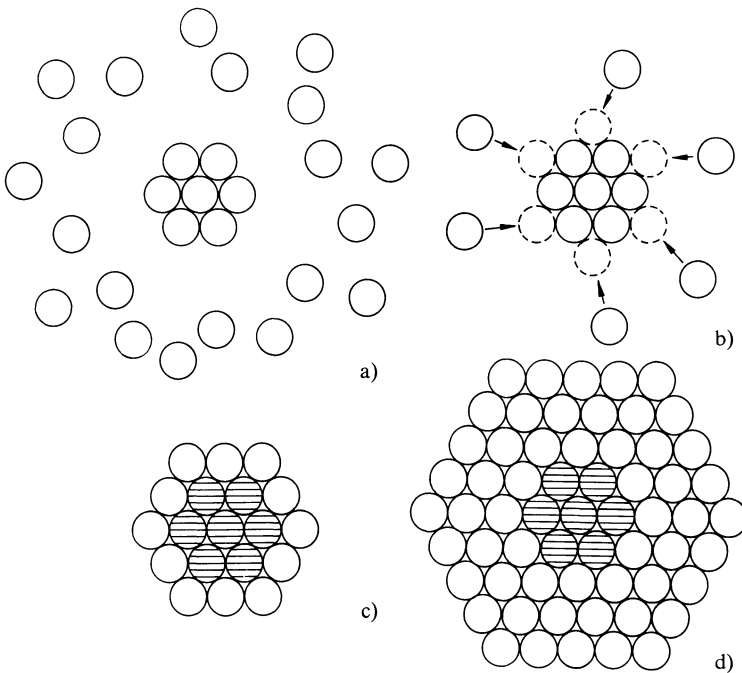


Fig. 4.4a–d. Nucleation and growth of the nucleus to a macrocrystal illustrated in two dimensions. **a** Nucleus, e.g. in a melt. **b** Atoms adhere to the nucleus. **c** Growth of a new layer on the faces of a nucleus. **d** The formation of a macrocrystal by the addition of further layers of atoms

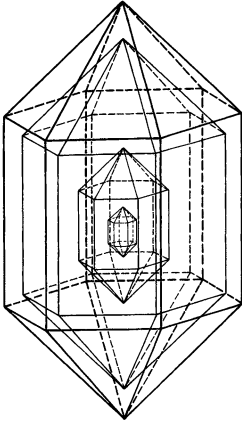


Fig. 4.5. Quartz crystal showing its stepwise growth

2. GROWTH OF A NUCLEUS TO A CRYSTAL. As the nucleus attracts further atoms, they take up positions on its faces in accordance with its three-dimensional periodicity. In this way, new lattice planes are formed (Fig. 4.4b–d). Note that the illustration is two-dimensional only. The growth of the nucleus, and then of the crystal, is characterised by a parallel displacement of its faces. *The rate of this displacement* is called the *rate of crystal growth*, and is a characteristic, anisotropic property of a crystal.

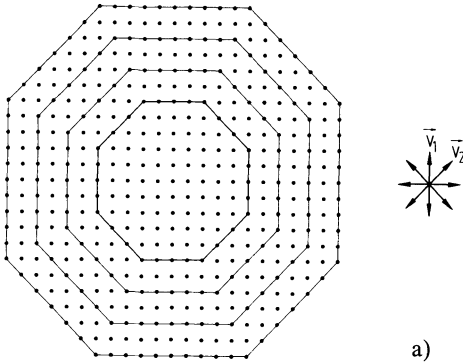
Figure 4.5 shows a few stages in the growth of a quartz crystal.

The nucleus shown in Fig. 4.6 is bounded by two different types of faces, and the rates of growth of these faces, v_1 and v_2 are thus, in principle, distinguishable. Figure 4.6a illustrates the case in which these rates of growth are similar, while in Fig. 4.6b, they are very different. A consequence of this difference is that the faces corresponding to the slow growth rate become steadily larger, while those corresponding to rapid growth disappear entirely. In addition, it should also be noted that crystal growth rates are affected by temperature, pressure, and degree of saturation of the solution. The actual crystal faces which eventually enclose the crystal depend on the ratios of the growth rates of the various faces, the slower-growing ones becoming more prominent than those that grow more rapidly. Those faces which do eventually develop generally have low Miller indices and are often densely populated with atoms.

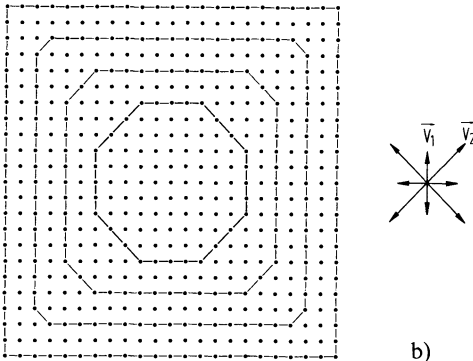
The three basic types of crystal habit may be understood in terms of the relative growth rates of the prism and pinacoid faces, which are indicated in Fig. 4.2 by arrows.

Figure 4.7 shows how crystals of different shapes can result from the same nucleus. Crystal I is regular in shape, while crystals II and III have become very much distorted as a result of external influences on the growth rate. None the less, the angles between the normals to the crystal faces remain constant, since the growing faces have simply been displaced along their normals. A parallel displacement of the faces cannot change interfacial angles. This observation applies equally to all growing faces of a crystal.

This observation is the basis of the *law of constancy of the angle*: *in different specimens of the same crystal, the angles between corresponding faces will be*



a)



b)

Fig. 4.6 a, b. Crystal growth showing a small (a) and a large (b) difference in growth rate with direction

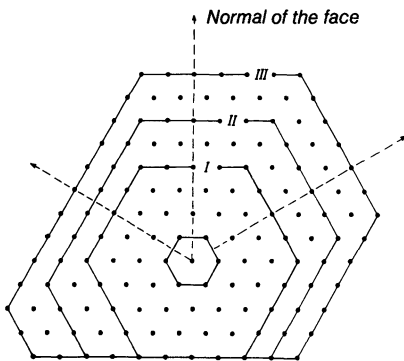


Fig. 4.7. Despite difference in rates of growth of different parts of a crystal, the angles between corresponding faces remain equal

equal. This law, which is valid at constant temperature and pressure, was first formulated by *N. Steno* in 1669, without any knowledge of crystal lattices!

The relative positions of the normals to the faces of the crystals in Fig. 4.7 remain constant. It is possible, by measurement of the angles between faces, to determine these relative positions and thus eliminate the distortion.

So far, our discussion has assumed the existence of a single crystal nucleus, or only a few, which can grow separately into single crystals like those shown in

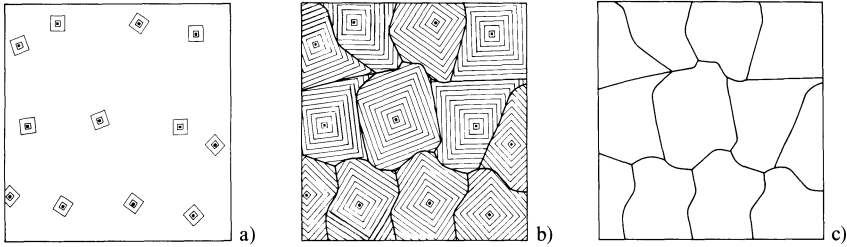


Fig. 4.8a–c. Development of a crystal aggregate. **a** Formation of several nuclei, which initially can grow independently. **b** Collision of growing crystallites leads to interference and irregularity in growth of the polyhedra. Eventually, the polyhedral shape of the crystallites is entirely lost. **c** The single crystal domains of the aggregate with their grain boundaries

Fig. 1.1. The term *single crystal*, as it is used here, implies one which has grown as such. It will normally display characteristic faces, but those grown in the laboratory often do not. If many nuclei are formed simultaneously, they may grow into one another in a random fashion, as illustrated in Fig. 4.8. This disturbance will prevent the development of crystal faces and forms. Instead, a *crystal aggregate* or polycrystal results. Figure 4.8 shows an example of single phases in the development of such an aggregate. The individual crystallites of an aggregate are themselves single crystals.

4.4 The Stereographic Projection

Since crystals are three-dimensional objects, it is necessary to use projections in order to work with them on a flat surface. One such projection is the parallel projection onto a plane, which was illustrated in Fig. 3.4c for representing a crystal structure.

For morphological studies, the stereographic projection has proved to be particularly useful. The principle of this projection is shown in Fig. 4.9. A crystal, in this case galena (PbS), is placed at the centre of a sphere. The normals to each face, if drawn from the centre of the sphere, will then cut the surface of the sphere in the indicated points, the *poles of the faces*. The angle between two poles is taken to mean the *angle between the normals* n , not the dihedral angle f between the faces. These two angles are simply related as: angle of normals $n = 180^\circ - \text{dihedral angle } f$ (Fig. 4.12). The poles are not randomly distributed over the surface of the sphere. In general they will lie on a few *great circles*, i.e. circles whose radius is that of the sphere. Those faces whose poles lie on a single great circle will belong to a single *zone*. The zone axis will lie perpendicular to the plane of the great circle. Considering the sphere as a terrestrial globe, a line from each of the poles in the northern hemisphere is projected to the south pole, and its intersection with the plane of the equator is marked with a point \bullet or a cross $+$ (see Fig. 4.10). Lines from poles in the southern hemisphere are similarly projected to the north pole, and their intersections with the equatorial plane are marked with an open circle \circ . For those poles lying exactly on the equator, a

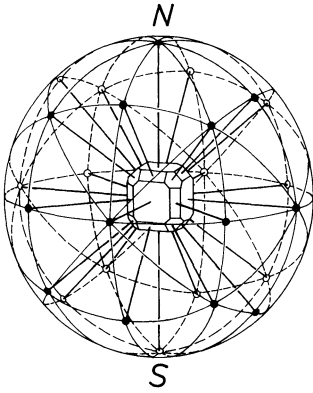


Fig. 4.9

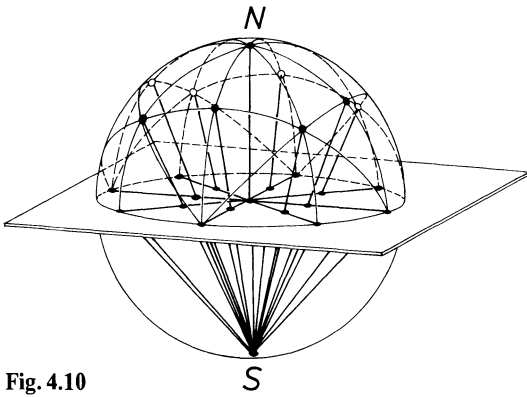


Fig. 4.10

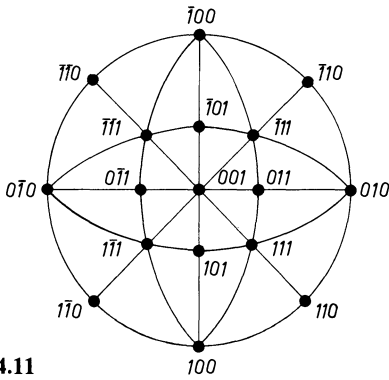


Fig. 4.11

Fig. 4.9. Crystal of galena at the centre of a sphere. The normals to the faces of the crystal cut the sphere at their poles, which lie on great circles

Fig. 4.10. In a stereographic projection, lines are drawn between the poles of the faces in the northern hemisphere and the south pole, and the intersection of these lines with the equatorial plane is recorded

Fig. 4.11. Stereographic projection of the crystal in Fig. 4.9; see also Fig. 4.1b

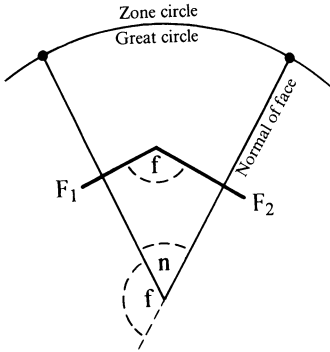


Fig. 4.12. Relationship between the angle of intersection of the normals (n) and the dihedral angle (f) between the faces F_1 and F_2 . The poles of the faces lie on a great circle, the zone circle

point or cross is used. The mathematical relationships of the stereographic projection are shown in Fig. 4.33.

Figure 4.11 shows the stereogram of the crystal in Fig. 4.9, only those planes belonging to the northern hemisphere being shown. Poles belonging to a single zone lie on the projections of the relevant great circles. The points resulting from the projections of each face are indexed.

Figure 4.13a shows the stereographic projection of a tetragonal prism and a pinacoid, while Fig. 4.13b gives that of a tetragonal pyramid and a *pedion*. A

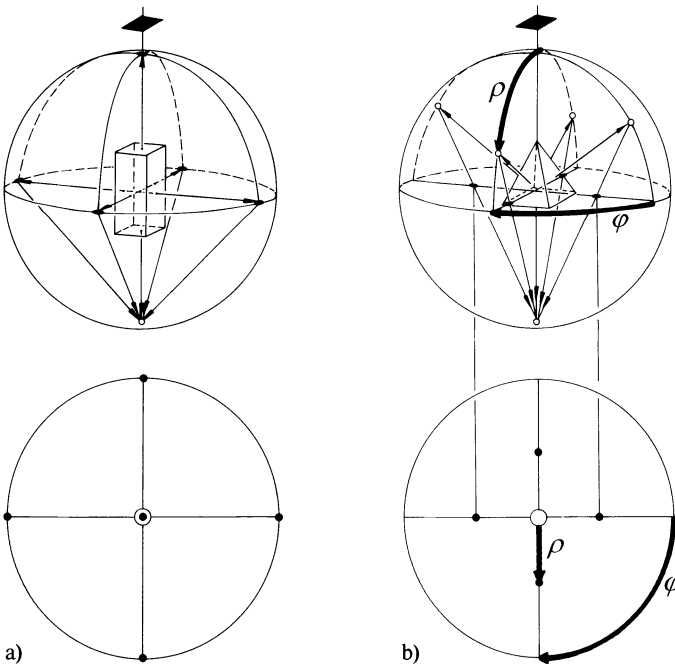


Fig. 4.13a, b. Stereographic projection of a tetragonal prism and a pinacoid (a) and of a tetragonal pyramid and a *pedion* (b). The angular coordinates φ and ρ are given for one of the pyramid faces

pedion is the name given to a crystal form which consists of a single face. In both cases, the altitude of the prism or pyramid is set in the N-S direction. Both the tetragonal prism and the tetragonal pyramid have square bases and square cross-sections. The faces of the prism are perpendicular to the plane of the stereographic projection, so their poles lie on the circumference of the circle of that projection. The faces of the pyramid make equal angles with the equatorial plane, so the poles of these faces are at equal distances from the centre of the plane of projection.

The representation of the stereographic projection in Fig. 4.9–11 is only intended to explain the principles of the method. In practice, the projection is based on the values of measured angles.

The stereographic projection is also very useful for the description of the point groups. In this case, there is a departure from the normal convention of plotting the stereogram. For rotation axes and rotoinversion axes, the symbols of these axes are used to indicate their intersection with the surface of the sphere of projection. Similarly, for mirror planes, the corresponding great circle of intersection is indicated (for an example, see Fig. 6.8e).

4.5 The Reflecting Goniometer

The angles between crystal faces may conveniently be measured with a *reflecting goniometer*. The crystal is mounted on a goniometer table, which is essentially a rotating plate with a graduated angle scale (see Fig. 4.14). The crystal mount (or goniometer head) is a construction of arcs and slides which makes it possible to bring a zone axis of the crystal into coincidence with the rotation axis of the goniometer table. The crystal is then rotated until the light beam from a lamp mounted horizontally is reflected from a crystal face onto the cross-hairs of a telescope, also mounted horizontally. The reading on the scale of the table then fixes the position of that crystal face. The table is then rotated until another face comes into the reflecting position, and the angular reading for this position is

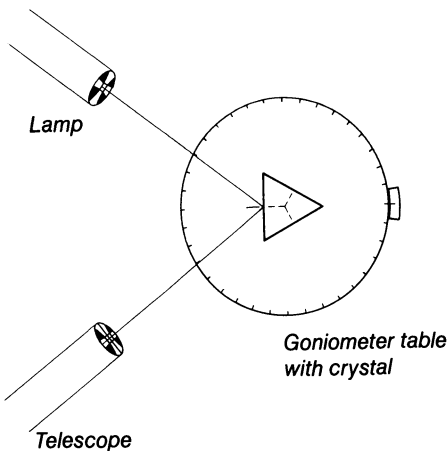


Fig. 4.14. Light path for a one-circle reflecting goniometer

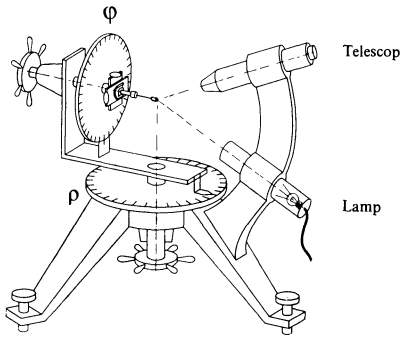


Fig. 4.15. Two-circle reflection goniometer with azimuthal circle ϕ and pole distance circle ρ (After [22])

taken. The difference between the two readings is the angle between the normals to the crystal faces. Continuing to rotate the table through 360° will allow the angles corresponding to the selected zone to be measured. This is the principle of the one-circle reflection goniometer. For the measurement of the angles corresponding to other zones on a one-circle reflecting goniometer, the crystal must be remounted.

A two-circle reflection goniometer makes it possible to rotate and measure the crystal about two mutually perpendicular axes (Fig. 4.15). In this way, all possible faces can be brought into the reflecting position. From the position of the two circles, the angular coordinates ϕ and ρ may be measured. These coordinates uniquely define the orientation of a crystal face, and the values can be directly plotted on a stereographic projection.

4.6 The Wulff Net

The Wulff net is a device to enable measured crystal angles to be plotted readily as a stereographic projection. The *Wulff net* is itself the stereographic projection of the grid of a conventional globe orientated so that the $N'-S'$ direction lies in the plane of projection (Fig. 4.16). The N-S direction of the stereographic

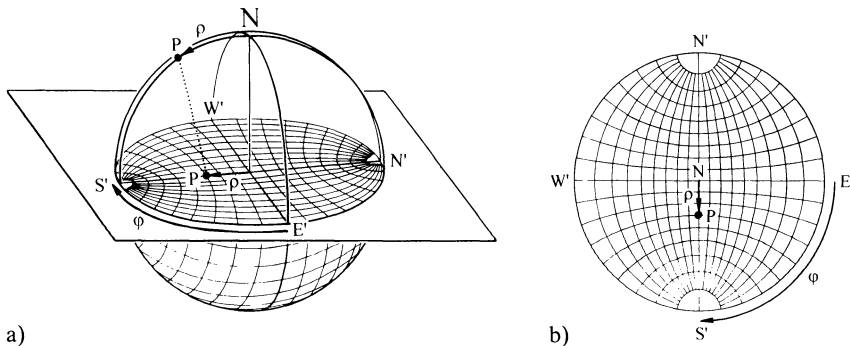


Fig. 4.16 a, b. The stereographic projection of the grid net of a globe ($N'-S' \perp N-S$) produces the Wulff net; the positions of the angular coordinates ϕ (the azimuthal angle) and ρ (the pole distance) are indicated. The pole P has coordinates $\phi = 90^\circ$ and $\rho = 30^\circ$

projection (Fig. 4.9) is thus perpendicular to the N'-S' direction both of the grid net of the globe and of the Wulff net (Fig. 4.16). Fig. 4.16a shows the grid of only one hemisphere. The equator and all meridians of the globe are great circles, while all of the parallels except the equator are small circles. With the help of the Wulff net, the angle between any two poles on the surface of the sphere can now be plotted directly on the stereographic projection. The angle measured between any two crystal faces is the angle between their normals or the angle between their poles. The two normals define the plane of a great circle (Fig. 4.9). The arc of the great circle between the two normals is the measured angular value. It is thus crucial that only arcs of great circles are used when angles are plotted on or estimated from a stereographic projection!

We shall now demonstrate the use of the Wulff net to plot the two angles measured with a two-circle goniometer (the azimuthal angle ϕ and the pole distance ρ) on a stereographic projection. The circle of the plane of projection is taken as the azimuth ϕ , so possible ϕ -values run from 0–360°. The front face of the tetragonal pyramid in Fig. 4.13b thus has a ϕ -value of 90°. The ρ -axis is perpendicular to the ϕ -axis. The faces of the tetragonal pyramid have ϕ -coordinates of 0°, 90°, 180° and 270° respectively and all faces have the same ρ -value.

A similar consideration of a tetragonal dipyrmaid, e.g. no. 6 in Exercise 4.4 results in the following angular coordinates (ϕ , ρ) for the eight faces: 0°, ρ ; 90°, ρ ; 180°, ρ ; 270°, ρ and 0°, $-\rho$; 90°, $-\rho$; 180°, $-\rho$; 270°, $-\rho$. Note that faces in the northern hemisphere are assigned values $0 \leq \rho \leq 90^\circ$, while those in the southern hemisphere have $-90^\circ \leq \rho \leq 0^\circ$ where both 90 and -90° represent positions on the equator. For an example, see the table of ϕ , ρ -values for the galena crystal in Exercise 4.13.

For practice, a Wulff net with a diameter of 20 cm and a 2°-grid is bound inside the rear cover. For best results, this should be carefully removed and pasted on a card with a minimum thickness of 1 mm. Drawings are then made on tracing paper secured by a pin at the centre of the net so as to be readily rotated.

The stereographic projection has two important properties:

1) The projections of two vectors onto the sphere intersect with the same angle as do the vectors themselves. The parallels and the meridians of the global net are mutually perpendicular. Since the Wulff net is the projection of these circles, the corresponding great and small circles of the Wulff net are perpendicular to one another, cf. Fig. 4.16.

2) All circles, great and small, on the sphere will project as circles on the equatorial plane (Fig. 4.17). Exceptionally, the meridians, which are parallel to the N-S-direction, will project as straight lines. This property has several consequences. For example, consider a circle with a radius of 30° on the surface of the sphere. Select a general point on the Wulff net, place the pole M there, and construct the locus of all points that are 30° from it. By rotating the tracing paper, the poles lying 30° from M on each of the great circles will be found (Fig. 4.18). These poles will indeed be found to lie on the circumference of a

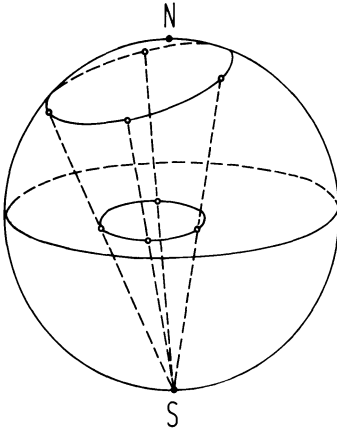


Fig. 4.17. A circle on the surface of a sphere remains a circle in its stereographic projection on the equatorial plane

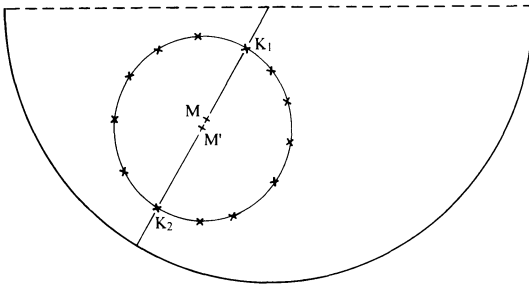


Fig. 4.18. Detail of the equatorial plane of a stereographic projection. Points 30° from a pole M are shown. These poles lie on the circumference of a circle, whose centre M' may be found by bisecting the diameter K_1K_2

circle. However, M is not at the center of this circle. The actual center M' may be found by bisecting the diameter K_1K_2 .

The following examples illustrate the principles of the stereographic projection and the use of the Wulff net.

1) Given the two poles 1 and 2, determine the angle between them: Place the tracing paper over the Wulff net and rotate it until both poles lie on a great circle, the zone circle (cf. Fig. 4.19a). The value of the angle can then be read from the great circle. If one of the poles lies in the southern hemisphere, it must be treated appropriately (cf. Fig. 4.19b).

2) Two faces define a zone. Their line of intersection is the zone axis, which is normal to the plane defined by the normals to the faces. (cf. Fig. 4.3). The zone circle is perpendicular to the pole of the zone axis.

a) Draw the pole corresponding to a zone circle: Rotate the zone circle onto a great circle of the Wulff net; the zone pole will then be 90° from the zone circle along the equator (cf. Fig. 4.20).

b) Draw the zone circle corresponding to a given zone pole: Rotate the pole onto the equator of the Wulff net. The zone circle is then the meridian 90° away from the pole (cf. fig. 4.20).

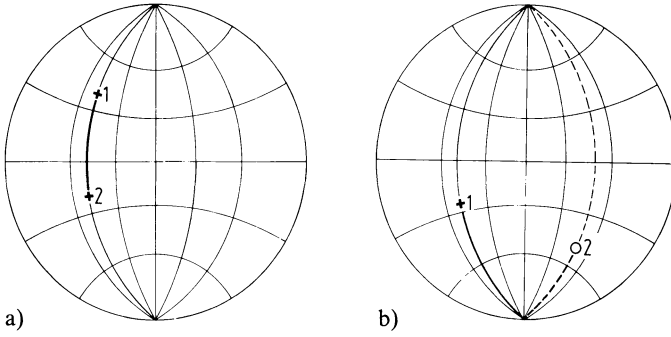


Fig. 4.19 a, b. The angle between two poles may be read from the great circle on which they both lie

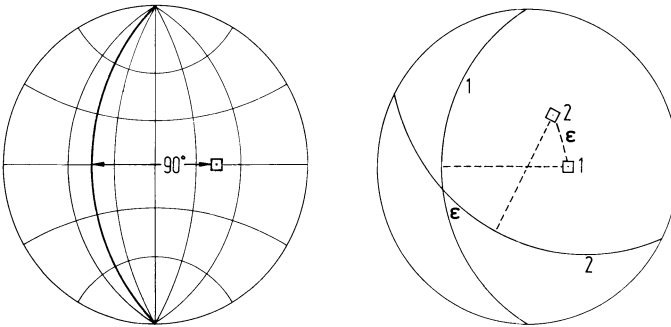


Fig. 4.20

Fig. 4.21

Fig. 4.20. The zone circle and the zone pole (□) are mutually perpendicular

Fig. 4.21. The angle ϵ between the planes of two zone-circles is the angle between the poles of the corresponding zones (□)

3) The angle ϵ between the planes of two zone-circles is the angle between the poles of the corresponding zones (cf. Fig. 4.21).

4) Find the pole 3, which is separated from pole 1 by an angle α and from pole 2 by an angle ω : This will lie at the intersections of the two circles with the given radii. Note that the centers and the radii of the circles must first be specified. The center of the α circle is the midpoint of the diameter $K_1 K_2$ (cf. Fig. 4.18); the center of the ω -circle is found by constructing the perpendicular bisector of a chord. Note that there are two solutions to this problem (cf. Fig. 4.22).

5) Change the plane of projection of a stereographic projection: An octahedron is a crystal form consisting of eight equilateral triangular faces (Fig. 4.23a). Fig. 4.23c gives the stereographic projection of this octahedron. The poles of the faces are marked with a cross; those lying in the southern hemisphere are not shown. The stereogram is now to be altered, so that the pole of one of the

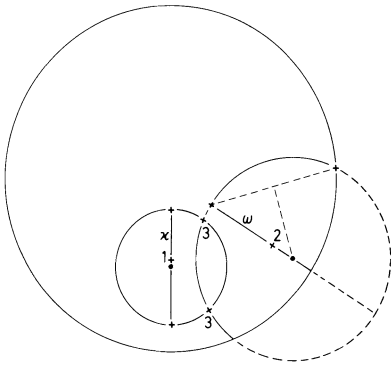


Fig. 4.22. Construction of the two poles 3, which make an angle α with pole 1, and an angle ω with pole 2

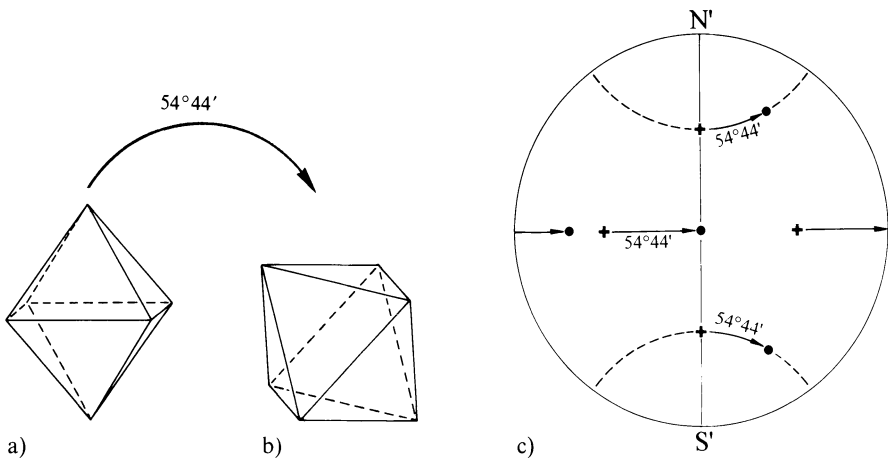


Fig. 4.23 a, b, c. The octahedron in (a) is rotated into the position in (b). This rotation is shown in the stereogram in (c). The crosses in the stereogram correspond to the faces in (a), the points to the faces in (b). The poles move along small circles

octahedral faces is moved to the centre of the plane of projection. This may be done by rotating one of the poles onto the equatorial plane of the Wulff net. The pole will lie on the equator at $54^{\circ}44'$ from its center. Rotating the pole about the $N'-S'$ axis of the net by $54^{\circ}44'$ then brings it to the centre of the projection. The other poles move along their own *small circles* by an angle of $54^{\circ}44'$. The new positions of the poles of the faces, which are shown by points in Fig. 4.23c, correspond to the orientation of the octahedron in Fig. 4.23b, which sits on a face.

4.7 Indexing of a Crystal

Today, it is rarely necessary to index a crystal whose lattice constants are unknown. In general, lattice constants give no indication of which faces of a crystal will actually be prominent, but it is possible to produce a stereogram

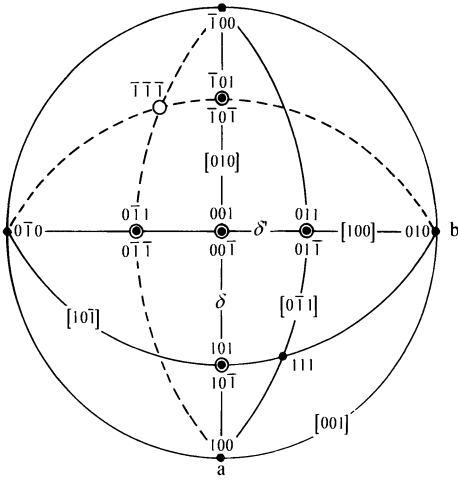


Fig. 4.24. Stereogram of the poles of a few of the faces of a topaz crystal allowed by the lattice which have low indices

showing all the poles representing faces that are possible for that lattice. Since crystals usually develop faces with low Miller indices, the number of poles which must be drawn is small.

We shall now draw the stereogram of the poles of a crystal of topaz. The lattice parameters are $a_0 = 4.65$, $b_0 = 8.80$, $c_0 = 8.40 \text{ \AA}$, $\alpha = \beta = \gamma = 90^\circ$. The six faces (100) , $(\bar{1}00)$, (010) , $(0\bar{1}0)$, (001) , $(00\bar{1})$ which are normal to the crystallographic axes can be entered immediately into the stereogram (Fig. 4.24). These faces lie on the following zone-circles: $[100] \equiv [(001)/(010)]$, $[010] \equiv [(100)/(001)]$, $[001] \equiv [(100)/(010)]$. The zone axis is normal to the plane of the zone-circle, and is parallel to the set of lattice lines which are common to the lattice planes making up the zone.

Figure 4.25 shows a (010) -section through the crystal lattice with the traces of the planes (100) , (101) , and (001) , which belong to the $[010]$ -zone. The

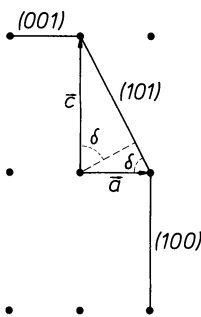


Fig. 4.25

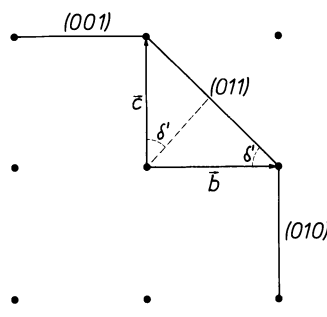


Fig. 4.26

Fig. 4.25. Section parallel to (010) through the lattice of a topaz crystal, showing the traces of the planes (001) , (101) and (100) , all of which belong to the zone $[010]$. δ is the angle between the normals to (001) and (101)

Fig. 4.26. Section parallel to (100) through the lattice of a topaz crystal, showing the traces of the planes (001) , (011) and (010) , all of which belong to the zone $[100]$. δ' is the angle between the normals to (001) and (011)

angle δ is the angle between the normals to (001) and (101). Since $\tan \delta = \frac{c_0}{a_0}$, $\delta = 61.03^\circ$. Similarly, Fig. 4.26, showing the (100)-section of the same lattice, gives the angle between the normals to (001) and (011). In this case, $\tan \delta' = \frac{c_0}{b_0}$, and $\delta' = 43.67^\circ$. With the help of the Wulff net, the angles δ and δ' can be placed on the great circles corresponding to the zones [010] and [100] respectively, giving the positions of the poles of the planes (101) and (011). Since the planes $(\bar{1}01)$, $(1\bar{0}\bar{1})$ and $(\bar{1}\bar{0}\bar{1})$ have the same inclination to the crystallographic axes as (101), while $(0\bar{1}\bar{1})$, $(01\bar{1})$ and $(0\bar{1}\bar{1})$ have that of (011), they may likewise be entered on the stereogram (Fig. 4.24).

The great circles for the zones [(100)/(011)] and [(101)/(010)] may now be drawn in, and the two intersections of these circles will occur at the poles with Miller indices (111) and $(\bar{1}\bar{1}\bar{1})$. These traces of zone-circles lying in the southern hemisphere are given as dashed lines.¹

The drawing in of the circles for further zones gives the poles for further faces. From these, the poles can be located for all faces with the same axial inclination as (111), viz. $(\bar{1}11)$, $(1\bar{1}1)$, $(\bar{1}\bar{1}1)$, $(11\bar{1})$, $(\bar{1}1\bar{1})$, $(1\bar{1}\bar{1})$ and $(\bar{1}\bar{1}\bar{1})$. For further faces, the zonal equation is used. Eventually, a stereogram, like that in Fig. 4.27 may be produced showing the poles for all faces (hkl) with $2 \leq h, k \leq 2$ and $0 \leq l \leq 2$.

An actual topaz crystal is shown in Fig. 4.28. Once such a crystal has been indexed with the aid of a stereogram, it is only necessary to measure a few angles on the actual crystal in order to bring the angles of the crystal into correspondence with the angles in the stereogram.

The indexing of the stereogram in Fig. 4.27 may be accomplished very easily using the complication rule, formulated by V. Goldschmidt. This rule allows all of the faces of a zone to be indexed by addition or subtraction of the indices of two standard faces. The application of this rule is shown in Fig. 4.29. Let the starting faces be (100) and (010). Addition of (100) + (010) gives (110); (010) + (110) gives (120); (110) + (120) gives (230), etc. It should be clear that subtraction will in the end lead to similar results. All of the calculated planes belong to the zone [001].

In Fig. 4.30, two zone circles are shown, each having two indexed poles on it. The complication rule may be used to index the pole at the point of intersection. In zone 1, (011) + $(1\bar{1}0)$ gives (101), while in zone 2, $(0\bar{1}0)$ + (211) gives (201). These poles lie between their generating poles. The problem is solved when further

¹ Application of the zonal equation leads to

$$\begin{array}{c|c|c|c|c} 1 & 0 & 0 & 1 & 0 \\ 0 & 1 & 1 & 0 & 1 \end{array} \quad \begin{array}{c|c} 0 & 0 \\ 1 & 1 \end{array} \quad \begin{array}{c|c|c|c|c} 1 & 0 & 0 & 1 & 0 \\ 0 & 1 & 1 & 0 & 1 \end{array} \quad \begin{array}{c} 0 \\ 1 \end{array} \quad \text{and} \quad \begin{array}{c|c|c|c|c} 1 & \bar{1} & 1 & 0 & \bar{1} \\ 0 & 0 & \bar{1} & 1 & 0 \end{array} \quad \begin{array}{c} 1 \\ \bar{1} \end{array}$$

$$\begin{array}{c} [0 \ \bar{1} \ 1] \end{array} \quad \begin{array}{c} [1 \ 0 \ \bar{1}] \end{array} \quad \begin{array}{c} (1 \ 1 \ 1) \end{array}$$

If the values of [uvw] are interchanged, the result is $(\bar{1}\bar{1}\bar{1})$. Two zone circles intersect in *two* poles. In morphology, (hkl) and $(\bar{h}\bar{k}\bar{l})$ represent *two* parallel faces, which are related to only *one* set of lattice planes, which may be designated as (hkl) or $(\bar{h}\bar{k}\bar{l})$.

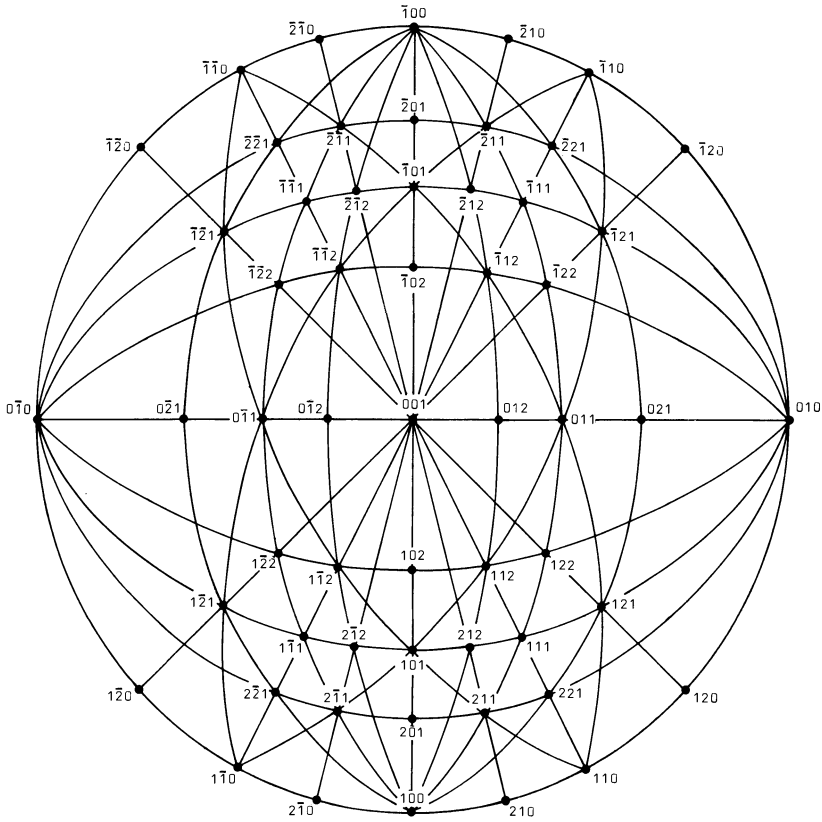


Fig. 4.27. Stereogram of the poles of those faces of a topaz crystal allowed by the lattice which have indices ($2 \leq h, k \leq 2; 0 \leq l \leq 2$)

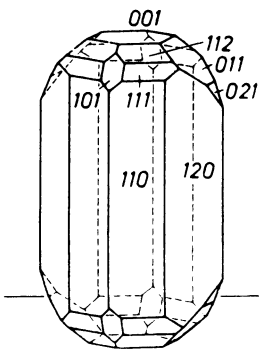


Fig. 4.28. Topaz crystal. (After [37])

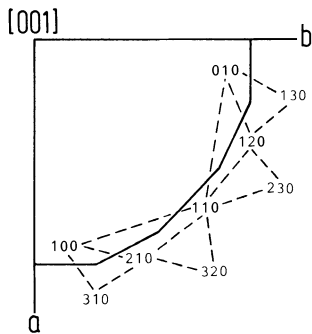


Fig. 4.29. Complication of the faces (100) and (010)

addition, or to be more precise subtraction, leads to a common point. In this case, from zone 1: $(1\bar{1}0) + (101)$ gives $(2\bar{1}1)$; while from zone 2, $(201) + (0\bar{1}0)$ gives $(2\bar{1}1)$, so the pole corresponding to the intersection has been indexed. This example is taken from Fig. 4.27. Note the relative positions of (101) and (201).

faces are to be indexed without reference to lattice constants. The crystallographic axes have been chosen to be parallel to the main zone axes of the stereographic projection. The faces normal to *a*, *b* and *c* can then be indexed directly. Since only (001) and (00 $\bar{1}$) actually appear in the crystal, the positions of (100), ($\bar{1}00$), (010) and (0 $\bar{1}0$) have been added as auxiliary poles, and represented by open circles. One plane must then be chosen as the unit face (111), which cuts each crystallographic axes *a*, *b*, *c*, at unit length. These unit lengths give the relative spacings at which the unit face cuts the crystallographic axes, *a*, *b*, *c*. They are calculated below. The only faces that can be considered for this purpose are 5 and 6, as only they cut *a*, *b* and *c* all in a positive sense. It is reasonable to choose face 6 as the unit face, as the zone circles including this pole contain more poles than those cutting 5. It is now possible to index faces making equal intercepts on *a*, *b* and *c*, viz. (111), ($\bar{1}11$), ($1\bar{1}1$) and ($\bar{1}\bar{1}1$), together with those having poles in the southern hemisphere, ($11\bar{1}$), ($\bar{1}1\bar{1}$), ($1\bar{1}\bar{1}$) and ($\bar{1}\bar{1}\bar{1}$). These last have not been included in the stereogram, nor have any others in the southern hemisphere, i.e. those with negative ρ . Using the complication rule, it is now possible to index the following faces and their equivalents:

$$\begin{aligned} (101) &= (100) + (001) = (111) + (1\bar{1}1), \\ (011) &= (010) + (001) = (111) + (\bar{1}11), \\ (110) &= (100) + (010) = (111) + (11\bar{1}). \end{aligned}$$

The remaining faces are then:

$$\begin{aligned} 5: (111) + (001) &= (101) + (011) = (112) \\ 3: (010) + (011) &= (111) + (\bar{1}10) = (021) \\ 4: (110) + (010) &= (111) - (0\bar{1}1) = (120) \end{aligned}$$

The crystal is now fully indexed, and is, in fact, the topaz crystal shown in Fig. 4.28.

The morphological axial ratios *a*:*b*:*c*, normally given as $\frac{a}{b} : 1 : \frac{c}{b}$, are characteristic of a crystal. The values for topaz can now be calculated: The (110) face cuts *a* and *b* at unit length (Fig. 4.32). The angle δ'' is the angle between (110) and (100), and from table 4.1 (7), it is $90^\circ - 62^\circ 08' = 27^\circ 52'$. Thus $\frac{a}{b} = \tan(27^\circ 52') = 0.529$. From Fig. 4.26, δ' is the angle between (011) and

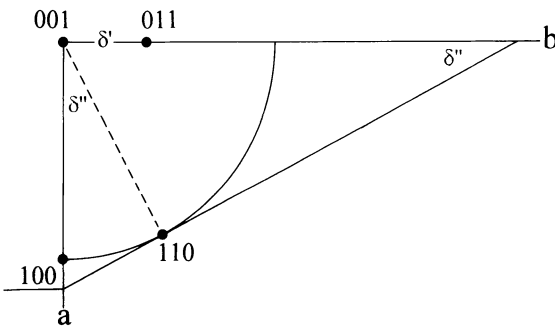


Fig. 4.32. The all-positive octant of the topaz stereogram from Fig. 4.31 with the constructed trace of the (110) face

(001), and from Tab. 4.1 (2), $\delta' = 43^\circ 39'$. Hence, $\frac{c}{b} = \tan(43^\circ 39') = 0.954$, and the normalized morphological axial ratios may be given as $\frac{a}{b} : 1 : \frac{c}{b} = 0.529 : 1 : 0.954$. The numbers 0.529, 1 and 0.954 give the relative spacings (unit lengths) at which the unit face cuts the crystallographic axes a , b and c .

Today, it is usual to formulate the structural axial ratio in terms of the lattice constants; for topaz $\frac{a_0}{b_0} : 1 : \frac{c_0}{b_0} = 0.528 : 1 : 0.955$ (cf. p. 42).

4.8 The Gnomonic and Orthographic Projections

In addition to the stereographic projection, mention should be made of the gnomonic and orthographic projections.

a) The gnomonic projection:

As in the stereographic projection, the crystal is considered to lie at the center of a sphere. The normals to the faces produce points P_G on a plane of projection, which is tangential to the sphere at the north pole (Fig. 4.33). The poles corresponding to the faces of a zone lie in straight lines on the projection plane. Fig. 4.34 shows a gnomonic projection of the galena crystal in Fig. 4.9. As ρ approaches 90° , the distances $N - P_G$ approach infinity. The poles of those faces with $\rho = 90^\circ$ are represented in the projection by arrows. The distance $N - P_G$ is $R \cdot \tan \rho$.

b) The orthographic projection:

As in the stereographic projection, the crystal is again considered to lie at the center of a sphere. In distinction to the stereographic projection, the

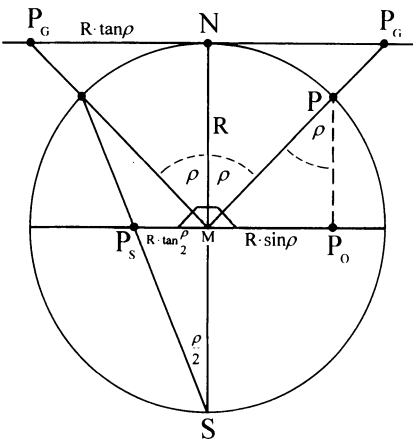
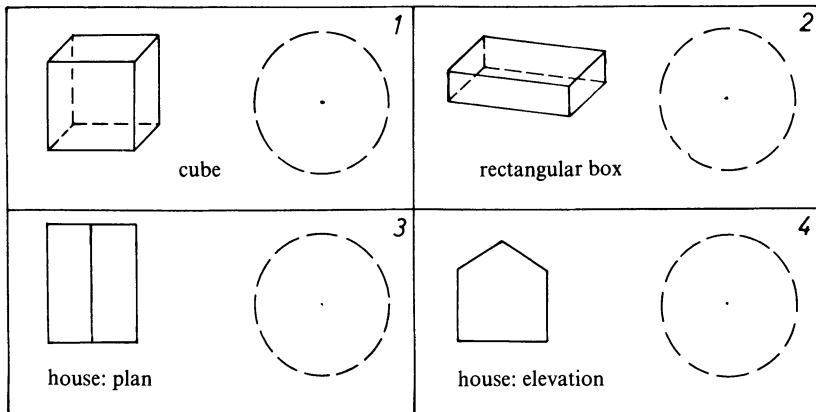


Fig. 4.33. The relationship of the stereographic, gnomonic and orthographic projections

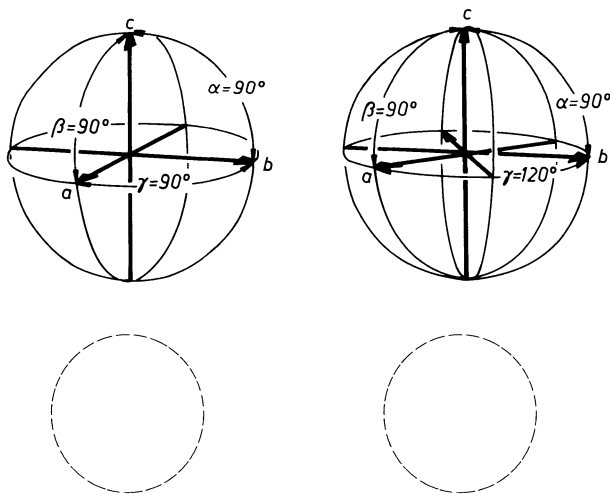
EXERCISES

Exercise 4.1. With the help of the pattern in Fig. 4.36, build a model of the galena crystal shown in Figs. 4.1 b and 4.9. Make a photocopy of the pattern, cut it out, and lightly score all the remaining lines. Fold away from you along the lines and stick sufficient neighbouring faces together with transparent tape to hold the model together.

Exercise 4.2. Plot the poles of the faces of the following objects on a stereogram.



Exercise 4.3. Plot the directions corresponding to the following axial systems on a stereogram.



1. Orthogonal axial system
(cubic, tetragonal,
orthorhombic)

2. Hexagonal axial system

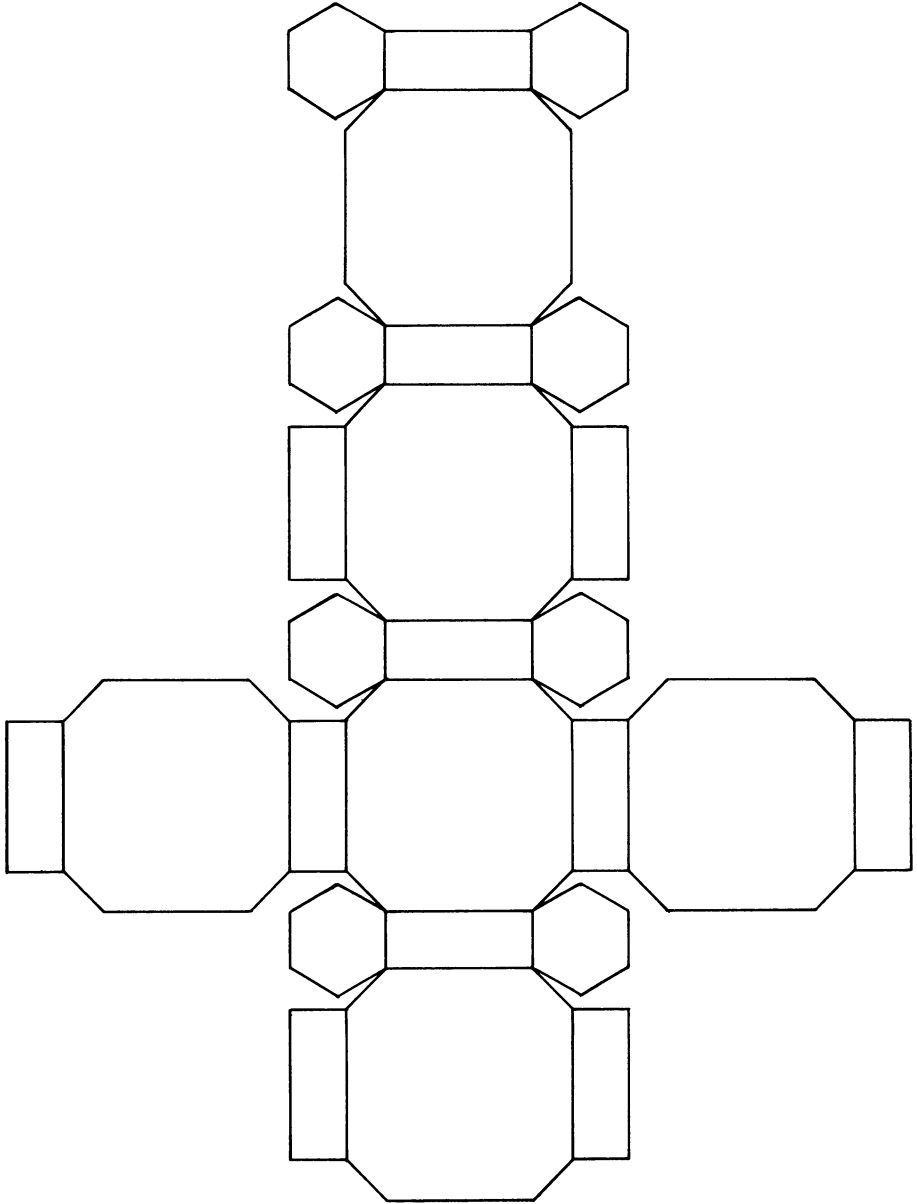


Fig. 4.36. Pattern for a model of a galena (PbS) crystal

Exercise 4.4. Photocopy and cut out the following patterns, which may be made into models of (a) a rhombic dipyramid, (b) a tetragonal pyramid with a pedion and (c) a hexagonal prism with a pinacoid (Fig. 4.37). With a little imagination, you can make similar models of the crystals in the following diagram (p. 52 and 53).

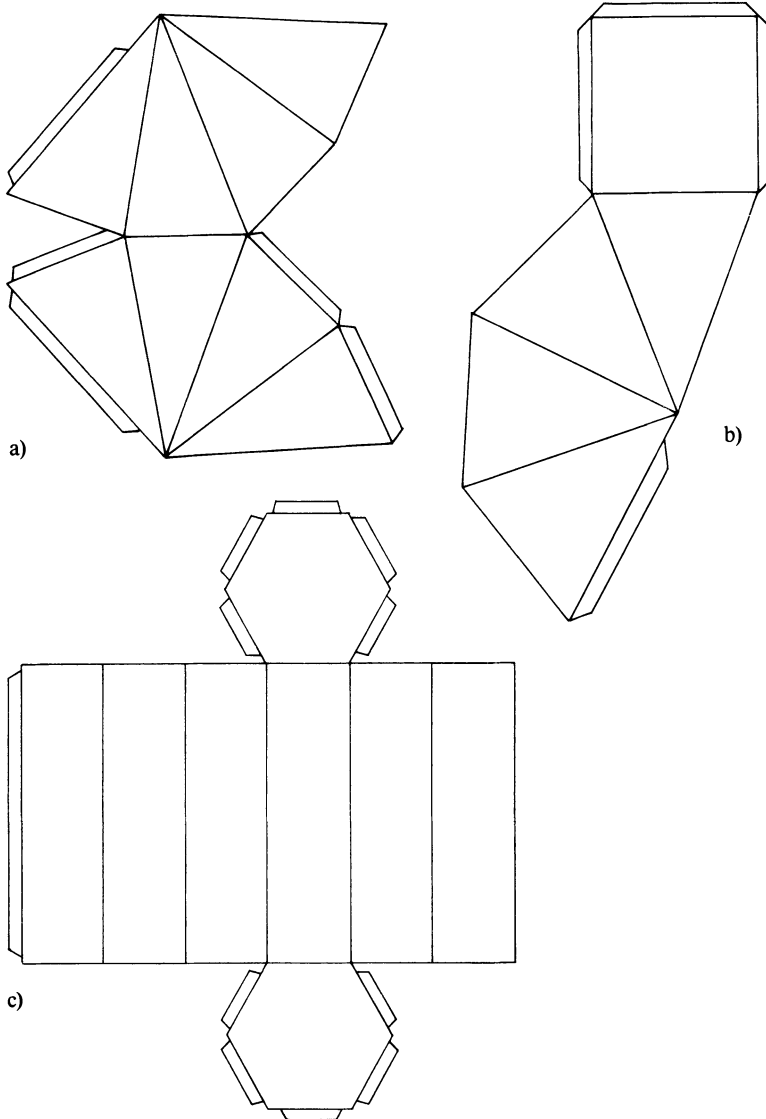
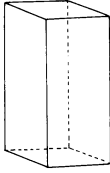
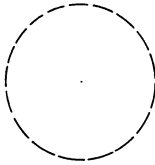
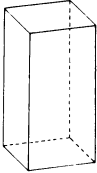
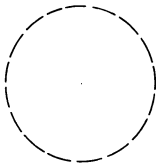
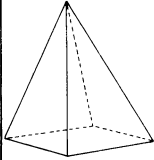
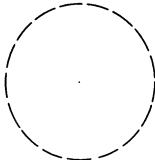
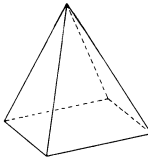
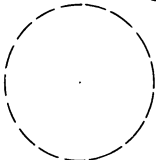
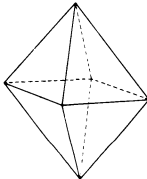
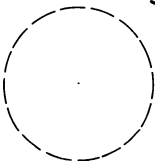
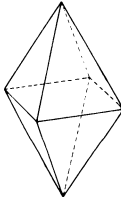
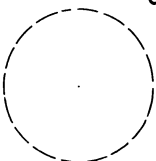
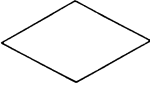

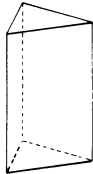
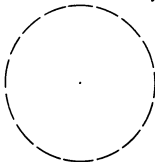

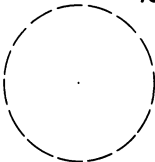
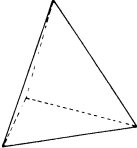
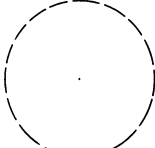
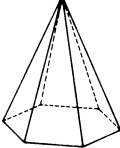
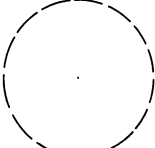
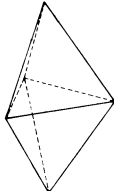
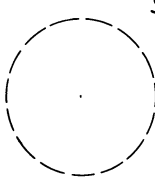
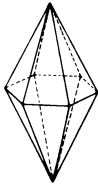
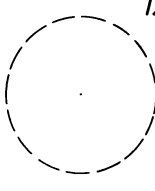

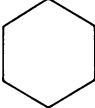


Fig. 4.37a-c. Pattern for models of a rhombic dipyramid (a), a tetragonal pyramid and pedion (b) and a hexagonal prism and pinacoid (c)

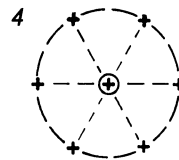
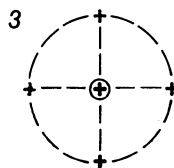
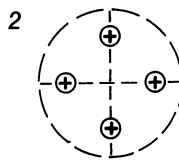
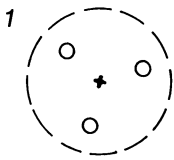
Plot the poles of the faces of the crystals you have made on a stereogram with the orientation chosen such that the altitude of each crystal is perpendicular to the plane of projection. The drawings below give the geometric shape of the base or of any section normal to the altitude.

	rhombic		tetragonal	
Prism		1 		4 
Pyramid		2 		5 
Dipyramid		3 		6 
Basal plane or section of the polyhedron	 Rhombus		 Square	

Exercise 4.5. Which faces of the hexagonal prism and pinacoid and of the tetragonal dipyramid belong to a single zone? Draw in the zone circle on the appropriate stereogram in Exercise 4.4.

	trigonal		hexagonal	
Prism		7 		10 
Pyramid		8 		11 
Dipyramid		9 		12 
Basal plane or section of the polyhedron	 Equilateral triangle		 Regular hexagon	

Exercise 4.6. What is represented by the following stereograms?



Exercise 4.7. In a stereographic projection, choose a pole at random and draw in points 30° away from it in all directions. What is the locus of the points produced?

Exercise 4.8. Construct a Wulff net using a ruler, a protractor and a compass. Make the circles at intervals of 30° .

Exercise 4.9. Insert poles on a stereographic projection with the following ϕ and ρ values: 1) $80^\circ, 60^\circ$; 2) $160^\circ, 32^\circ$; 3) $130^\circ, 70^\circ$. Determine the angle between a) 1 and 2; b) 1 and 3; c) 2 and 3. Indicate the zone pole for the zones determined by a) 1 and 2; b) 1 and 3; c) 2 and 3, and give the ϕ and ρ values for their positions.

Exercise 4.10. The poles for the faces with angular coordinates $40^\circ, 50^\circ$ and $140^\circ, 60^\circ$ lie on zone circle A, while the poles $80^\circ, 70^\circ$ and $190^\circ, 30^\circ$ are on zone circle B. These zone circles have two points of intersection. Determine the angular coordinates ϕ, ρ for these points. How are these faces orientated relative to each other?

Exercise 4.11. What is the relationship among the normals to the faces comprising a zone? How are they related to the zone axis?

Exercise 4.12. In the cubic unit cell shown in Fig. 4.38 three different sorts of axes are shown. Three axes (\square) pass through the midpoints of opposite faces ($x, \frac{1}{2}, \frac{1}{2}, \frac{1}{2}, y, \frac{1}{2}$; and $\frac{1}{2}, \frac{1}{2}, z$). Four axes (Δ) lie along the body diagonals. Six axes (\circ) pass through the midpoints of opposite edges. All of these axes intersect in the centre of the unit cell.

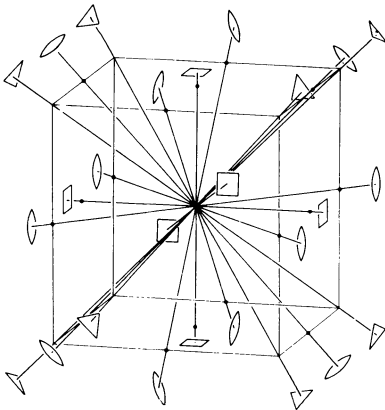


Fig. 4.38. Cubic unit cell showing the axes through the midpoints of opposite faces (\square), along the body diagonals (Δ), and through the midpoints of opposite edges (\circ). (After [6])

Draw the axes on a stereographic projection making use of the Wulff net. It is convenient to place one of the axes (\square) at the centre of the plane of projection. The angles between the various axes may be taken from Fig. 4.39 and 4.40, which show cross-sections through the centre of the cube.

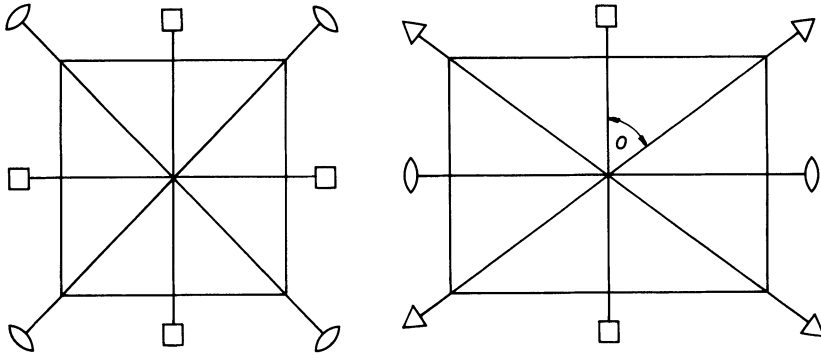


Fig. 4.39. Section through the centre of the cubic unit cell in Fig. 4.38 parallel to a cube face ($\frac{1}{2}, y, z$ or $x, \frac{1}{2}, z$ or $x, y, \frac{1}{2}$)

Fig. 4.40. Section x, x, z or $x, 1-x, z$ through the cubic unit cell of Figure 4.38. The angle θ is 54.73° , half of the tetrahedral angle (the H-C-H angle in methane) of 109.46°

Exercise 4.13. The galena crystal in Fig. 4.41 (see also Fig. 4.1) was measured using a reflection goniometer. The angular coordinates ϕ and ϱ are given in the accompanying table.

- a) Draw the stereogram of the pole faces.
- b) Compare this stereogram with that of the axes in the cube drawn in Exercise 4.12.

Face	ϕ	ϱ
1,1'	-	$\pm 0^\circ$
2,2'	0°	$\pm 45^\circ$
3	0°	90°
4,4'	45°	$\pm 54.73^\circ$
5	45°	90°
6,6'	90°	$\pm 45^\circ$
7	90°	90°
8,8'	135°	$\pm 54.73^\circ$
9	135°	90°
10,10'	180°	$\pm 45^\circ$
11	180°	90°
12,12'	225°	$\pm 54.73^\circ$
13	225°	90°
14,14'	270°	$\pm 45^\circ$
15	270°	90°
16,16'	315°	$\pm 54.73^\circ$
17	315°	90°

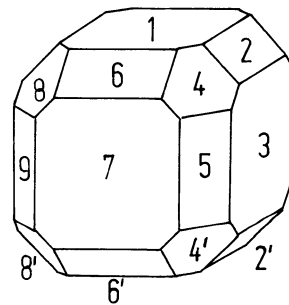


Fig. 4.41. Crystal of galena

Exercise 4.14. Draw a stereogram showing the pole faces of a crystal of rutile. The lattice parameters are given in Table 9.5. Compare your stereogram with the crystal given in Table 8.11.15.

Exercise 4.15. Draw the stereogram of a cube in its normal setting, i.e. with one face normal to the N-S direction. Rotate the cube to bring a body diagonal of the cube parallel to N-S, and draw the resulting poles of the faces on the stereographic projection.

Exercise 4.16. Draw the orthographic projection of the axes of the cube-shaped unit cell shown in Fig. 4.38. The necessary angular values may be taken from exercise 4.12. Sketch the main zone circles.

Exercise 4.17. Draw a gnomonic projection of the topaz crystal in Fig. 4.28. The lattice constants are given on p. 42.

5 Principles of Symmetry

Up to now, the only repetition operation that we have used formally has been the lattice translation: the operation of three non-coplanar lattice translations on a point which gives rise to the space lattice.

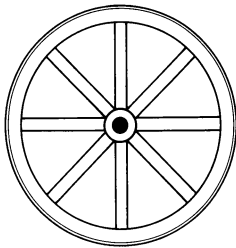


Fig. 5.1. This wheel may be considered either as derived from an object consisting of a single spoke which is repeated by rotation every 45° or as an object which is brought into coincidence with itself by a rotation of 45°

In addition to lattice translations, there are other repetition operations, such as rotations and reflections. In these cases, an object is brought into a coincidence with itself by rotation about an axis or reflection in a plane.

All repetition operations are called symmetry operations. Symmetry consists of the repetition of a pattern by the application of specific rules.

In the wheel illustrated in Fig. 5.1, the spokes are repetitions of one another at intervals of 45° , or alternatively, as the wheel rotates, it is brought into coincidence with itself by every rotation of 45° . *When a symmetry operation has a "locus", that is a point, a line, or a plane that is left unchanged by the operation, this locus is referred to as the symmetry element.*

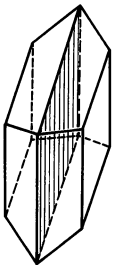


Fig. 5.2. Reflection of either side of this gypsum crystal in the hatched plane indicated brings it into coincidence with the other side. This plane is called a mirror plane

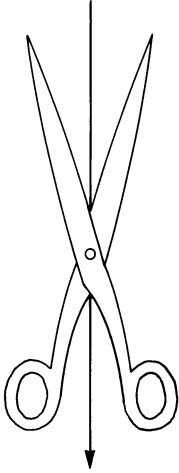


Fig. 5.3. Rotation of the pair of scissors through 180° about the axis marked with an *arrow* brings it into coincidence with itself. This axis is called a rotation axis

Figure 5.2 is an illustration of a crystal of gypsum. The right-hand half of the crystal can be brought into coincidence with the left-hand half through a *reflection* in the hatched plane, which will equally bring the left-hand side into coincidence with the right. Every point in the crystal will be moved by this reflection operation except those which actually lie on the reflection plane itself. The plane containing these points is thus the *symmetry element* corresponding to the *symmetry operation* of reflection; it is called a *mirror plane*.

Rotation through 180° about the axis marked with an arrow will bring either half of the pair of scissors in Fig. 5.3 into coincidence with the other half. Alternatively, rotation of the pair of scissors through 180° brings it into coincidence with itself. Every point on the scissors moves during this operation except those that lie on the rotation axis (the arrow) itself. The points comprising this axis make up the symmetry element corresponding to the *symmetry operation of rotation*: the *rotation axis*.

Another type of symmetry is shown by the pair of irregular pentagons in Fig. 5.4. Reflection of either pentagon through the indicated point will bring it into coincidence with the other pentagon. In this symmetry operation, which is called *inversion*, only a single point remains unchanged, it is the symmetry element of the symmetry operation inversion and is called an *inversion centre* or a centre of symmetry.

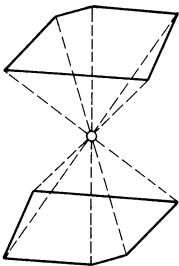


Fig. 5.4. Either pentagon is brought into coincidence with the other by reflection in a point. This is called inversion, and the point which remains unmoved by the operation is called an inversion centre or centre of symmetry

5.1 Rotation Axes

What symmetry elements are present in a general plane lattice, such as that shown in Fig. 5.5? Make a copy of the figure on tracing paper and lay the copy directly over the original. Then rotate the copy about the central lattice point A until both lattices come into coincidence once more. In this case, this will happen after a rotation of 180° , and a further rotation of 180° makes a full 360° rotation, returning the upper lattice to its original position.

The symmetry element corresponding to the symmetry operation of rotation is called a *rotation axis*. The order of the axis is given by X where $X = \frac{360^\circ}{\epsilon}$, and ϵ is the minimum angle (in degrees) required to reach a position indistinguishable from the starting point. In the above case, $X = \frac{360^\circ}{180^\circ} = 2$, and the axis is called a *2-fold rotation axis*. The symbol for this operation is simply the digit 2. In a diagram, it is represented as $()$ if it is normal to the plane of the paper, or as \rightarrow if it is parallel to it.

Whenever a 2-fold axis passes through a point A, a 2-fold axis must pass through all points equivalent by translation to A. 2-fold axes normal to the lattice plane will also pass through all points B, C and D which lie on the midpoints of a translation vector. There are thus an infinite number of rotation axes normal to this plane.

Objects are said to be *equivalent* to one another if they can be brought into coincidence by the application of a symmetry operation. If no symmetry

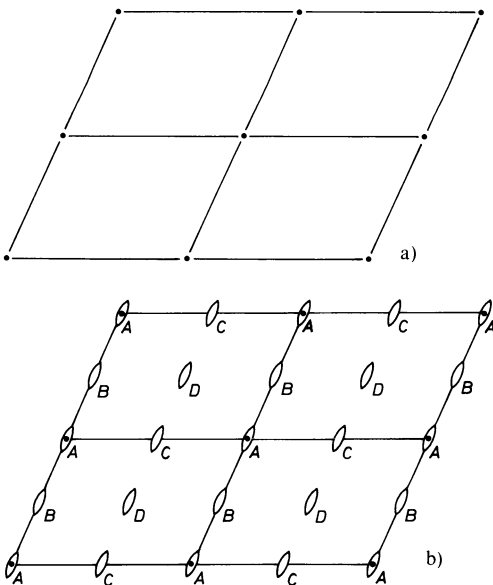


Fig. 5.5a, b. A general plane lattice (a) and its symmetry (b). Symmetry elements marked with the same letter are equivalent to one another

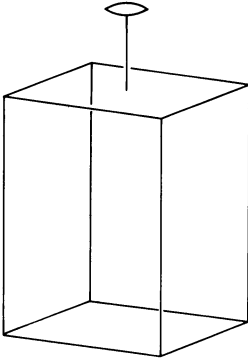


Fig. 5.6. A crystal with upper and lower parallelogram faces and sides perpendicular to them has – so far as its morphology is concerned – only a single 2-fold axis

operation except lattice translation is involved, the objects are said to be “*equivalent by translation*” or “*identical*”.

In Fig. 5.5, all rotation axes A are equivalent to one another, as are all axes B, C and D. On the other hand, the axes A are not equivalent to B, and so forth.

A crystal, in which congruent lattice planes (Fig. 5.5) lie directly one above the other, may develop a morphology in which the lower and upper faces are corresponding parallelograms (pinacoid), and the side faces are all perpendicular to these (Fig. 5.6). Such a crystal will come into coincidence with itself if it is rotated through 180° about an axis through the middle of the upper and lower faces. It thus contains a single 2-fold axis. This observation may be generalised as follows:

The morphology of a single crystal will show only one symmetry element of a particular type in a particular direction, although both its lattice and its crystal structure will show infinitely many parallel elements.

Let us now consider whether it is possible to have axes of order higher than 2. An axis with $X > 2$ operating on a point will produce at least two other points lying in a plane normal to it. Since three non-colinear points define a plane, this must be a lattice plane. Thus, rotation axes must invariably be normal to lattice planes, and we must decide whether the points generated by a rotation axis can fulfill the conditions for being a lattice plane, specifically, that parallel lattice lines will have the same translation period.

a) *Threefold Rotation Axis:* 3 (graphical symbol Δ). Figure 5.7a shows a 3-fold rotation axis normal to the plane of the paper. By its operation, a rotation of 120° $\left(= \frac{360^\circ}{3} \right)$, point I comes into coincidence with point II, and, by a second rotation of 120° with point III. A further rotation of 120° returns it to its original location. A lattice translation moves point I to point IV, and the four points thus generated produce the unit mesh of a lattice plane. Thus, 3-fold axes are compatible with space lattices.

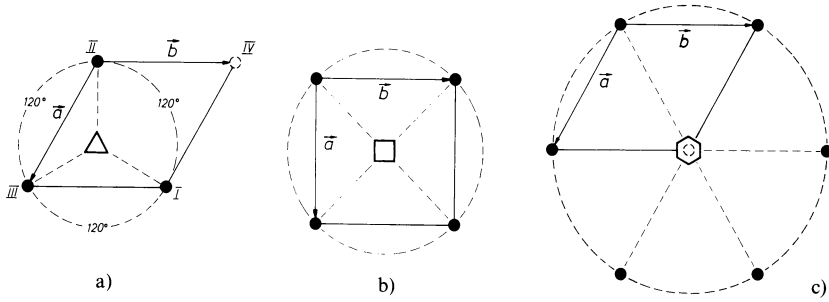


Fig. 5.7a–c. The arrays of points resulting from the operation on a point of a 3-fold, b 4-fold, and c 6-fold axes normal to the plane of the paper can lead to lattice planes. \odot additional points produced by lattice translations

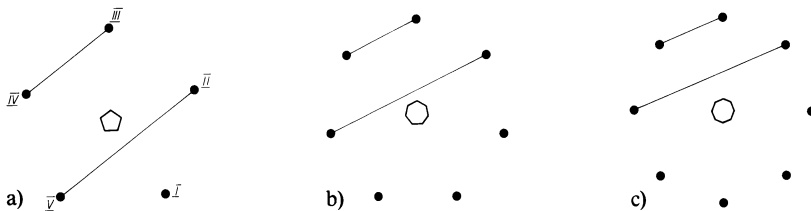


Fig. 5.8a–c. The arrays of points resulting from the operation on a point of a 5-fold, b 7-fold, and c 8-fold axes do *not* fulfil the conditions for a lattice plane, in that parallel lines through equivalent points do not have equal spacings. These rotation symmetries cannot occur in lattices

b) *Fourfold Rotation Axis 4* (graphical symbol \square). Fourfold axes are also compatible with space lattices. As shown in Fig. 5.7b, the action of a 4-fold axis on a point results in a square of points which is also the unit mesh of a lattice plane.

c) *Fivefold Rotation Axis 5*. The operation of this axis on a point results in a regular pentagon of points, as shown in Fig. 5.8a. The line through points III and IV is parallel to that through II and V. If these are to be lattice lines, the spacings of the two pairs of points must either be equal or have an integral ratio. Since this is clearly not the case, the points in Fig. 5.8a do not constitute a lattice plane, and we may conclude that 5-fold axes are impossible in space lattices!

d) *Sixfold Rotation Axis 6* (graphical symbol \hexagon)¹. This operation, applied to a single point, results in a regular hexagon (Fig. 5.7c). A lattice translation places

¹ The standard international symbols for 2, 3, 4 and 6 are \bullet , \blacktriangle , \blacksquare and \bullet , respectively. For convenience, \circ , \triangle , \square and \circ are also used here. In Chapter 8, filled and unfilled symbols are used to distinguish the ends of a polar rotation axis X_p .

a lattice point on the axis itself, and the resulting array meets the condition for a lattice plane. Inspection of Fig. 5.7a and c will show that the lattices resulting from 6-fold and 3-fold axes are, in fact, equal.

e) *Rotation Axes of Order Higher Than 6.* Figure 5.8b and c shows the effect of attempting to build up a lattice plane by applying 7-fold and 8-fold axes to a point. The results are analogous to those for the 5-fold axis described in paragraph (c) above. These arrays do not produce equal spacings of points in parallel lines and so cannot occur in lattices. The same result will occur for any rotation axis with $X > 6$.

In space lattices and consequently in crystals, only 1-, 2-, 3-, 4-, and 6-fold rotation axes can occur.

Note that the wheel in Fig. 5.1 contains an 8-fold axis.

5.2 The Mirror Plane

A further symmetry operation is *reflection* and the corresponding symmetry element is called a plane of symmetry or, more commonly, a *mirror plane*, and given the symbol m . The graphical symbol for a plane normal to the paper is a bold line, as in Fig. 5.9. A mirror plane parallel to the paper is represented by a bold angle; an example of this is in Chap. 14.2. Any point or object on one side of a mirror plane is matched by the generation of an equivalent point or object on the other side at the same distance from the plane along a line normal to it (Fig. 5.9).

Figure 5.10 shows the operation of a mirror plane on a lattice line A , generating another lattice line A' . Whether the line A is parallel to the mirror plane or not, the result is a rectangular unit mesh. The generation of the lattice plane in Fig. 5.10b requires that a lattice point lies on m ; this lattice contains two points per unit mesh and is called centred. A primitive mesh is not chosen in this case since the rectangular cell (with the symmetry plane parallel to an edge) is easier to work with.

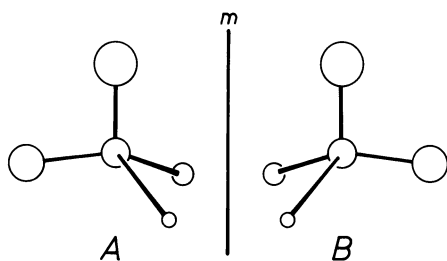


Fig. 5.9. The operation of a mirror plane m on an asymmetric molecule. The mirror plane, perpendicular to the paper, transforms A into B and likewise B into A

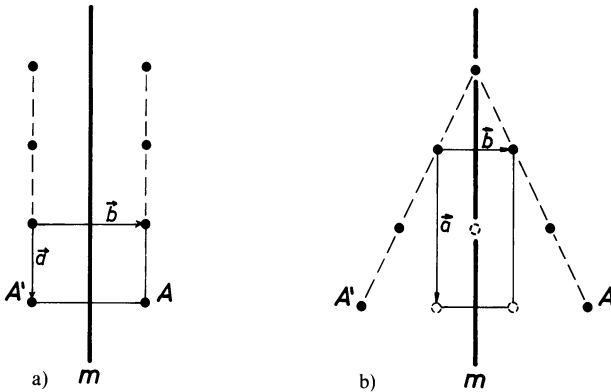


Fig. 5.10 a, b. Operation of m on a lattice line: in **a** the lattice line is parallel to m . The resultant plane lattice is primitive with a rectangular unit cell. In **b**, the lattice line is tilted with respect to m . The resultant plane lattice again has a rectangular unit cell, but is now centred. \circ additional points produced by lattice translations

5.3 The Inversion Centre

The symmetry operation called *inversion* relates pairs of points or objects which are equidistant from and on opposite sides of a central point (called an *inversion centre* or centre of symmetry). The symbol for this operation is $\bar{1}$, and is explained in Section 5.4.1a. An illustration of this operation on a molecule is given in Fig. 5.11. The graphical symbol for an inversion centre is a small circle. Every space lattice has this operation and is thus *centrosymmetric*, see Fig. 5.12.

The operation of an inversion centre on a crystal face generates a parallel face on the opposite side of the crystal. An example of this is the crystal of malonic acid in Table 8.11.2 which has no symmetry other than inversion, and is

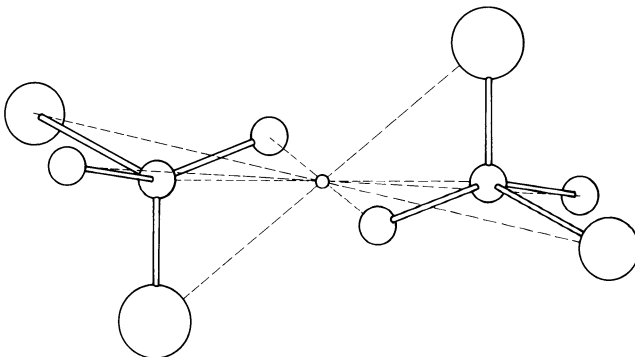


Fig. 5.11. The operation of an inversion centre (\circ) on asymmetric molecules

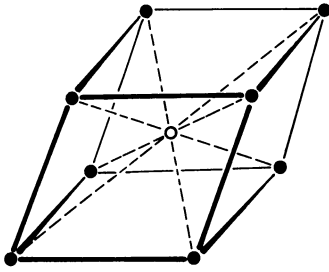


Fig. 5.12. The unit cell of a general lattice, showing the inversion at $\frac{1}{2}, \frac{1}{2}, \frac{1}{2}$. All lattices are centrosymmetric

entirely enclosed by pairs of such parallel faces (or pinacoids). The occurrence of such pairs of parallel faces is important for the detection of inversion symmetry in crystals.

5.4 Compound Symmetry Operations

The operations of rotation, inversion, reflection and lattice translation may be linked with one another. There are two possibilities to be considered here:

a) *Compound Symmetry Operation.* Two symmetry operations are performed in sequence as a single event. This produces a new symmetry operation but the individual operations of which it is composed are lost.

b) *Combination of Symmetry Operations.* In this case, two or more individual symmetry operations are combined which are themselves symmetry operations. Both they and any combination of them must be compatible with the space lattice.

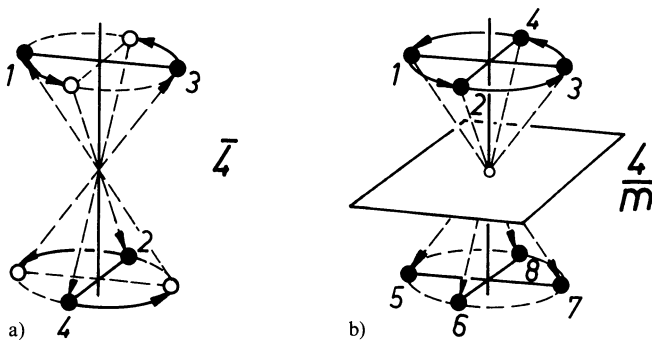


Fig. 5.13 a, b. Compound symmetry operation a and combination of symmetry elements b of a 4-fold rotation and an inversion, illustrated by the effect on the point 1. In a the rotation and the inversion are not present; in b they are present. The open circles in a represent auxiliary points occupied when only one part of the compound operation has been applied. In b, the combination of the rotation and the inversion results also in a mirror plane normal to the axis

Table 5.1. Compound symmetry operations of simple operations. The corresponding symmetry elements are given in round brackets

	Rotation	Reflection	Inversion	Translation
Rotation	×	Roto-reflection	Roto-inversion	Screw rotation
Reflection	(Roto-reflection axis)	×	2-fold rotation	Glide reflection
Inversion	(Roto-inversion axis)	(2-fold rotation axis)	×	Inversion
Translation	(Screw axis)	(Glide plane)	(Inversion centre)	×

These different cases may be illustrated for 4-fold rotation and inversion by considering the examples given in Fig. 5.13.

a) *Compound Symmetry Operation.* Figure 5.13a shows an operation which consists of a rotation of 90° about an axis followed by an inversion through a point on the axis. Successive applications of this compound operation move a point at 1 to 2, 3, 4, and back to 1. Note that the resulting array has neither an inversion centre nor a 4-fold rotation axis.

b) *Combination of Symmetry Operations.* Figure 5.13b illustrates the result of the operations 4-fold rotation and inversion also being present themselves. Successive operations of the 4-fold axis move a point from 1 to 2, 3, 4 and back to 1, while the inversion centre moves it from each of those positions to 7, 8, 5 and 6 respectively.

Combinations of symmetry operations will be further examined in Chapters 6, 8 and 9. Compound symmetry operations are summarised in Table 5.1, where the names of the symmetry elements corresponding to the symmetry operations are given in round brackets. Neither reflection plus inversion nor translation plus inversion results in a new operation. Glide and screw operations are beyond the needs of the present discussion and will be covered in Chapter 9.1.

5.4.1 Rotoinversion Axes

The compound symmetry operation of rotation and inversion is called *rotoinversion*. Its symmetry elements are the *rotoinversion axes*, with the general symbol \bar{X} (pronounced X-bar or bar-X). There are only five possible rotation axes X: 1, 2, 3, 4 and 6, and five corresponding rotoinversion axes \bar{X} : $\bar{1}$, $\bar{2}$, $\bar{3}$, $\bar{4}$ and $\bar{6}$.

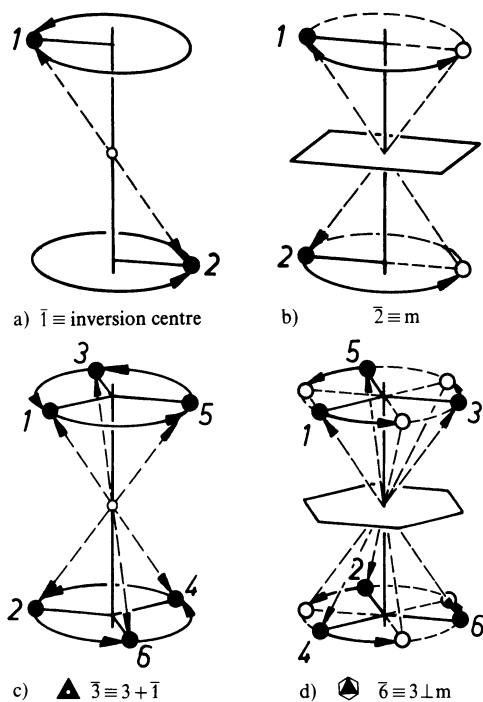
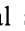



Fig. 5.14a-d. The operation of rotoinversion axes on a point 1: **a** $\bar{1}$. **b** $\bar{2} \equiv m$. **c** $\bar{3} \equiv 3 + \bar{1}$. **d** $\bar{6} \equiv 3 \perp m$. For $\bar{4}$, see Fig. 5.10a. The *unfilled circles* represent auxiliary points which are not occupied when the two operations of which the compound operation is composed are not themselves present

a) Rotoinversion Axis $\bar{1}$ (Fig. 5.14a). $\bar{1}$ implies a rotation of 360° followed by inversion through a point on the 1-fold rotoinversion axis. The operation of $\bar{1}$ on a point 1 returns it to its starting position, and the subsequent inversion takes it to point 2. The rotoinversion operation $\bar{1}$ is thus identical to inversion through an inversion centre. For this reason, $\bar{1}$ is used as a symbol for the inversion centre.

b) Rotoinversion Axis $\bar{2}$ (Fig. 5.14b). The effect of rotation through an angle of 180° followed by inversion is to take a point from 1 to 2. A repetition of this compound operation returns it to its original position. The two points are, however, also related to one another by reflection in a plane normal to the axis. The operation $\bar{2}$ is thus identical with m , and need not be considered further. *Note, however, that $\bar{2}$ represents a direction normal to m .*

c) Rotoinversion Axis $\bar{3}$ (graphical Symbol \blacktriangle) (Fig. 5.14c). Successive applications of the operation $\bar{3}$ move a point to altogether six equivalent positions. In this case, both of the simple operations 3 and $\bar{1}$ are necessarily present – $\bar{3} \equiv 3 + \bar{1}$, so the compound symmetry operation is here a combination of symmetry operations.

d) *Rotoinversion Axis* $\bar{4}$ (graphical symbol ) (Fig. 5.13a). The $\bar{4}$ axis has already been analysed in the previous section. As may be seen in Fig. 5.13a, and as the graphical symbol indicates, $\bar{4}$ implies the presence of a parallel 2.

e) *Rotoinversion Axis* $\bar{6}$ (graphical symbol ) (Fig. 5.14d). Successive applications of $\bar{6}$ move a point to altogether six equivalent positions. It can be seen that $\bar{6}$ implies the presence of a parallel 3 and a perpendicular $m - \bar{6} \equiv 3 \perp m$.

The unambiguous demonstration of the relationships: $\bar{1} \equiv$ inversion centre, $\bar{2} \equiv m$, $\bar{3} \equiv 3 + \bar{1}$, $\bar{4}$ implies 2, and $\bar{6} \equiv 3 \perp m$ in Figs. 5.13a and 5.14 is only possible when an object such as an unsymmetrical pyramid is operated upon by symmetry operations (see exercise 5.1a). Note particularly that *only rotoinversion axes of odd order imply the presence of an inversion centre*, viz. $\bar{1}$ and $\bar{3}$.


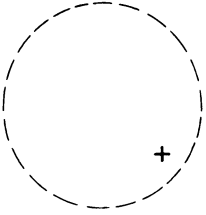
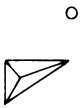
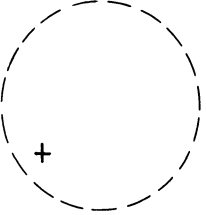
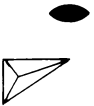
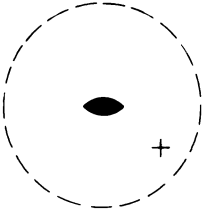
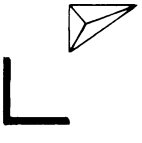
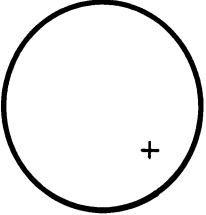
5.4.2 Rotoreflexion Axes

Like the rotoinversion axes, *rotoreflexion* axes S_1 , S_2 , S_3 , S_4 , and S_6 may be defined. Rotoreflexion implies the compound operation of rotation and reflection in a plane normal to the axis. However, these axes represent nothing new, since it is easy to demonstrate the correspondence $S_1 \equiv m$; $S_2 \equiv \bar{1}$; $S_3 \equiv \bar{6}$; $S_4 \equiv \bar{4}$; $S_6 \equiv \bar{3}$. Rotoinversion axes are now invariably used in crystallography.

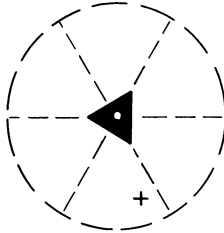
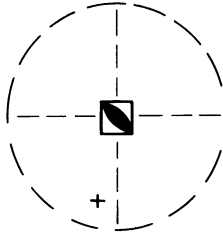
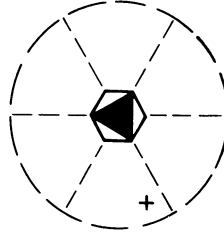
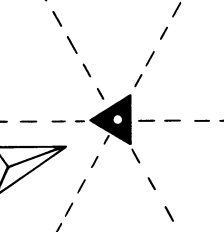
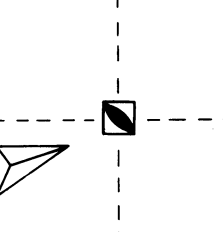
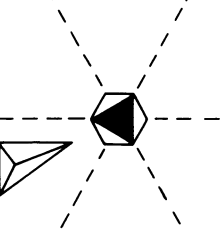
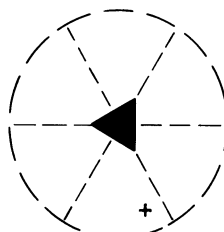
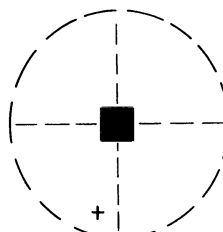
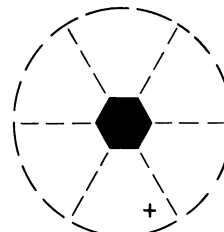
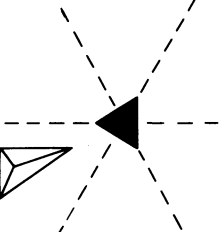
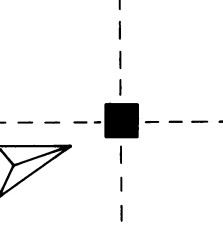
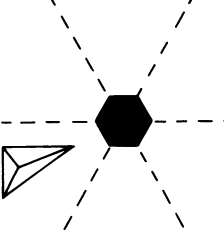
The symmetry elements with which the crystallographer is concerned are the *proper rotation axes* X (1, 2, 3, 4 and 6) and the *rotoinversion or improper axes* \bar{X} ($\bar{1} \equiv$ inversion centre, $(\bar{2}) \equiv m$, $\bar{3}$, $\bar{4}$ and $\bar{6}$). In addition to these, there are screw axes and glide planes (see Chap. 9.1).

The axes X and \bar{X} , including $\bar{1}$ and m , are called point-symmetry elements, since their operations always leave at least one point unmoved.

For 1, this property applies to every point in space, for m to every point on the plane, for 2, 3, 4, 6, to every point on the axis, and for $\bar{1}$, $\bar{3}$, $\bar{4}$ and $\bar{6}$ to a single point.

X	a	b	a	b	\bar{X}
1					$\bar{1}$
2					$\bar{2} \equiv m$

Exercise 5.1 (p. 70)

X	3	4	6
b			
a			
b			
a			
X	3	4	6

Exercise 5.1 (p. 70)

EXERCISES

Exercise 5.1. The ten crystallographic point symmetry operations are shown on pp. 68 and 69. Carry out these operations on:

- An unsymmetrical pyramid, whose base lies into the plane of the paper. Sketch the appearance of the generated pyramids, using dotted lines for those lying below the paper.
- A general pole on a stereographic projection.

Exercise 5.2. Carry out the rotoreflection operations S_1 , S_2 , S_3 , S_4 and S_6 on a general pole on a stereographic projection, and compare these with the stereograms of the rotation-inversion axes $\bar{1}$, $\bar{2} = m$, $\bar{3}$, $\bar{4}$ and $\bar{6}$ in Exercise 5.1.

Exercise 5.3. When two faces are related by an inversion centre $\bar{1}$, how must they lie with respect to one another?

Exercise 5.4. Carry out the rotoinversion operation a) $\bar{5}$ b) $\bar{8}$ c) $\bar{10}$ on a general pole on a stereographic projection.

Exercise 5.5. Analyse the rotoinversion axes (cf. exercises 5.1 and 5.4) into simple symmetry elements, if it is possible.

Exercise 5.6. Which rotoinversion axes contain an inversion centre?

Exercise 5.7. What crystal form is developed by the faces whose poles result from the operation of $\bar{3}$, $\bar{4}$, $\bar{6}$ and $\bar{6}$ on a general pole? (see Exercise 5.1 b).

Exercise 5.8. What shape is implied for the section of a prism which has a 2-, 3, 4, or 6-fold axis?

Exercise 5.9. Determine the location of the rotation axes of a cube.

6 The 14 Bravais Lattices

The general space lattice, with no restrictions on the shape of the unit cell, may be used to describe all crystals. In most cases, however, the lattices which occur are special in that they have special features, such as unit cell dimensions (lattice parameters) which are equal in two or three directions or angles between cell edges with particular values, such as 60° , 90° , 120° or 54.73° . The general lattice has no point symmetry elements except inversion centres. The presence of rotation axes and mirror planes will restrict the cell parameters in some way, and give special lattices. These special lattices give rise to simplifications in the crystal morphology and in physical properties.

When lattice translations in two directions are equivalent, all physical properties are equal in these directions.

In addition to the general space lattice, there are several special lattices. Before we consider these space lattices, however, it is useful to develop the concepts by consideration of general and special plane lattices.

The General (Oblique) Plane Lattice

If we take a point 1, and operate on it with a 2-fold axis, we will generate an equivalent point 2 (Fig. 6.1 a). The application of a lattice translation \vec{a} to point 1 generates an identical point 3 (Fig. 6.1 b), and the 2-fold axis then relates point 3 to point 4 (Fig. 6.1 c). We have now generated a unit mesh of the lattice. It has the shape of an oblique parallelogram, where $a_0 \neq b_0$ and $\gamma \neq 90^\circ$.

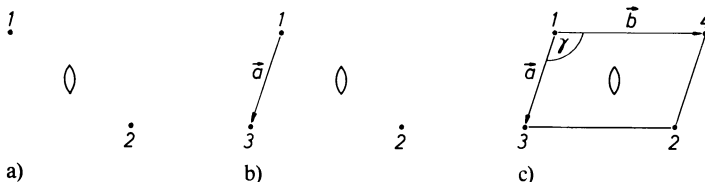


Fig. 6.1 a-c. Development of the general plane lattice, with an oblique unit mesh

Note that here and throughout this book, in reference to symmetry, \neq means need not be equivalent while $=$ means are required by symmetry to be equivalent.

It is possible to vary a_0 , b_0 and γ in any way we like without losing the 2-fold axis. Thus this lattice is fully general.

Special Plane Lattices

a) Returning to Fig. 6.1 a, point 3 could have been chosen so that the points 1, 2 and 3 described a right triangle, with the right angle at point 3 (Fig. 6.2a). The operation of the 2-fold axis now results in a rectangular unit mesh, $a_0 \neq b_0$, $\gamma = 90^\circ$. The arrangements of the points is now “special”, as further symmetry has been introduced, namely two mutually perpendicular mirror planes, parallel to the 2-fold axis (Fig. 6.2b).

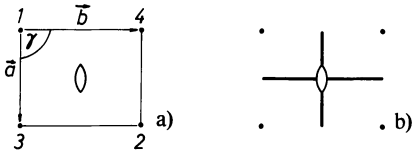


Fig. 6.2a, b. Development of the special plane lattice with a rectangular unit mesh (a) and its symmetry (b)

b) A further possibility in Fig. 6.1 a would be to choose the location of point 3 so that points 1, 2 and 3 formed an isosceles triangle with the two equal edges meeting at point 3. The unit mesh of the resulting lattice is a rhombus: $a_0 = b_0$, $\gamma \neq 60^\circ, 90^\circ$ or 120° (Fig. 6.3a). Extension of the edges 1–4 and 1–3 a further unit translation on the other side of 1, an alternative choice of unit mesh arises (Fig. 6.3b). It is rectangular ($a'_0 \neq b'_0$, $\gamma = 90^\circ$), and is called centred because it has a point at its centre identical to those at the vertices. Consideration of the symmetry of this cell shows that there are a pair of mirror planes, similar to those in Fig. 6.2b, and several 2-fold axes (Fig. 6.3c).

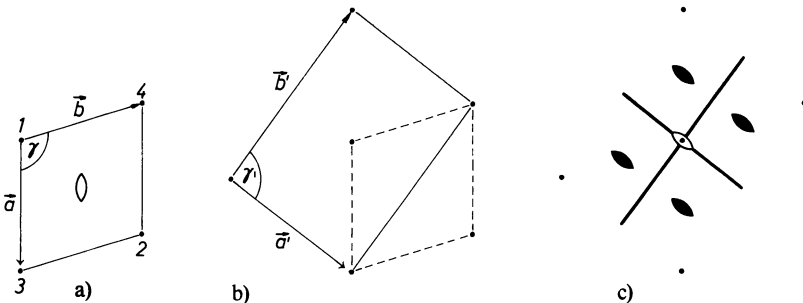


Fig. 6.3a–c. Development of the special plane lattice with a rhombic unit mesh (a), and its alternative description by a centred rectangular mesh (b). Symmetry of the plane lattice (c)

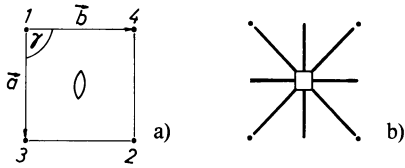


Fig. 6.4 a, b. Development of the special plane lattice with a square unit mesh and its symmetry

c) Returning once more to Fig. 6.1 a, we choose the position of point 3 in such a way as to make the points 1, 2 and 3 describe an isosceles right triangle, with the right angle at 3. The resultant lattice now has a square unit mesh: $a_0 = b_0$, $\gamma = 90^\circ$. As shown in Fig. 6.4b, there are now a 4-fold axis and four mirror planes parallel to it in the cell.

d) Finally, let us choose the position of point 3 in Fig. 6.1 a such that the points 1, 2 and 3 make an equilateral triangle (Fig. 6.5 a). The unit mesh of the resulting hexagonal lattice is now a 120° rhombus, or $a_0 = b_0$, $\gamma = 120^\circ$. In addition to the 2-fold axis, there are now 3- and 6-fold axes as well as several mirror planes. The axes are shown in Fig. 6.5 b (see also Fig. 5.7 a, c).

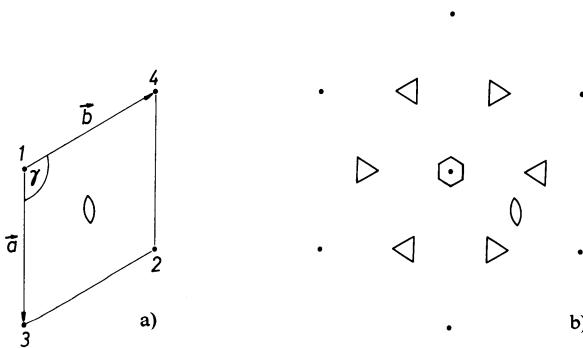


Fig. 6.5 a, b. Development of the special hexagonal plane lattice and its symmetry. The unit mesh is a 120° rhombus

We have now developed all four of the possible special lattice planes (which were, in fact, introduced in a different way in Chapter 5) from the general plane lattice. These plane lattices are summarised in Table 6.1 with their characteristic symmetry elements. The general lattice (see Fig. 5.5) possesses 2-fold axes only, but the special lattices (a)–(d) all have further symmetry elements, which are shown on their diagrams in Fig. 6.6. It should be noted that only point symmetry elements are shown here. There are compound symmetry elements involving translation, glide planes (see Chap. 9.1).

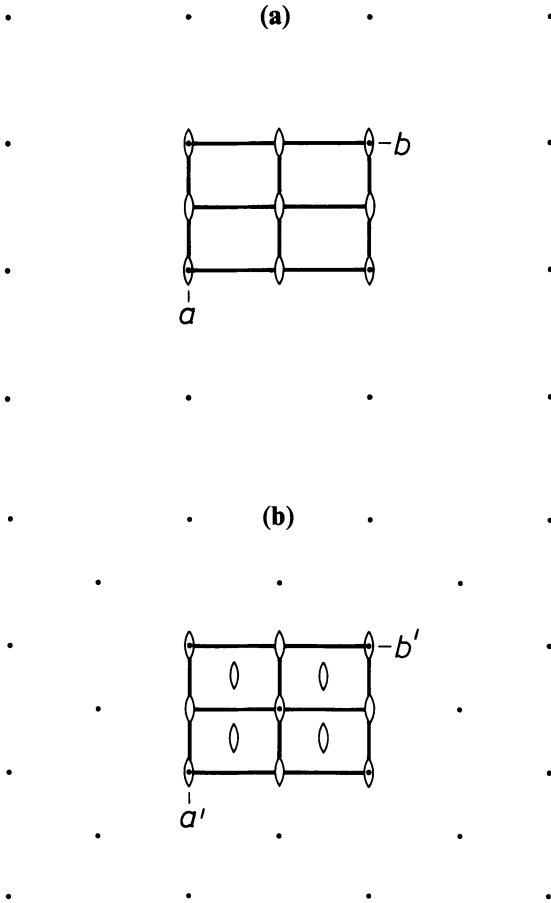


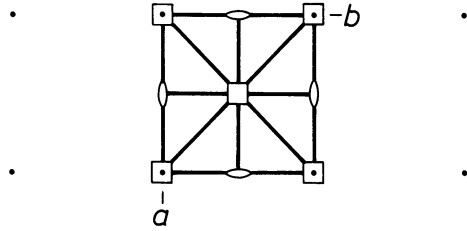
Fig. 6.6 a–d. Symmetry elements of the special lattice planes with a primitive (a) and a centred (b) rectangular unit mesh, and a square (c) and a hexagonal (120° rhombus) (d) unit mesh

6.1 The Primitive Space Lattices (P-Lattices)

The relationships between lattices and symmetry elements in three dimensions are similar to those in two. From the general space lattice, several special space lattices may be derived, in which congruent lattice planes are stacked above one another. If the symmetry of the lattice planes is not changed, the five space lattices with primitive unit cells (P-lattices) are produced. These are given in Table 6.2.

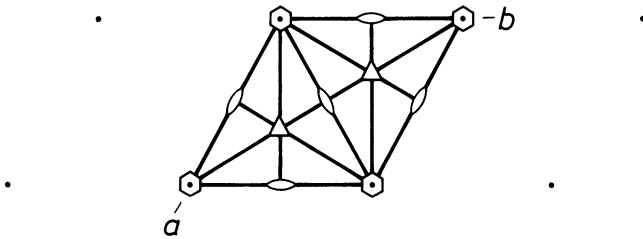
Compare the stacking processes illustrated in Figs. 6.8–6.10a, b; 6.12 and 6.13a, b. Notice that the centred rectangular plane lattice (b) does not occur. The square lattice may be stacked either with $c_0 \neq a_0 = b_0$ or $c_0 = a_0 = b_0$; the former develops the tetragonal P-lattice and the latter the cubic P-lattice. The cubic lattice is a special case of the tetragonal, since new, characteristic symmetry

• • (c) • •



• • • •

• (d) • • •



• • • •

elements appear (three-fold rotation axes along the body diagonals of the unit cell). The generation of the general or triclinic P-lattice by stacking is shown in Fig. 6.7a. All of the P-lattices are illustrated in Table 6.3.

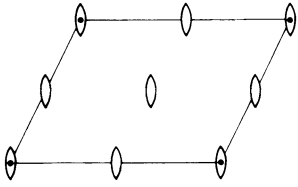
Table 6.1. Plane lattices

	Shape of unit mesh	Lattice parameters	Characteristic symmetry elements	Figure
General plane lattices	Parallelogram	$a_0 \neq b_0$ $\gamma \neq 90^\circ$	2	5.5 6.1 c
Special plane lattice	a Rectangle (primitive)	$a_0 \neq b_0$ $\gamma = 90^\circ$	m	6.2a 6.6a
	b Rectangle (centred)	$a_0 \neq b_0$ $\gamma = 90^\circ$	m	6.3b 6.6b
	c Square	$a_0 = b_0$ $\gamma = 90^\circ$	4	6.4a 6.6c
	d 120° Rhombus	$a_0 = b_0$ $\gamma = 120^\circ$	6 (3)	6.5a 6.6d

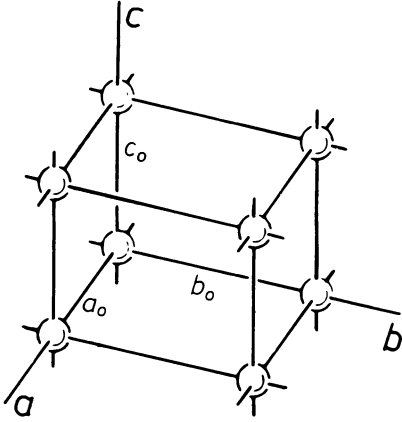
Table 6.2. P-Lattices

Shape of unit mesh in stacked layers	Interplanar spacing	Lattice	Figure
Parallelogram ^a ($a_0 \neq c_0$)	b_0	Monoclinic P	6.8a, b
Rectangle ($a_0 \neq b_0$)	c_0	Orthorhombic P	6.9a, b
Square ($a_0 = b_0$)	$c_0 \neq (a_0 = b_0)$	Tetragonal P	6.10a, b
Square ($a_0 = b_0$)	$c_0 = (a_0 = b_0)$	Cubic P	6.13a, b
120°-Rhombus ($a_0 = b_0$)	c_0	Hexagonal P	6.12a, b

^a Note that for historical reasons, the description $a_0 \neq b_0, \gamma \neq 90^\circ$ has been changed in this case to $a_0 \neq c_0, \beta \neq 90^\circ$.

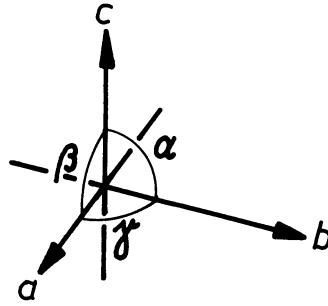


a Plane lattice with oblique unit mesh showing its symmetry. Stacking of such planes directly above one another leads to the monoclinic P-lattice (cf. Fig. 6.8a, b). If, however, the lattice points of the stacked planes do not coincide with the 2-fold axes, these are lost, and the triclinic P-lattice has been generated. (cf. b)



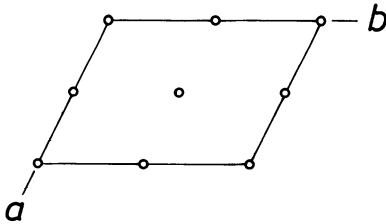
b Triclinic P-lattice, lattice parameters in the unit cell are:

$$a_0 \neq b_0 \neq c_0 \\ \alpha \neq \beta \neq \gamma$$



c Triclinic axial system:

$$a \neq b \neq c \\ \alpha \neq \beta \neq \gamma$$

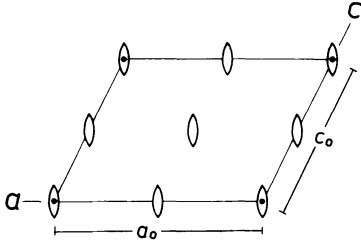


d Space group $P\bar{1}$.
Projection of the symmetry elements of the triclinic P-lattice parallel to c onto the plane $x, y, 0$. This is the space group of highest symmetry in the triclinic system

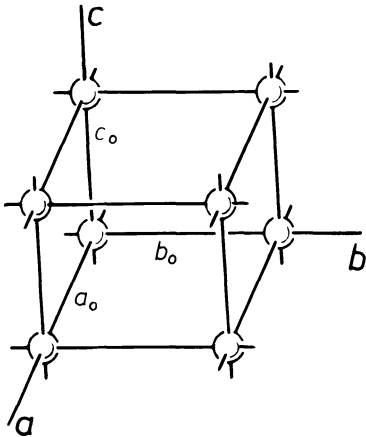
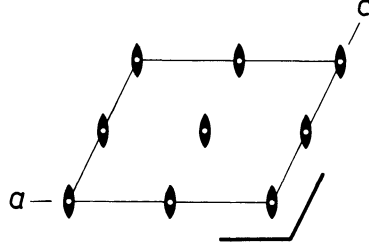
(O)
e Point group $\bar{1}$.
Symmetry of a lattice point in a triclinic P-lattice. This is the point group of highest symmetry in the triclinic system

f 1 is the triclinic point group of lower symmetry than $\bar{1}$ (formed by removal of $\bar{1}$)

Fig. 6.7a-f. The triclinic crystal system



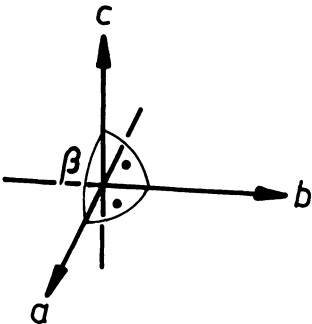
a Plane lattice with oblique unit mesh showing its symmetry. Stacking of such planes directly above one another with interplanar spacing b_0 leads to the monoclinic P-lattice (cf. b)



b Monoclinic P-lattice, lattice parameters in the unit cell are:

$$a_0 \neq b_0 \neq c_0$$

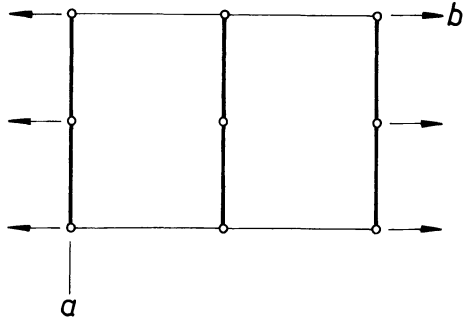
$$\alpha = \gamma = 90^\circ \quad \beta > 90^\circ$$



c Monoclinic axial system:

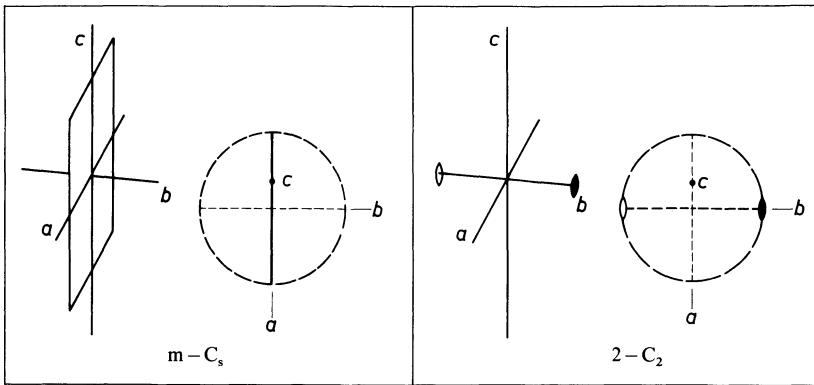
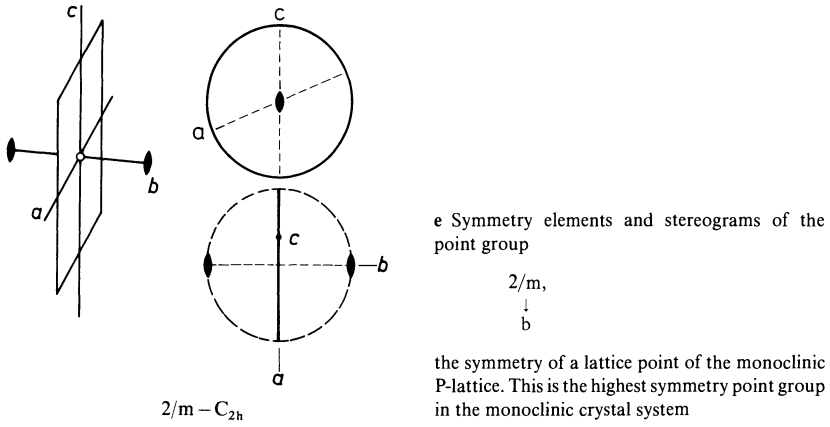
$$a \neq b \neq c$$

$$\alpha = \gamma = 90^\circ \quad \beta > 90^\circ$$



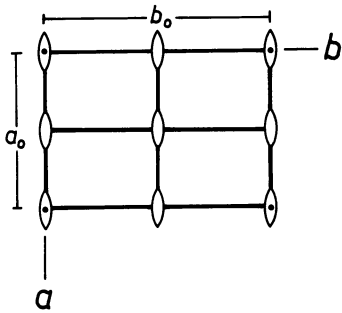
d Space group P 2/m.

Projection of the symmetry elements of the monoclinic P-lattice on $x, 0, z$ (above) and on $x, y, 0$ (below). This is one of the space groups of highest symmetry in the monoclinic system

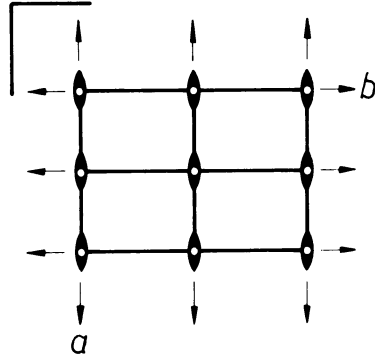


f Symmetry elements and stereograms of the monoclinic point groups of lower symmetry than $2/m$ (formed by removal of symmetry elements from it).

Fig. 6.8a-f. The monoclinic crystal system

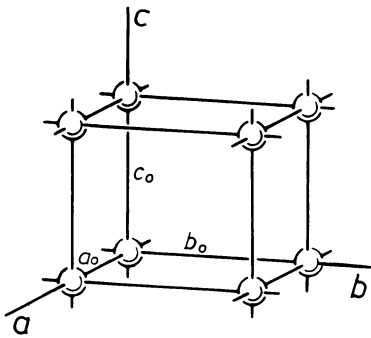


a Plane lattice with rectangular unit mesh showing its symmetry. Stacking of such planes directly above one another with interplanar spacing c_0 leads to the orthorhombic P-lattice (cf. b)



d Space group
 $P\ 2/m\ 2/m\ 2/m\ (Pmmm)$
 $\downarrow\ \downarrow\ \downarrow$
 $a\ \ b\ \ c$

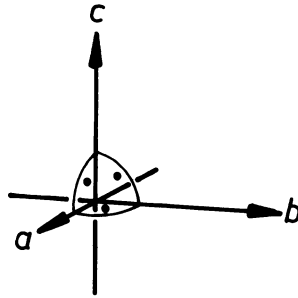
Projection of the symmetry elements of the orthorhombic P-lattice on $x, y, 0$. This is one of the space groups of highest symmetry in the orthorhombic system



b Orthorhombic P-lattice, lattice parameters in the unit cell are:

$$a_0 \neq b_0 \neq c_0$$

$$\alpha = \beta = \gamma = 90^\circ$$

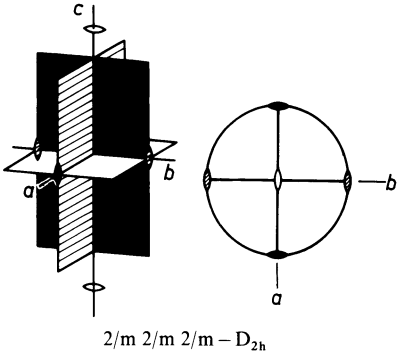


c Orthorhombic axial system

$$a \neq b \neq c$$

$$\alpha = \beta = \gamma = 90^\circ$$

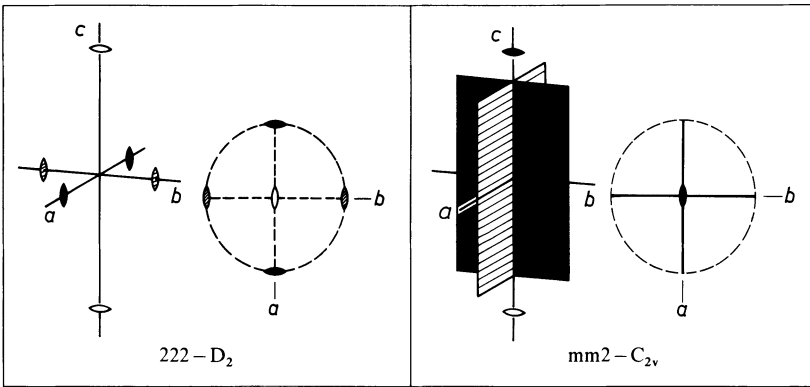
Fig. 6.9 a-f. The orthorhombic crystal system



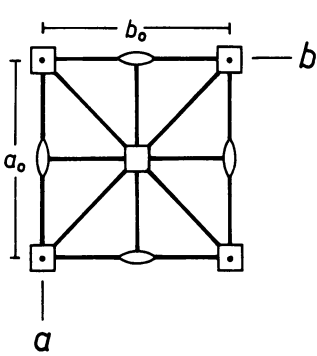
e Symmetry elements and stereogram of the point group

$$\begin{array}{ccc}
 2/m & 2/m & 2/m \text{ (mmm)}, \\
 \downarrow & \downarrow & \downarrow \\
 a & b & c
 \end{array}$$

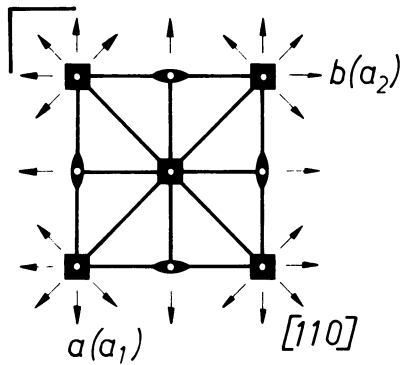
the symmetry of a lattice point of the orthorhombic P-lattice. This is the highest symmetry point group in the orthorhombic crystal system



f Symmetry elements and stereograms of the orthorhombic point groups of lower symmetry than $2/m\ 2/m\ 2/m$ (formed by removal of symmetry elements from it)

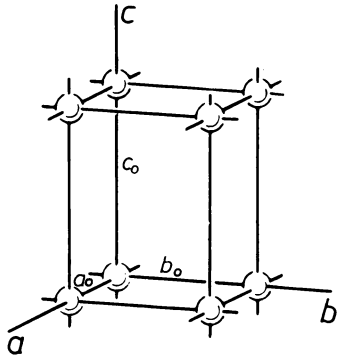


a Plane lattice with square unit mesh showing its symmetry. Stacking of such planes directly above one another with interplanar spacing $c_0 \neq a_0 = b_0$ leads to the tetragonal P-lattice (cf. b)

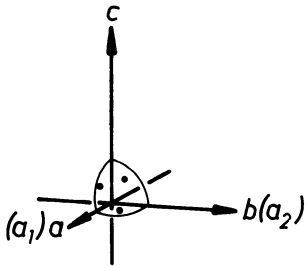


d Space group
 $P 4/m 2/m 2/m$ ($P 4/mmm$)
 $\downarrow \quad \downarrow \quad \downarrow$
 $c \quad \langle a \rangle \quad \langle 110 \rangle$

Projection of the symmetry elements of the tetragonal P-lattice on $x, y, 0$. This is one of the space groups of highest symmetry in the tetragonal system

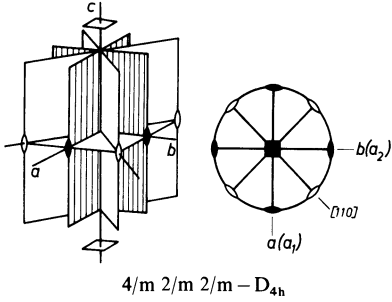


b Tetragonal P-lattice, lattice parameters in the unit cell are:
 $a_0 = b_0 \neq c_0$
 $\alpha = \beta = \gamma = 90^\circ$



c Tetragonal axial system
 $a = b \neq c$ ($a_1 = a_2 \neq c$)
 $\alpha = \beta = \gamma = 90^\circ$

Fig. 6.10a-f. The tetragonal crystal system

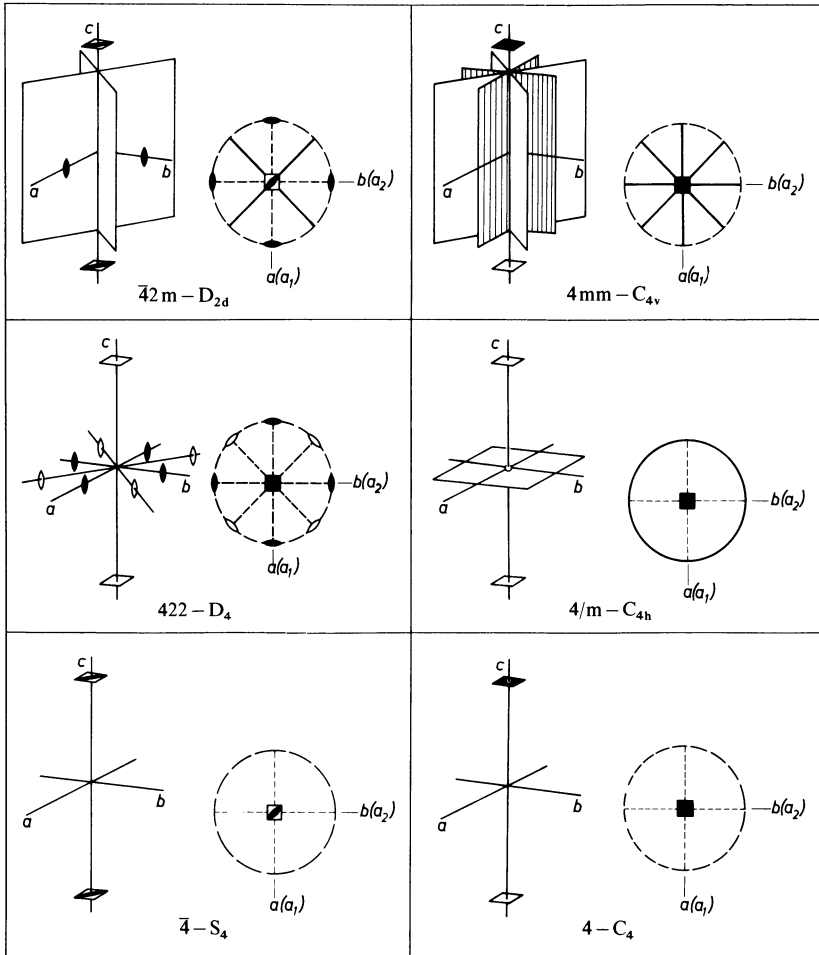


e Symmetry elements and stereogram of the point group

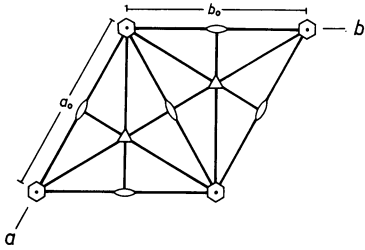
$$4/m\ 2/m\ 2/m\ (4/mmm),$$

$$\begin{matrix} \downarrow & \downarrow & \downarrow \\ c & (a) & (110) \end{matrix}$$

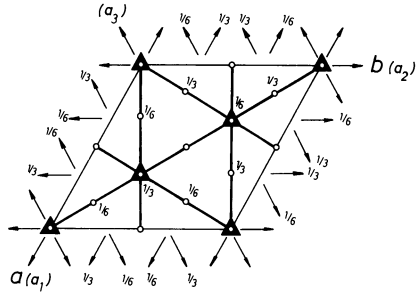
the symmetry of a lattice point of the tetragonal P-lattice. This is the highest symmetry point group in the tetragonal crystal system



f Symmetry elements and stereograms of the tetragonal point groups of lower symmetry than $4/m\ 2/m\ 2/m$ (formed by removal of symmetry elements from it). Note that a change in choice of axes in the point group $42m$ gives a point group $4m2$ ($(a \perp m)$). The two settings are equally satisfactory



a Plane lattice with 120° rhombus unit mesh showing its symmetry. Stacking of such planes above one another so that the second lattice plane is at a height of $c_0/3$ with a lattice point on a 3 fold axis, while the third plane is at a height of $2/3c_0$ with its lattice point on the other 3-fold axis. The fourth plane will then come directly above the first. This arrangement reduces the 6-fold axes to 3-fold, and removes the symmetry planes in $x, 0, z$; $0, y, z$ and x, x, z as well as the two-fold axis parallel to c (cf. b)

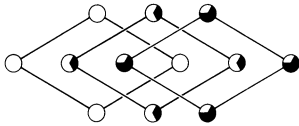


d Space group

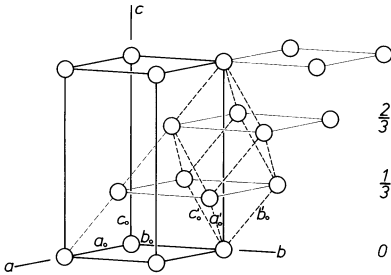
$$R \bar{3} 2/m (R \bar{3}m)$$

$$\begin{matrix} \downarrow & \downarrow \\ c & (a) \end{matrix}$$

Projection of the symmetry elements of the trigonal R-lattice on $x, y, 0$. This is one of the space groups of highest symmetry in the trigonal system



c Axial system: see Fig. 6.12c



b From this arrangement of lattice points, two distinct unit cells may be chosen:

I) Trigonal R-lattice; the lattice parameters of the cell are:

$$a_0 = b_0 \neq c_0$$

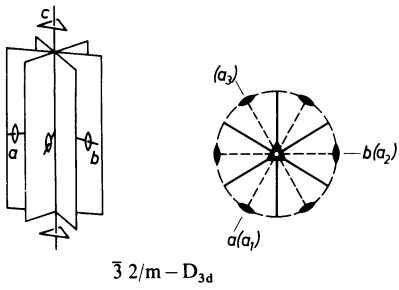
$$\alpha = \beta = 90^\circ, \quad \gamma = 120^\circ$$

II. Rhombohedral P-lattice; the lattice parameters of the cell are:

$$a'_0 = b'_0 = c'_0$$

$$\alpha' = \beta' = \gamma'$$

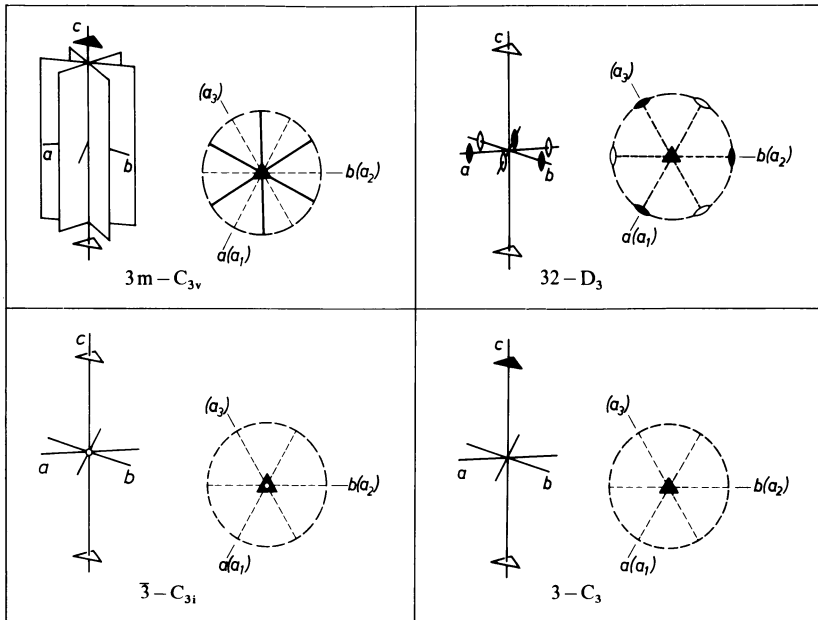
Fig. 6.11 a-f. The trigonal crystal system



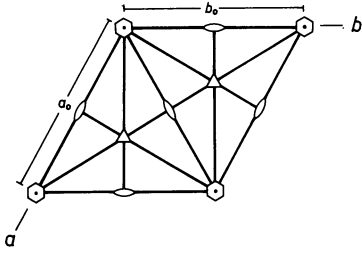
e Symmetry elements and stereogram of the point group

$$\begin{array}{c} \bar{3} 2/m (\bar{3}m), \\ \downarrow \downarrow \\ c \quad (a) \end{array}$$

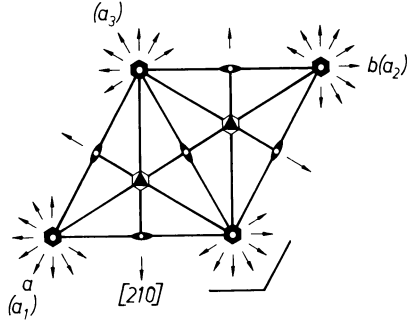
the symmetry of a lattice point of the trigonal R-lattice. This is the highest symmetry point group in the trigonal crystal system



f Symmetry elements and stereograms of the trigonal point groups of lower symmetry than $\bar{3} 2/m$ (formed by removal of symmetry elements from it)

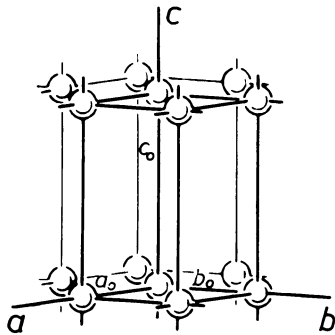


a Plane lattice with 120° rhombus unit mesh showing its symmetry. Stacking of such planes directly above one another with interplanar spacing c_0 leads to the hexagonal P-lattice (cf. b)



d Space group
 $P 6/m 2/m 2/m (P6/mmm)$
 $\downarrow \quad \downarrow \quad \downarrow$
 $c \quad \langle a \rangle \langle 210 \rangle$

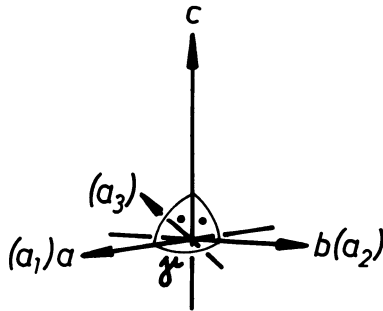
Projection of the symmetry elements of the hexagonal P-lattice on $x, y, 0$. This is the space group of highest symmetry in the hexagonal system



b Hexagonal P-lattice, lattice parameters in the unit cell are:

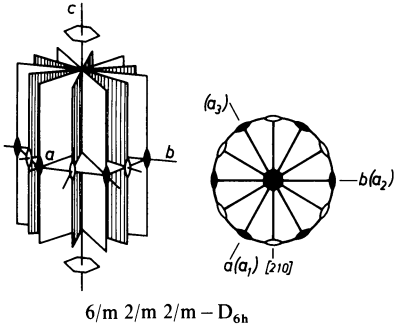
$$a_0 = b_0 \neq c_0$$

$$\alpha = \beta = 90^\circ, \quad \gamma = 120^\circ$$



c Hexagonal axial system
 $a = b \neq c \quad (a_1 = a_2 = a_3 \neq c)$
 $\alpha = \beta = 90^\circ, \quad \gamma = 120^\circ$

Fig. 6.12a-f. The hexagonal crystal system

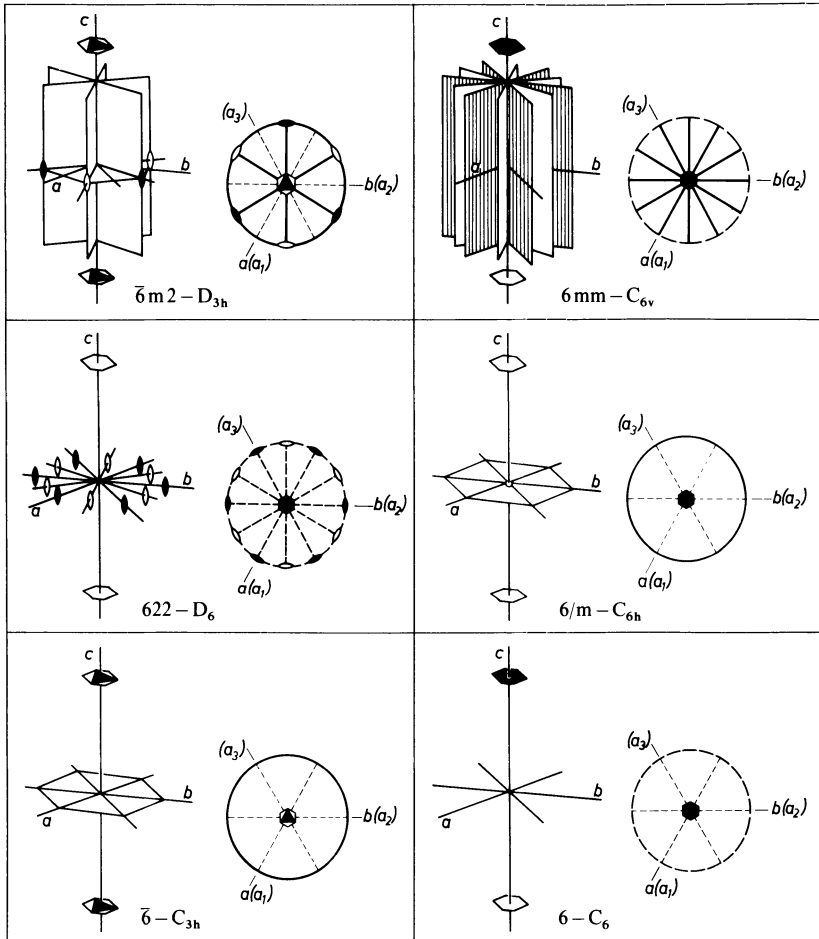


e Symmetry elements and stereogram of the point group

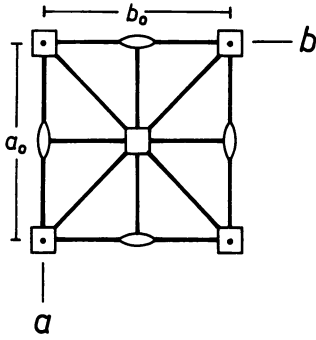
$$6/m\ 2/m\ 2/m\ (6/mmm),$$

$$\begin{matrix} \downarrow & \downarrow & \downarrow \\ c & \langle a \rangle & \langle 210 \rangle \end{matrix}$$

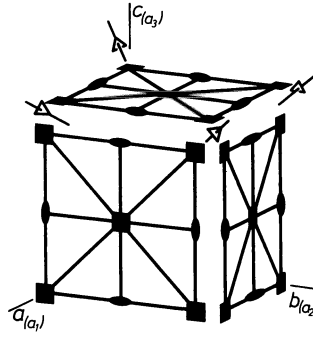
the symmetry of a lattice point of the hexagonal P-lattice. This is the highest symmetry point group in the hexagonal crystal system



f Symmetry elements and stereograms of the hexagonal point groups of lower symmetry than $6/m\ 2/m\ 2/m$ (formed by removal of symmetry elements from it). Note that a change in choice of axes in the point group $\bar{6}m\ 2$ gives a point group $\bar{6}2m$ ($\langle a \rangle \parallel 2$). The two settings are equally satisfactory.



a Plane lattice with square unit cell showing its symmetry. Stacking of such planes directly above one another with interplanar spacing $c_0 = a_0 = b_0$ leads to the cubic P-lattice (cf. b).

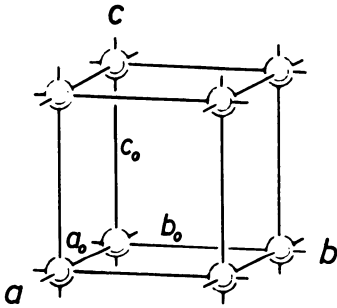


d Space group

$$P 4/m \bar{3} 2/m (Pm\bar{3}m)$$

$$\begin{matrix} \downarrow & \downarrow & \downarrow \\ (a) & (111) & (110) \end{matrix}$$

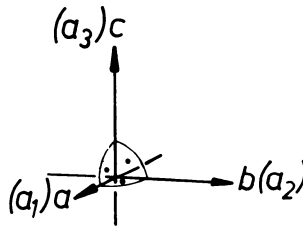
Symmetry elements (incomplete) of the cubic P-lattice. This is one of the space groups of highest symmetry in the cubic system



b Cubic P-lattice, lattice parameters in the unit cell are:

$$a_0 = b_0 = c_0$$

$$\alpha = \beta = \gamma = 90^\circ$$

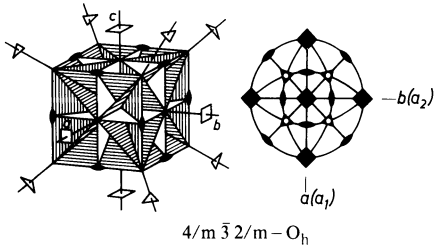


c Cubic axial system

$$a = b = c \quad (a_1 = a_2 = a_3)$$

$$\alpha = \beta = \gamma = 90^\circ$$

Fig. 6.13a-f. The cubic crystal system

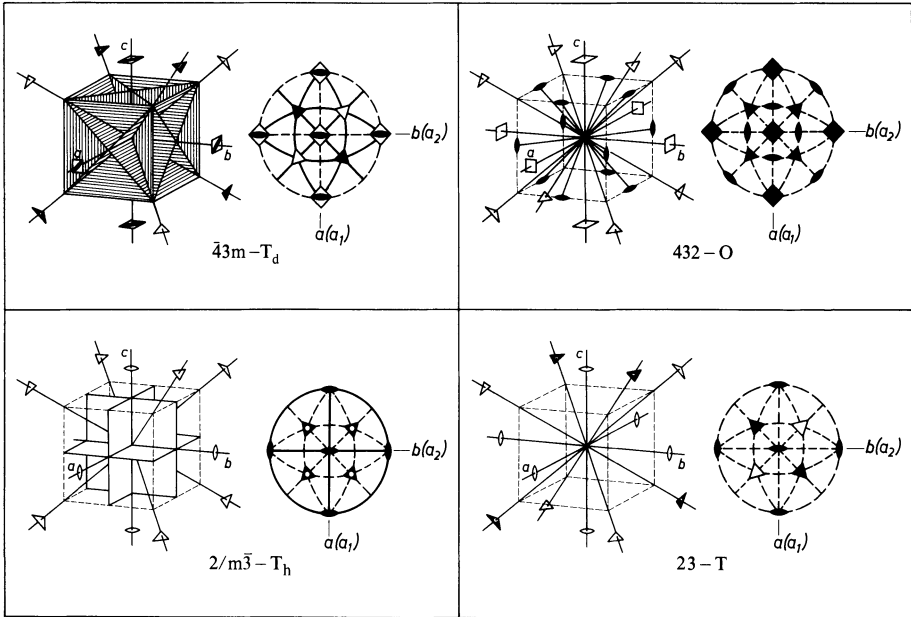


e Symmetry elements and stereogram of the point group

$$P \ 4/m \ \bar{3} \ 2/m \ (m\bar{3}m),$$

$$\begin{matrix} \downarrow & \downarrow & \downarrow \\ \langle a \rangle & \langle 111 \rangle & \langle 110 \rangle \end{matrix}$$

the symmetry of a lattice point of the cubic P-lattice. This is the highest symmetry point group in the cubic crystal system

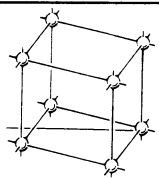
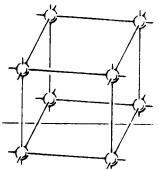
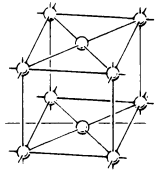
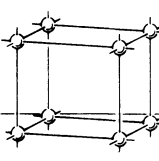
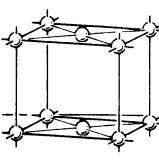
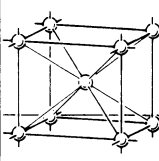
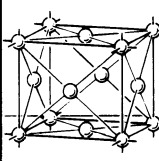
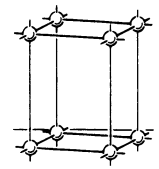
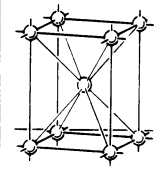
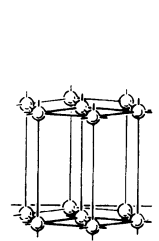
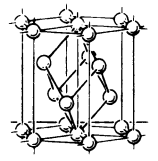
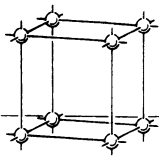
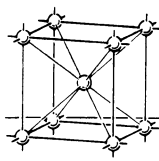
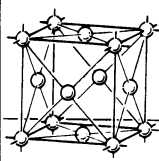


f Symmetry elements and stereograms of the cubic point groups of lower symmetry than $4/m \bar{3} 2/m$ (formed by removal of symmetry elements from it)

6.2 The Symmetry of the Primitive Lattices

Before considering the symmetry of lattices, it is useful to learn two rules governing the generation of a symmetry element by the combination of two others. In the following two cases, *the presence of any two of the given symmetry elements implies the presence of the third* (cf. p. 91). Combination of symmetry elements is no casual occurrence; it is fundamental to the nature of symmetry.

Table 6.3. The 14 Bravais Lattices

	P	C	I	F
Triclinic				
Monoclinic				
Orthorhombic				
Tetragonal				
Trigonal				
Hexagonal				
Cubic				

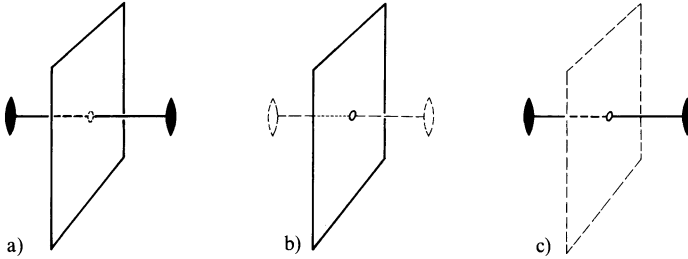


Fig. 6.14a-c. Symmetry rule I: **a** $2 \perp m \rightarrow \bar{1}$ (at the intersection of 2 and m); **b** $\bar{1}$ on $m \rightarrow 2$ (passing through $\bar{1}$ and normal to m); **c** $\bar{1}$ on $2 \rightarrow m$ (passing through $\bar{1}$ and normal to 2)

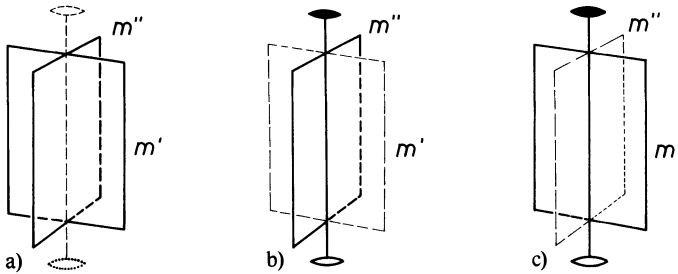


Fig. 6.15a-c. Symmetry rule II: **a** $m' \perp m'' \rightarrow 2$ (along the intersection of m' and m''); **b** 2 on $m'' \rightarrow m' \perp m''$ (with 2 as the line of intersection); **c** 2 on $m' \rightarrow m'' \perp m'$ (with 2 as the line of intersection)

In the following two rules the presence of any two of the given symmetry elements implies the presence of the third:

Rule I. A rotation axis of even order ($X_e = 2, 4$ or 6), a mirror plane normal to X_e , and an inversion centre at the point of intersection of X_e and m (Fig. 6.14)¹.

Rule II. Two mutually perpendicular mirror planes and a 2-fold axis along their line of intersection (Fig. 6.15).

Every lattice is centrosymmetric and has inversion centres on the lattice points and midway between any two of them. Thus, in a P-lattice, there are inversion centres at $0, 0, 0$; $\frac{1}{2}, 0, 0$; $0, \frac{1}{2}, 0$; $0, 0, \frac{1}{2}$; $\frac{1}{2}, \frac{1}{2}, 0$; $\frac{1}{2}, 0, \frac{1}{2}$; $0, \frac{1}{2}, \frac{1}{2}$ and $\frac{1}{2}, \frac{1}{2}, \frac{1}{2}$.

Symmetry of the Triclinic P-Lattice. The only point symmetry elements of the triclinic lattice are inversion centres (Fig. 6.16) at the coordinates given above. A projection of the symmetry elements parallel to c onto $x, y, 0$ is shown in Fig. 6.17. The z -coordinates implied for the inversion centres are 0 and $\frac{1}{2}$.

¹ $X_e = 2, 4$ or 6 . The illustration only includes the case $X_e = 2$. The rule is not completely general, since $m + \bar{1}$ can only generate 2.

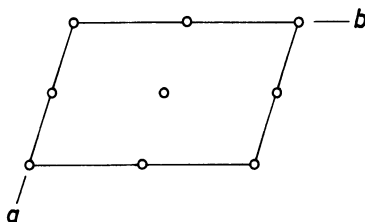
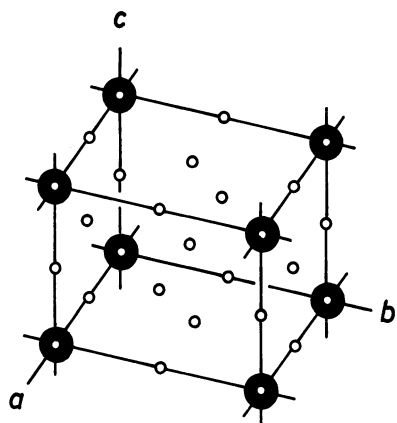


Fig. 6.17. Projection of the symmetry elements of space group $P\bar{1}$ onto $x, y, 0$. The z -coordinates of $\bar{1}$ are 0 and $\frac{1}{2}$, cf. Fig. 6.16

◀ Fig. 6.16. Triclinic P-lattice with the symmetry elements of space group $P\bar{1}$ (● $\bar{1}$ on lattice point)

Definition

The complete set of symmetry operations in a lattice or a crystal structure, or a group of symmetry operations including lattice translations is called a space group.

The space group of a primitive lattice which has only $\bar{1}$ is called $P\bar{1}$, and the conditions for its unit cell parameters: $a_0 \neq b_0 \neq c_0$; $\alpha \neq \beta \neq \gamma$.

Symmetry of the Monoclinic P-Lattice. The set of lattice planes from which we generated the monoclinic P-lattice (Fig. 6.8a) contain a set of 2-fold axes parallel to b . In addition, there are mirror planes normal to b at $x, 0, z$ and $x, \frac{1}{2}, z$ as well as the inversion centres that were present in the triclinic case. The location of the mirror planes follows from our first rule: (2 and $\bar{1}$ generate $m \perp 2$ at $\bar{1}$.) The array of symmetry elements of the lattice is shown in Fig. 6.8d in projections on $x, 0, z$ and $x, y, 0$.² Since the 2 is normal to the m , this combination is given the symbol $2/m$, pronounced “two over m ”. It is not necessary to represent the inversion centre, since $2/m$ implies $\bar{1}$, by Rule I.

The space group of the monoclinic P-lattice is $P2/m$, where it is conventional to choose the b -axis parallel to 2 and normal to m . The b -axis is called the *symmetry direction*. The a - and c -directions thus lie in the plane of m . This is called the “second setting”. Occasionally, the so-called “first setting” is encountered, with the c -direction parallel to 2 and normal to m . When this convention is used, the lattice is formed in the more usual way by the stacking of parallel lattice planes with $a_0 \neq b_0$, $\gamma \neq 90^\circ$, and a spacing of c_0 .

² In the diagrams, the symbol $\text{—}/$ indicates a mirror plane parallel to the plane of the page at heights of 0 and $\frac{1}{2}$. When the planes lie at other heights, such as $\frac{1}{4}$ and $\frac{3}{4}$, this is shown by adding $\frac{1}{4}$. Note that if there is an m , 2 or $\bar{1}$ at 0, it is also found at $\frac{1}{2}$; if it lies at $\frac{1}{4}$, it is also at $\frac{3}{4}$, etc.

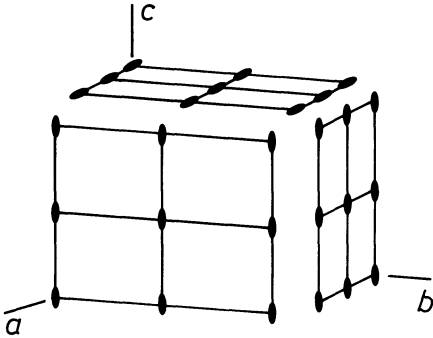


Fig. 6.18. Symmetry elements of space group $P 2/m 2/m 2/m$. The inversion centres are not shown

Symmetry of the Orthorhombic P-Lattice. In addition to the symmetry of the stacked planes (Fig. 6.9a), the orthorhombic P-lattice (Fig. 6.9b) has mirror planes normal to c at $x, y, 0$ and $x, y, \frac{1}{2}$ and inversion centres (Fig. 6.9d). Further, the application of rule I ($m + \bar{1} \Rightarrow 2 \perp m$) or rule II ($m \perp m \Rightarrow 2$) generates 2-fold axes at $x, 0, 0$; $x, 0, \frac{1}{2}$; $x, \frac{1}{2}, 0$; $x, \frac{1}{2}, \frac{1}{2}$; $0, y, 0$; $0, y, \frac{1}{2}$; $\frac{1}{2}, y, 0$ and $\frac{1}{2}, y, \frac{1}{2}$.

An alternative approach, which leads to the same result is the following: the unit cell of the orthorhombic P-lattice is a rectangular parallelepiped; it is bounded by three pairs of lattice planes with primitive rectangular unit meshes. These planes all have the same symmetry, that shown in Fig. 6.9a. The arrangement of symmetry elements is shown in Fig. 6.18, which should be compared with Fig. 6.9d. This set of symmetry elements can be given a symbol. The symmetry elements are arranged in the order of the crystallographic axes: a, b, c . Each axis has a 2-fold rotation axis parallel to it and mirror planes normal to it. Thus, the symbol for this space group is: $P 2/m 2/m 2/m$.

\downarrow \downarrow \downarrow
 a b c

Here the a -, b - and c -axes are all called *symmetry directions*. Fig. 6.19, gives a projection of all point symmetry elements of space group $P2/m2/m 2/m$, and separate projections showing those elements related to the symmetry directions a, b and c .

Symmetry of the Tetragonal P-Lattice. In addition to the symmetry of the stacked planes (Fig. 6.10a), the tetragonal P-lattice (Fig. 6.10b) has mirror planes $\perp c$ at $x, y, 0$ and $x, y, \frac{1}{2}$ and inversion centres (Fig. 6.10d). Further, the application of Rule I ($m + \bar{1} \Rightarrow 2 \perp m$) or rule II ($m \perp m \Rightarrow 2$) generates several 2-fold axes. It should be noted in passing that the projection of the symmetry elements for this space group in Fig. 6.10d is incomplete, since there are also glide planes present (Section 9.1). The same is true for the space groups in Figs. 6.11d–6.13d, which in addition contain screw axes. These symmetry elements are essentially irrelevant to our present purpose, and will not be considered further here.

The unit cell of a tetragonal P-lattice has the shape of a tetragonal prism; it is bounded by two lattice planes with square unit meshes and four planes with rectangular meshes, the symmetries of which are shown in Fig. 6.20. Compare Fig. 6.20 with Fig. 6.10d, noting that the 2-fold axes parallel to $[110]$ and $[\bar{1}\bar{1}0]$ do not appear in Fig. 6.20.

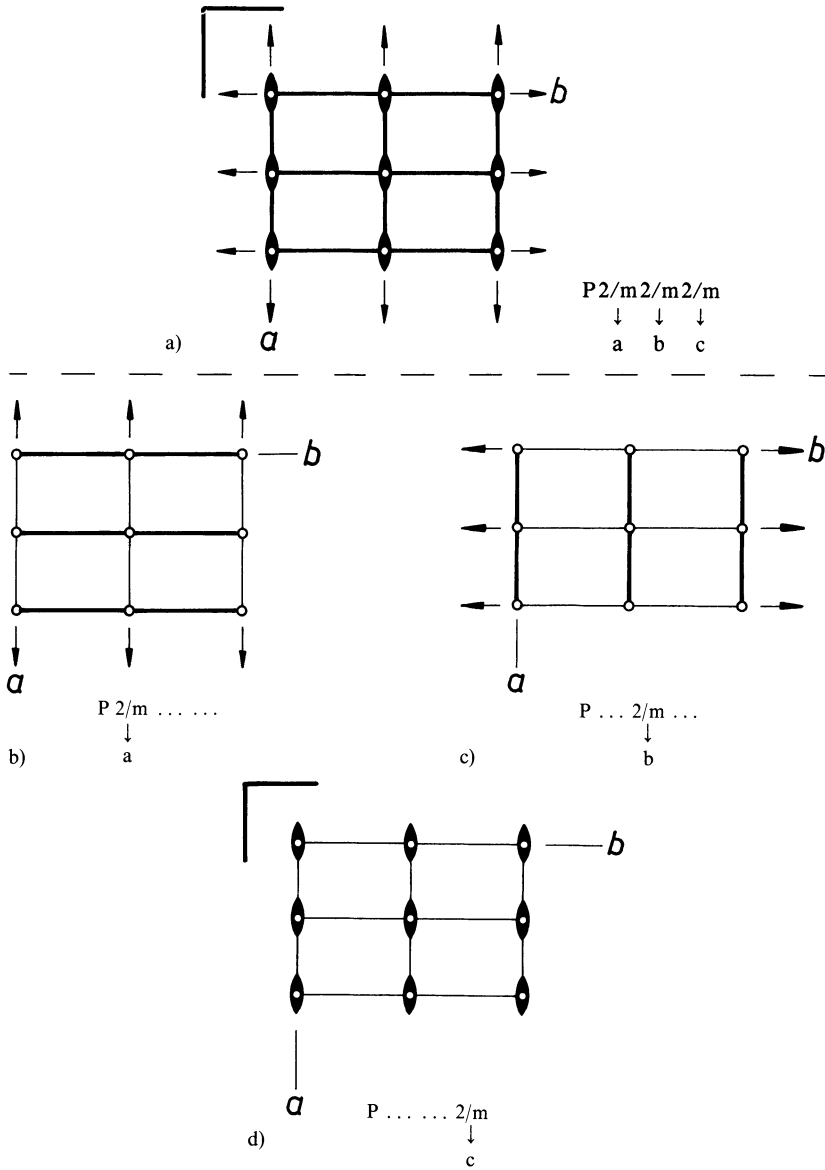


Fig. 6.19. a Space group $P 2/m 2/m 2/m$. In the other diagrams, only the symmetry elements corresponding to the symmetry directions a , b , c are shown:

b $P 2/m \dots \dots$, c $P \dots 2/m \dots$, d $P \dots \dots 2/m$
 $\downarrow \quad \downarrow \quad \downarrow$
 $a \quad b \quad c$

The 4-fold axes have the effect of making a and b equivalent, and they are often denoted as a_1 and a_2 , as in Fig. 6.10d. Similarly, the directions $[110]$ and $[\bar{1}\bar{1}0]$ are equivalent to one another. We must now introduce a further type of brackets, pointed brackets $\langle \rangle$. The symbol $\langle uvw \rangle$ denotes the lattice direction

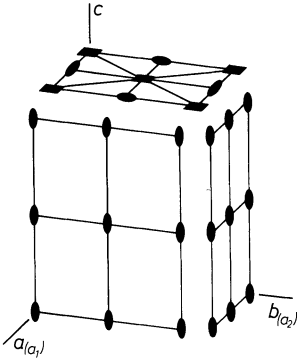


Fig. 6.20. Symmetry elements of space group $P 4/m 2/m 2/m$. The 2 along $\langle 110 \rangle$ and the inversion centres are not shown

$[uvw]$ and all directions equivalent to it. Similarly, $\langle a \rangle$ denotes the a-axis and all equivalent axes. For the tetragonal lattice, $\langle 110 \rangle$ implies both the $[110]$ and the $[\bar{1}\bar{1}0]$ directions, and $\langle a \rangle$ implies both the a- and b-axes.

In the space group symbol, the symmetry elements are given in the order: c, $\langle a \rangle$, diagonal of the $\langle a \rangle$ -axes, viz. $\langle 110 \rangle$, all of which are called *symmetry directions*. Thus, equivalent symmetry operations are given only once. The space group symbol is thus $P 4/m 2/m 2/m$.

$$\begin{array}{ccc} \downarrow & \downarrow & \downarrow \\ c & \langle a \rangle & \langle 110 \rangle. \end{array}$$

Figure 6.21 gives a projection of all point symmetry elements of space group $P4/m 2/m 2/m$, and separate projections showing those elements related to the *symmetry directions* c, $\langle a \rangle$ and $\langle 110 \rangle$.

Symmetry of the Hexagonal P-Lattice. In addition to the symmetry of the stacked planes, the hexagonal P-lattice, like the orthorhombic and tetragonal lattices, has mirror planes $\perp c$ at $x, y, 0$ and $x, y, \frac{1}{2}$, and inversion centres (Fig. 6.12d), so the application of Rule I ($m + \bar{1} \Rightarrow 2 \perp m$) or rule II ($m \perp m \Rightarrow 2$) generates several 2-fold axes.

Figure 6.22 shows the projection of a hexagonal P-lattice on (001). The 6-fold axis makes $a = b$, and a and b may also be written as a_1 and a_2 . Another direction, called the a_3 -axis, may then be added, making an angle of 120° with a_1 and a_2 , and equivalent to them both. Thus, $\langle a \rangle$ now represents a_1, a_2, a_3 . The diagonals bisecting the $\langle a \rangle$ -axes are $[210]$, $[\bar{1}\bar{2}0]$ and $[\bar{1}\bar{1}0]$. As for the tetragonal lattice, the symmetry elements are arranged in the space group symbol in the order, c, $\langle a \rangle$, diagonals of the $\langle a \rangle$ axes, viz. $\langle 210 \rangle$, all of which are called *symmetry directions*.

The space group symbol is thus: $P 6/m 2/m 2/m$.

$$\begin{array}{ccc} \downarrow & \downarrow & \downarrow \\ c & \langle a \rangle & \langle 210 \rangle. \end{array}$$

Figure 6.23 gives a projection of all the point-symmetry elements of space group $P6/m2/m2/m$, and separate diagrams showing those elements related to the *symmetry directions* c, $\langle a \rangle$ and $\langle 210 \rangle$.

Symmetry of the Cubic P-Lattice. The symmetry of the stacking planes is shown in Fig. 6.13a. The stacking results in a lattice with a cubic unit cell

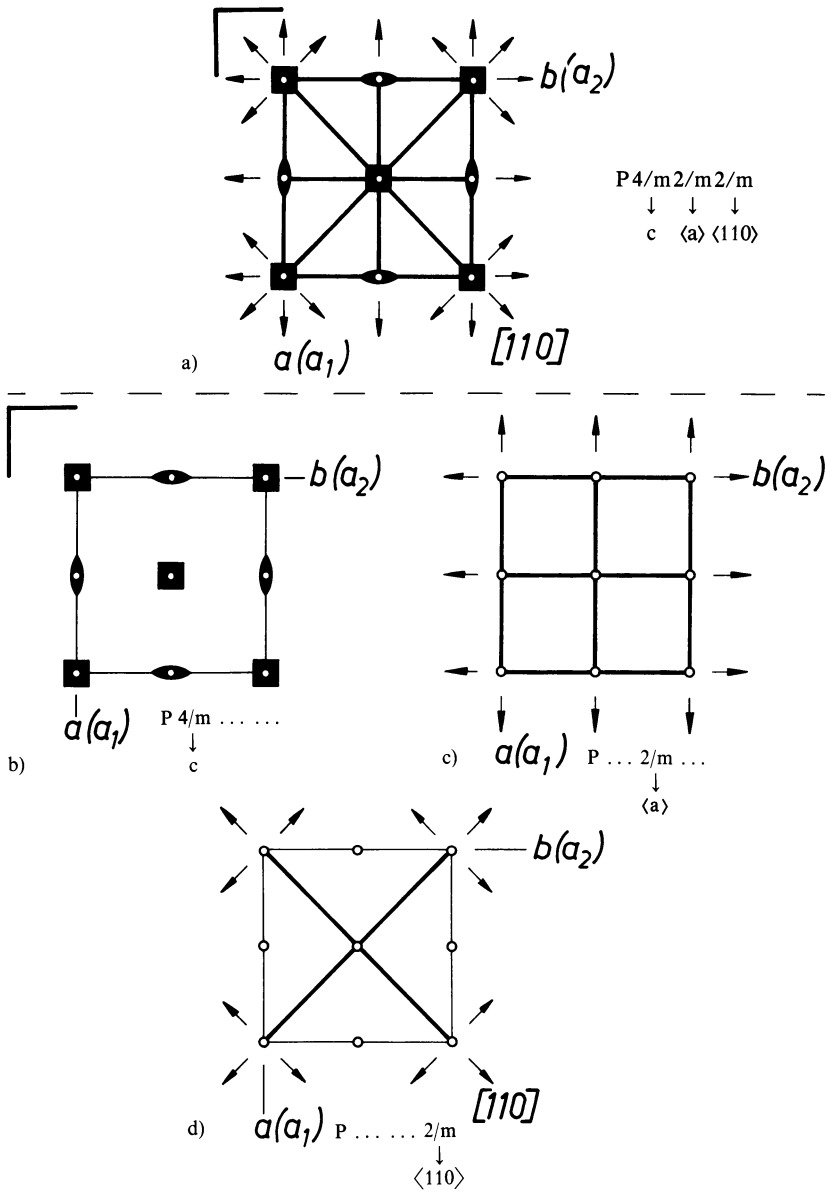


Fig. 6.21. a Space group $P4/m2/m2/m$. In the other diagrams, only the symmetry elements corresponding to the symmetry directions c , $\langle a \rangle$, $\langle 110 \rangle$ are shown:

b $P4/m \dots \dots$, c $P \dots 2/m \dots$, d $P \dots \dots 2/m$
 $\downarrow \quad \quad \quad \downarrow \quad \quad \quad \downarrow$
 $c \quad \quad \quad \langle a \rangle \quad \quad \quad \langle 110 \rangle$

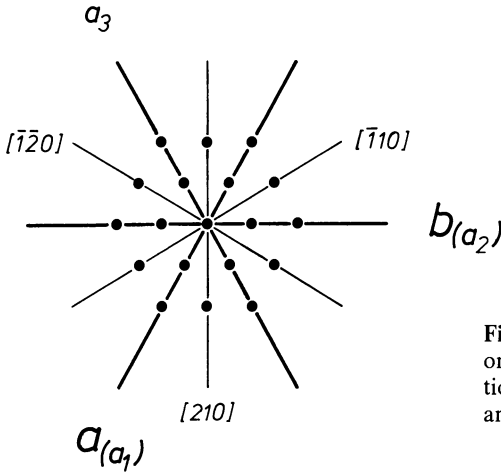


Fig. 6.22. Hexagonal P-lattice projected on (001) emphasising the symmetry directions $\langle a \rangle = a_1, a_2, a_3$ and $\langle 210 \rangle = [210], [\bar{1}10]$ and $[\bar{1}20]$

($a_0 = b_0 = c_0$). This means that the lattice planes $0, x, z$ and $x, 0, z$ have the same symmetry as $x, y, 0$, see Fig. 6.13d. This equivalence of the planes generates four 3-fold axes along the body diagonals of the unit cell as well as inversion centres, so these axes are represented as $\bar{3} (\equiv 3 + \bar{1})$. Application of rule I ($m + \bar{1} \Rightarrow 2 \perp m$) or rule II ($m \perp m \Rightarrow 2$) generates 2-fold axes parallel to $[110]$ and equivalent directions. (These 2-fold axes are not included in Fig. 6.13d).

In the space group symbol, the symmetry elements are given in the order: $\langle a \rangle, \langle 111 \rangle =$ body diagonals of the unit cell, $\langle 110 \rangle =$ face diagonals of the unit cell. The space group symbol for the cubic P-lattice is thus: $P 4/m \bar{3} 2/m$.

$\downarrow \quad \downarrow \quad \downarrow$
 $\langle a \rangle \quad \langle 111 \rangle \quad \langle 110 \rangle$

Figure 6.24 gives a projection of all the point-symmetry elements of space group $P4/m \bar{3} 2/m$, and separate diagrams showing those elements related to the symmetry directions $\langle a \rangle, \langle 111 \rangle$ and $\langle 110 \rangle$.

6.3 The Centred Lattices

Consideration of the primitive lattices we have so far generated raises the question as to whether it is possible to import into the P-lattices one or more further lattice planes without destroying the symmetry. Let us first consider the monoclinic P-lattice.

Figure 6.25 shows the monoclinic P-lattice and its symmetry, $P2/m$, projected onto $x, 0, z$ (see also Fig. 6.8d). Each point of the lattice has $2/m$ symmetry, which implies the presence of an inversion centre in the point. Insertion of new lattice planes parallel to (010) into the lattice is only possible if the lattice points fall on a position which also has symmetry $2/m$, i.e. on $\frac{1}{2}, 0, 0; 0, \frac{1}{2}, 0; 0, 0, \frac{1}{2}; \frac{1}{2}, \frac{1}{2}, 0; \frac{1}{2}, 0, \frac{1}{2}; 0, \frac{1}{2}, \frac{1}{2}$, or $\frac{1}{2}, \frac{1}{2}, \frac{1}{2}$. These possibilities must each be considered.

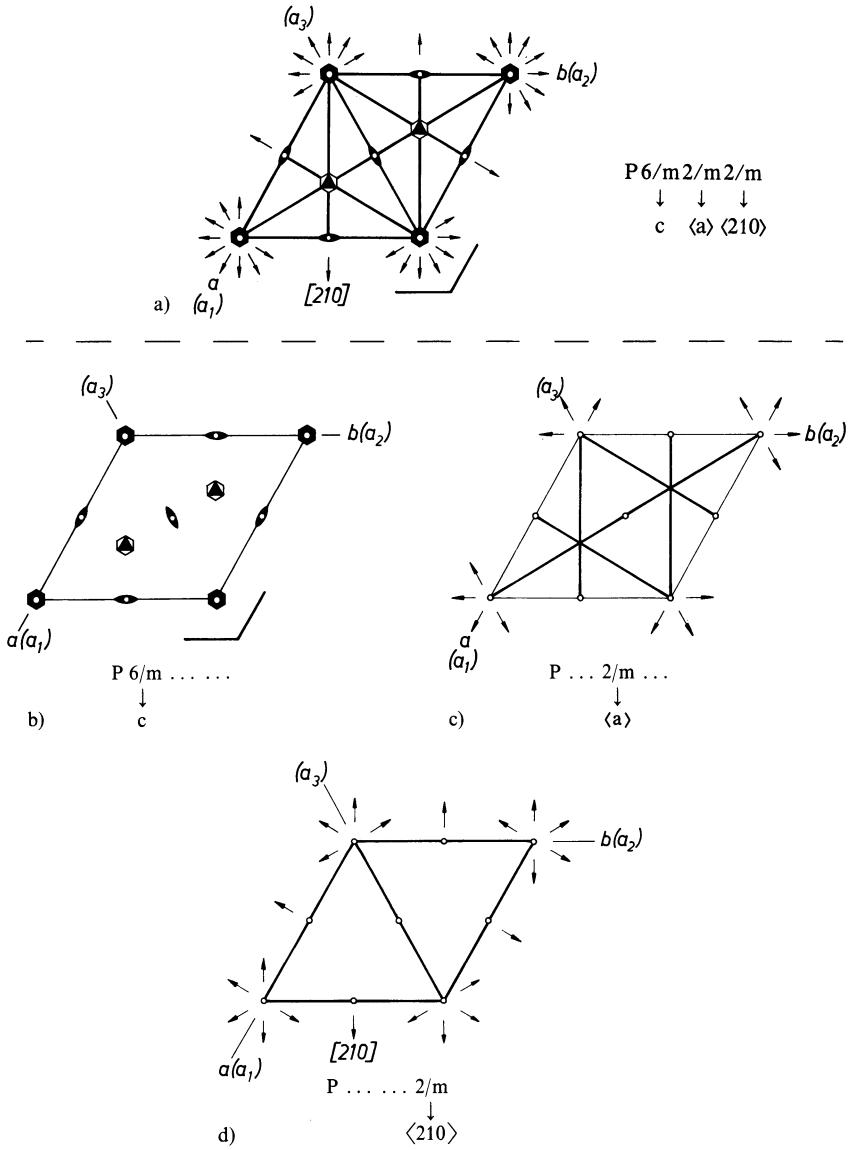


Fig. 6.23. a Space group $P 6/m 2/m 2/m$. In the other diagrams, only the symmetry elements corresponding to the symmetry directions c , $\langle a \rangle$, $\langle 210 \rangle$ are shown:

b $P 6/m \dots \dots$, c $P \dots 2/m \dots$, d $P \dots \dots 2/m$
 $\downarrow \quad \quad \downarrow \quad \quad \downarrow$
 $c \quad \quad \langle a \rangle \quad \quad \langle 210 \rangle$

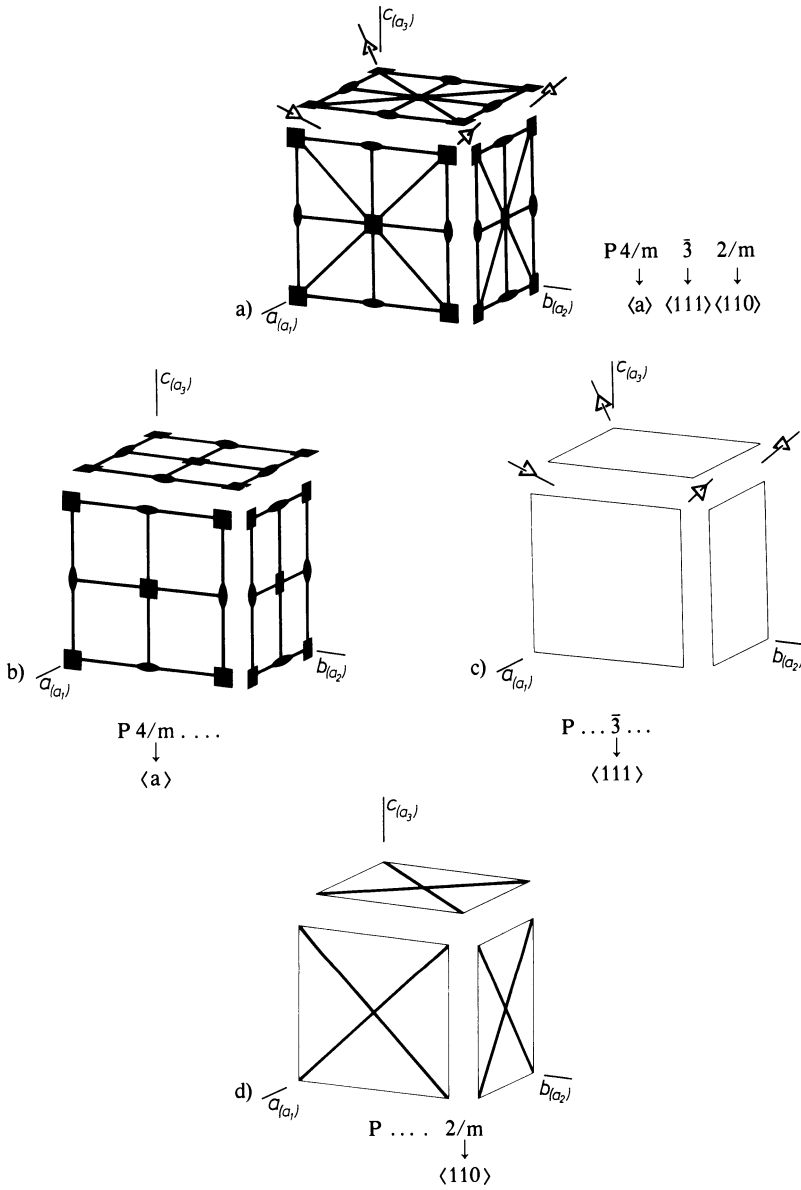


Fig. 6.24. a Space group $P 4/m \bar{3} 2/m$. In the other diagrams, only the symmetry elements corresponding to the symmetry directions $\langle a \rangle$, $\langle 111 \rangle$, $\langle 110 \rangle$ are shown.

b $P 4/m \dots$, **c** $P \dots \bar{3} \dots$, **d** $P \dots 2/m$
 $\downarrow \quad \quad \downarrow \quad \quad \downarrow$
 $\langle a \rangle \quad \quad \langle 111 \rangle \quad \quad \langle 110 \rangle$

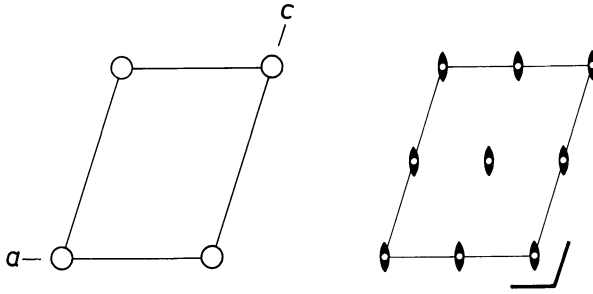


Fig. 6.25. The monoclinic P-lattice and its symmetry elements projected onto $x, 0, z$ (\circ lattice point with $y = 0$)

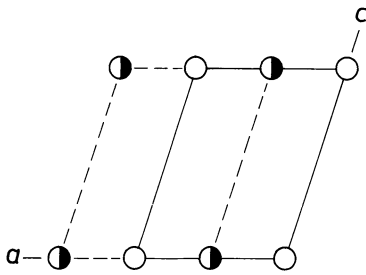


Fig. 6.26. The monoclinic C-lattice projected on $x, 0, z$ (\bullet represents a lattice point with $y = \frac{1}{2}$)

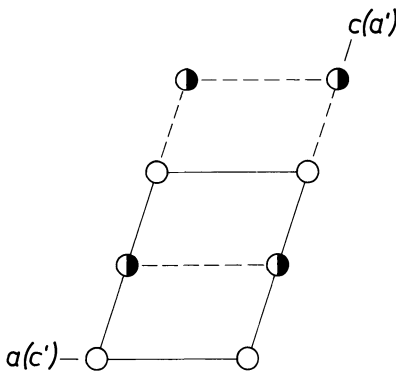


Fig. 6.27. The monoclinic A-lattice (a_0, b_0, c_0) can, by interchanging a and c , be converted to a monoclinic C-lattice (a'_0, b_0, c'_0)

a) *Lattice Plane with Lattice Point at $\frac{1}{2}, \frac{1}{2}, 0$* (Fig. 6.26). These new lattice points centre the a, b -face of the unit cell. This is called a C-face centred lattice, or more simply a *C-lattice*, although this name is formally inexact, being used to describe a “lattice with a C-face centred unit cell”. The monoclinic C-lattice is illustrated in Table 6.3.

b) *Lattice Plane with Lattice Point at $0, \frac{1}{2}, \frac{1}{2}$* (Fig. 6.27). If the new plane centres the b, c -face, the result will be an A-face centred lattice. Since, however, in monoclinic cells, the a and c axes may lie anywhere in the mirror plane, they may be swapped, converting the A-lattice into a C-lattice.

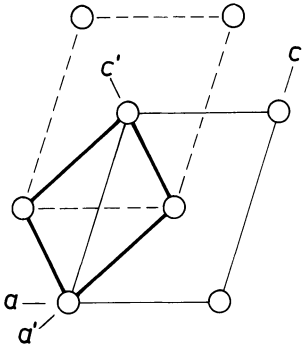


Fig. 6.28. The monoclinic B-lattice (a_0, b_0, c_0) can be converted to a smaller monoclinic P-lattice (a'_0, b_0, c'_0)

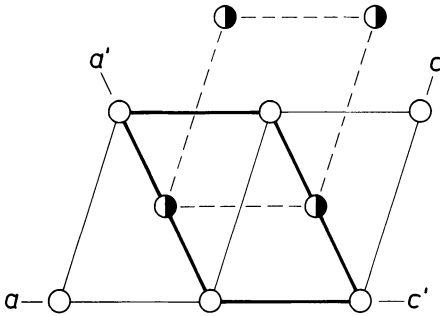


Fig. 6.29. The monoclinic I-lattice (a_0, b_0, c_0) can be converted to a monoclinic C-lattice (a'_0, b_0, c'_0)

c) *Lattice Plane with Lattice Point at $\frac{1}{2}, 0, \frac{1}{2}$* (Fig. 6.28). The result is now a B-lattice, from which a smaller, primitive unit cell can be chosen (outlined in bold) that still has monoclinic symmetry.

d) *Lattice Plane with Lattice Point at $\frac{1}{2}, \frac{1}{2}, \frac{1}{2}$* (Fig. 6.29). A lattice is formed, with a lattice point at the body centre of the unit cell. This is called a body centred or I-lattice (from the German *innenzentriert*). As with the A-lattice, choice of different axes convert this to a monoclinic C-lattice.

e) *Lattice Plane with Lattice Point at $\frac{1}{2}, 0, 0$; $0, \frac{1}{2}, 0$ or $0, 0, \frac{1}{2}$* . In any of these cases, the result is simply to halve the cell; no new type of lattice is formed.

f) It is also possible to introduce two lattice planes at the same time, for example, as in both a) and b), giving additional lattice points at $\frac{1}{2}, \frac{1}{2}, 0$ and $0, \frac{1}{2}, \frac{1}{2}$ (Fig. 6.30a). Since it is necessary that all lattice points have the same environment, and parallel lattice lines the same period a further lattice point (shown with a dashed outline) must be added at $\frac{1}{2}, 0, \frac{1}{2}$. Thus, all the faces of the unit cell are now centred, giving an all-face centred or F-lattice.

A general principle following from this is that *a lattice centred on two faces cannot exist because the requirement that all lattice points are identical and parallel lattice lines have the same lattice period will convert it to an all-face centred lattice.*

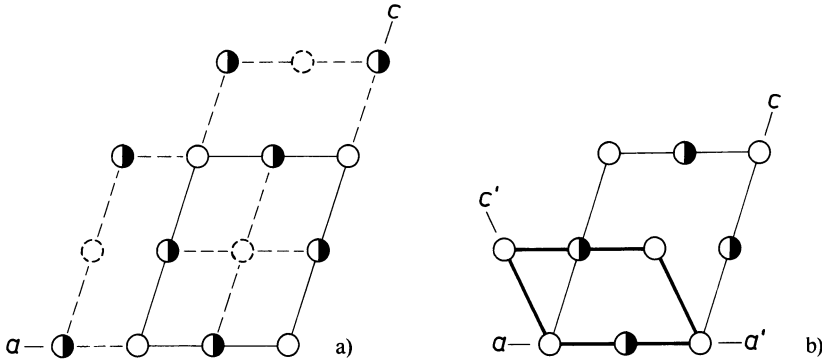


Fig. 6.30 a, b. The development of the monoclinic F-lattice a. The monoclinic F-lattice (a_0, b_0, c_0) can be converted to a monoclinic C-lattice (a'_0, b_0, c'_0) b

The monoclinic F-lattice can, in fact, be reduced to a C-lattice of half the volume, as is shown in Fig. 6.30b.

We have now considered all the possibilities for introducing extra lattice planes into the monoclinic P-lattice, and have shown that all of these may be represented either as P- or C-lattices ($A, I, F \rightarrow C$; $B \rightarrow P$).

The orthorhombic lattice may be developed in the same way, giving rise of orthorhombic A-, B-, C-, I- and F-lattices. The I- and F-lattices are now not reducible as they were in the monoclinic case. The A-, B- and C-lattices are alternative representations of the same lattice; the a -, b -, and c -axes can always be chosen so as to generate a C-lattice. There are a few space groups which are customarily treated as having an A-lattice (see Table 9.2). The C-lattice may also be developed by the vertical stacking of planes with the centred rectangular unit mesh (Fig. 6.6b).

Similar considerations to those in the monoclinic case lead from the tetragonal P-lattice to the tetragonal I-lattice, and from the cubic P-lattice to the cubic I- and F-lattices (Table 6.3).

An examination of the hexagonal P-lattice will show that the only point with the same symmetry as $0, 0, 0$ is $0, 0, \frac{1}{2}$. The addition of a lattice plane there will merely halve the size of the unit cell.

A 6-fold axis always contains a 3-fold axis. Starting from this fact, the plane lattice with a 120° rhombus as unit mesh contains a 3-fold axes at $0, 0, z$; $\frac{1}{3}, \frac{2}{3}, z$ and $\frac{2}{3}, \frac{1}{3}, z$ (Fig. 6.11a). It is possible to add a second plane at a height of $\frac{1}{3}c_0$ with a lattice point on the 3-fold axis at $\frac{2}{3}, \frac{1}{3}, z$ and a third plane at a height of $\frac{2}{3}c_0$ with a lattice point on the 3-fold axis at $\frac{1}{3}, \frac{2}{3}, z$ (Fig. 6.11 b). The fourth plane will then come at a height of c_0 , directly above the first. This new arrangement of lattice points reduces the 6-fold axes to 3-fold and removes the mirror planes at $x, 0, z$; $0, y, z$ and x, x, z as well as the 2-fold axes parallel to the c -axis. The resulting lattice has the shape of a hexagonal lattice ($a_0 = b_0 \neq c_0$, $\alpha = \beta = 90^\circ$, $\gamma = 120^\circ$) but contains three lattice points per unit cell ($0, 0, 0$; $\frac{2}{3}, \frac{1}{3}, \frac{1}{3}$; $\frac{1}{3}, \frac{2}{3}, \frac{2}{3}$).

It is possible, however, to describe this lattice by a primitive unit cell ($a'_0 = b'_0 = c'_0$, $\alpha' = \beta' = \gamma'$). If the first cell is used to describe the lattice, it is called

a trigonal R-lattice, if the second is used, the lattice is called rhombohedral P (Fig. 6.11b). The unit cell of the rhombohedral P-lattice has indeed the shape of a rhombohedron, with six rhombi as faces.

Special cases of the rhombohedral P-lattice are: (a) $\alpha' = 90^\circ$ gives the cubic P-lattice; (b) $\alpha' = 60^\circ$ gives the cubic F-lattice and (c) $\alpha' = 109.47^\circ$ gives the cubic I-lattice.

6.4 The Symmetry of the Centred Lattices

With the exception of the trigonal R-lattice, the derivation above of the centred lattices always paid strict attention to retaining the full symmetry of the corresponding P-lattice. All the symmetry elements of the P-lattice remained, only the translation properties were altered. The centring does indeed introduce new symmetry elements, notably screw axes and glide planes (see Chap. 9.1). In spite of this, the symbols for the space groups of the centred lattices may easily be given, since the new symmetry elements do not appear in them.

Now it is not difficult to derive the symbol for the trigonal R-lattice from the reduced symmetry of the lattice planes. There are, in addition to the normal ones, further inversion centres, which, by Rule I ($m + \bar{1} \Rightarrow 2 \perp m$), generate a set of 2-fold axes parallel to a_1, a_2, a_3 (Fig. 6.11 d). The 3-fold axis becomes $\bar{3}$ since $3 + \bar{1} \Rightarrow \bar{3}$. The order of the symmetry directions here is: c, $\langle a \rangle$, giving the symbol $R \bar{3} 2/m$.

$\downarrow \quad \downarrow$
 c $\langle a \rangle$.

The space group symbols of the 14 Bravais lattices are given in Table 6.4 in the same order as Table 6.3.

Table 6.3 contains the 14 lattices, which are usually known as the *Bravais lattices*.

Table 6.4. The space group symbols for the 14 Bravais lattices

	P	C	I	F
Triclinic	$P\bar{1}$			
Monoclinic	$P2/m$	$C2/m$		
Orthorhombic	$P2/m2/m2/m$	$C2/m2/m2/m$	$I2/m2/m2/m$	$F2/m2/m2/m$
Tetragonal	$P4/m2/m2/m$		$I4/m2/m2/m$	
Trigonal	$P6/m2/m2/m$	$R\bar{3}2/m$		
Hexagonal				
Cubic	$P4/m\bar{3}2/m$		$I4/m\bar{3}2/m$	$F4/m\bar{3}2/m$

Table 6.5. Number and coordinates of the lattice points in the unit cells of the Bravais lattices

Lattice	No. of lattice points in unit cell	Coordinates of lattice points in unit cell
P	1	0, 0, 0
A	2	0, 0, 0; $0, \frac{1}{2}, \frac{1}{2}$
B	2	0, 0, 0; $\frac{1}{2}, 0, \frac{1}{2}$
C	2	0, 0, 0; $\frac{1}{2}, \frac{1}{2}, 0$
I	2	0, 0, 0; $\frac{1}{2}, \frac{1}{2}, \frac{1}{2}$
R	3	0, 0, 0; $\frac{2}{3}, \frac{1}{3}, \frac{1}{3}$; $\frac{1}{3}, \frac{2}{3}, \frac{2}{3}$
F	4	0, 0, 0; $\frac{1}{2}, \frac{1}{2}, 0$; $\frac{1}{2}, 0, \frac{1}{2}$; $0, \frac{1}{2}, \frac{1}{2}$

The 14 Bravais lattices represent the 14 and only ways in which it is possible to fill space by a three-dimensional periodic array of points.

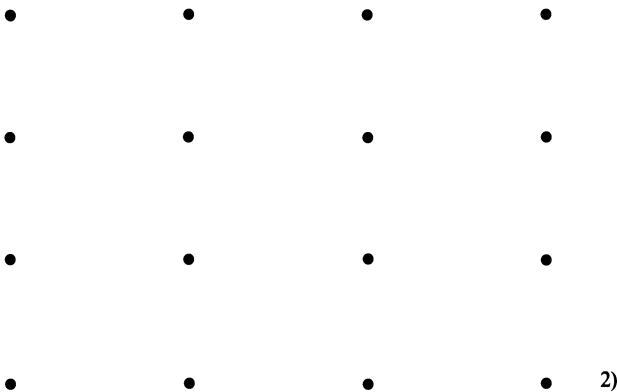
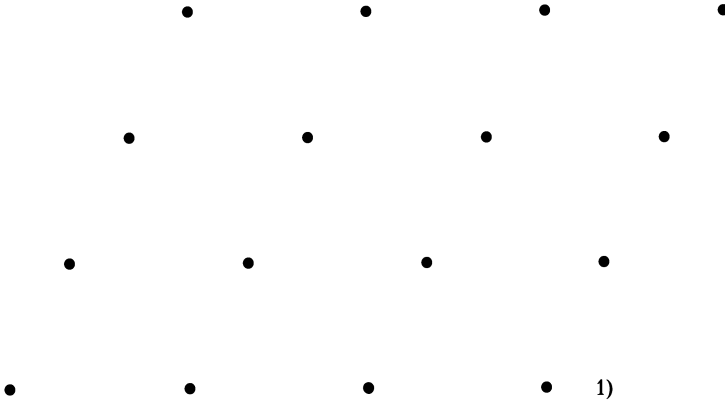
All crystals are built up on one of these lattices. In Chapter 3, we defined a crystal structure as a lattice plus a basis. While the number of lattices is fixed at 14, there are infinitely many possible ways of arranging atoms in cell. *Any crystal structure, however, has only one Bravais lattice.*

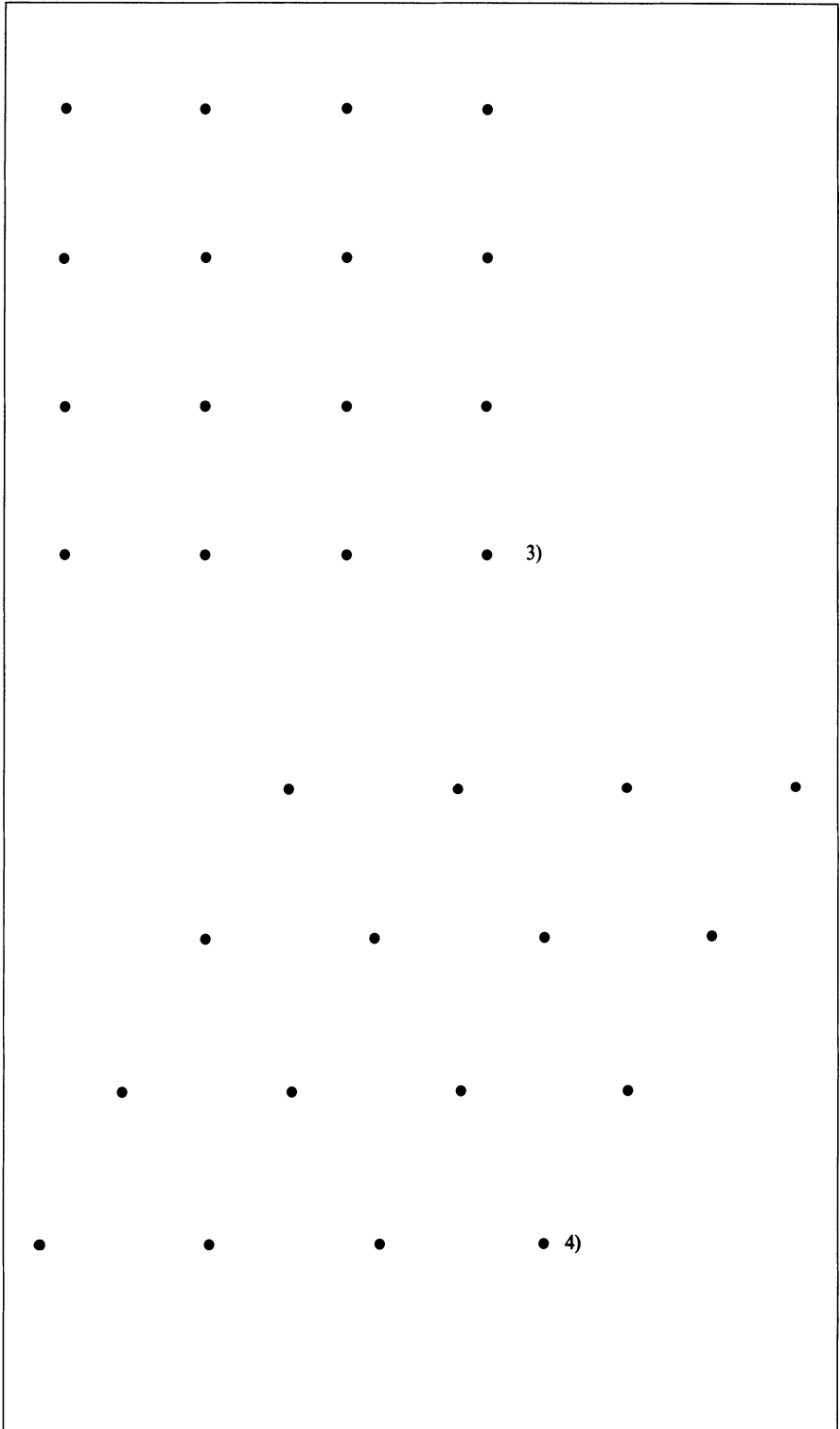
The number and coordinates of the lattice points in the unit cells of the Bravais lattices is given in Table 6.5.

EXERCISES

Exercise 6.1. Symmetry of plane lattices.

- Determine the symmetry elements for the given plane lattices, and draw these in their places on the lattice. Note that only m , 2, 3, 4 and 6 normal to the plane of the paper need be considered.
- Draw in the edges of the unit mesh and give the lattice parameters. Which lattice parameters are equivalent and why?
- Determine which symmetry elements are themselves equivalent by symmetry.

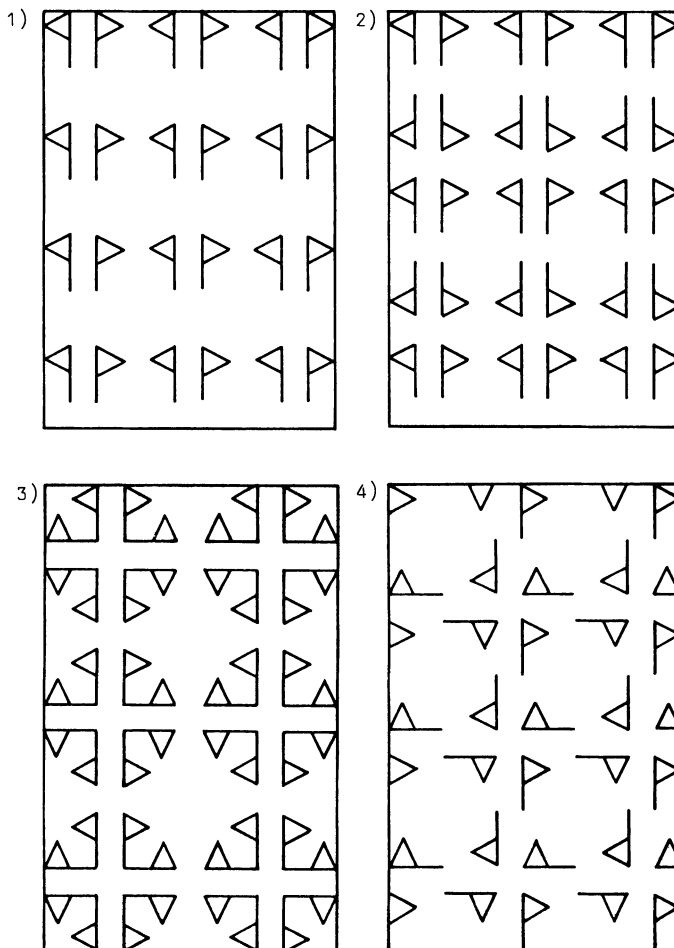


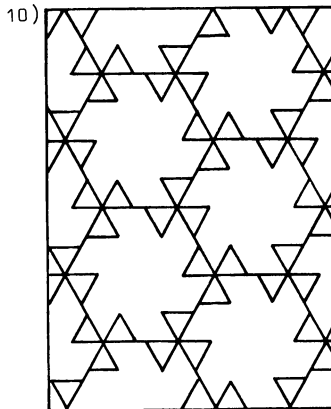
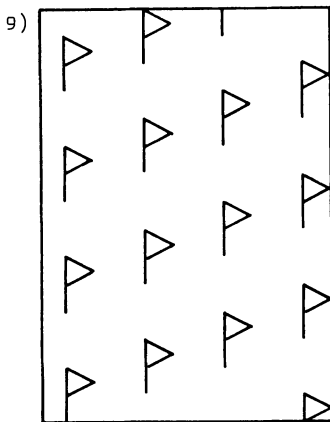
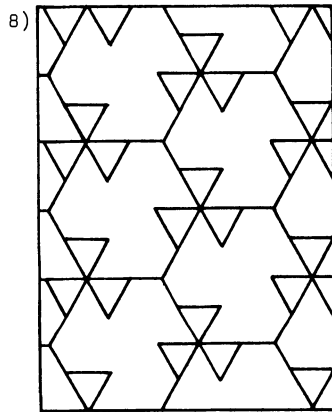
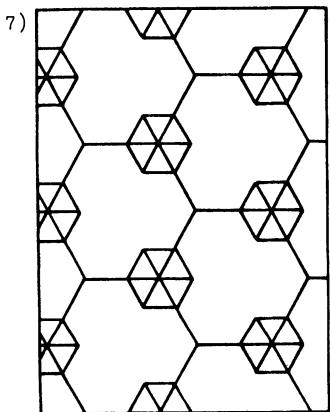
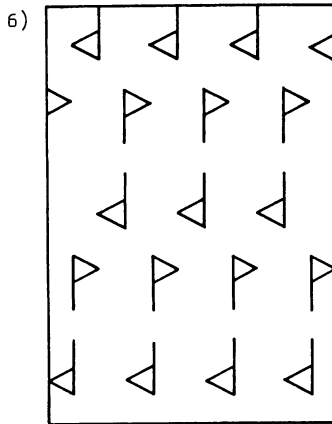
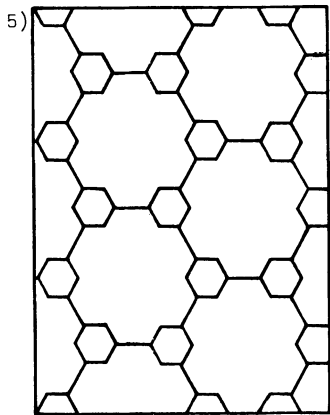


Exercise 6.2. For the given two-dimensional structures, determine:

- The unit mesh.
- The symmetry elements. It is only necessary to indicate those symmetry elements which lie within the unit mesh. As in Exercise 6.1, only m , 2 , 3 , 4 and 6 normal to the plane of the paper need be considered.

Two-dimensional structures after Kockel





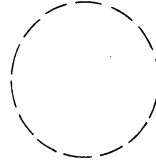
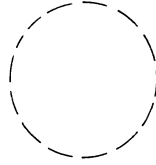
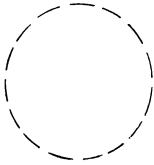
Exercise 6.3. (Refer to Symmetry Rule I)

a) Draw the given combinations of two symmetry elements on the stereographic projection. As the inversion centre is a single point, it cannot be shown on the stereogram, but may be taken to lie at the centre of the projection. Draw in a pole which does not lie on any symmetry element, and allow the symmetry elements to operate on it. On the basis of the positions of the resulting poles, determine the third symmetry element generated by the combination of the given symmetry elements, and draw it on the stereogram.

1) $2 \perp m$

2) $2 + \bar{1}$

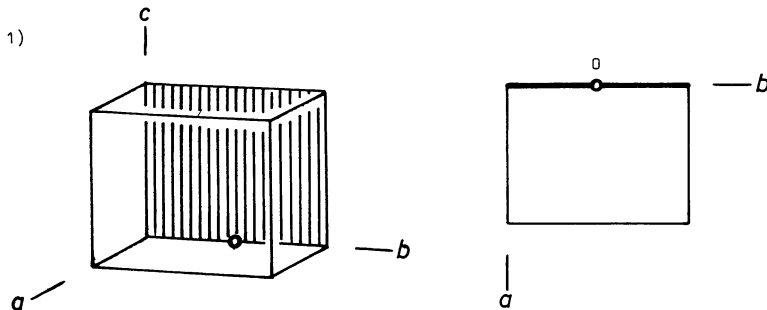
3) $m + \bar{1}$



Demonstrate that:

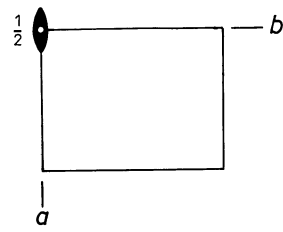
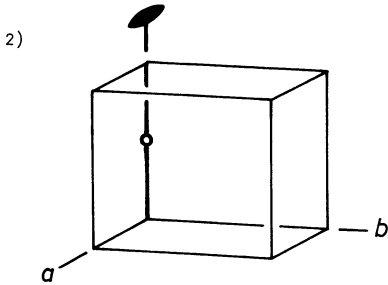
$4 \perp m \rightarrow \bar{1}$	$4 + \bar{1} \rightarrow m$	but $m + \bar{1} \rightarrow 2.$
$6 \perp m \rightarrow \bar{1}$	$6 + \bar{1} \rightarrow m$	

b) Below are given an orthorhombic unit cell and its projection on $x, y, 0$. Draw the third symmetry element generated by the two given elements on either or both of these, give its symbol and the coordinates of its position. Note that only one symmetry element of each type is drawn in the cell.

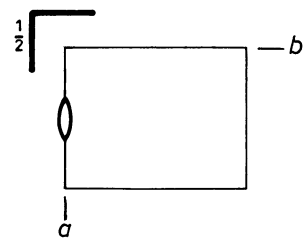
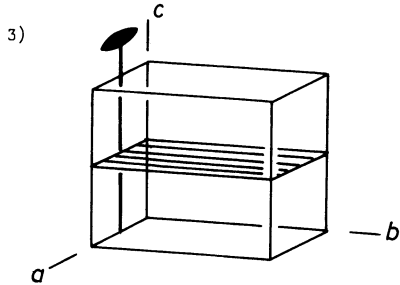


m at $0, y, z$ and $\bar{1}$ at $0, \frac{1}{2}, 0$ generate ... at ...

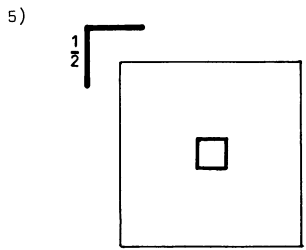
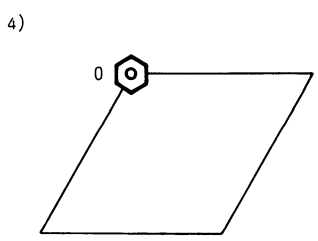




2 at $0, 0, z$ and $\bar{1}$ at $0, 0, \frac{1}{2}$ generate ... at ...

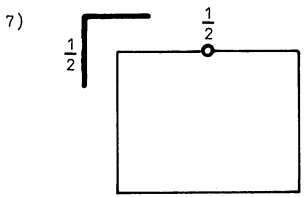
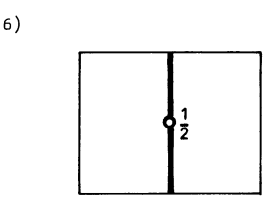


2 at $\frac{1}{2}, 0, z$ and m at $x, y, \frac{1}{2}$ generate ... at ...



6 at $0, 0, z$ and $\bar{1}$ at $0, 0, 0$ generate ... at ...

4 at $\frac{1}{2}, \frac{1}{2}, z$ and m at $x, y, \frac{1}{2}$ generate ... at ...

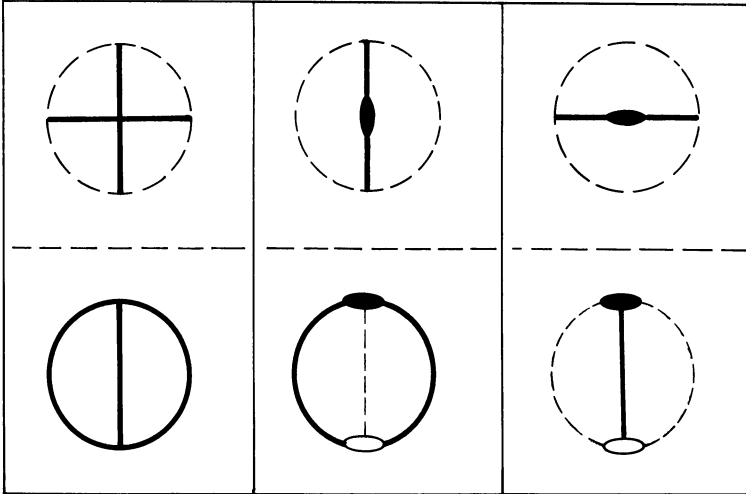


m at $x, \frac{1}{2}, z$ and $\bar{1}$ at $\frac{1}{2}, \frac{1}{2}, \frac{1}{2}$ generate ... at ...

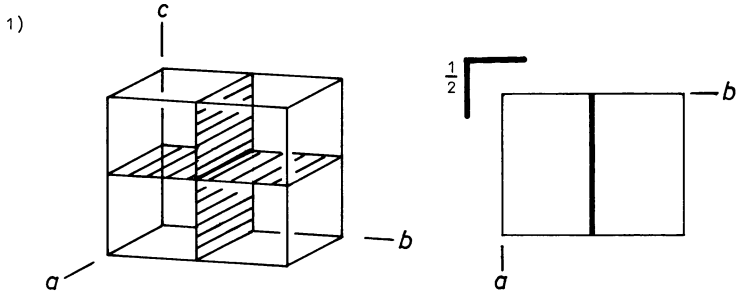
m at $x, y, \frac{1}{2}$ and $\bar{1}$ at $0, \frac{1}{2}, \frac{1}{2}$ generate ... at ...

Exercise 6.4. (Refer to symmetry rule II)

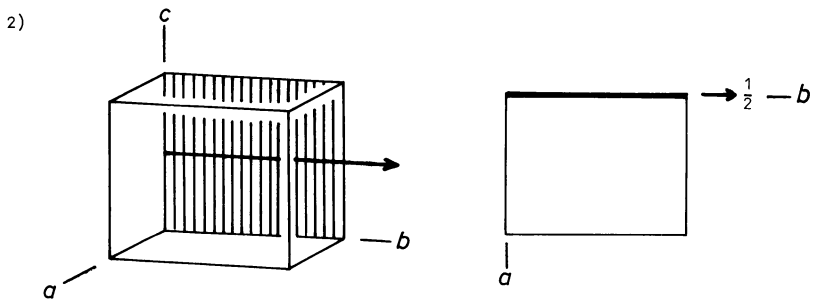
- a) On the following stereograms, draw in the third symmetry element generated by the combination of the given two.



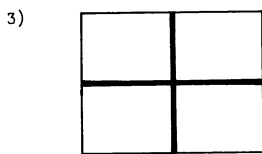
b) An orthorhombic unit cell and its projection on $x, y, 0$ are given below. On either of them, draw the third symmetry element generated by the two given elements, and give its symbol and the coordinates of its position.



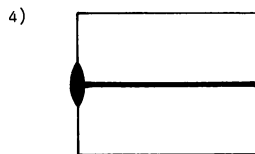
m at $x, \frac{1}{2}, z$ and at $x, y, \frac{1}{2}$ generate ... at ...



m at $0, y, z$ and 2 at $0, y, \frac{1}{2}$ generate ... at ...



m at $x, \frac{1}{2}, z$ and at $\frac{1}{2}, y, z$ generate ... at ...

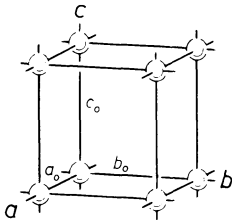


m at $\frac{1}{2}, y, z$ and 2 at $\frac{1}{2}, 0, z$ generate ... at ...

Exercise 6.5.

Which of the 14 Bravais lattices are each of the following?

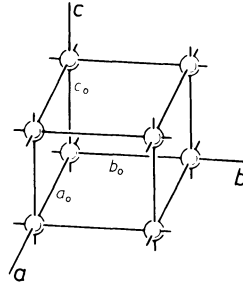
a)



$$a_0 = b_0 = c_0$$

$$\alpha = \beta = \gamma = 90^\circ$$

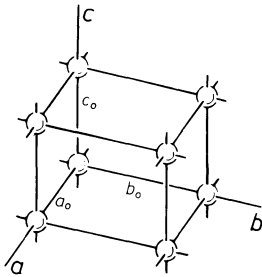
b)



$$a_0 \neq b_0 \neq c_0$$

$$\alpha = \gamma = 90^\circ \quad \beta > 90^\circ$$

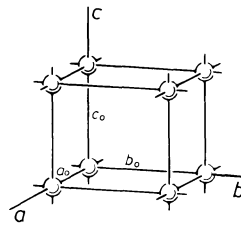
c)



$$a_0 \neq b_0 \neq c_0$$

$$\alpha \neq \beta \neq \gamma$$

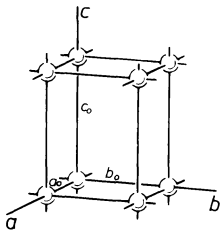
d)



$$a_0 \neq b_0 \neq c_0$$

$$\alpha = \beta = \gamma = 90^\circ$$

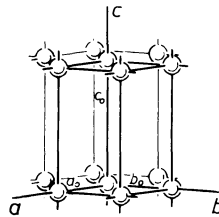
e)



$$a_0 = b_0 \neq c_0$$

$$\alpha = \beta = \gamma = 90^\circ$$

f)



$$a_0 = b_0 \neq c_0$$

$$\alpha = \beta = 90^\circ \quad \gamma = 120^\circ$$

Exercise 6.6.

- a) Draw the unit cells of each of the following lattices as a projection on $x, y, 0$, or, in the monoclinic case, on $x, 0, z$. Use a scale of $1 \text{ \AA} = 1 \text{ cm}$.

Monoclinic P: $a_0 = 5.5, b_0 = 4.0, c_0 = 4.0 \text{ \AA}; \beta = 105^\circ$

Orthorhombic P: $a_0 = 3.0, b_0 = 4.5, c_0 = 4.0 \text{ \AA}$

Tetragonal P: $a_0 = 4.0, c_0 = 3.0 \text{ \AA}$

Hexagonal P: $a_0 = 4.0, c_0 = 3.0 \text{ \AA}$

Trigonal R: $a_0 = 4.5, c_0 = 3.0 \text{ \AA}$

- b) Determine the symmetry operations of lattices you have drawn, and plot the symmetry elements on the projection of the lattice.
- c) Now use a coloured pen to colour the symmetry elements, using colours so that symmetry elements have the same colour if they belong to the same symmetry direction (i.e. one of the various symmetry directions used in the space group symbol).
- d) Give the space group symbol for each lattice, making use of the colours of symmetry elements you have chosen in (c).

Exercise 6.7. Derive the three centred orthorhombic lattices (cf. Section 6.3).

- a) What is the symmetry of a lattice point in the orthorhombic P-lattice?
- b) Which points in the unit cell of the P-lattice have the same symmetry as the lattice points? Give their coordinates.
- c) Bring a lattice plane, parallel to (001) into a position such that a lattice point comes into coincidence with each of the positions you have determined in (b). Repeat the above exercise with two planes.

Exercise 6.8. Similarly, derive the centred tetragonal lattices.

7 The Seven Crystal Systems

In the various lattices, the vectors \vec{a} , \vec{b} and \vec{c} must be chosen and associated with a system of suitable crystallographic axes, $\mathbf{a}, \mathbf{b}, \mathbf{c}$. This is not done arbitrarily. Generally, so far as is possible, the choices are made so that the direction of rotation axes, rotoinversion axes and the normals to mirror planes are parallel to $\vec{a}, \vec{b}, \vec{c}$ and to $\mathbf{a}, \mathbf{b}, \mathbf{c}$:

$$\vec{a}, \vec{b}, \vec{c}; \mathbf{a}, \mathbf{b}, \mathbf{c} // X, \bar{X}, \text{normal to } m.$$

It is possible to distinguish six axial systems (systems of crystallographic axes), which are given in Figs. 6.7c–6.13c and which correspond to the six primitive lattices. These axial systems naturally apply equally to the centred lattices. On this basis, we may define a crystal system:

Definition

All lattices, all crystal structures and all crystal morphologies which can be defined by the same axial system belong to the same crystal system.

This definition distinguishes six crystal systems. It is, however, usual to separate the system of crystallographic axes based on $a = b \neq c$, $\alpha = \beta = 90^\circ$, $\gamma = 120^\circ$ into a hexagonal and a trigonal crystal system. The hexagonal system is characterised by the presence of 6 or $\bar{6}$, while the trigonal is characterised by 3.

In Table 7.1, the seven crystal systems are listed along with the restrictions on the axial system. It is important to remember, however, that equivalence of crystallographic axes and special values of the angles are simply a consequence of the underlying symmetry. Those symmetry elements which cause equivalences to arise between crystallographic axes are listed. A full list of the symmetry elements characterising the various crystal systems is given in Table 8.9.

The space groups of the lattices themselves have the highest symmetry which can occur in that crystal system (cf. Table 6.4). Symmetry elements in each crystal system can only be orientated in certain directions with respect to one another, since it is not those symmetry elements alone, but they and all their combinations which must be in accordance with the properties of the space lattice. The symmetry of the lattice automatically determines all the angles

Table 7.1. The seven crystal systems

Crystal system	Restrictions on the axial system	Figure	Equivalences of crystallographic axes caused by:
Triclinic	$a \neq b \neq c \quad \alpha \neq \beta \neq \gamma^a$	6.7c	
Monoclinic	$a \neq b \neq c \quad \alpha = \gamma = 90^\circ, \quad \beta > 90^\circ$	6.8c	
Orthorhombic	$a \neq b \neq c \quad \alpha = \beta = \gamma = 90^\circ$	6.9c	
Tetragonal	$a = b \neq c \quad \alpha = \beta = \gamma = 90^\circ$ ($a_1 = a_2 \neq c$)	6.10c	$4, \bar{4}/c$
Trigonal ^b	$a = b \neq c \quad \alpha = \beta = 90^\circ, \quad \gamma = 120^\circ$ ($a_1 = a_2 \neq c$)	6.12c	$3//c$
Hexagonal		6.12c	$6, \bar{6}/c$
Cubic	$a = b = c \quad \alpha = \beta = \gamma = 90^\circ$ ($a_1 = a_2 = a_3$)	6.13c	$3//\langle 111 \rangle$

^a As usual, the signs = and \neq are to be read as *must be equivalent* and *need not be equivalent* respectively as a consequence of symmetry.

^b An alternative definition divides the hexagonal and trigonal systems differently, giving a hexagonal and a rhombohedral system. The rhombohedral system (see Fig. 6.11 b) has the restrictions on its axial system: $a' = b' = c'$; $\alpha' = \beta' = \gamma'$.

which the symmetry elements of the particular crystal system may make with one another.

The symmetry directions in crystal systems are summarised in Table 7.2. These symmetry directions are used for point groups (Chap. 8) and space groups (Chap. 9). Symmetry directions are defined differently for each crystal system. For some subgroups, a symmetry element does not necessarily exist in the second and/or third position of the symmetry directions (cf. Table 8.10).

The normalized axial ratios from morphology $\frac{a}{b} : 1 : \frac{c}{b}$ or from the crystal structure $\frac{a_0}{b_0} : 1 : \frac{c_0}{b_0}$ for an orthorhombic crystal are discussed in section 4.7. These ratios are summarised in Table 7.3 for all crystal systems. They may be expressed more simply for systems of higher symmetry.

The U.S. Department of Commerce: National Bureau of Standards and the International Center for Diffraction Data have produced a series of volumes *Crystal Data - Determinative Tables*. These contain an extensive listing of important crystallographic data. Triclinic (anorthic), monoclinic and ortho-

Table 7.2. Symmetry directions in the seven crystal systems

	Position in the international symbol		
	1st	2nd	3rd
Triclinic	–		
Monoclinic	b		
Orthorhombic	a	b	c
Tetragonal	c	⟨a⟩	⟨110⟩
Trigonal	c	⟨a⟩	– ^c
Hexagonal	c	⟨a⟩	⟨210⟩
Cubic	⟨a⟩	⟨111⟩	⟨110⟩

^c There are a few trigonal space groups with a 3rd. symmetry direction ⟨210⟩ as in the hexagonal system, for example P31m or P312 with m or 2 in ⟨210⟩, cf. Table 9.2

Table 7.3. Normalized axial ratios as used for the various crystal systems.

Crystal system	Axial ratios	
	morphological	structural
Triclinic Monoclinic Orthorhombic	$\frac{a}{b} : 1 : \frac{c}{b}$	$\frac{a_0}{b_0} : 1 : \frac{c_0}{b_0}$
Tetragonal Trigonal Hexagonal	$\frac{c}{a}$	$\frac{c_0}{a_0}$
Cubic	–	a_0

rhombic crystals are listed in the order of the $\frac{a_0}{b_0}$ ratio, where $c_0 < a_0 < b_0$. Tetragonal, trigonal and hexagonal crystals are arranged by the $\frac{c_0}{a_0}$ ratio, and cubic crystals by the value of the lattice constant a_0 .

8 Point Groups

8.1 The 32 Point Groups

As has been noted, the space groups of the Bravais lattices are those with the highest possible symmetry for the corresponding crystal systems. When the lattice points are now replaced by actual atoms, ions or molecules, they must themselves possess at least the full symmetry of the lattice point if the space group is to remain unchanged. Now the symmetry of a lattice point is easily determined from the space group; it consists of all of the point symmetry elements of the space group that pass through the point (X, \bar{X}, m) or lie on it ($\bar{1}$). In each crystal system, only the space group of the P-lattice or, in the trigonal system the R-lattice, need be considered (see Figs. 6.7d–6.13d), since the centred lattices in each system define identical points. Lattice translations, the most important of all the symmetry operations for space groups, are now discarded, and the set of symmetry elements remaining is called a *point group*. The symmetry elements of these point groups and their stereographic projections are set out in Figs. 6.7e–6.13e, and the conversion from space group to point group in Table 8.1. There is a great deal of useful information in the diagrams, and it is worth taking the trouble to study them carefully.

Table 8.1. Correspondence of one of the space groups of highest symmetry in each crystal system with the point group of highest symmetry in that crystal system

Crystal system	Space group	Point group	Fig.
Triclinic	$P \bar{1}$	$\rightarrow \bar{1}$	6.7d, e
Monoclinic	$P 2/m$	$\rightarrow 2/m$	6.8d, e
Orthorhombic	$P 2/m 2/m 2/m$	$\rightarrow 2/m 2/m 2/m$	6.9d, e
Tetragonal	$P 4/m 2/m 2/m$	$\rightarrow 4/m 2/m 2/m$	6.10d, e
Trigonal	$R \bar{3} 2/m$	$\rightarrow \bar{3} 2/m$	6.11d, e
Hexagonal	$P 6/m 2/m 2/m$	$\rightarrow 6/m 2/m 2/m$	6.12d, e
Cubic	$P 4/m \bar{3} 2/m$	$\rightarrow 4/m \bar{3} 2/m$	6.13d, e

The point groups are made up from point symmetry operations and combinations of them. Formally, *a point group is defined as a group of point symmetry operations whose operation leaves at least one point unmoved. Any operation involving lattice translation is excluded.*

The symmetry directions have the same relationship to the symmetry elements of the point group as they do to those of the space group (Table 7.2). Those point groups derived from the space groups of the lattices are also the highest symmetry possible for the particular crystal system.

These point groups of highest symmetry in each crystal system all contain the symmetry elements of one or more point groups of lower symmetry (subgroups). These will be developed below for some crystal systems:

a) TRICLINIC. The only subgroup of $\bar{1}$ is 1. Starting from the space group $P\bar{1}$ (Fig. 6.16), all points which do not lie on inversion centres have the point symmetry 1.

b) MONOCLINIC. $2/m$ has the subgroups 2, m , $\bar{1}$ (cf. Symmetry rule I) and 1. Since $\bar{1}$ and 1 belong to the triclinic system, only 2 and m are monoclinic point groups (cf. Fig. 6.8f). They possess sufficient symmetry to define the monoclinic system: $m \perp b$ in the a, c -plane, and 2 parallel to b and normal to the a, c -plane. In the space group $P2/m$ (Fig. 6.8d), the point $0, 0, 0$ has the point symmetry $2/m$, while any point on $x, \frac{1}{2}, z$ has point symmetry m , and any point on the line $\frac{1}{2}, y, \frac{1}{2}$ has point symmetry 2 (cf. Fig. 9.13)

c) ORTHORHOMBIC. If inversion symmetry is removed from point group $2/m$ $2/m$ $2/m$, each $2/m$ must be reduced either to 2 or to m (Symmetry rule I). The possible orthorhombic subgroups are thus mmm , $mm2$ (or $m2m$ or $2mm$), $m22$ (or $2m2$ or $22m$) and 222 . The symmetry elements of mmm are given on the stereogram in Fig. 8.1. By Symmetry rule II ($m \perp m \Rightarrow 2$), 2-fold rotation axes are formed at each intersection of planes, and the point group $2/m$ $2/m$ $2/m$ has been reformed. Similarly, the combination $22m$ also regenerates $2/m$ $2/m$ $2/m$ (cf. Fig. 8.2). The orthorhombic subgroups of $2/m$ $2/m$ $2/m$ are thus 222 and $mm2$ (Fig. 6.9f). As an example, in the space group $P2/m$ $2/m$ $2/m$ (Fig. 6.9d), all points on $\frac{1}{2}, \frac{1}{2}, z$ ($z \neq 0$ or $\frac{1}{2}$) have point symmetry $mm2$.

In a similar way, the other crystal systems may be treated, giving in total 32 point groups or crystal classes, which are summarised in Table 8.2. They are called the crystallographic point groups.

All crystallographic point groups are subgroups of either $4/m$ $\bar{3}$ $2/m$ or $6/m$ $2/m$ $2/m$ or both. The hierarchy of the subgroups is illustrated in Fig. 8.3.

Some point groups have overdefined symbols, as we have seen for $2/m$ $2/m$ $2/m$ (Fig. 8.1). In some of these cases, the symbol is abbreviated; the abbreviated symbols are shown in round brackets in Table 8.2. These

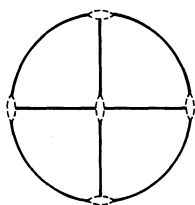


Fig. 8.1. The three mutually perpendicular mirror planes of mmm showing with *dashed outline* the automatically developed 2-fold axes (Symmetry rule II). Thus mmm is in fact $2/m\ 2/m\ 2/m$ and is used as an abbreviated symbol for it

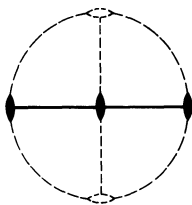


Fig. 8.2. The symmetry elements of $m22$ (fully drawn in) on the stereogram, automatically generate (Symmetry rule II) the other symmetry elements shown with *dashed outline*, generating $2/m\ 2/m\ 2/m$. Thus, $m22$ is in fact identical with $2/m\ 2/m\ 2/m$

Table 8.2. The 32 point groups

Crystal system	Point groups		Symmetry and stereograms of the point groups in Fig.
Triclinic	$\bar{1}$	1	
Monoclinic	$2/m$	$m, 2$	6.8e, f
Orthorhombic	$2/m\ 2/m\ 2/m$ (mmm)	$mm2, 222$	6.9e, f
Tetragonal	$4/m\ 2/m\ 2/m$ ($4/mmm$)	$\bar{4}2m, 4mm, 422$ $4/m, \bar{4}, 4$	6.10e, f
Trigonal	$\bar{3}\ 2/m$ ($\bar{3}m$)	$3m, 32, \bar{3}, 3$	6.11e, f
Hexagonal	$6/m\ 2/m\ 2/m$ ($6/mmm$)	$\bar{6}m2, 6mm, 622$ $6/m, \bar{6}, 6$	6.12e, f
Cubic	$4/m\ \bar{3}\ 2/m$ ($m\bar{3}m$)	$\bar{4}3m, 432, 2/m\bar{3}, 23$ ($m\bar{3}$)	6.13e, f

abbreviated forms are also used for space groups (Chap. 9). They are called *short symbols* to distinguish them from the *full symbols*.

Up to now, symmetry symbols have always been used in relation to the symmetry directions. The symbol on its own, however, clearly shows the relative orientation of the various symmetry elements. Thus:

- X2: rotation axis X and 2-fold axes perpendicular to it, e.g. $42(2)$ (Fig. 6.10f).
 Xm: rotation axis X and mirror planes parallel to it, e.g. $3m$ (Fig. 6.11f).

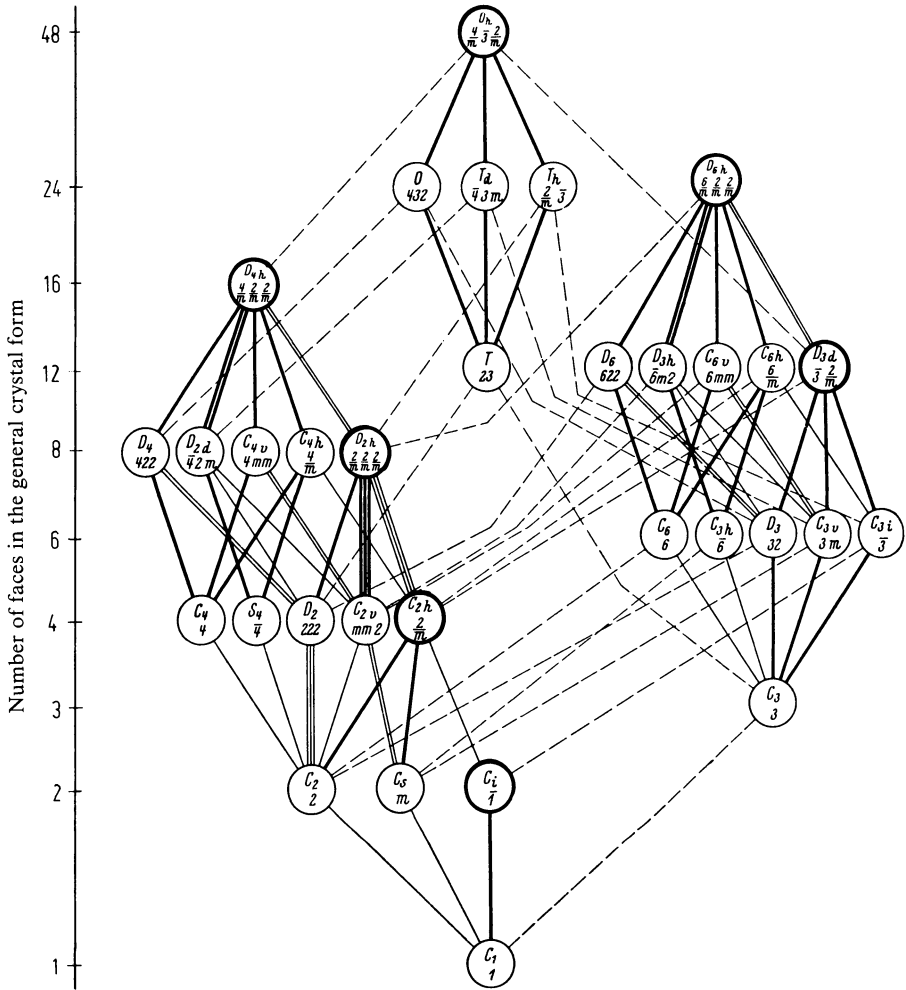


Fig. 8.3. The crystallographic point groups and their subgroups, after Hermann [18]. The circles corresponding to the highest symmetry group of each crystal system are *outlined in bold*. *Double or triple lines* indicate that the supergroup is related to the subgroup in two or three inequivalent settings. Connecting lines between point groups of the same crystal system are bold, all others are *plain* or *dashed*. The presence of a line of any sort indicates that the lower group is a subgroup of the higher. On the ordinate is given the order of the point group, i.e. the number of faces in the general crystal form

- $\bar{X}2$: rotoinversion axis \bar{X} and 2-fold axes perpendicular to it, e.g. $\bar{4}2(m)$ (Fig. 6.10f).
- $\bar{X}m$: rotoinversion axis \bar{X} and mirror planes parallel to it, e.g. $\bar{6}m(2)$ (Fig. 6.12f).
- X/mm : rotation axis X and mirror planes both parallel and perpendicular to it, e.g. $4/mm(m)$ (Fig. 6.10f).

Table 8.3. The Schönflies symbols for the point groups with the equivalent International symbols C_n : n-fold rotation axis; identical with X

C_n	C_1	C_2	C_3	C_4	C_6
X	1	2	3	4	6

 C_{ni} : odd-order rotation axis and inversion centre $i \equiv \bar{X}$ (odd) C_s : (s for German Spiegelebene) = mirror plane; S_n : n-fold rotoreflection axis (only S_4 and S_6 used)

	C_i	C_s	$C_{3i} \equiv S_6$	S_4	
\bar{X}	$\bar{1}$	$(\bar{2} \equiv)$ m	$\bar{3}$	$\bar{4}$	

 C_{nh} : n-fold axis normal to mirror plane $\equiv X/m$

C_{nh}		C_{2h}	C_{3h}	C_{4h}	C_{6h}
X/m		2/m	$(3/m \equiv)$ $\bar{6}$	4/m	6/m

 C_{nv} : n-fold axis parallel to n mirror planes $\equiv Xm$

C_{nv}		C_{2v}	C_{3v}	C_{4v}	C_{6v}
Xm		mm2	3m	4mm	6mm

 D_n : n-fold axis normal to n 2-fold axes $\equiv X2$

D_n		D_2	D_3	D_4	D_6
X2		222	32	422	622

 D_{nd} : as D_n plus mirror planes bisecting 2-fold axes

D_{nd}		D_{2d}	D_{3d}		
$\bar{X}m$		$\bar{4}2m$	$\bar{3}m$		

 D_{nh} : as D_n plus mirror plane normal to n-fold axis

D_{nh}		D_{2h}	D_{3h}	D_{4h}	D_{6h}
X/mmm		mmm	$(3/mmm \equiv)$ $\bar{6}m2$	4/mmm	6/mmm

T (tetrahedral) and O (octahedral) groups

	T	T_h	O	T_d	O_h
	23	$m\bar{3}$	432	$\bar{4}3m$	$m\bar{3}m$

The symbols we have been using so far for space groups and point groups are known as the *International* or *Hermann-Mauguin symbols*. In physics and chemistry, the older *Schönflies* symbols are widely used. Unfortunately, Schönflies symbols are impossible to adapt as useful space group symbols. Although they are adequate to define point groups, there is no particular advantage to using them. Table 8.3 gives the International equivalents of all the Schönflies symbols for the crystallographic point groups.

8.2 Crystal Symmetry

A space group reveals the entire symmetry of a crystal structure. When we consider only the morphology of a crystal, the lattice translations which characterise the space group are no longer relevant, and what is left is the point group which is implied by that space group. If the crystal is bounded by plane faces, the symmetry of its morphology will be the symmetry of that point group.

Figure 8.4 illustrates the symmetry of a crystal of PbS (galena) (cf. Fig. 4.1). The symmetry elements which are apparent in the crystal are summarised on the stereographic projection. The point group of the crystal is $4/m \bar{3} 2/m$. In Table 8.11, examples of crystals in various point groups are given in the right-hand column.

8.2.1 Crystal Forms

In Chapter 4.2, crystal form was provisionally defined as a set of “equal” faces. We are now in a position to give an exact definition.

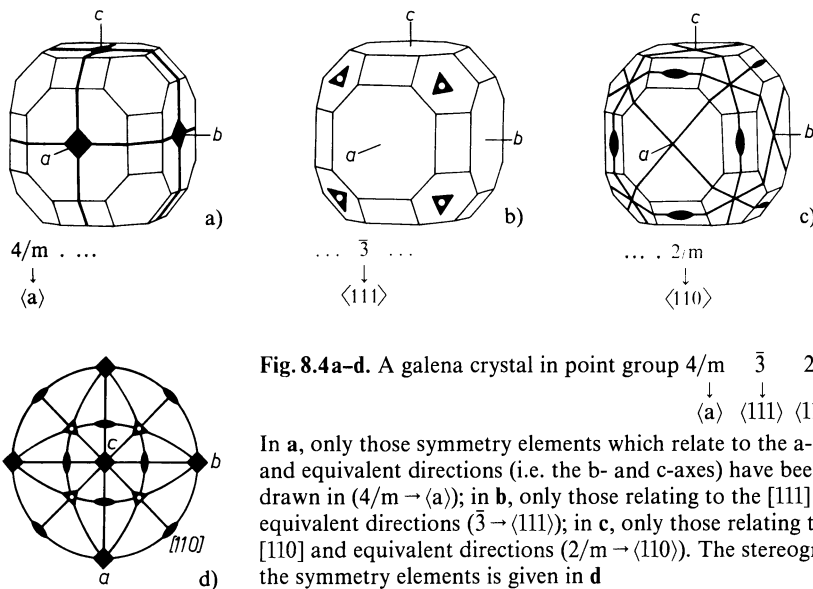


Fig. 8.4a-d. A galena crystal in point group $4/m \bar{3} 2/m$.
 $\downarrow \quad \downarrow \quad \downarrow$
 $\langle a \rangle \quad \langle 111 \rangle \quad \langle 110 \rangle$

In a, only those symmetry elements which relate to the a-axis and equivalent directions (i.e. the b- and c-axes) have been drawn in ($4/m \rightarrow \langle a \rangle$); in b, only those relating to the $[111]$ and equivalent directions ($\bar{3} \rightarrow \langle 111 \rangle$); in c, only those relating to the $[110]$ and equivalent directions ($2/m \rightarrow \langle 110 \rangle$). The stereogram of the symmetry elements is given in d

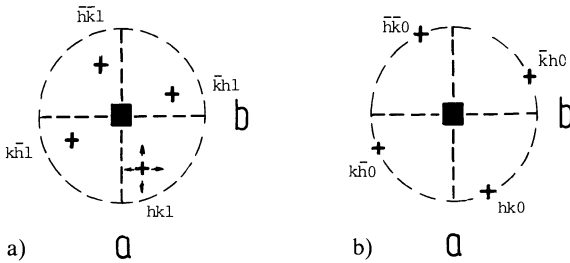


Fig. 8.5a,b. Stereograms of point group 4. **a** General form, tetragonal pyramid $\{hkl\}$. **b** Limiting form tetragonal prism $\{hk0\}$ of general form tetragonal pyramid $\{hkl\}$

When the symmetry operations of a point group are applied to a crystal face, a number of equivalent faces will be produced. Thus, as shown in the stereographic projection in Fig. 8.5a, application of the symmetry operation of the point group 4 on the pole of a face produces a tetragonal pyramid.

A set of equivalent faces is called a crystal form.

Exercise 5.1b gives a manipulation which will always result in the production of the stereogram of a crystal form.

The individual faces of the tetragonal pyramid in Fig. 8.5a have been indexed, i.e. assigned the values of their Miller indices. A scheme for indexing the faces of tetragonal crystals will be given later (Fig. 8.8). A crystal form is identified by the indices of one of the faces belonging to that form. In the case of a form, the indices are placed in braces, thus: $\{hkl\}$, in order to distinguish between a face and a form. The relationship between (hkl) and $\{hkl\}$ is the same as that between $[uvw]$ and $\langle uvw \rangle$.

Each face of the tetragonal pyramid in Fig. 8.5a is itself unsymmetrical, as there is no symmetry element normal to it. On its own, it thus has face symmetry 1.

Three types of crystal forms must now be distinguished: a general form, a special form and a limiting form.

A general form is a set of equivalent faces, each of which has face symmetry 1.

In other words, when the poles of the faces of a general form are placed on a stereogram of the symmetry elements, they do not lie on any of them. General forms have general indices $\{hkl\}$. The tetragonal pyramid $\{hkl\}$ in Fig. 8.5a is such a general form. The poles of the faces of a general form have two degrees of freedom, shown as arrows in the figure. The face can be displaced in two directions without causing the tetragonal pyramid to cease to be a crystal form. All that happens is that the inclination of the faces to one another is altered.

The variation of the indices $\{hkl\}$ gives rise not to only one, but to an infinite number of general crystal forms. In some point groups, care must be taken with the signs of the indices. In any case, the possibility of infinitely many crystal

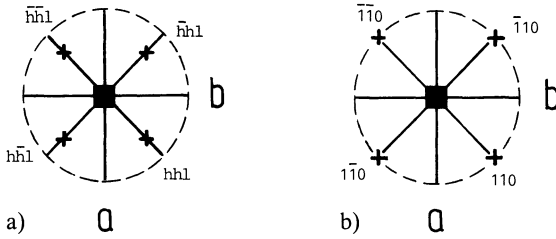


Fig. 8.6a,b. Stereograms of point group $4mm$. **a** Special form, tetragonal pyramid $\{hhl\}$. **b** Limiting form, tetragonal prism $\{110\}$ of special form, tetragonal pyramid $\{hhl\}$

forms is only of theoretical interest, since in practice, crystals rarely have faces with large values of h , k or l .

A special form is a set of equivalent crystal faces which themselves have a face symmetry higher than 1.

In a stereogram of the symmetry elements, the poles of the faces of a special form lie on at least one of them. Figure 8.6a shows the stereogram of the symmetry elements of the point group $4mm$. If the pole of a face (hhl) is entered, the application of the symmetry elements gives a tetragonal pyramid $\{hhl\}$. This is a special form, as the faces lie on a symmetry element, and each has face symmetry $\dots m$. The symmetry is given as $\dots m$ with reference to the order of the symmetry directions used for point groups of the tetragonal system: c , $\langle a \rangle$, $\langle 110 \rangle$. The mirror planes with which we are concerned here are those normal to $\langle 110 \rangle$. The poles of the faces of this special form have only a single degree of freedom. The form will remain a tetragonal pyramid only as long as the pole remains on the mirror plane $\dots m$. Should the pole move until it coincides with the 4-fold axis, another special form arises, the pedion $\{001\}$ with face symmetry $4mm$. This form no longer has any degree of freedom. A special form always has indices which are a special case of $\{hkl\}$, such as $\{hhl\}$, $\{h0l\}$ or $\{100\}$.

A limiting form is a special case of either a general or a special form. It has the same number of faces, each of which has the same face symmetry, but the faces are differently arranged.

Consider the situation in Fig. 8.5a if the pole moves to the periphery of the equatorial plane of the stereographic projection. The result is a tetragonal prism $\{hk0\}$ which is the limiting form of the general form tetragonal pyramid $\{hkl\}$ with face symmetry 1. A similar movement of the pole $\{hhl\}$ in Fig. 8.6b, along the mirror plane to the periphery of the equator gives rise to the tetragonal prism $\{110\}$, the limiting form of the special form $\{hhl\}$ with face symmetry $\dots m$.

Each point group has characteristic forms. What follows is a description of those of the point group $4/mmm$, the point group of highest symmetry in the tetragonal system. Figure 8.7a is a stereogram of the symmetry elements of this point group. A single, asymmetric face unit is shown hatched in Fig. 8.7a.

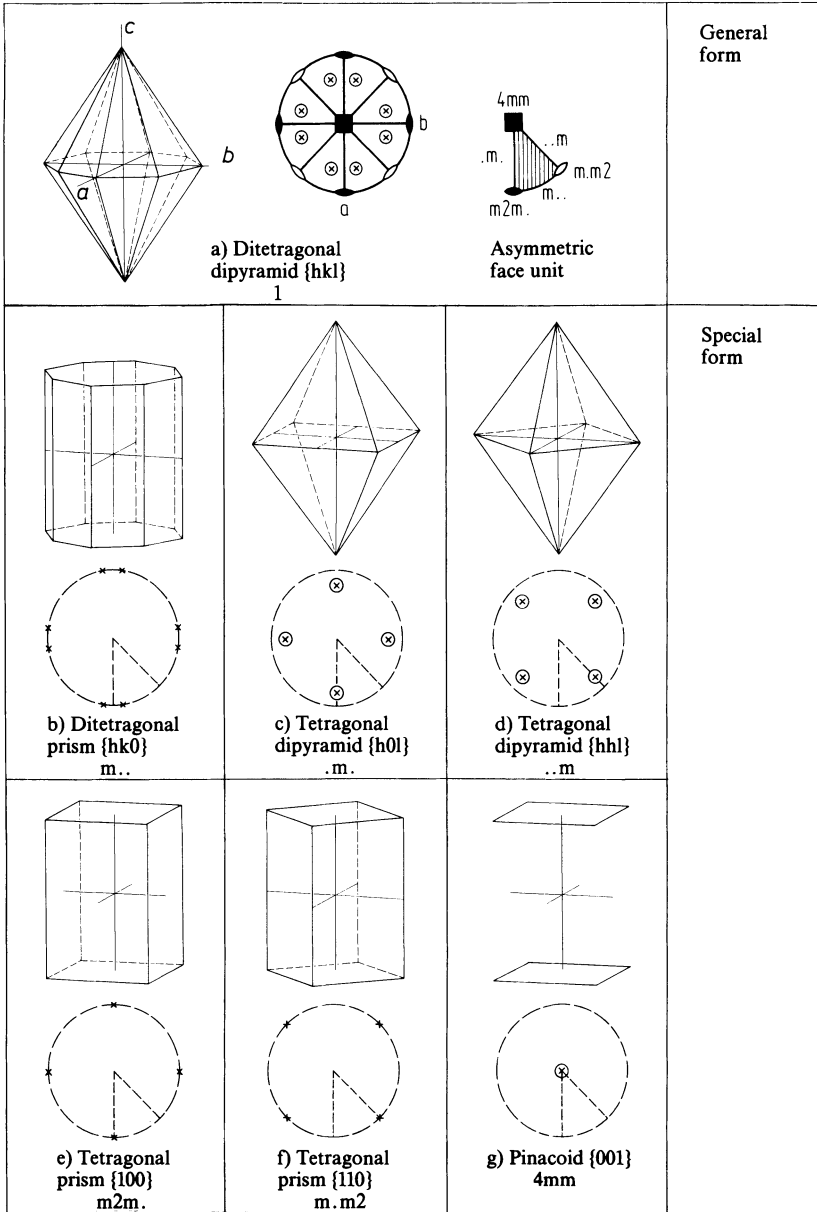


Fig. 8.7a-g. Crystal forms of point group $4/mmm$, with their face symmetries. A stereogram of the symmetry elements is given, with the asymmetric face unit and stereograms of each form

The asymmetric face unit of a point group, in terms of its stereographic projection, is the smallest part of the surface of the sphere which, by the application of the symmetry operations, will generate the entire surface of the sphere.

This particular asymmetric face unit is bounded by $m..$, $.m.$ and $..m.$. The vertices have face symmetry $4mm$, $m2m.$ and $m.m2$. If a pole is entered in the asymmetric face unit on the stereogram and operated on by the symmetry, the result is a ditetragonal dipyrmaid, $\{hkl\}$, shown in Fig. 8.7a. This form has two degrees of freedom. A ditetragonal dipyrmaid will be generated as long as the pole does not move onto one of the symmetry elements which constitute the boundary of the asymmetric face unit. The ditetragonal dipyrmaid is a general form (face symmetry 1, two degrees of freedom, $\{hkl\}$). The size of the asymmetric face unit is simply the ratio of the surface area of the sphere to the number of faces in a general form.

$$f_{\text{asym. face unit}} = \frac{f_{\text{surface area of the sphere}}}{\text{number of faces in the general form}}$$

In this case, the number of such faces is 16, so the asymmetric face unit shown hatched in Fig. 8.7a is $\frac{1}{16}$ of the total surface area of the sphere.

An asymmetric face unit of a point group contains all the information necessary for the complete description of the crystal forms in this point group. (This definition may be compared with that of the asymmetric unit on p. 198.)

If the general pole (hkl) is moved onto the mirror plane $m..$, this pole, and all the others in the general form $\{hkl\}$ will undergo a change. As the poles approach this mirror plane, the angle between (hkl) and $(hk\bar{l})$ becomes progressively smaller, and is equal to 0 at the mirror plane. At this point, the two faces (hkl) and $(hk\bar{l})$ have coalesced into a single face $(hk0)$. As shown in Fig. 8.7b, the ditetragonal dipyrmaid has become a ditetragonal prism $\{hk0\}$.

Figure 8.8 shows the stereographic projection of a ditetragonal prism $\{hk0\}$ and the indices of the poles of its faces. In the stereogram, a section through the ditetragonal prism is shown in bold lines which are extended (dashed lines) to show the intercepts on the axes better, $(hk0) = (210)$.

A pole of a face on the mirror plane $.m.$ gives, after the application of the symmetry operations, a tetragonal dipyrmaid, $\{h0l\}$, shown in Fig. 8.7c. A pole of a face on $..m$ gives a tetragonal dipyrmaid $\{hhl\}$, shown in Fig. 8.7d. The three forms $\{hk0\}$, $\{h0l\}$ and $\{hhl\}$ all have eight faces, i.e. half of the number of faces of the ditetragonal dipyrmaid. These three forms each have one degree of freedom. Each form retains its identity so long as the pole remains on the appropriate edge (m) of the asymmetric face unit.

The poles of faces on the vertices of the asymmetric face unit have no degree of freedom. The application of the symmetry operations to a pole with face symmetry $m2m.$ gives a tetragonal prism $\{100\}$ (Fig. 8.7e). Similarly the pole

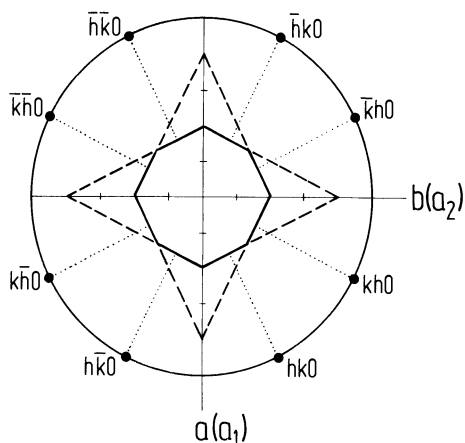


Fig. 8.8. Section through a ditetragonal prism (*outlined*), in the equatorial plane of a stereographic projection, with the poles of the relevant faces and their indices, $\{hk0\}$ ($=\{210\}$) shown. The *dashed lines* serve to indicate the intercepts of the faces on the axes

with face symmetry $m.m2$ gives a tetragonal prism $\{110\}$ (Fig. 8.7f), while that on $4mm$ gives a pinacoid $\{001\}$ (Fig. 8.7g).

The forms $\{hk0\}$, $\{h0l\}$, $\{hhl\}$, $\{100\}$, $\{110\}$ and $\{001\}$ have the face symmetries given in Fig. 8.7 and are thus special forms.

Figure 8.9 shows a stereogram with the poles of the crystal forms of point group $4/mmm$, the highest point symmetry of the tetragonal system. The poles of the faces with negative indices $\bar{1}$ are not shown. The heavy lines divide the surface into the 16 asymmetric face units of the point group $4/mmm$. Those poles which lie on the corners of the asymmetric face unit have no degree of freedom. Those on the edges of the asymmetric face unit have one degree of freedom, and represent all other poles lying on the same edge. The poles lying within the asymmetric face unit have two degrees of freedom and represent all faces whose poles lie in this area. In every case, taken together, these faces produce ditetragonal dipyramids.

If the poles of the faces of a ditetragonal prism $\{hk0\}$ (Fig. 8.8) are split and moved an equal amount in the directions of (001) and $(00\bar{1})$, a ditetragonal dipyramid $\{hkl\}$ will be formed. The indexing of the faces of this form arise from the $\{hk0\}$ of the ditetragonal prism by the replacement of 0 with l and $\bar{1}$, as in Fig. 8.9, the indices of all 16 faces of the ditetragonal dipyramid can be read from the stereogram in Fig. 8.9, as can the indices for the faces of all of the tetragonal forms.

In $4/mmm$, there are $n=16$ poles for faces of the general form, and $2n+2=34$ poles for faces of special forms, each type of form being considered only once. The same relationship between the numbers of faces for the general form and the total number of faces for all special forms also applies to the point group of highest symmetry in the orthorhombic, hexagonal and cubic systems.

Starting from the point group of highest symmetry in a crystal system, the subgroups can be developed – see Section 8.1. There is a similar relationship between the general crystal form of the point group of highest symmetry and those of its subgroups belonging to the same crystal system. These may be illustrated by starting from the stereogram of the crystal forms of $4/mmm$ in Fig. 8.9 and developing those of the subgroup $4mm$.

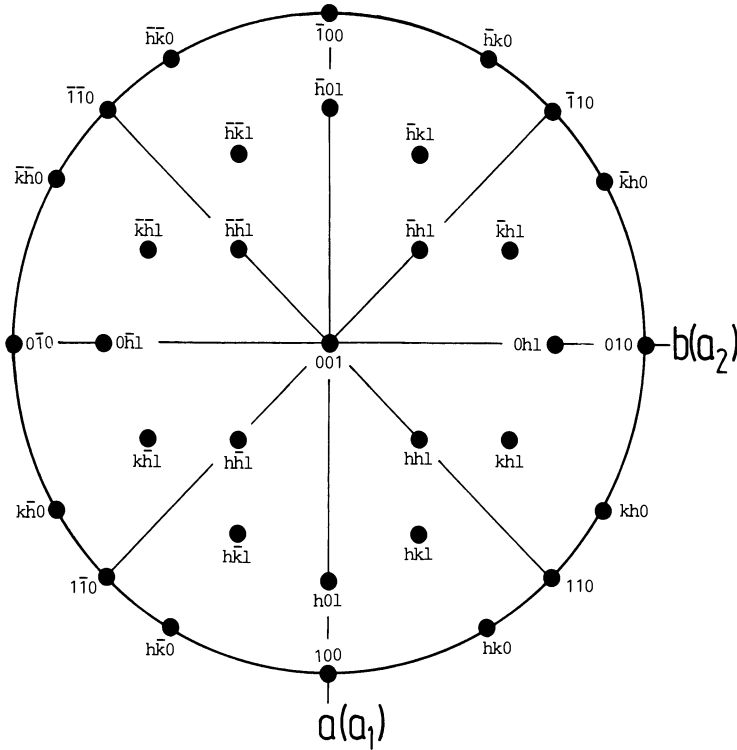


Fig. 8.9. Stereogram of the poles of the faces of all crystal forms of 4/mmm, the point group of highest symmetry in the tetragonal system. The stereogram shows the position and the indices for each face in each form. Poles of faces with negative values of l are not included. The spherical triangle with vertices (001), (100) and (110) is an asymmetric face unit of the point group 4/mmm

Place a piece of tracing paper over the stereogram in Fig. 8.9, choose suitable symmetry directions and mark on it those symmetry elements which belong to 4mm. A possible asymmetric face unit for this point group is a region bounded by the pole faces (001), (100), (00 $\bar{1}$) and (110). Because half of this asymmetric face unit lies in the southern hemisphere, it is shown checked in Fig. 8.10a. It is twice the size of the asymmetric face unit of 4/mmm, and is made up by combining two such asymmetric face units.

Now enter on the tracing paper the pole of the general face (hkl), and allow the symmetry operations of 4mm to act on it. The result is eight poles which define a ditetragonal pyramid {hkl} (Fig. 8.10a₁). The pole (hk \bar{l}) which belongs to the same asymmetric unit as (hkl) in 4mm gives a second ditetragonal pyramid {hk \bar{l} } (Fig. 8.10a₂). Thus, the ditetragonal dipyramid which is the general form in 4/mmm reduces to two ditetragonal pyramids in 4mm. The doubling of the size of the asymmetric face unit results in a halving of the number of faces in the general form.

In the same way, the general forms of the other tetragonal point groups may be developed. The relevant asymmetric face units are given in Table 8.4.

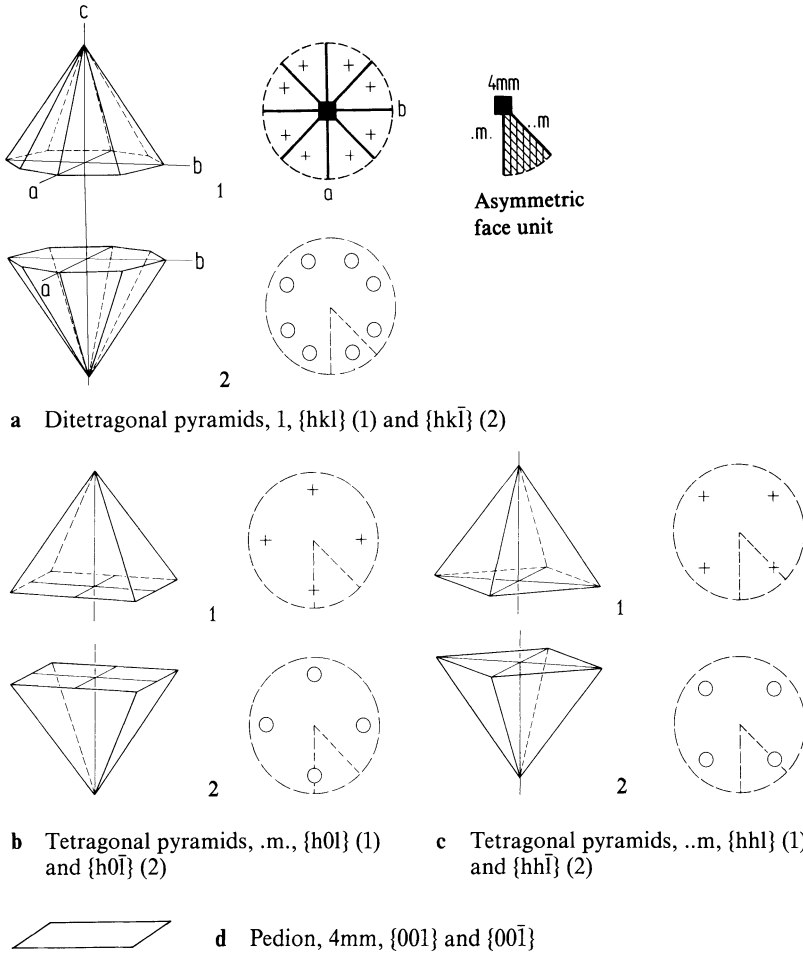


Fig. 8.10a-d. Crystal forms of point group $4mm$, in so far as these differ from those in point group $4/mmm$ (Fig. 8.7), with their face symmetries. A stereogram of the symmetry elements is given, with the asymmetric face unit and stereograms of each form.

The general form of point group $4/m$ is a tetragonal dipyramid. The poles $\{hkl\}$ and $\{h\bar{k}l\}$ both give tetragonal dipyramids, $\{hkl\}$ and $\{h\bar{k}l\}$, by the action of the symmetry operations, and these two dipyramids may be distinguished by their positions. Figure 8.11 shows the square cross-sections of $\{hkl\}$ and $\{h\bar{k}l\}$. Taking them together, and ignoring the dashed lines, they make up the cross-section of the ditetragonal dipyramid $\{hkl\}$ of $4/mmm$.

The general form of $42m$ is the tetragonal scalenohedron, and of 422 the tetragonal trapezohedron [Table 14.1.2 (13) and (11)]. The combination of $\{hkl\}$ and $\{h\bar{k}l\}$ regenerates in both point groups the ditetragonal dipyramid.

The asymmetric face unit for 4 and $\bar{4}$ is four times the size of that of $4/mmm$ (Table 8.4). In 4 , the ditetragonal dipyramid is split into four tetragonal pyramids, $\{hkl\}$, $\{h\bar{k}l\}$, $\{hkl\}$ and $\{h\bar{k}l\}$, while in $\bar{4}$, it becomes four tetragonal disphenoids, $\{hkl\}$, $\{h\bar{k}l\}$, $\{khl\}$ and $\{k\bar{h}l\}$ [Table 14.1.2 (9)].

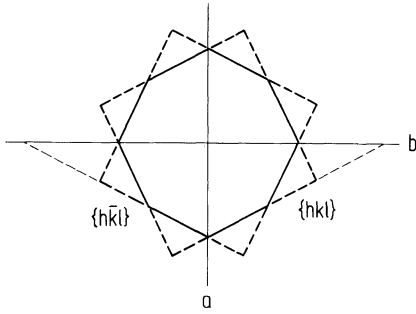


Fig. 8.11. Square cross-sections through the tetragonal dipyrramids $\{hk\bar{l}\}$ and $\{hkl\}$, general forms in point group $4/m$. Together, they make up the fully outlined ditetragonal cross section of the ditetragonal pyramid. The same relationship holds for the four tetragonal pyramids $\{hkl\}$, $\{hk\bar{l}\}$, $\{h\bar{k}l\}$ and $\{h\bar{k}\bar{l}\}$, general forms in point group 4

The special forms of point group $4/mmm$ in Fig. 8.7 are given in Table 8.4 with their face symmetries.

With the help of the stereogram in Fig. 8.9, we may derive the limiting and special forms of point group $4mm$. As in $4/mmm$, the pole of the face $\{hk0\}$ gives rise to the ditetragonal prism $\{hk0\}$ (Fig. 8.7b). This ditetragonal prism is the limiting form of the general form ditetragonal pyramid $\{hkl\}$. These forms both have face symmetry 1 and a total of eight faces.

Application of the symmetry operations $4mm$ to the pole of the face $\{h0l\}$ results in a tetragonal pyramid $\{h0l\}$ (Fig. 8.10b₁), having point symmetry $.m.$, a special form. Similarly, $\{h0\bar{l}\}$ is a tetragonal pyramid (Fig. 8.10b₂). These pyramids are distinguished only by their settings, and their combination gives the tetragonal dipyrmaid $\{h0l\}$ of point group $4/mmm$. The tetragonal prism $\{100\}$ is a limiting form of the special form tetragonal pyramid $\{h0l\}$, also having face symmetry $.m.$, and a total of four faces.

Tetragonal pyramids are also generated by $\{hhl\}$ and $\{hh\bar{l}\}$ (Fig. 8.10c), this time with face symmetry $..m$. These forms combine to give the tetragonal dipyrmaid $\{hhl\}$ of $4/mmm$. The tetragonal prism $\{110\}$ is a limiting form of the special form tetragonal pyramid $\{hhl\}$. Finally, the pole of the face $\{001\}$ gives the pedion $\{001\}$, with face symmetry $4mm$. All of the forms of the point group $4mm$ are given in Table 8.4.

The special and limiting forms of the rest of the tetragonal point groups are also to be found in Table 8.4. It will be seen that the various forms of the point groups of lower symmetry are greatly simplified. For point group 4, for example, all that remains beside the general form tetragonal pyramid is a single limiting form, the tetragonal prism, and a single special form, the pedion.

In Table 8.4, the general forms and their limiting forms are separated from special forms by heavy lines, while dashed lines are used to separate the general forms from their limiting forms. Equal forms with the same face symmetry are collected together, as is also done in Tables 8.5–8.7.

The face symmetries in Table 8.4 are always derived from a three-component symbol for the point group, which is expanded as required, e.g. $4/m(1)$ (1). Thus, the face symmetry in $\{hk0\}$ is given as $m..$, and that in $\{001\}$ is given as $4...$. The same expansion is used for those point groups in other crystal systems which have symbols with only 1 or 2 components, e.g. $3m(1)$, $23(1)$, etc.

Crystal forms in the other crystal systems can be developed in the same way to that we have done for the tetragonal system. In the following pages, the crystal forms for the hexagonal (trigonal), cubic and orthorhombic systems are set out to show their interrelationships and to provide an aid in the indexing of faces. The crystal forms are first given for each system (Tables 8.4–8.7), and Table 14.1 gives a summary of the 47 fundamental forms. The names used here are those in the *International Tables for Crystallography* [14].

Crystal Forms in the Hexagonal and Trigonal Systems

In each crystal system, an axial system a , b , c must be chosen which is appropriate for the symmetry. For the hexagonal and trigonal systems, in addition to the unique c -axis, it is convenient to choose three equivalent axes a_1 , a_2 and a_3 (cf. p. 95 and Fig. 6.22) and to use the Bravais-Miller indices (hki) . The index i corresponds to the a_3 axis. The indices h , k and i are not independent, but are related by $h + k + i = 0$ or $h + k = \bar{i}$. The application of this relationship can be seen in Fig. 8.12. Joint consideration of the hexagonal and trigonal systems is useful since all of the trigonal forms may be derived from the dihexagonal dipyrmaid, the general form of $6/m\ 2/m\ 2/m$, the highest symmetry point group of the hexagonal system (see Figs. 8.12 and 8.13 and Table 8.5). The trigonal and hexagonal crystal forms are all set out in Table 14.1.3.

Crystal Forms in the Cubic System

The cubic crystal forms are collected in Table 14.1.4; see also Figs. 8.14 and 8.15 and Table 8.6.

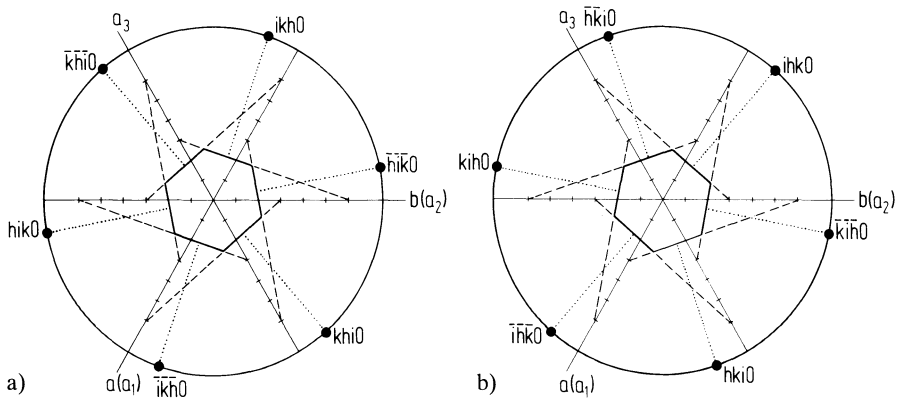


Fig. 8.12a, b. Section through a hexagonal prism $\{hki0\}$ (a) and $\{khi0\}$ (b), in the equatorial plane of a stereographic projection, with the poles of the relevant faces and their indices indicated. The *dashed lines* serve to indicate the intercepts of the faces on the axes [$(hki0) = (21\bar{3}0)$; $(khi0) = (12\bar{3}0)$]

Table 8.4. Crystal forms in the tetragonal system and their face symmetries

Point group	Asymmetric face unit and face symmetry	Special forms		General and limiting forms {hkl}	Special and limiting forms			
		{hhl}	{h0l}		{hk0}	{100}	{110}	{001}
$4/m\ 2/m\ 2/m$ ($4/mmm$)		Tetragonal dipyramid ..m	Tetragonal dipyramid .m.	Ditetragonal dipyramid 1	Ditetragonal prism m..	Tetragonal prism m2m.	Tetragonal prism m.m2	Pinacoid 4mm
4mm		Tetragonal pyramid ..m	Tetragonal pyramid .m.	Ditetragonal pyramid 1		Tetragonal prism .m.	Tetragonal prism ..m	Pedion 4mm
$\bar{4}2m$		Tetragonal disphenoid ..m		Tetragonal scalenohedron 1			Ditetragonal prism 1	Pinacoid 2..mm
422		Tetragonal dipyramid 1		Tetragonal trapezohedron 1			Tetragonal prism .2.	Tetragonal prism ..2

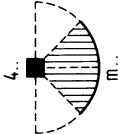
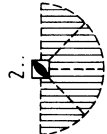
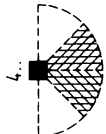
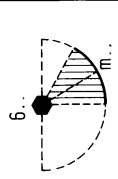
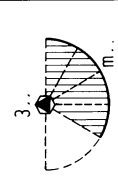
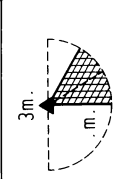
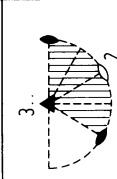
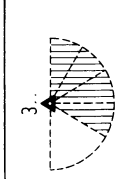
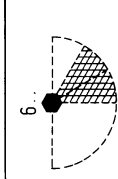
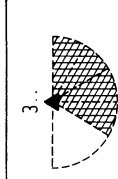
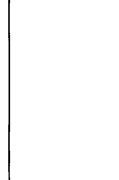
<p>$4/m$</p>		<p>Tetragonal dipyramid 1</p>	<p>Tetragonal prism m..</p>	<p>Pinacoid 4..</p>
<p>$\bar{4}$</p>		<p>Tetragonal disphenoid 1</p>	<p>Tetragonal prism 1</p>	<p>Pinacoid 2..</p>
<p>4</p>		<p>Tetragonal pyramid 1</p>		<p>Pedion 4..</p>

Table 8.5. Crystal forms in the hexagonal/trigonal system and their face symmetries

Point group	Asymmetric face unit and face symmetry	Special forms		General and limiting forms {hkl}	Special and limiting forms			
		{h $\bar{0}$ h}	{hh $\bar{2}$ h}		{hki0}	{11 $\bar{2}$ 0}	{10 $\bar{1}$ 0}	{0001}
6/m 2/m 2/m (6/mmm)		Hexagonal dipyramid .m.	Hexagonal dipyramid ..m	Dihexagonal dipyramid 1	Dihexagonal prism m...	Hexagonal prism m2m	Hexagonal prism mm2	Pinacoid 6mm
$\bar{6}m2$		Trigonal dipyramid .m.	Hexagonal dipyramid 1	Ditrigonal dipyramid 1	Ditrigonal prism m...	Hexagonal prism m..	Trigonal prism mm2	Pinacoid 3m.
$\bar{3}2/m$ ($\bar{3}m$)		Rhombohedral .m.		Ditrigonal scalenohedron 1		Hexagonal prism .2.	Hexagonal prism .m.	
6mm		Hexagonal pyramid .m.	Hexagonal pyramid ..m	Dihexagonal pyramid 1	Dihexagonal prism 1	Hexagonal prism ..m	Hexagonal prism .m.	Pedion 6mm
622		Hexagonal dipyramid 1		Hexagonal trapezohedron 1		Hexagonal prism .2.	Hexagonal prism ..2	Pinacoid 6..

$6/m$		Hexagonal dipyrmaid 1	Hexagonal prism m..	Pinacoid 6..
$\bar{6}$		Trigonal dipyrmaid 1	Trigonal prism m..	Pinacoid 3..
$3m$		Trigonal pyramid .m.	Hexagonal pyramid 1	Pedion 3m.
32		Ditrigonal pyramid 1	Ditrigonal prism 1	
		Trigonal trapezohedron 1	Trigonal dipyrmaid 1	Hexagonal prism 1
3		Rhombohedron 1	Rhombohedron 1	Pinacoid 3..
6		Hexagonal pyramid 1	Hexagonal prism 1	Pedion 6..
3		Trigonal pyramid 1	Trigonal prism 1	Pedion 3..

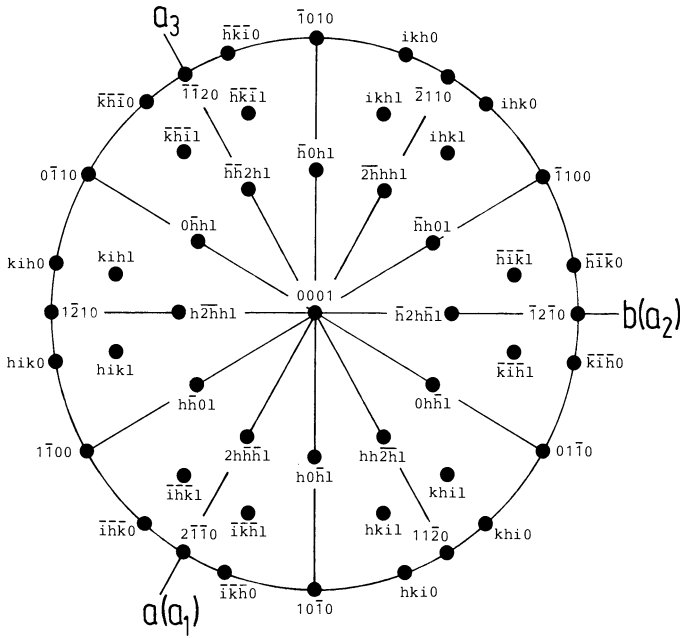


Fig. 8.13. Stereogram of the poles of the faces in all crystal forms of the point group of highest symmetry in the hexagonal system, $6/m\ 2/m\ 2/m$. The stereogram shows the positions and the indices of all hexagonal and trigonal forms. The poles of faces with negative l are excluded. The spherical triangle with vertices $(10\bar{1}0)$, (0001) , $(11\bar{2}0)$ is an asymmetric face unit for the point group $6/m\ 2/m\ 2/m$

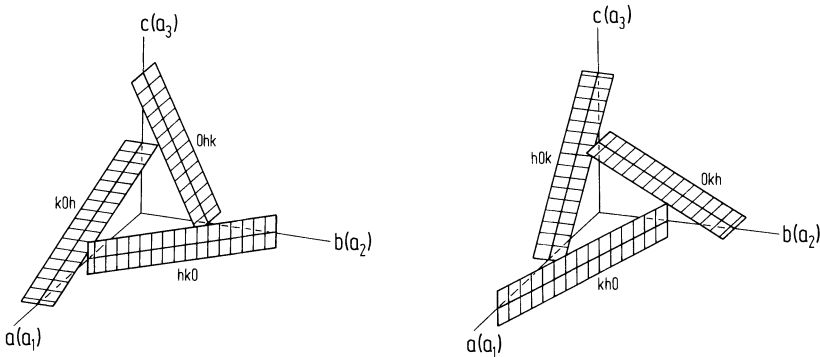


Fig. 8.14. Indices for the cubic faces belonging to the form $\{hk0\}$ ($=\{210\}$). If these are shifted from their special position so that their poles move toward the pole of the (111) face, faces will be obtained with general indices $\{hkl\}$ in the point group $4/m\ \bar{3}\ 2/m$ (cf. Fig. 8.15)

In the cubic, hexagonal (including trigonal) and tetragonal systems, all crystal forms except the pinacoid and the pedion are characteristic of the system.

Table 8.6. Crystal forms in the cubic system and their face symmetries

Point group	Asymmetric face unit and face symmetry	Special forms		General and limiting forms {hkl}	Special and limiting forms			
		{hkk}	{hhk}		{hk0}	{110}	{111}	{100}
$4/m \bar{3} 2/m$ ($m\bar{3}m$)		Trapezohedron ..m	Tris-octahedron ..m	Hexaoc-tahedron 1	Tetra-hexahedron m..	Rhomb-dodecahedron m.m2	Octahedron .3m	Hexahedron 4m.m
$\bar{4}3m$		Tristetra-hedron ..m	Deltoid-dodecahedron ..m	Hexatetra-hedron 1	Tetra-hexahedron 1	Rhomb-dodecahedron ..m	Tetrahedron .3m	Hexahedron 2..mm
$2/m \bar{3}$ ($m\bar{3}$)		Trapezo-hedron 1	Tris-octahedron 1	Diploid 1	Pyrito-hedron m..	Rhomb-dodecahedron m..	Octahedron .3.	Hexahedron 2m..
432		Tristetra-hedron 1	Deltoid-dodecahedron 1	Gyroid 1	Tetra-hexahedron 1	Rhomb-dodecahedron ..2	Octahedron .3.	Hexahedron 4..
23		Tristetra-hedron 1	Deltoid-dodecahedron 1	Tetartoid 1	Pyritohedron 1	Rhomb-dodecahedron 1	Tetrahedron .3.	Hexahedron 2..

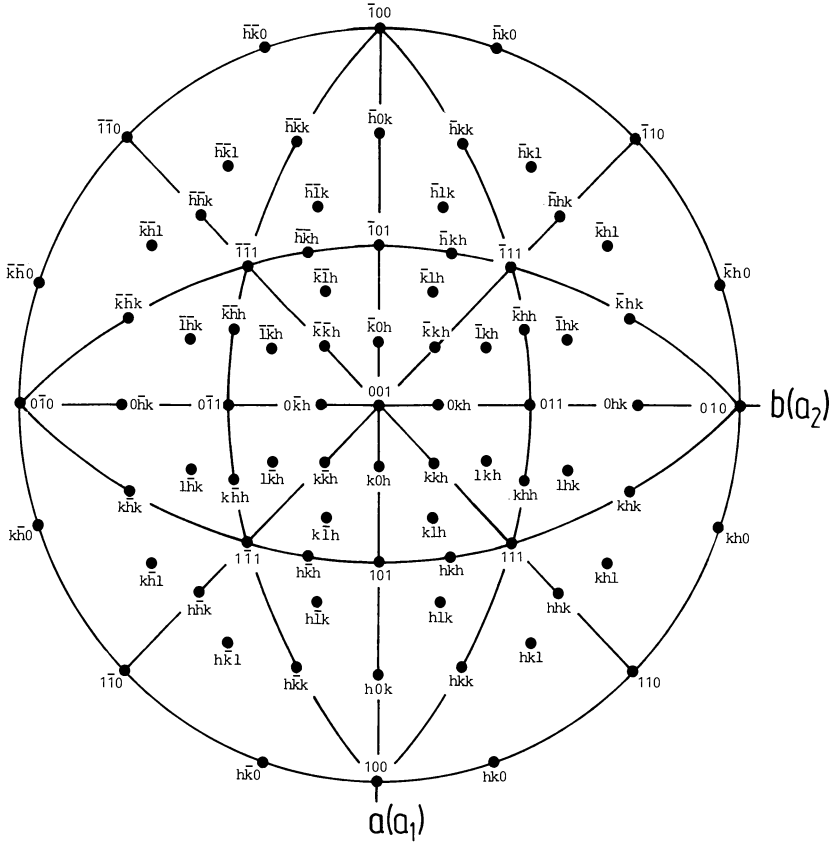


Fig. 8.15. Stereogram of the poles of the faces in all crystal forms of the point group of highest symmetry in the cubic system, $4/m \bar{3} 2/m$. The stereogram shows the positions and the indices of all cubic forms $(hk0) = (310)$, $(hkk) = (311)$, $(hhk) = (221)$, $(hkl) = (321)$. The poles of faces with the third index negative are excluded. The spherical triangle with vertices (100) , (110) , (111) is an asymmetric face unit for the point group $4/m \bar{3} 2/m$

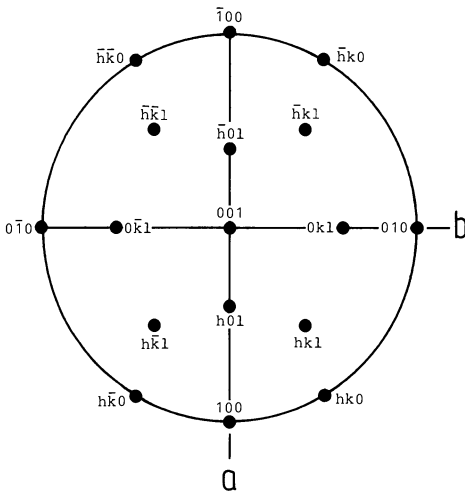


Fig. 8.16. Stereogram of the poles of the faces in all crystal forms of the point group of highest symmetry in the orthorhombic system, $2/m 2/m 2/m$. The stereogram shows the positions and the indices of all orthorhombic forms. The poles of faces with negative l are excluded. The spherical triangle with vertices (100) , (010) , (001) is an asymmetric face unit for the point group $2/m 2/m 2/m$

Table 8.7. Crystal forms in the orthorhombic system and their face symmetries

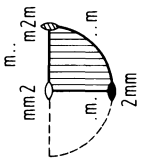
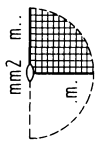
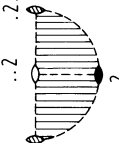
Point group	Asymmetric face unit and face symmetry	Special forms		General and limiting forms {hkl}	Special and limiting forms			
		{h0}	{0kl}		{hk0}	{100}	{010}	{001}
2/m 2/m 2/m (mmm)		Rhombic prism .m.	Rhombic prism m...	Rhombic dipyramid 1	Rhombic prism ..m	Pinacoid 2mm	Pinacoid m2m	Pinacoid mm2
mm2		Dihedron .m.	Dihedron m...	Rhombic pyramid 1	Rhombic prism 1	Pinacoid .m.	Pinacoid m..	Pedion mm2
222		Rhombic prism 1		Rhombic disphenoid 1		Pinacoid 2..	Pinacoid .2.	Pinacoid ..2

Table 8.8. Eigensymmetry and generating symmetry of the tetragonal forms

	Eigensymmetry	Generating symmetry
Tetragonal pyramid	4mm	4, 4mm
Tetragonal disphenoid	$\bar{4}2m$	$\bar{4}$, $\bar{4}2m$
Tetragonal prism	4/mmm	4, $\bar{4}$, 4/m, 422, 4mm 42m, 4/mmm
Tetragonal trapezohedron	422	422
Ditetragonal pyramid	4mm	4mm
Tetragonal scalenohedron	$\bar{4}2m$	$\bar{4}2m$
Tetragonal dipyrmaid	4/mmm	4/m, 422, $\bar{4}2m$, 4/mmm
Ditetragonal prism	4/mmm	422, 4mm, $\bar{4}2m$, 4/mmm
Ditetragonal dipyrmaid	4/mmm	4/mmm

Crystal Forms in the Orthorhombic, Monoclinic and Triclinic Systems

All of the “rhombic” forms are listed in Table 14.1.1, see Fig. 8.16 and Table 8.7.

Only relatively simple forms occur in the monoclinic system. The general form in 2/m is the rhombic prism; in m and 2, the general forms are both dihedra: a dome in m and a sphenoid in 2 (Table 14.1.1). The pinacoid and the pedion are special or limiting forms.

The triclinic system gives only the pinacoid ($\bar{1}$) and the pedion (1).

The symmetry of a crystal form can be considered in two separate ways. A tetragonal pyramid is generated by the symmetry operations of 4; that is its *generating symmetry*. On the other hand, a tetragonal pyramid actually displays the symmetry of 4mm; that is its *eigensymmetry*¹. In Table 8.8, these eigensymmetries and generating symmetries are given for all tetragonal forms.

Normally, crystals are not characterised by a single form but by a combination of forms, which must, of course, all conform to the point group of the crystal. The rutile crystal in Table 8.11.15 is a combination of a tetragonal dipyrmaid {111}, and two tetragonal prisms, {100} and {110}.

¹ eigen (German) = own

8.3 Molecular Symmetry

Point symmetry is a very great help in the description of molecules, by which term we include polyatomic ions of any charge. Figure 8.17a shows a molecule of H_2O , on which the symmetry elements, two mirror planes and a 2-fold rotation axis, have been drawn. The point group $mm2$ (C_{2v}) is shown on the stereogram in Fig. 8.17b.

In Table 8.11.1–37 (left hand column) molecular examples are given for several point groups. The stereogram for the point group is in most cases in the same orientation as the example molecule.

The point groups of molecules are not limited to the 32 crystallographic groups. They may contain such symmetry elements as 5-fold axes which are incompatible with a crystal lattice. Table 8.11.33–37 and Fig. 11.6b give a few examples of important *non-crystallographic point groups* with molecular examples.

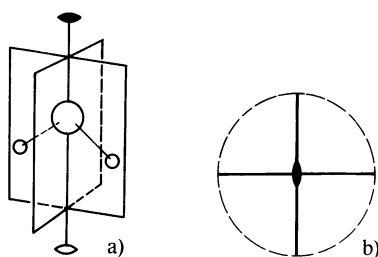


Fig. 8.17a. Point symmetry ($mm2 - C_{2v}$) of the H_2O molecule. **b** Stereogram of the symmetry elements of this point group

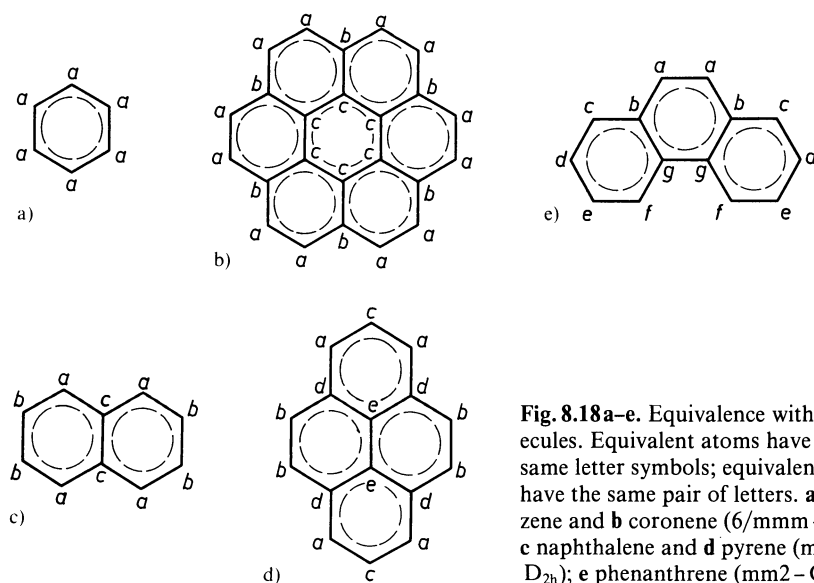


Fig. 8.18a–e. Equivalence within molecules. Equivalent atoms have the same letter symbols; equivalent bonds have the same pair of letters. **a** Benzene and **b** coronene ($6/mmm - D_{6h}$); **c** naphthalene and **d** pyrene ($mmm - D_{2h}$); **e** phenanthrene ($mm2 - C_{2v}$)

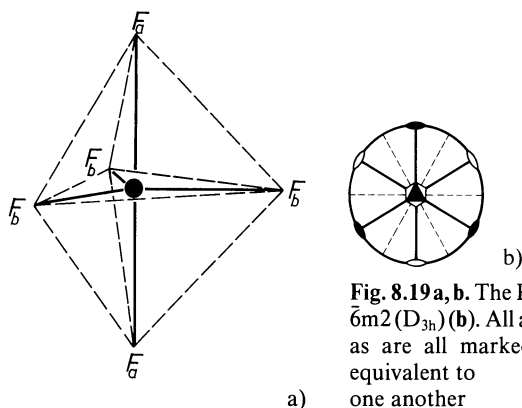


Fig. 8.19 a, b. The PF_5 molecule (a) has point group $\bar{6}m2 (D_{3h})$ (b). All atoms marked F_a are equivalent, as are all marked F_b , but F_a and F_b are not equivalent to one another

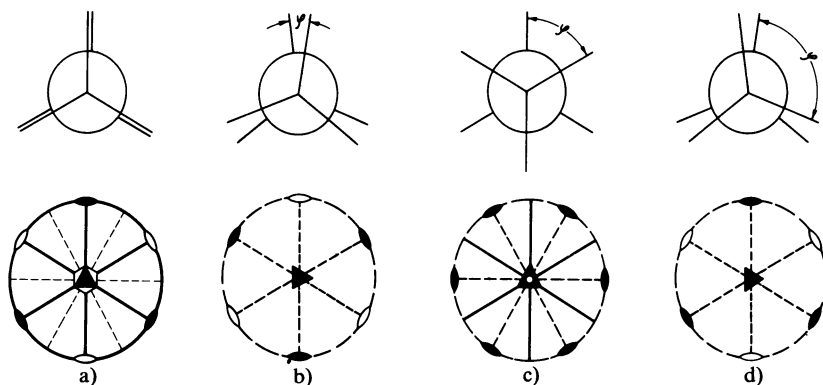


Fig. 8.20 a-d. Conformations of ethane. **a** Eclipsed: $\varphi = 0$ or 120 or 240° : ($\bar{6}m2 - D_{3h}$). **b** Skew: $0 < \varphi < 60^\circ$, $120 < \varphi < 180^\circ$ or $240 < \varphi < 300^\circ$: ($32 - D_3$). **c** Staggered: $\varphi = 60$ or 180 or 300° : ($\bar{3}m - D_{3d}$). **d** Skew: $60 < \varphi < 120^\circ$, $180 < \varphi < 240^\circ$ or $300 < \varphi < 360^\circ$: ($32 - D_3$). The conformations in **b** and **d** are enantiomorphs

The point group of a molecule indicates which atoms and which bonds are equivalent. Thus, in benzene, C_6H_6 , with point group $6/mmm - D_{6h}$ all C-atoms and all H-atoms are equivalent, as are all C-H and C-C bonds (Fig. 8.18a, and also Table 8.11.27). Coronene, $\text{C}_{24}\text{H}_{12}$, also belongs to point group $6/mmm - D_{6h}$. In Fig. 8.18b, equivalent carbon atoms are indicated by the letters a or b or c, and all bonds between pairs of similarly labelled atoms are equivalent. There are thus four symmetry independent C-C bonds in coronene (a-a, a-b, b-c and c-c). Further examples are naphthalene, C_{10}H_8 , and pyrene, $\text{C}_{16}\text{H}_{10}$, both ($mmm - D_{2h}$) (Fig. 8.18c), and phenanthrene, $\text{C}_{14}\text{H}_{10}$, ($mm2 - C_{2v}$) (Fig. 8.18e). The equivalences can be particularly clearly shown by copying the stereogram of the appropriate point group (Table 8.11.7, 8 and 27) onto transparent paper and superimposing it on the molecules in Fig. 8.18.

In PF_5 , phosphorus is surrounded by five fluorine atoms. Were this a planar pentagonal molecule, all F-atoms and all P-F bonds would be equivalent

(point group $5/m\bar{m}2$ ($\bar{1}0m2$), Table 8.11.35). In fact, the molecule has the shape of a trigonal dipyramid (Fig. 8.19) with the P-atom at the centre, and point symmetry $\bar{6}m2$ (D_{3h}). Thus, the two atoms labelled F_a are equivalent, as are the three labelled F_b , but F_a and F_b are not equivalent to one another.

If one of the methyl groups of an ethane molecule is rotated about the C–C bond through 360° with respect to the other, various different *conformations* will be generated. These are illustrated in Fig. 8.20 together with the stereograms of the respective point groups. Conformations are the spatial arrangements of the atoms of a molecule which result from rotation about a chemical single bond.

8.4 Determination of Point Groups

Before the determination of the point group of a crystal (or a molecule having a crystallographic point group), it should be assigned to one of the seven crystal systems. For this, it is necessary to know the *characteristic symmetry elements* of the crystal systems; these are given in Table 8.9, and can be derived from the symmetry information given in Table 8.10.

Table 8.9. Characteristic symmetry elements of the seven crystal systems

Crystal system	Point groups ^a	Characteristic symmetry elements
Cubic	$4/m\bar{3}2/m$ $\bar{4}3m, \bar{4}32, 2/m\bar{3}, 23$	4 ▲
Hexagonal	$6/m2/m2/m$ $\bar{6}m2, 6mm, 622,$ $6/m, \bar{6}, \bar{6}$	⬡ or ⬢
Tetragonal	$4/m2/m2/m$ $\bar{4}2m, 4mm, \bar{4}22,$ $4/m, \bar{4}, \bar{4}$	1 ■ or 1 ▧ (3 ■ or 3 ▧ ⇒ cubic)
Trigonal	$\bar{3}2/m$ $\bar{3}m, \bar{3}2, \bar{3}, \bar{3}$	1 ▲ (remember that m normal to 3 gives $\bar{6}$ = hexagonal)
Orthorhombic	$2/m2/m2/m$ $mm2, 222$	2 and/or m in three orthogonal directions
Monoclinic	$2/m$ $m, \bar{2}$	2 and/or m in one direction
Triclinic	$\bar{1}$ 1	$\bar{1}$ or 1 only

^a Characteric symmetry elements are underlined.

In determining the point group of molecules or crystals, it is in general not necessary to find each and every symmetry element. Using Tables 8.9 and 8.10, it may generally be done by answering a few, well-chosen questions. In practice, it is best to consider first an important property of rotation axes. All rotation axes are polar. This means that they have distinct properties in parallel and antiparallel directions. Various other symmetry elements can destroy this polarity, viz.:

- (a) $\bar{1}$ (b) $m \perp X$ (c) $2 \perp X$

The 2 in Fig. 8.17 and Table 8.11.18 and the 3 in Table 8.11.19 are examples of polar rotation axes. The ends of polar axes are represented in symmetry diagrams and stereograms by one solid and one open symbol (cf. Figs. 6.8f–6.13f).

Questions to use for point-group determination:

1. Are rotation axes higher than 2 present (3, 4, 6)?
2. Are these axes polar? or
Is an inversion centre present?
(crystals with an inversion centre are characterised by sets of parallel faces opposite one another.)

Point group determination will be illustrated by two examples:

- a) The methane molecule (CH_4) (Table 8.11.31). It is easily seen that a polar 3-fold axis lies on each C–H bond. As there are four of these, the point group must belong to the cubic system, and it must be one with polar 3-fold axes (indicated in Table 8.10 by a subscript p by the graphical symbol (e.g. \blacktriangle_p). This indicates either 23 or $\bar{4}3m$ (Table 8.10). These are readily distinguished, since only $\bar{4}3m$ has mirror planes. These planes are readily seen in CH_4 , so the point group is $\bar{4}3m$.
- b) A crystal of magnesium (Table 8.11.27). The crystal contains a 6-fold rotation axis, and so must belong to the hexagonal system. An inversion centre is also easily found. This limits the point group to $6/m$ and $6/mmm$ (Table 8.10). These may be distinguished by the mirror planes parallel to 6 in $6/mmm$ and not in $6/m$. Since these planes are evident in the crystal, the magnesium crystal may be assigned to point group $6/mmm$.

Determination of the symmetry of a crystal is not always unambiguous. For example, the cube (hexahedron) occurs as a form in all five cubic point groups (Table 8.6). Determining the symmetry of a cube will naturally lead to the point group of highest symmetry, $m\bar{3}m$ (Table 8.11.32). The mineral pyrites, FeS_2 (point group $m\bar{3}$) has cube-shaped crystals. The cube-faces, however, frequently have characteristic striations which indicate the lower symmetry (Table 8.11.29).

In other ambiguous cases, “etch-figures” will indicate the true symmetry of a crystal face and hence of the entire crystal. These figures are bounded by faces with high Miller indices and arise from the action of a solvent on a crystal face.

Table 8.10. Crystal systems, point groups, symmetric directions and symmetry-dependent physical properties

Crystal systems	Point groups			Symmetry elements ^c	Symmetry elements and symmetry directions ^d			Enantiorphism	Optical activity	Piezoelectricity	Pyroelectricity	Lave groups
	Nr.	Sch ^a	H.-M. ^b		a	b	c					
	Triclinic $a \neq b \neq c$ $\alpha \neq \beta \neq \gamma$	1	C_1		1		-					
	2	C_i	$\bar{1}$	$\bar{1}$	-	-	-					
Monoclinic $a \neq b \neq c$ $\alpha = \gamma = 90^\circ$ $\beta > 90^\circ$	3	C_2	2	\bullet_p	-	2	-	+	+	+	+	$2/m$
	4	C_s	m	m	-	m	-		(+)	+	+	
	5	C_{2h}	$2/m$	$\bullet \perp m$	-	$2/m$	-					
Orthorhombic $a \neq b \neq c$ $\alpha = \beta = \gamma = 90^\circ$	6	D_2	222	$\bullet + \bullet + \bullet$	2	2	2	+	+	+	+	
	7	C_{2v}	mm2	$m + m + \bullet_p$	m	m	2		(+)	+	+	
	8	D_{2h}	mmm ($2/m2/m2/m$)	$(\bullet \perp m) + (\bullet \perp m) + (\bullet \perp m)$	$2/m$	$2/m$	$2/m$					

^a Schönflies symbol.
^b Hermann-Mauguin symbol (International symbol).
^c The number of symmetry elements of each type is given, p signifies polar.
^d Rotation axes, rotoinversion axes and the normals to mirror planes are parallel to the respective symmetry directions.
 continuation p. 148 and 149

Table 8.10 (continuation)

Crystal systems	Point groups			Symmetry elements ^c	Symmetry elements and symmetry directions ^d						Enantiom.	Optical act.	Piezoelectr.	Pyroelectr.	Lauve groups			
	Nr.	Sch ^a	H.-M. ^b		c	$\langle a \rangle$	$\langle 110 \rangle$	Optical act.								Piezoelectr.		
								+	(+)	-						+	(+)	-
Tetragonal $a = b \neq c$ $\alpha = \beta = \gamma = 90^\circ$	9	C_4	4	\blacksquare_P	4	-	-	+	+	+	+	+	+	4/m				
	10	S_4	$\bar{4}$	\blacksquare	$\bar{4}$	-	-	(+)	(+)	+	+	+	+					
	11	C_{4h}	4/m	$\blacksquare \perp m$	$\bar{1}$	4/m	-	-										
	12	D_4	422	$\blacksquare + 2\uparrow + 2\downarrow$		4	2	2	+	+	+	+	+					
	13	C_{4v}	4mm	$\blacksquare_P + 2m + 2m$		4	m	m			+	+	+	4/mmm				
	14	D_{2d}	$\bar{4}2m$	$\blacksquare + 2\uparrow + 2m$		$\bar{4}$	2	m		(+)	+	+	+					
	15	D_{4h}	4/mmm (4/m2/m2/m)	$(\blacksquare \perp m) + 2(\uparrow \perp m) + 2(\downarrow \perp m)$	$\bar{1}$	4/m	2/m	2/m										
Trigonal $a = b \neq c$ $\alpha = \beta = 90^\circ$ $\gamma = 120^\circ$	16	C_3	3	\blacktriangle_P	c	$\langle a \rangle$	-	+	+	+	+	+	$\bar{3}$					
	17	C_{3i}	$\bar{3}$	\blacktriangle	3	-	-											
	18	D_3	32	$\blacktriangle + 3\uparrow_P$		3	2	2	+	+	+	+	$\bar{3}m$					
	19	C_{3v}	3m	$\blacktriangle_P + 3m$		3	m	-			+	+						
	20	D_{3d}	$\bar{3}m$ ($\bar{3}2/m$)	$\blacktriangle + 3(\uparrow \perp m)$	$\bar{1}$	$\bar{3}$	2/m	2/m										

Crystals of the mineral nepheline (Table 8.11.21) have a morphology (a hexagonal prism and a pinacoid) which indicate the point group 6/mmm. The etch figures show that the true symmetry is only 6.

8.5 Enantiomorphism

The point group 1 (C_1) is *asymmetric*. All other point groups with no symmetry other than rotation axes are called *chiral* or *dissymmetric*. The relevant point groups are:

X: (1), 2, 3, 4, 6	C_n : (C_1), C_2 , C_3 , C_4 , C_6
X2: 222, 32, 422, 622	D_n : D_2 , D_3 , D_4 , D_6
X3: 23, 432	T, O

Asymmetric and dissymmetric crystals and molecules are those which are not superimposable on their mirror images by rotation or translation. These mirror images are said to be the *enantiomorphs* of each other. In Fig. 5.9 and Table 8.11.3 and 18, examples are given of enantiomorphic crystals and molecules. Enantiomorphic molecules are also called *enantiomeric*.

8.6 Point Groups and Physical Properties

We shall now examine a few properties of molecules and crystals which are related to their point groups, or whose effects may be traced back to specific symmetry considerations.

8.6.1 Optical Activity

Optical activity refers to the ability of certain crystals and molecules to rotate the plane of polarised light. It can only arise in those point groups which are enantiomorphic (cf. Sect. 8.5 and Table 8.10). Two sorts of optical activity may be distinguished:

a) *Optical Activity as a Property of a Crystal*. The crystal is optically active, and this activity is lost when the crystal is melted or dissolved. Examples include $MgSO_4 \cdot 7H_2O$, SiO_2 (low-quartz), $NaClO_3$ (Table 8.11.6, 18 and 28). Not only the morphology but also the crystal structures exist in two enantiomorphic forms. The “left” form rotates the plane of polarised light to the left, and the “right” form an equal amount to the right.

b) *Optical Activity as the Property of Molecules*. Some molecules are themselves enantiomeric, and both their solutions and the crystals they form are optically active. Well-known examples of this type of optical activity are the crystals of

D- and L-tartaric acid (Table 8.11.3). In contrast, the “racemate” DL-tartaric acid is optically inactive and gives crystals with point group $\bar{1}$ (C_i). Molecules of the isomeric form *meso*-tartaric acid ($\bar{1}$, (C_i), Table 8.11.2) are centrosymmetric and hence optically inactive.

Optical activity is not limited to the 11 point groups in which enantiomorphism occurs (Sect. 8.5). It can also occur in crystals in the point groups m (C_s), $mm2$ (C_{2v}), $\bar{4}$ (S_4) and $\bar{4}2m$ (D_{2d}), cf. Table 8.10.

8.6.2 Piezoelectricity

Some crystals, when subjected to pressure or tension in certain directions develop an electric charge; this property is called *piezoelectricity*. This effect is clearly seen in plates of quartz (point group 32), cut normal to the a -axis or any polar 2-fold rotation axis (Fig. 8.21). The direction of the applied pressure or tension must be along a polar axis. Polar axes are those which have distinct physical properties in the parallel and antiparallel directions. These directions must thus not be themselves related by symmetry. It follows that within the crystal there will be an asymmetric charge distribution along polar axes. The opposite faces, normal to the polar axis, develop electric charges when a pressure is applied along the axis. The direction of this electric field is reversed when the pressure is replaced by a tension.

Piezoelectricity is only observed in crystals which have polar axes. Polar directions only exist in point groups without a centre of symmetry. There are 21 such point groups, as is shown in Table 8.10. The point group 432 is also excluded, as the symmetry is too high for the effect to develop.

The piezoelectric effect is reversible. If an electric field is applied in the direction of the polar axis of a quartz plate, the crystal will undergo compression or expansion. The application of an alternating field will cause the crystal to vibrate.

Other crystals which show piezoelectricity include D- and L-tartaric acid ($2 - C_2$), Table 8.11.3; tourmaline ($3m - C_{3v}$), Table 8.11.19; NaClO_3 ($23 - T$), Table 8.11.28; ZnS (sphalerite) ($\bar{4}3m - T_d$), Table 8.11.31.

Piezoelectricity has many technical applications, including ultrasonic generators, amplifiers, microphones and quartz time-pieces.

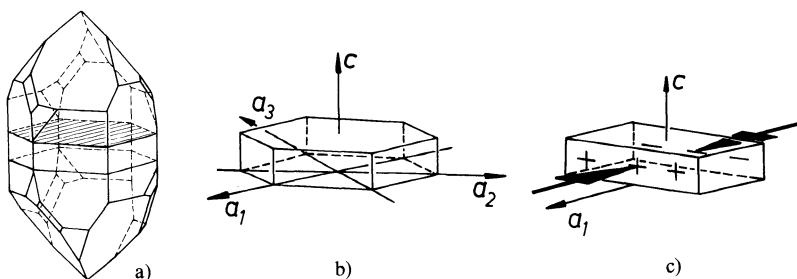


Fig. 8.21 a-c. The piezoelectric effect in a quartz plate arising from pressure along a polar axis, here parallel to the a_1 axis

8.6.3 Pyroelectricity

When a crystal of tourmaline (Table 8.11.19) is heated, the polar ends of the crystal develop electric charges. Heating causes the positive end of the *c*-axis to become positively charged relative to the negative end, and cooling has the opposite effect. This effect results from the fact that tourmaline has a permanent electric dipole. The charge which builds up is soon dissipated by conduction into the surroundings. Changes in temperature change the size of the electric dipole.

The dipole moment is a vector. Pyroelectricity can only arise when the point group has no symmetry operations which alter the direction of this dipole. The vector must remain unchanged by all the symmetry operations. Point groups having this property include those with only a single rotation axis: $2(C_2)$, $3(C_3)$, $4(C_4)$ and $6(C_6)$ as well as those which have only these axes plus mirror planes parallel to them: $mm2(C_{2v})$, $3m(C_{3v})$, $4mm(C_{4v})$ and $6mm(C_{6v})$. The dipole-moment vector lies in the rotation axis. The conditions for the presence of a dipole moment are also found in the point groups *m* (for all directions parallel to the mirror plane) and *1* (for every direction), cf. Table 8.10.

Knowledge of the symmetry gives only a qualitative indication of the possible presence of pyroelectricity. It does not indicate the size of the dipole moment or the directions of the positive and negative ends.

Sucrose, $C_{12}H_{22}O_{11}$, ($2 - C_2$) and hemimorphite, $Zn_4[(OH)_2/Si_2O_7] \cdot H_2O$ ($mm2 - C_{2v}$) are examples of crystals showing pyroelectricity.

8.6.4 Molecular Dipole Moments

Many molecules have an asymmetric distribution of electric charge and hence an electric *dipole moment*. The relationship between the point group of a molecule and the direction of its dipole is the same as that developed above for the pyroelectricity of crystals (cf. Sect. 8.6.3).

The measurement of a dipole moment can give important information about the shape of a molecule. PF_3 has a dipole moment, while BF_3 does not. Molecules of the formula AB_3 may have the shape of an equilateral triangle with A at the centre [$\bar{6}m2(D_{3d})$] or a triangular pyramid with A at the apex [$3m(C_{3v})$], cf. Table 8.11.19 and 26. The shape of BF_3 is thus the former, while PF_3 is the latter.

Table 8.11. Examples of molecules and crystals for the point groups

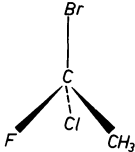

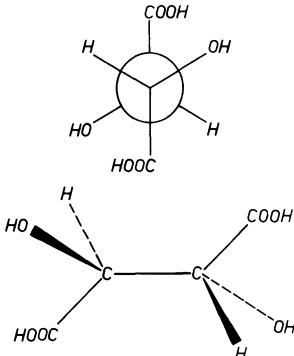
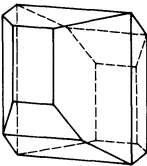
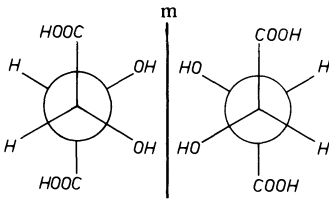
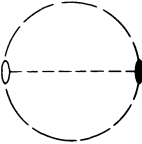
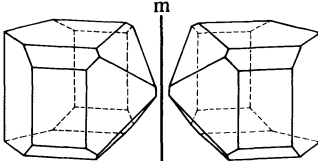
Molecules	Point group	Crystals
	$1 - C_1$	<div style="text-align: right;">1</div>  <hr/> $SrH_2(C_4H_4O_6)_2 \cdot 4H_2O$ $CaS_2O_3 \cdot 6H_2O$
 <p style="text-align: center;"><i>Meso</i>-Tartaric acid</p>	σ $\bar{1} - C_i$	<div style="text-align: right;">2</div>  <hr/> $CH_2(COOH)_2$ (Malonic acid) <hr/> H_3BO_3 , $CuSO_4 \cdot 5H_2O$ $MnSiO_3$ (Rhodonite) $NaAlSi_3O_8$ (Albite)
 <p>The enantiomers of tartaric acid</p>	 $2 - C_2$	<div style="text-align: right;">3</div>  <p style="text-align: center;">D- L- Tartaric acid</p> <hr/> $Li_2SO_4 \cdot H_2O$ $C_{12}H_{22}O_{11}$ (Sucrose) $C_{14}H_{10}$ (Phenanthrene)

Table 8.11 (continuation)

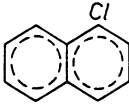
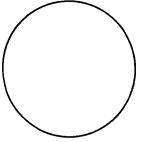
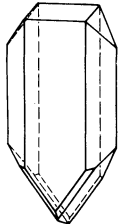
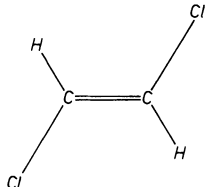
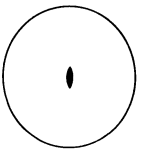
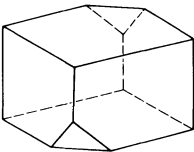
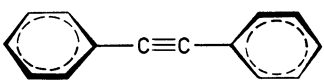
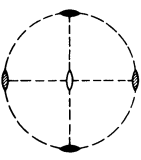
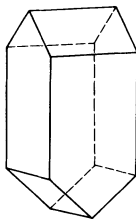
Molecules	Point group	Crystals
 <p style="text-align: center;">— NOCl</p>	 <p style="text-align: center;">$m - C_s$</p>	<p style="text-align: right;">4</p>  <p style="text-align: center;">$K_2S_4O_6$ $CuSO_4 \cdot 3H_2O$</p>
 <p style="text-align: center;"><i>Trans</i>-1,2-Dichloroethene</p>	 <p style="text-align: center;">$2/m - C_{2h}$</p>	<p style="text-align: right;">5</p>  <p style="text-align: center;">$KClO_3$</p> <p style="text-align: center;">$CaSO_4 \cdot 2H_2O$ (Gypsum) Fig. 5.6 $FeSO_4 \cdot 7H_2O$ $KAlSi_3O_8$ (Sanidine), S $C_{10}H_8$, $C_{14}H_{10}$ (Anthracene) $(COOH)_2 \cdot 2H_2O$</p>
 <p style="text-align: center;">Diphenylethine</p>	 <p style="text-align: center;">$222 - D_2$</p>	<p style="text-align: right;">6</p>  <p style="text-align: center;">$MgSO_4 \cdot 7H_2O$ (Epsomite)</p> <p style="text-align: center;">Vitamin B_{12} (Fig. 1.1b) $KNaC_4H_4O_6 \cdot 4H_2O$ (Rochelle salt)</p>

Table 8.11 (continuation)

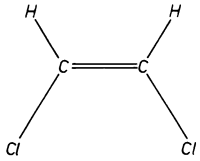
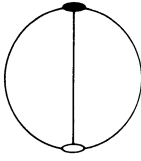
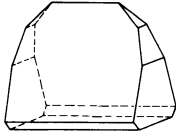
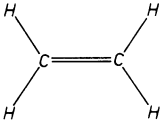
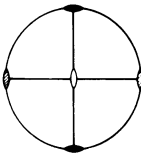
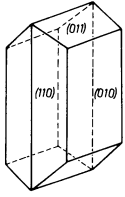
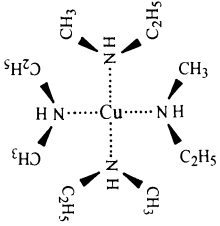
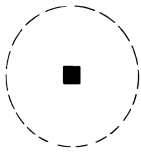
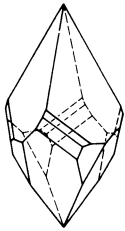
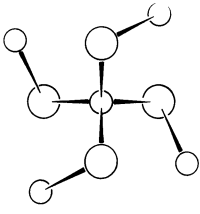
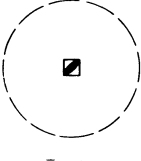
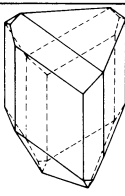
Molecules	Point group	Crystals
 <p data-bbox="209 412 409 437"><i>Cis</i>-1,2-Dichloroethene</p>	 <p data-bbox="518 402 612 426">mm2 – C_{2v}</p>	 <p data-bbox="950 248 959 266">7</p> <p data-bbox="667 402 926 426">NH₄MgPO₄ · 6H₂O (Struvite)</p> <hr/> <p data-bbox="667 448 879 518">C₆H₄(OH)₂ (Resorcinol) Ag₃Sb (Dyskrasite) FeAlO₃</p>
 <p data-bbox="279 707 350 732">Ethene</p>	 <p data-bbox="518 719 612 744">mmm – D_{2h}</p>	 <p data-bbox="950 548 959 566">8</p> <p data-bbox="667 737 844 762">CaCO₃ (Aragonite)</p> <hr/> <p data-bbox="667 783 950 853">CaSO₄ (Anhydrite), KClO₄ BaSO₄ (Barytes), S (COOH)₂ (Oxalic acid), C₆H₆, I₂</p>
 <p data-bbox="444 889 468 906">2+</p>	 <p data-bbox="542 1107 589 1132">4 – C₄</p>	 <p data-bbox="950 883 959 901">9</p> <p data-bbox="667 1107 856 1132">PbMoO₄ (Wulfenite)</p> <hr/> <p data-bbox="667 1153 914 1178">(CH₃CHO)₄ (Metaldehyde)</p>
 <p data-bbox="248 1425 373 1450">C – (S – CH₃)₄</p>	 <p data-bbox="542 1407 589 1432">4 – S₄</p>	 <p data-bbox="950 1201 959 1218">10</p> <p data-bbox="667 1382 926 1407">Ca₂[AsO₄/B(OH)₄] (Cahnite)</p> <hr/> <p data-bbox="667 1428 926 1471">BPO₄, BaSO₄ C(CH₂OH)₄ (Pentaerythritol)</p>

Table 8.11 (continuation)

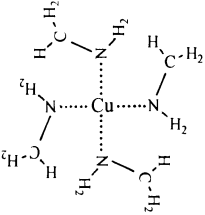
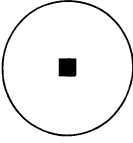
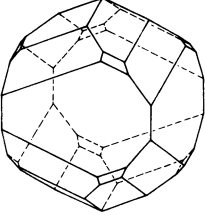
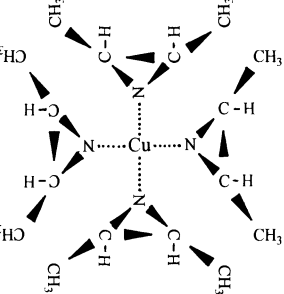
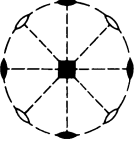
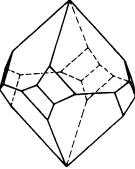
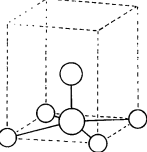
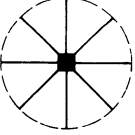
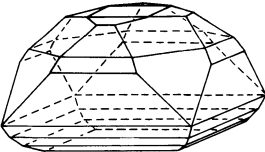
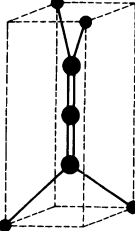
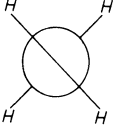
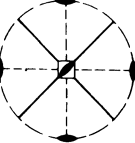
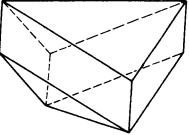
Molecules	Point group	Crystals
 <p style="text-align: right; margin-right: 10px;">2+</p>	 <p style="text-align: center;">4/m - C_{4h}</p>	 <p style="text-align: right;">11</p> <p>CH₂OH · (CHOH)₂ · CH₂OH (Isoerythritol)</p> <hr/> <p>CaWO₄ (Scheelite) NaIO₄, BaMoO₄</p>
 <p style="text-align: right; margin-right: 10px;">2+</p>	 <p style="text-align: center;">422 - D₄</p>	 <p style="text-align: right;">12</p> <p>CCl₃COOK · CCl₃COOH</p> <hr/> <p>NiSO₄ · 6H₂O</p>
 <p style="text-align: center;">XeOF₄</p>	 <p style="text-align: center;">4mm - C_{4v}</p>	 <p style="text-align: right;">13</p> <p>Diaboleite Pb₂Cu(OH)₄Cl₂</p>
 <p style="text-align: center;">C₃H₄ (Allene)</p> 	 <p style="text-align: center;">42m - D_{2d}</p>	 <p style="text-align: right;">14</p> <p>Hg(CN)₂</p> <hr/> <p>KH₂PO₄, CO(NH₂)₂ (Urea) CuFeS₂ (Chalcopyrite)</p>

Table 8.11 (continuation)

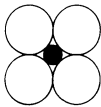
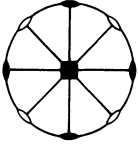
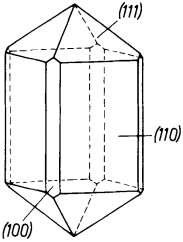
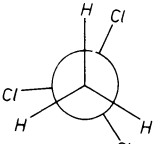
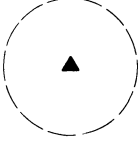
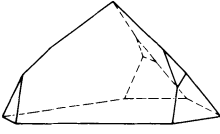
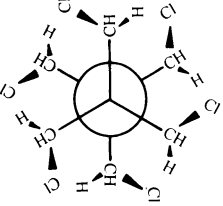
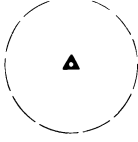
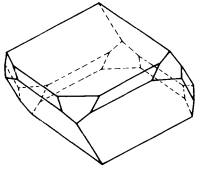
Molecules	Point group	Crystals
 <p data-bbox="291 455 345 483">PtCl_4^{2-}</p>	 <p data-bbox="509 478 630 506">$4/mmm - D_{4h}$</p>	<p data-bbox="941 248 961 276">15</p>  <p data-bbox="673 543 785 571">TiO_2 (Rutile)</p> <hr/> <p data-bbox="673 601 826 672">SnO_2 (Cassiterite) TiO_2 (Anatase) ZrSiO_4 (Zircon)</p>
 <p data-bbox="279 922 356 950">CH_3CCl_3</p>	 <p data-bbox="544 922 595 950">$3 - C_3$</p>	<p data-bbox="941 719 961 747">16</p>  <p data-bbox="673 936 791 964">$\text{NaIO}_4 \cdot 3\text{H}_2\text{O}$</p> <hr/> <p data-bbox="673 984 712 1012">Ti_2S</p>
	 <p data-bbox="544 1319 595 1347">$\bar{3} - C_{3i}$</p>	<p data-bbox="941 1090 961 1118">17</p>  <p data-bbox="673 1354 885 1382">$\text{CaMg}(\text{CO}_3)_2$ (Dolomite)</p> <hr/> <p data-bbox="673 1407 844 1478">FeTiO_3 (Ilmenite) Be_2SiO_4 (Phenacite) Li_2BeF_4</p>

Table 8.11 (continuation)

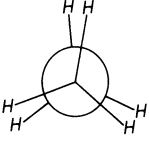
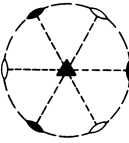
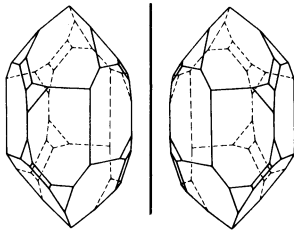
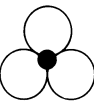
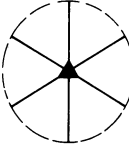
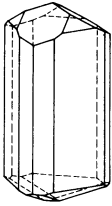
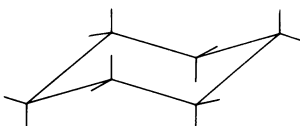
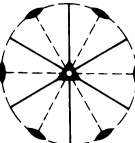
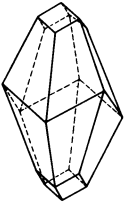
Molecules	Point group	Crystals
 <p data-bbox="199 476 435 502">C_2H_6 (Skew conformation)</p>	 <p data-bbox="546 476 605 502">$32 - D_3$</p>	<p data-bbox="946 238 970 264">18</p>  <p data-bbox="746 529 923 582">L- Low-quartz SiO_2 R-</p> <hr/> <p data-bbox="676 599 923 652">$AlPO_4$, Se, Te, HgS, $K_2S_2O_6$ $(C_6H_5CO)_2$ (Benzil)</p>
 <p data-bbox="241 864 405 899">IO_3^-, SeO_3^{2-}, AsO_3^{3-}</p>	 <p data-bbox="540 899 611 926">$3m - C_{3v}$</p>	<p data-bbox="946 679 970 705">19</p>  <p data-bbox="676 917 782 943">Tourmaline</p> <hr/> <p data-bbox="676 961 870 1031">Ag_3SbS_3 (Pyrargyrite) NiS (Millerite) $LiNaSO_4$</p>
 <p data-bbox="176 1314 464 1349">C_6H_{12} Cyclohexane (Chair-form)</p>	 <p data-bbox="535 1278 623 1305">$\bar{3}m - D_{3d}$</p>	<p data-bbox="946 1067 970 1093">20</p>  <p data-bbox="676 1314 823 1349">$CaCO_3$ (Calcite)</p> <hr/> <p data-bbox="676 1367 905 1464">As, Sb, Bi, $CdCl_2$, $NaNO_3$ Al_2O_3 (Corundum) Fe_2O_3 (Haematite) $Mg(OH)_2$ (Brucite)</p>

Table 8.11 (continuation)

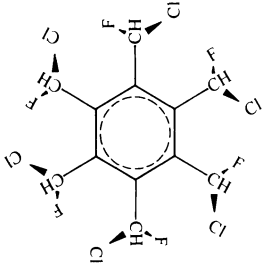
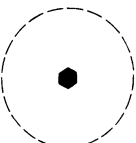
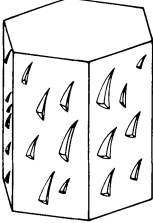
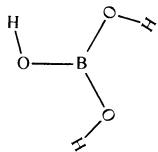
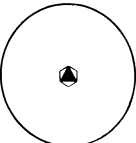
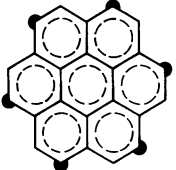
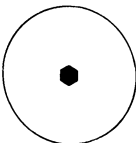
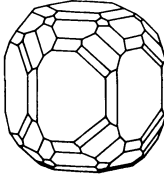
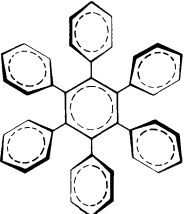
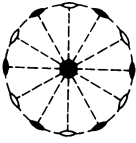
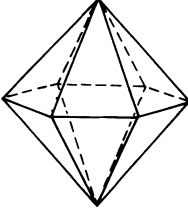
Molecules	Point group	Crystals
 <p style="text-align: center;">CHFCl = R</p> <p style="text-align: center;">Hexa-R-Benzene</p>	 <p style="text-align: center;">$6 - C_6$</p>	<p style="text-align: right;">21</p>  <p style="text-align: center;">KNa₃(AlSiO₄)₄ (Nepheline) with etch-figures</p> <hr/> <p style="text-align: center;">LiKSO₄ CHI₃</p>
 <p style="text-align: center;">B(OH)₃</p>	 <p style="text-align: center;">$\bar{6} - C_{3h}$</p>	<p style="text-align: right;">22</p> <p style="text-align: center;">Li₂O₂</p>
 <p style="text-align: center;">Hexaazacorone</p>	 <p style="text-align: center;">$6/m - C_{6h}$</p>	<p style="text-align: right;">23</p>  <p style="text-align: center;">Ca₅[F/(PO₄)₃] (Apatite)</p> <hr/> <p style="text-align: center;">Ce₂(SO₄)₃ · 9H₂O</p>
 <p style="text-align: center;">Hexaphenylbenzene</p>	 <p style="text-align: center;">$622 - D_6$</p>	<p style="text-align: right;">24</p>  <p style="text-align: center;">KAlSiO₄ (Kaliophilite) SiO₂ (High-quartz)</p>

Table 8.11 (continuation)

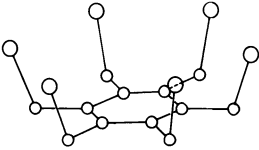
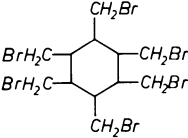
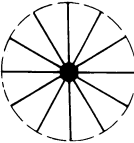
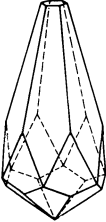
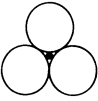
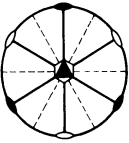
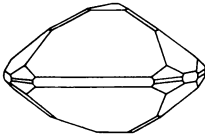

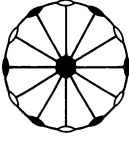
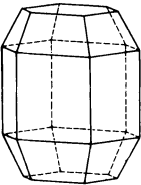
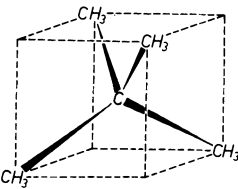
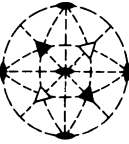
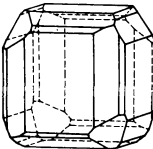
Molecules	Point group	Crystals
  Hexabromomethylbenzene	 $6\text{mm} - C_{6v}$	25  AgI <hr/> ZnS (Wurtzite), CdS ZnO, BeO
 $\text{NO}_3^-, \text{CO}_3^{2-}$	 $\bar{3}m2 - D_{3h}$	26  BaTi(Si ₃ O ₉) (Benitoite)
 Benzene	 $6/mmm - D_{6h}$	27  Mg <hr/> Be, Zn, CuS, NiAs, Be ₃ Al ₂ Si ₆ O ₁₈ (Beryl) C (Graphite), MoS ₂ C ₂ H ₆
 Tetramethylmethane	 $23 - T$	28  Left-NaClO ₃ <hr/> NaBrO ₃

Table 8.11 (continuation)

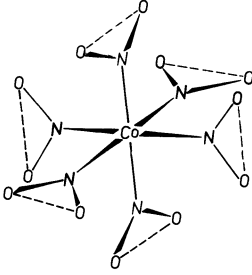
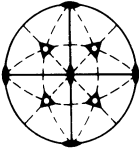
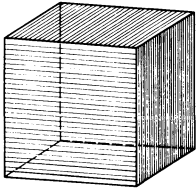
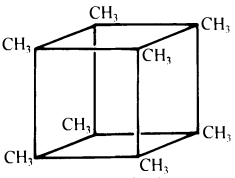
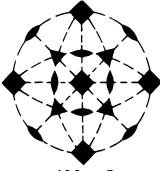
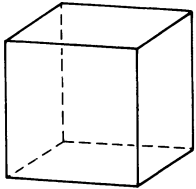
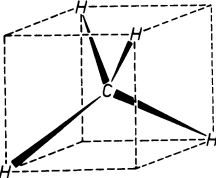
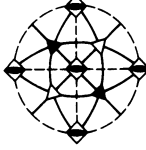
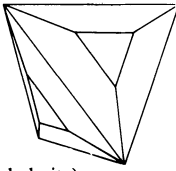
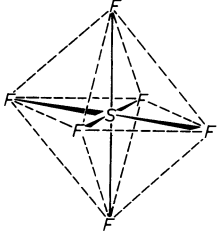
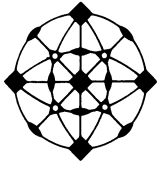
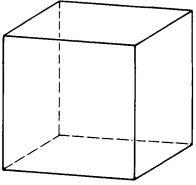
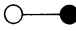
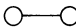
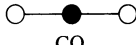
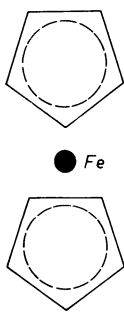
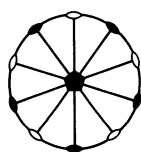
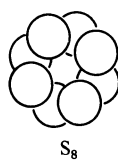
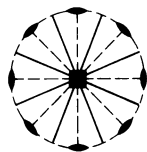
Molecules	Point group	Crystals
 <p data-bbox="252 515 373 543">$[\text{Co}(\text{NO}_2)_6]^{3-}$</p>	 <p data-bbox="531 462 602 490">$m\bar{3} - T_h$</p>	 <p data-bbox="938 243 954 268">29</p> <p data-bbox="667 437 938 479">FeS_2 (Pyrite) with Striations on the cube faces</p> <p data-bbox="667 508 938 532">Alums (e.g. $\text{KAl}(\text{SO}_4)_2 \cdot 12\text{H}_2\text{O}$)</p>
 <p data-bbox="209 779 373 802">Octamethylcubane</p>	 <p data-bbox="531 772 602 797">$432 - O$</p>	 <p data-bbox="938 560 954 585">30</p> <p data-bbox="667 744 860 769">SiO_2 (Melanophlogite)</p> <p data-bbox="667 779 754 804">Ag_3AuTe_2</p>
 <p data-bbox="279 1009 355 1033">Methane</p>	 <p data-bbox="531 1001 609 1026">$\bar{4}3m - T_d$</p>	 <p data-bbox="938 843 954 867">31</p> <p data-bbox="667 1001 809 1026">ZnS (Sphalerite)</p> <p data-bbox="667 1044 825 1097">CuCl, CuBr, CuI $\text{Al}(\text{PO}_3)_3$, Ag_3PO_4</p>
 <p data-bbox="291 1379 331 1404">SF_6</p> <p data-bbox="138 1425 272 1450">C_8H_8 (Cubane)</p>	 <p data-bbox="519 1337 609 1361">$m\bar{3}m - O_h$</p>	 <p data-bbox="938 1132 954 1157">32</p> <p data-bbox="667 1326 872 1351">NaCl, KCl, CaF_2, MgO</p> <p data-bbox="667 1368 891 1467">PbS (Fig. 4.1), CsCl Garnet (Fig. 1.1a) Cu, Ag, Au, Pt, Fe, W, Si C (Diamond)</p>

Table 8.11 (continuation)

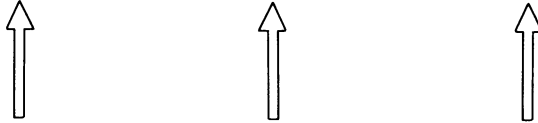
A few non-crystallographic point groups

Molecules	Point group	Crystals
 CO, HCl, CN ⁻	An ∞ -fold rotation axis with infinitely many mirror planes parallel to it. $\infty m - C_{\infty v}$	33 Impossible
 H ₂ O ₂ Cl ₂  CO ₂ <hr/> C ₂ H ₂	An ∞ -fold rotation axis with infinitely many mirror planes parallel to it and infinitely many 2-fold axes normal to it, a mirror plane normal to it $\infty/mm - D_{\infty h}$	34 Impossible
 Ferrocene (eclipsed conformation)	 $5/mm2 (\bar{1}0m2) - D_{5h}$	35 Impossible
 S ₈	 $\bar{8}2m - D_{4d}$	36 Impossible
C ₆₀ (Fig. 11.6a)	$2/m \bar{3} 5 - I_h$ (Fig. 11.6b)	37 Impossible

EXERCISES

Exercise 8.1.

- a) What is meant by a polar rotation axis?
 b) Which symmetry elements can compensate the polarity of a rotation axis? The arrows in the diagram represent X-fold polar rotation axes, X_p . The polarity will be compensated by a symmetry operation which reverses the head of the arrows. Draw in the location of symmetry elements which can do this.



- c) How can polar rotation axes be recognised in symmetry diagrams and in the stereograms of point groups?

Exercise 8.2. Are there polar rotoinversion axes? If so, specify which; if not, state why not.

Exercise 8.3. Combine the operations $1 + \bar{1}$, $2 + \bar{1}$, $3 + \bar{1}$, $4 + \bar{1}$, $6 + \bar{1}$. Which point groups result? Give their symbols.

Exercise 8.4. Combine the operations (A) $2 + 2$, (B) $m + m$ and (C) $2 + m$, where the elements intersect at angles of 30, 45, 60 and 90°. Take the direction of m to be the direction of its normal.

Complete the stereographic projections shown in Table 8.12. Which symmetry elements are generated? What are the resultant point groups? Give the symbols for each.

Copy the stereograms of the point groups in columns A, B or C into column D, and add $\bar{1}$. Which new point groups are generated? Give their symbols.

For each point group, choose an axial system and assign each point group to a crystal system.

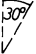
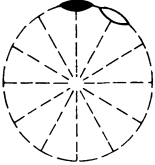
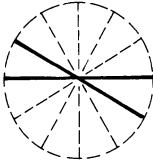
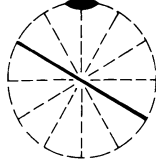
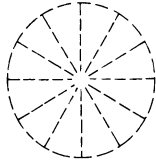
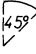
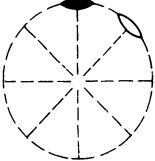
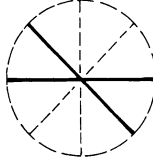
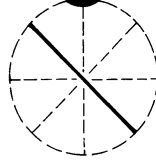
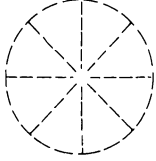
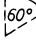
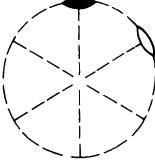
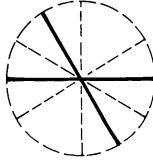
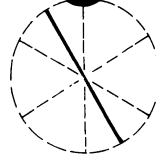
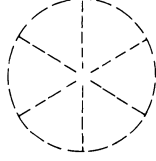
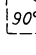
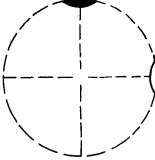
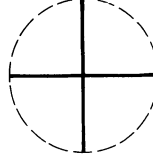
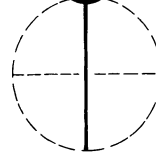
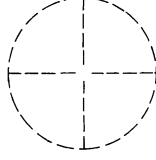
The solution of that part of the exercise will explain the following symmetry rules:

- A) The combination of two 2-fold axes at an angle of $\frac{\epsilon}{2}$ produces an X-fold axis through their point of intersection perpendicular to their common plane.

$$X = \frac{360^\circ}{\epsilon}.$$

- B) The combination of two mirror planes at an angle of $\frac{\epsilon}{2}$ produces an X-fold axis along their line of intersection. $X = \frac{360^\circ}{\epsilon}$.

Table 8.12

	A $2+2$	B $m+m$	C $2+m$	D A or B or C $+i$
				
				
				
				

- C) The combination of a 2-fold axis with a mirror plane at an angle of $\frac{\epsilon}{2}$ produces an \bar{X} axis through the point of intersection of the axis with the normal to the plane and perpendicular to the common plane of the axis and the normal.

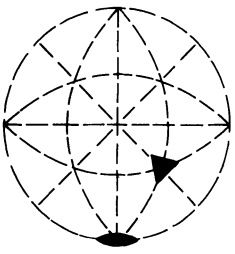
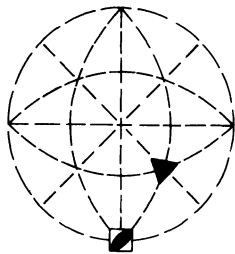
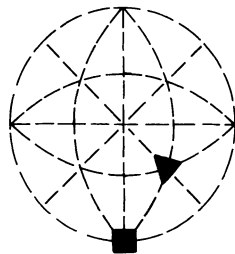
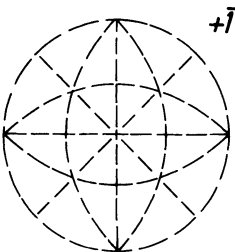
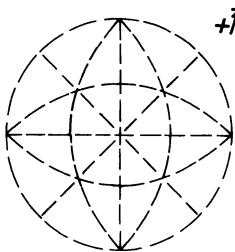
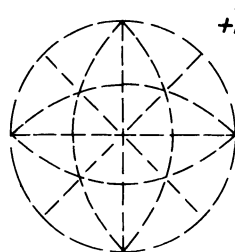
$$\bar{X} = \frac{360^\circ}{\epsilon}$$

Since only $X=1, 2, 3, 4$ and 6 or $\bar{X}=\bar{1}, \bar{2} \equiv m, \bar{3}, \bar{4}$ and $\bar{6}$ are permitted, $\frac{\epsilon}{2}$ can only have the values $30, 45, 60, 90$ and 180° . The combinations at an angle of 180° are not included in Table 8.12.

Exercise 8.5. Combine the operations of (E) $2+3$, (F) $\bar{4}+3$ and (G) $4+3$, where the elements intersect at an angle of 54.73° (the angle between the edge and the body diagonal of a cube).

Complete the stereographic projections shown in Table 8.13, and give the symbols for the resultant point groups. Copy the stereograms in E, F and G into H, I and K and add $\bar{1}$ to them. Give the symbols of the point groups which now result.

Table 8.13

$2+3$	$\bar{4}+3$	$4+3$
		
<i>E</i>	<i>F</i>	<i>G</i>
		
<i>H</i>	<i>I</i>	<i>K</i>

Exercise 8.6. Starting from the point of highest symmetry in the trigonal system $\bar{3} 2/m$, develop its trigonal subgroups.

Exercise 8.7. Colour the circles of the point groups in Fig. 8.3, using the same colour for all point groups belonging to the same crystal system.

Exercise 8.8.

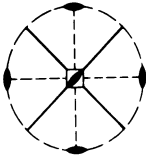
- a) How is it possible to identify the crystal system of a point group from its International symbol?
- b) For each crystal system, give the characteristic point-symmetry elements, and, if necessary, the number of such elements or their relationship to one another. Mark the position these elements occupy in the International point-group symbol, and give an example for each crystal system.

Crystal system	Characteristic symmetry elements number and relationship to one another	Position of characteristic symmetry element(s) in the symbol			Example
		1st	2nd	3rd	
Triclinic					
Monoclinic					
Orthorhombic					
Tetragonal					
Trigonal					
Hexagonal					
Cubic					

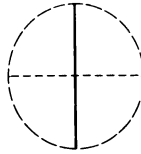
Exercise 8.9. Determine the International symbol for the point groups whose symmetry elements are illustrated in the following stereograms:

- First, find the symmetry elements that characterise the crystal system.
- Indicate the crystallographic axes a , b , c on the stereogram, bearing in mind the orientation of the symmetry directions for the crystal system.
- Give the International symbol and, in brackets, the Schönflies symbol.

1)



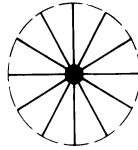
2)



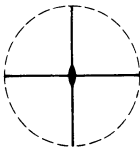
3)



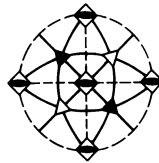
4)



5)



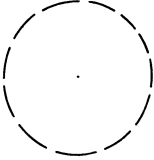
6)



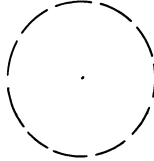
Exercise 8.10. In the stereograms below, indicate the symmetry elements for the given point group:

- Determine the crystal system.
- Draw the appropriate axial system on the stereogram. The c-axis should always be perpendicular to the plane of projection.
- Analyse the point group symbol with respect to the symmetry directions.
- Finally, draw the symmetry elements on the stereogram. *Remember that rotations and rotoinversion axes, as well as the normals to mirror planes are arranged parallel to their symmetry directions.*

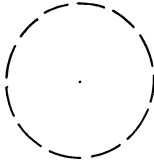
222



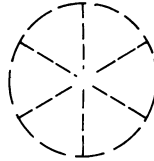
2/m



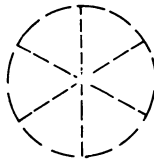
4mm



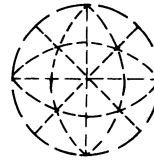
$\bar{6}m2$



$\bar{3} 2/m$
($\bar{3}m$)



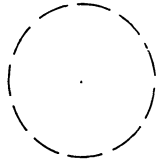
$\bar{4}3m$



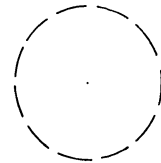
Exercise 8.11. Determination of point groups

Determine the point groups of the molecules and ions given below, using the method described in Section 8.4. Give the International symbol and the Schönflies symbol, and draw the symmetry elements on the stereographic projection.

1 Benzene



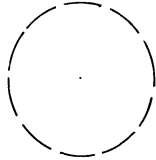
2 Chlorobenzene



3 1,2-Dichlorobenzene



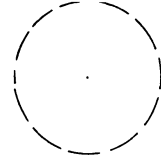
1.2 -



4 1,3-Dichlorobenzene



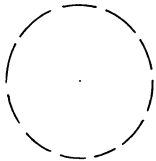
1.3 -



5 1,4-Dichlorobenzene



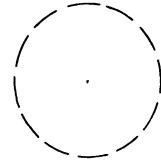
1.4 -



6 1,2,3-Trichlorobenzene



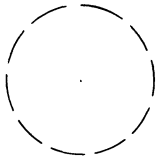
1.2.3 -



7 1,2,4-Trichlorobenzene



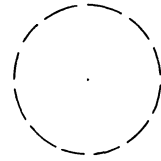
1.2.4 -

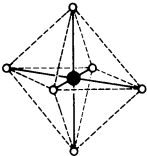
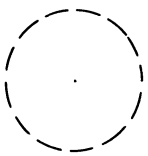
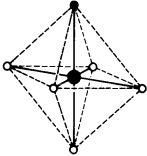
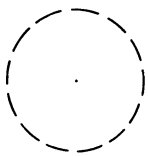
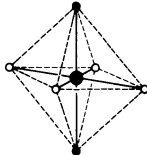
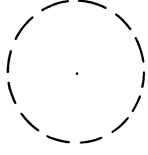
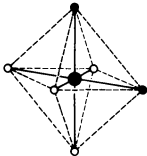
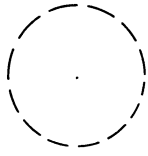
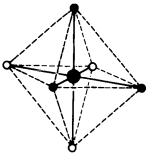
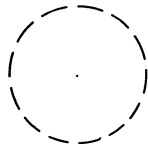
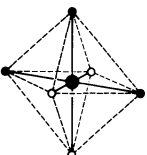
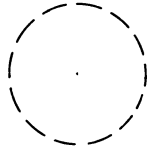


8 1,3,5-Trichlorobenzene



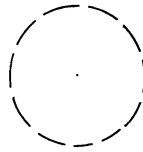
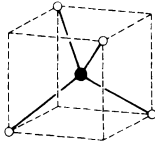
1.3.5 -



9	SF_6		
10	SF_5X		
11	SF_4X_2		
12			
13	SF_3X_3		
14			

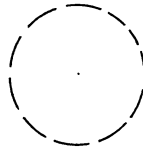
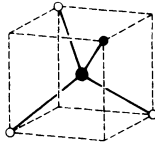
15

Methane
 CH_4



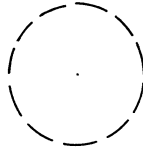
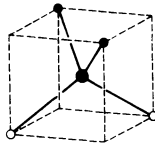
16

Chloromethane
 CH_3Cl



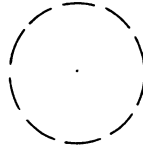
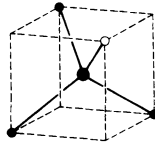
17

Dichloromethane
 CH_2Cl_2



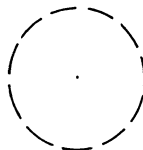
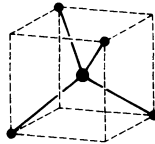
18

Chloroform
 CHCl_3



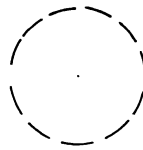
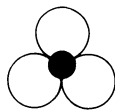
19

Carbon tetrachloride
 CCl_4



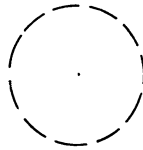
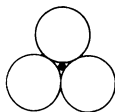
20

IO_3^-
 SeO_3^{2-}
 AsO_3^{3-}



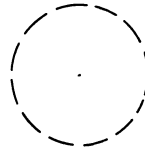
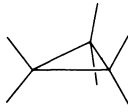
21

NO_3^-
 CO_3^{2-}



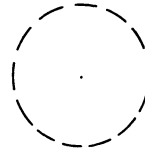
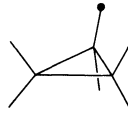
22

Cyclopropane
 C_3H_6



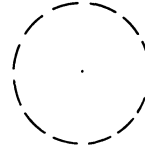
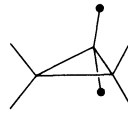
23

Monochlorocyclopropane
 C_3H_5Cl

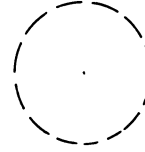
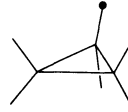


24

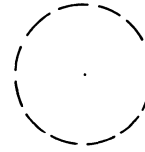
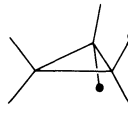
Dichlorocyclopropane
 $C_3H_4Cl_2$



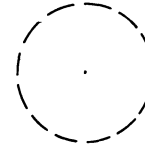
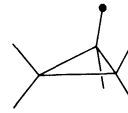
25



26

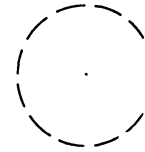
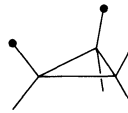


27



28

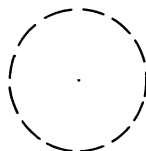
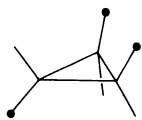
Trichlorocyclopropane
 $C_3H_3Cl_3$



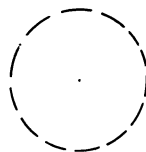
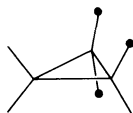
Trichlorocyclopropane



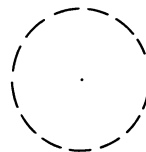
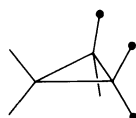
29



30

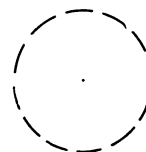
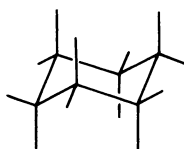


31



32

chair form

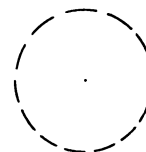
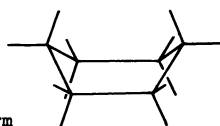


Cyclohexane

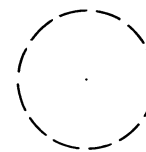
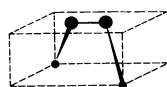


33

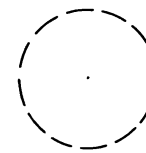
boat form



34

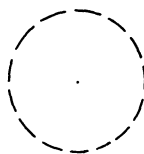


35



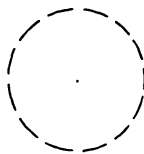
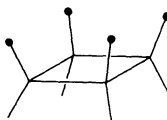
36

Cyclobutane
 C_4H_8

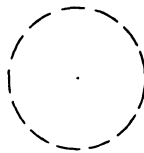


37

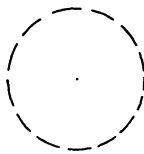
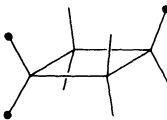
Tetrachlorocyclobutane
 $C_4H_4Cl_4$



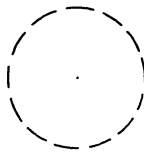
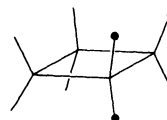
38



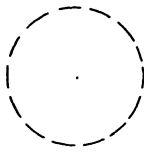
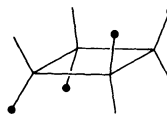
39



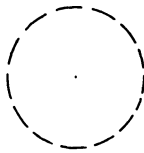
40



41



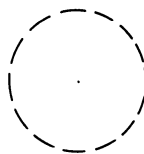
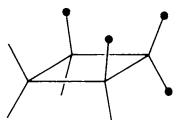
42



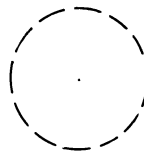
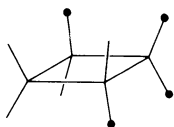
Tetrachlorocyclobutane



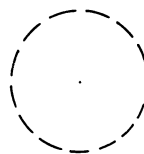
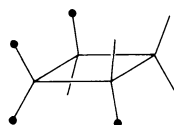
43



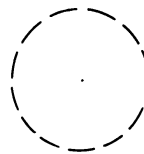
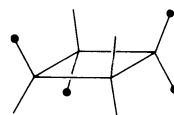
44



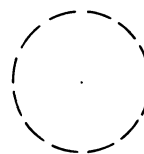
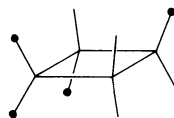
45



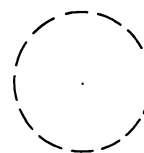
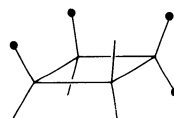
46



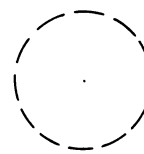
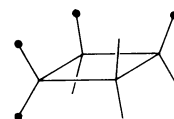
47



48

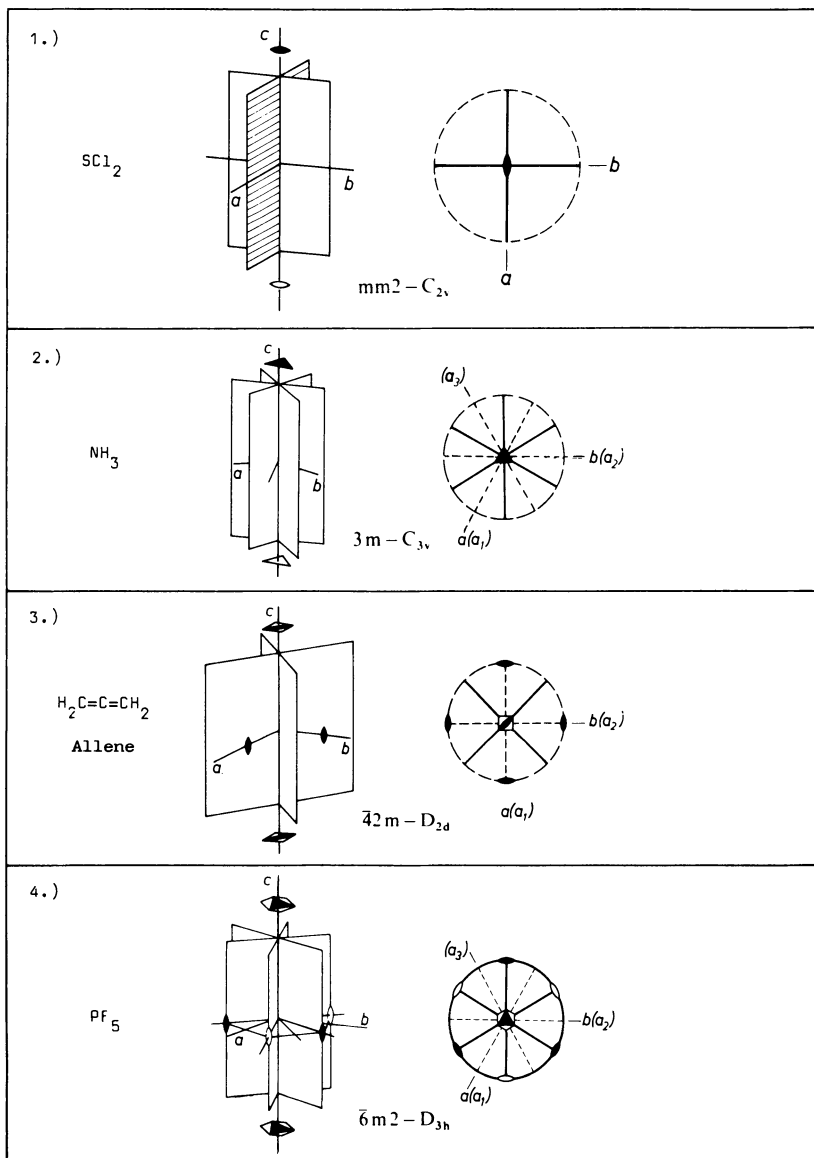


49

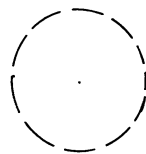
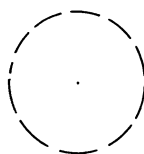
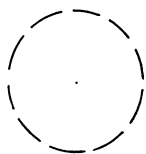
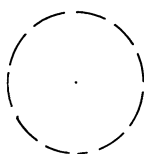
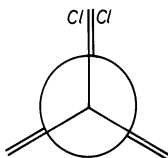


- a) Which isomers of tetrachlorocyclobutane are enantiomers?
 b) Which molecules possess a dipole moment?

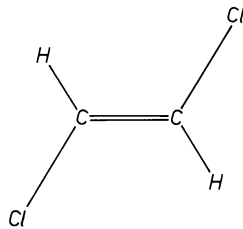
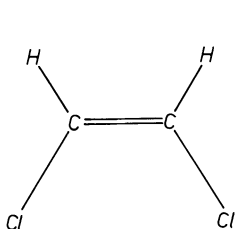
Exercise 8.12. What information about the spatial arrangement of the atoms in the following molecules can you infer from the point group symmetry?



Exercise 8.13. Rotate one of the CH_2Cl groups of a 1,2-dichloroethane molecule about the $\text{C}-\text{C}$ bond stepwise through 360° with respect to the other. Which symmetry distinct conformations are encountered? Give their point groups, and compare them with the corresponding conformations of ethane in Fig. 8.20.

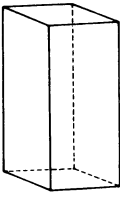
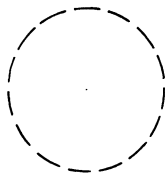
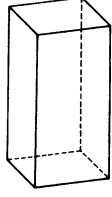
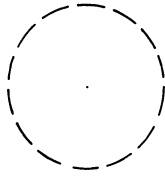

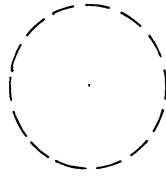
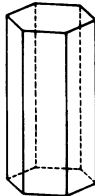
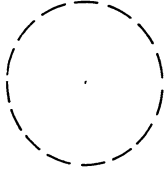
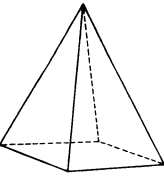
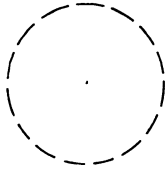
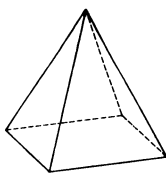
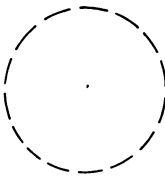
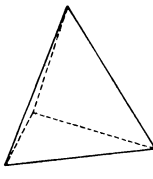
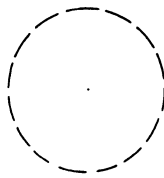
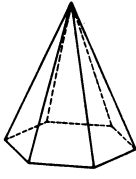
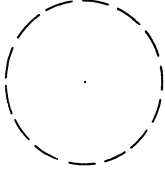


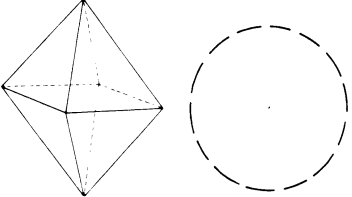
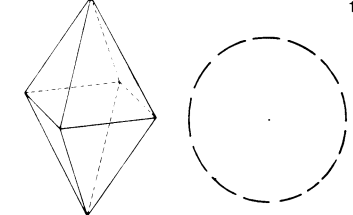
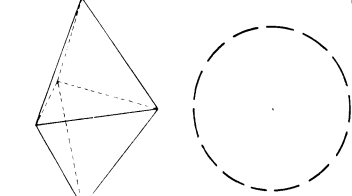
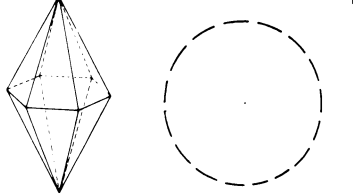
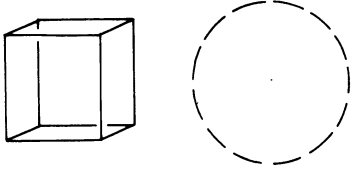
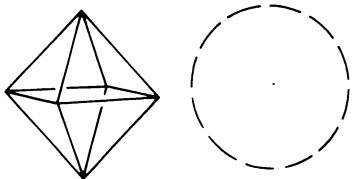
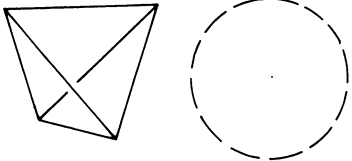
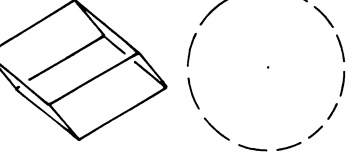
Exercise 8.14. Will measurements of their dipole moments distinguish the *cis* and *trans* forms of dichloroethene?



Exercise 8.15.

- Determine the point groups of the following crystals with the help of Table 8.10 and crystal models such as those illustrated in Exercise 4.4. Draw the symmetry elements on the stereogram, and give the International symbol for the point group.
- Indicate the position of the crystallographic axes on the stereograms and the crystal diagrams.
- Estimate by eye the positions of the crystal faces, and enter the poles on the stereogram, using different colours for different forms.
- Index the crystal forms.

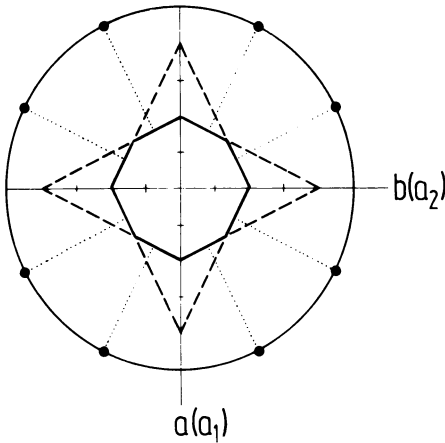
 <p>Rhombic prism</p>	 <p>1</p>	 <p>Tetragonal prism</p>	 <p>2</p>
 <p>Trigonal prism</p>	 <p>3</p>	 <p>Hexagonal prism</p>	 <p>4</p>
 <p>Rhombic pyramid</p>	 <p>5</p>	 <p>Tetragonal pyramid</p>	 <p>6</p>
 <p>Trigonal pyramid</p>	 <p>7</p>	 <p>Hexagonal pyramid</p>	 <p>8</p>

<p style="text-align: right;">9</p>  <p>Rhombic dipyramid</p>	<p style="text-align: right;">10</p>  <p>Tetragonal dipyramid</p>
<p style="text-align: right;">11</p>  <p>Trigonal dipyramid</p>	<p style="text-align: right;">12</p>  <p>Hexagonal dipyramid</p>
<p style="text-align: right;">13</p>  <p>Hexahedron</p>	<p style="text-align: right;">14</p>  <p>Octahedron</p>
<p style="text-align: right;">15</p>  <p>Tetrahedron</p>	<p style="text-align: right;">16</p>  <p>Rhombohedron</p>

Exercise 8.16. Which of the crystals in Exercise 8.15 might, on the basis of its crystal forms, show the piezo-electric effect? Mark the appropriate diagrams "Piezo-elect."

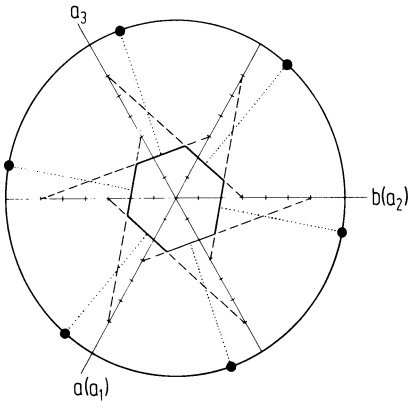
Exercise 8.17. There is a simple relationship between the numbers of faces, edges and vertices of a polyhedron. Work out what it is.

Exercise 8.18. The figure shows the cross-section of a ditetragonal prism on the equatorial plane of a stereographic projection, together with the corresponding poles. The dashed lines have been added to point out the axial intercepts of the faces.



- a) Index all the faces of the crystal form $\{hk0\}$ or $\{210\}$.
- b) If the faces of a ditetragonal prism are inclined by a given angle in the direction of the positive and negative c -axis, the poles of the faces move a corresponding amount away from the periphery in the $[001]$ and $[00\bar{1}]$ directions. What is the resulting crystal form? Index all the faces of this form.

Exercise 8.19. The figure shows the cross-section of a hexagonal prism on the equatorial plane of a stereographic projection, together with the corresponding poles. The dashed lines have been added to point out the axial intercepts of the faces.



- Index all the faces of the crystal form $\{hki0\}$ or $\{21\bar{3}0\}$.
- If the faces of a hexagonal prism are inclined by a given angle in the direction of the positive and negative c -axis, the poles of the faces move a corresponding amount away from the periphery in the $[0001]$ and $[000\bar{1}]$ directions. What is the resulting crystal form? Index all the faces of this form.

Exercise 8.20. Derive the crystal forms of the following point groups:

- Use the characteristic symmetry elements to determine the crystal system (cf. Table 8.9).
- Look up the stereogram of the poles of the forms for the point group of highest symmetry in that system: Fig. 8.16 for orthorhombic, Fig. 8.9 for tetragonal, Fig. 8.13 for hexagonal or trigonal, and Fig. 8.15 for cubic.
- Place a piece of tracing paper over the stereogram, and draw in the symmetry elements for the point group, appropriately orientated to the crystallographic axes.
- Indicate the asymmetric face unit.
- Draw in first the poles for the faces of the general form. What is it called? Index all the faces.
- If the general form has limiting forms, draw these in and name and index them.
- Draw in the special forms and their limiting forms (if any). Name and index them and give the point symmetry of their faces.

(It is a good idea to use several pieces of tracing paper!)

- | | |
|----------------|----------------|
| 1) $\bar{4}2m$ | 5) $6/mmm$ |
| 2) 4 | 6) 622 |
| 3) mmm | 7) $3m$ |
| 4) $mm2$ | 8) $m\bar{3}m$ |
| | 9) $\bar{4}3m$ |

Exercise 8.21. In *International Tables for Crystallography*, Vol. A, for the point group $4/m\bar{3}2/m$, the trapezohedron (or deltoidicositetrahedron), is given as the special form $\{hhl\}$, $|h| < |l|$ and the trisoctahedron for $\{hhl\}$, $|h| > |l|$. In Table 8.6, however, the trapezohedron is given for $\{hkk\}$ and the trisoctahedron for $\{hkk\}$. Explain this apparent inconsistency.

Exercise 8.22. Which special forms in the hexagonal and trigonal systems have limiting forms?

9 Space Groups

9.1 Glide Planes and Screw Axes

The 32 point groups are the symmetry groups of many molecules and of all crystals, so long as only the morphology is considered. Space groups give the symmetry not only of crystal lattices, but also of crystal structures.

In Table 6.4 are given the space-group symbols for the 14 Bravais lattices; the space-group symbol does not in general enumerate all the symmetry elements of the space group. In particular, the space groups of centred lattices contain new symmetry operations. These are compound symmetry operations which arise through reflection and translation (1) and rotation and translation (2) (cf. Chap. 5.4 and Table 5.1).

1. In the orthorhombic C-lattice, reflection through a plane (---) at $\frac{1}{4}, y, z$, followed by a translation of $\frac{\vec{b}}{2}$ moves the lattice point $0, 0, 0$ to $\frac{1}{2}, \frac{1}{2}, 0$ (Fig. 9.1 a). This symmetry operation is called a *glide reflection*, and the corresponding element is a *glide plane* (in this case, a b-glide plane).

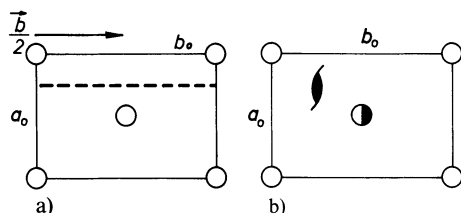


Fig. 9.1. a Location of a b-glide plane in an orthorhombic C-lattice. b Position of 2-fold screw axis in an orthorhombic I-lattice. (● lattice point with $z = \frac{1}{2}$)

2. In the orthorhombic I-lattice, a 180° rotation about an axis (●) at $\frac{1}{4}, \frac{1}{4}, z$, followed by a translation of $\frac{\vec{c}}{2}$, moves the lattice point $0, 0, 0$ to $\frac{1}{2}, \frac{1}{2}, \frac{1}{2}$ (Fig. 9.1 b). This symmetry operation is called a *screw rotation*, and the corresponding element is a *screw axis* (in this case, a 2-fold screw axis).

9.1.1 Glide Planes

The compound symmetry operation “glide reflection” implies:

- A) a reflection and
- B) a translation by the vector \vec{g} parallel to the plane of glide reflection where $|\vec{g}|$ is called the *glide component*.

Figure 9.2 contrasts the operation of a mirror plane with that of a glide plane on a point lying off the planes.

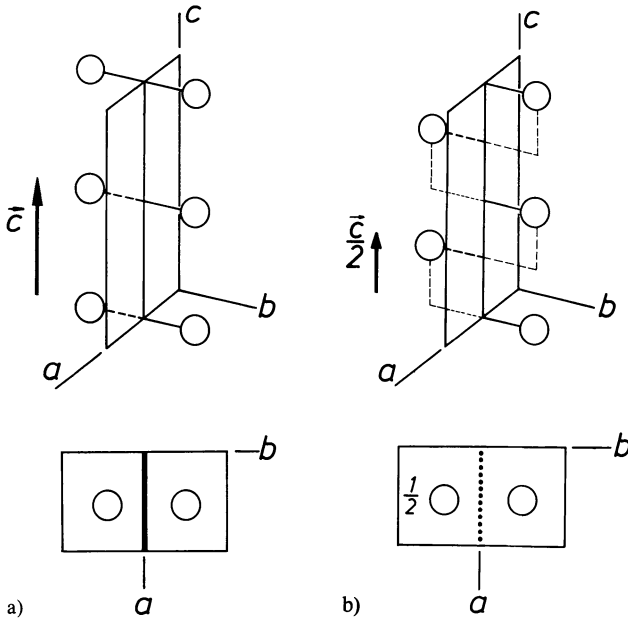


Fig. 9.2a, b. Operation of a mirror plane m (a) and of a glide plane c (b) on a point shown in perspective and as a projection on (001)

A second application of the glide reflection brings one to a point identical to the starting point.

\vec{g} is one-half of a lattice translation parallel to the glide plane, $|\vec{g}| = \frac{1}{2}|\vec{r}|$.

Glide planes are developments of mirror planes, and can only occur in an orientation that is possible for a mirror plane.

For this reason, in the orthorhombic system, glide planes only occur parallel to (100), (010) and (001). Compare the space group $P2/m\ 2/m\ 2/m$ in Fig. 6.9d with the point group $2/m\ 2/m\ 2/m$ in Fig. 6.9e. Since the glide component $|\vec{g}|$ must be half of a lattice translation parallel to the glide plane, in an orthorhombic space group the only possible glide planes parallel to (100) will have glide components $\frac{1}{2}|\vec{b}|$, $\frac{1}{2}|\vec{c}|$, $\frac{1}{2}|\vec{b} + \vec{c}|$ and $\frac{1}{4}|\vec{b} + \vec{c}|$, and this last type will only occur in centred lattices, where $\frac{1}{4}|\vec{b} + \vec{c}|$ can be half of a lattice translation. In Fig. 9.3, these cases are illustrated, together with those parallel to (010) and (001).

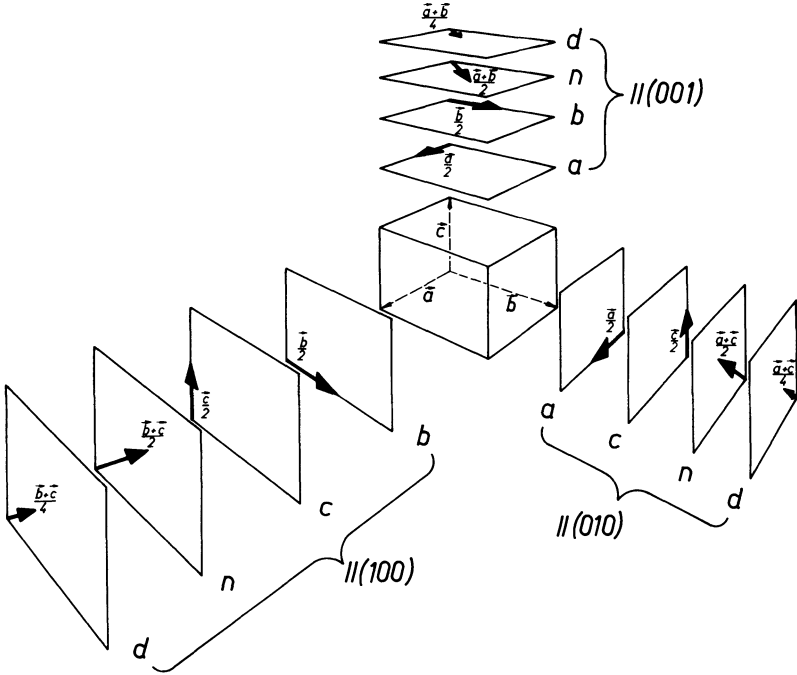


Fig. 9.3. Glide planes in the orthorhombic system

Glide planes are designated by symbols indicating the relationship of their glide components to lattice vectors \vec{a} , \vec{b} and \vec{c} . Those with axial components: $\frac{1}{2}|\vec{a}|$, $\frac{1}{2}|\vec{b}|$ or $\frac{1}{2}|\vec{c}|$ are given the symbols **a**, **b** and **c** respectively, those with diagonal components $\frac{1}{2}|\vec{\tau}_1 + \vec{\tau}_2|$ have the symbol **n**, while those with the component $\frac{1}{4}|\vec{\tau}_1 \pm \vec{\tau}_2|$, known as diamond glides, have the symbol **d**.

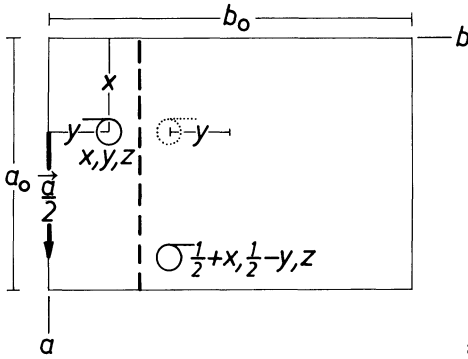
Since glide planes play so important a role in space groups, the operation of a few examples will be given in an orthorhombic cell projected on $x, y, 0$. In these projection diagrams, only a single glide plane is shown – see Chapter 14.2 for an explanation of the graphical symbols.

a) In Fig. 9.4a, an a-glide is shown at $x, \frac{1}{4}, z$. Reflection of a point x, y, z in this plane gives $x, \frac{1}{2} - y, z$, called an “auxiliary” point and the translation $\frac{1}{2}\vec{a}$ then moves this auxiliary point to $\frac{1}{2} + x, \frac{1}{2} - y, z$.

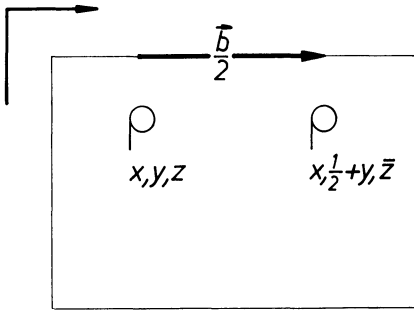
b) The b-glide plane at $x, y, 0$ in Fig. 9.4b reflects a point x, y, z to the auxiliary point x, y, \bar{z} , which the translation of $\frac{1}{2}\vec{b}$ then moves to $x, \frac{1}{2} + y, \bar{z}$.

c) The c-glide plane at $x, \frac{1}{2}, z$ in Fig. 9.4c reflects a point x, y, z to the auxiliary point, $x, 1 - y, z$ which the translation of $\frac{1}{2}\vec{c}$ then moves to $x, 1 - y, \frac{1}{2} + z$.

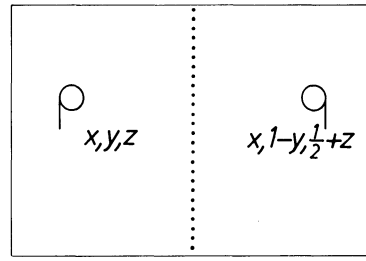
d) The n-glide plane at $x, y, \frac{1}{4}$ in Fig. 9.4d is parallel to the a,b-plane, and thus has a glide component $\frac{1}{2}|\vec{a} + \vec{b}|$. It reflects a point x, y, z to the auxiliary point $x, y, \frac{1}{2} - z$, which the translation of $\frac{1}{2}(\vec{a} + \vec{b})$ then moves to $\frac{1}{2} + x, \frac{1}{2} + y, \frac{1}{2} - z$.



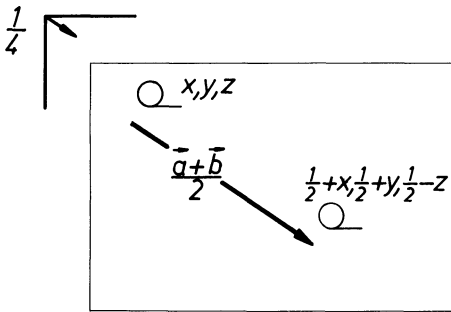
a a-glide at $x, \frac{1}{4}z$



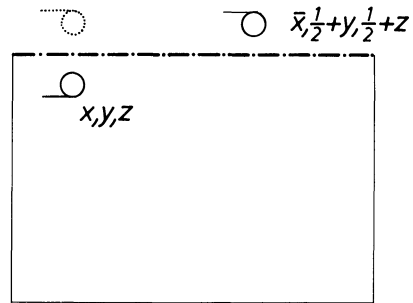
b b-glide at $x, y, 0$



c c-glide at $x, \frac{1}{2}, z$



d n-glide at $x, y, \frac{1}{4}$ with glide component $\frac{1}{2}|\bar{a} + \bar{b}|$



e n-glide at $0, y, z$ with glide component $\frac{1}{2}|\bar{b} + \bar{c}|$

Fig. 9.4 a-e. Operation of glide planes on a point. In each case, only a single glide plane is shown projected on $x, y, 0$ in an orthorhombic cell.

e) The n -glide plane at $0, y, z$ in Fig. 9.4e has a glide component $\frac{1}{2}|\vec{b} + \vec{c}|$. It reflects a point x, y, z to the auxiliary point \bar{x}, y, z , which the translation of $\frac{1}{2}(\vec{b} + \vec{c})$ then moves to $\bar{x}, \frac{1}{2} + y, \frac{1}{2} + z$.

9.1.2 Screw Axes

The compound symmetry operation “screw rotation” implies:

- A) a rotation of an angle $\varepsilon = \frac{360^\circ}{X}$; ($X = 1, 2, 3, 4, 6$) and
- B) a translation by a vector \vec{s} parallel to the axis, where $|\vec{s}|$ is called the *screw component*.

For rotation axes and rotoinversion axes, the direction of rotation was unimportant. This is not the case for screw axes; for a right-handed axial system, X, Y, Z (Fig. 9.5, see also Chap. 2.3) a rotation about an axis on Z from the X -axis toward the Y -axis is linked with a positive translation along Z . This is the motion of a right-handed screw, which corresponds to the motion of advancing the thumb of the right hand in the direction of the vector \vec{s} as the fingers of this hand point in the sense of rotation.

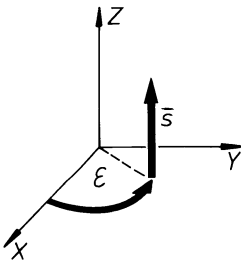


Fig. 9.5. The handedness of a screw axis

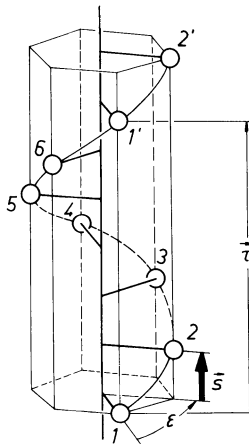


Fig. 9.6. Operation of a 6-fold screw axis 6_1 on a point lying off the axis

Figure 9.6 shows the operation of a 6-fold screw axis ($\varepsilon = 60^\circ$) on a point lying off the axis. The points 1, 2, 3 ... are arranged like the treads of a spiral staircase. After X rotations ($X = 6$) through the angle ε ($X \cdot \varepsilon = 360^\circ$), the point 1 will return to its starting point. In this case, however, the rotations have been accompanied by a translation of $X \cdot \vec{s}$, and the point 1' has been reached, which is identical to the starting point. The vector $1-1'$ is not necessarily a single lattice translation \vec{t} , but may be any integral multiple σ of \vec{t} .

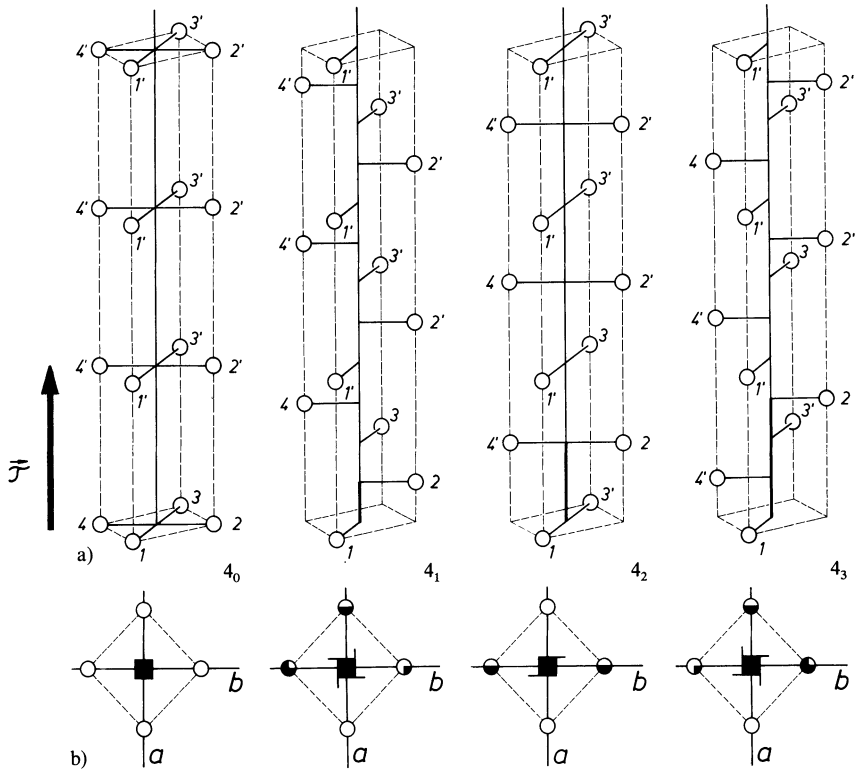


Fig. 9.7a, b. Operation of a 4-fold rotation axis and the three 4-fold screw axes on a point lying off the axes. a shows perspective views and b projections on $x, y, 0$

$$X \cdot |\vec{s}| = \sigma |\vec{r}| \quad \text{or}$$

$$|\vec{s}| = \frac{\sigma}{X} |\vec{r}|.$$

Since $|\vec{s}| < |\vec{r}|$, $\sigma < X$ and can have the following values:

$$\sigma = 0, 1, 2, \dots, X - 1$$

and

$$|\vec{s}| = 0, \frac{1}{X} |\vec{r}|, \frac{2}{X} |\vec{r}|, \dots, \frac{X-1}{X} |\vec{r}|$$

since the screw component

$$|\vec{s}| = \frac{\sigma}{X} |\vec{r}|,$$

screw axes are designated $X_\sigma = X_0, X_1, X_2, \dots, X_{X-1}$.

For $X=4$, $\sigma=0, 1, 2, 3$. The resulting screw axes are 4_0 (a 4-fold rotation axis), 4_1 , 4_2 and 4_3 , with screw components $0, \frac{1}{4}|\vec{r}|, \frac{2}{4}|\vec{r}|$ and $\frac{3}{4}|\vec{r}|$. (Note that the screw component is directly derivable from the symbol, by inverting it and considering it as a fraction, e.g. $4_1 \rightarrow \frac{1}{4}$.) The 4-fold rotation and screw

axes are compared in Fig. 9.7. Successive operations of the 4-fold screw axes on a point lying off the axis move point 1 to 2, 3 and 4. A lattice translation of τ generated the points 1', 2', 3' and 4'. The operations of the screw axes are also illustrated in Fig. 9.7b by projection of the points within a single lattice translation onto the plane normal to the axis. Note that the sets of points generated by 4_1 and 4_3 are mirror images of one another, i.e. they are a pair of enantiomorphs. Since 4_1 represents a right-handed screw, 4_3 may be described as a left-handed screw with a screw component $|\vec{s}'| = \frac{1}{4}|\vec{\tau}|$ also.

Figure 9.8 shows all of the other screw and rotation axes possible for crystals (see also Chap. 14.2). The enantiomorphous pairs are 3_1 and 3_2 , 4_1 and 4_3 , 6_1 and 6_5 , and 6_2 and 6_4 .

Screw axes can only occur in crystals parallel to those directions which are possible for rotation axes in the corresponding point group.

9.2 The 230 Space Groups

The 32 crystallographic point groups have been derived from the point groups of highest symmetry in each crystal system (see Table 8.2). All of the space groups can be derived in a similar manner. Starting from the space groups of highest symmetry in each crystal system, i.e. those of the 14 Bravais lattices (see Table 6.4), it is possible to derive an analogous scheme for determining all of their subgroups. It must, however, be borne in mind that screw axes can replace rotation axes, and glide planes mirror planes thus:

$$\begin{aligned} 2 &\leftarrow 2_1 \\ 3 &\leftarrow 3_1, 3_2 \\ 4 &\leftarrow 4_1, 4_2, 4_3 \\ 6 &\leftarrow 6_1, 6_2, 6_3, 6_4, 6_5 \\ m &\leftarrow a, b, c, n, d. \end{aligned}$$

The space groups of the monoclinic system will be derived as an example for all crystal systems. We start from the two monoclinic space groups of highest symmetry; $P2/m$ and $C2/m$ (Fig. 9.9). Additionally, in $C2/m$, there are a-glide planes at $x, \frac{1}{4}, z$ and $x, \frac{3}{4}, z$, and 2₁-axes at $\frac{1}{4}, y, 0$; $\frac{1}{4}, y, \frac{1}{2}$; $\frac{3}{4}, y, 0$ and $\frac{3}{4}, y, \frac{1}{2}$.

The monoclinic subgroups of the point group $2/m$ are m and 2 . The point-symmetry elements 2 and m can be replaced by 2_1 and a glide plane respectively. Since m is parallel to (010) , only a-, c- and n-glides are possible. However, a different choice of the a and c axes will convert either an a- or an n-glide into a c-glide (Fig. 9.10). Thus, only the c-glide need be considered.

Replacement of 2 and m by 2_1 and c results in the 13 monoclinic space groups shown in Table 9.1 as subgroups of $P2/m$ and $C2/m$.

The sets of symmetry elements for these space groups are shown in Fig. 9.9, in the same order as Table 9.1, as projections on $x, y, 0$. Additionally, a- and n-glide planes occur in C-centred space groups. Thus it can be seen that the pairs of symbols $C2/m$ and $C2_1/m$, $C2/c$ and $C2_1/c$, and $C2$ and $C2_1$ represent only a single space group each, cf. exercise 9.4.

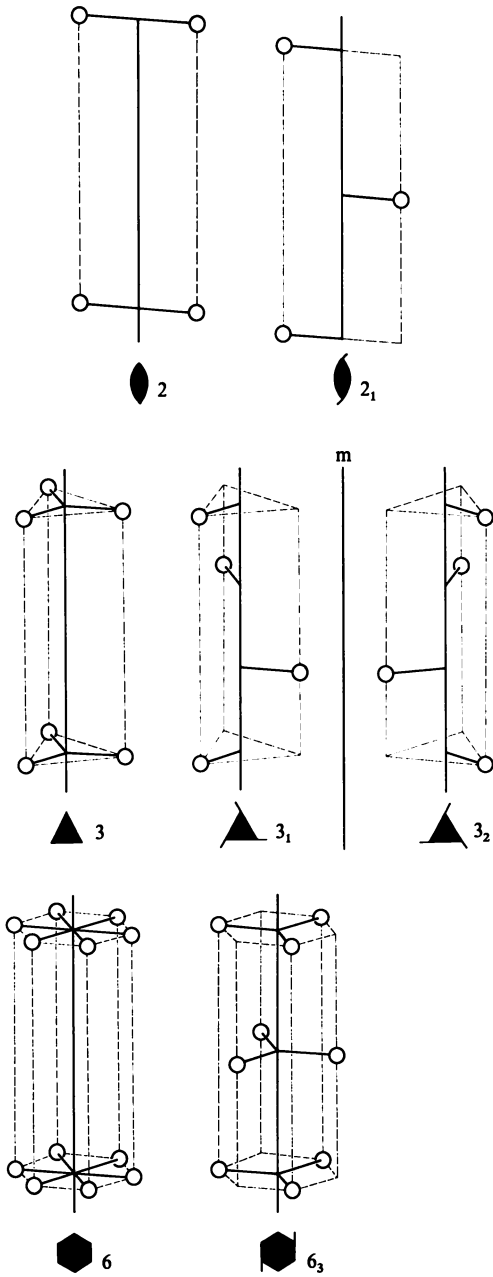


Fig. 9.8. Operation of rotation and screw axes on a point lying off them. The enantiomorphous pairs 3₁-3₂, 6₁-6₅ and 6₂-6₄ are given together. 4, 4₁, 4₂ and 4₃ are shown in Fig. 9.7

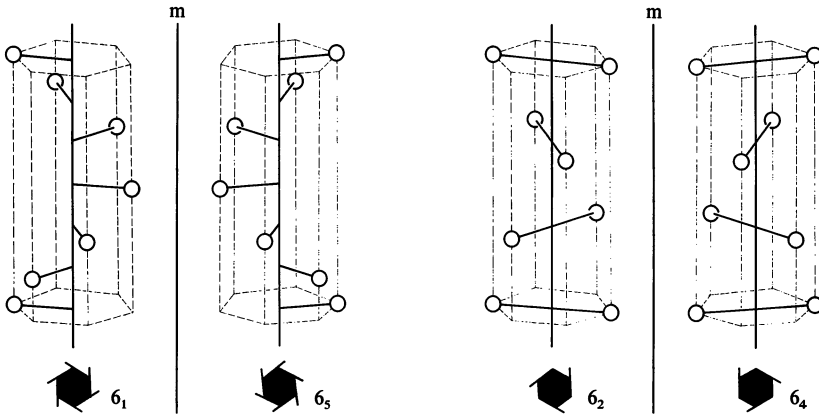


Fig. 9.8 (continued)

In the same way, inspection of the other crystal systems leads to the entire 230 space groups. These 230 space groups are listed in Table 9.2, sorted by crystal system and point group. Only the standard abbreviated symbols (short symbols) are given.

In every case, the point group is easily derived from the space group symbol. The screw axes are replaced by the corresponding rotation axis, the glide planes by a mirror plane, and the lattice symbol is omitted, the result being the point group to which the space group belongs.

It would be useful to revise the space groups of the Bravais lattices, which are given in Figs. 6.7d–6.13d.

The *International (Hermann-Mauguin) symbols* thus indicate the symmetry of each space group clearly. *Schönflies symbols*, on the other hand, merely assign an arbitrary number to each space group within a given point group. Thus, for point group $m(C_s)$, we have:

$$Pm: (C_s^1), \quad Pc: (C_s^2), \quad Cm: (C_s^3), \quad Cc: (C_s^4).$$

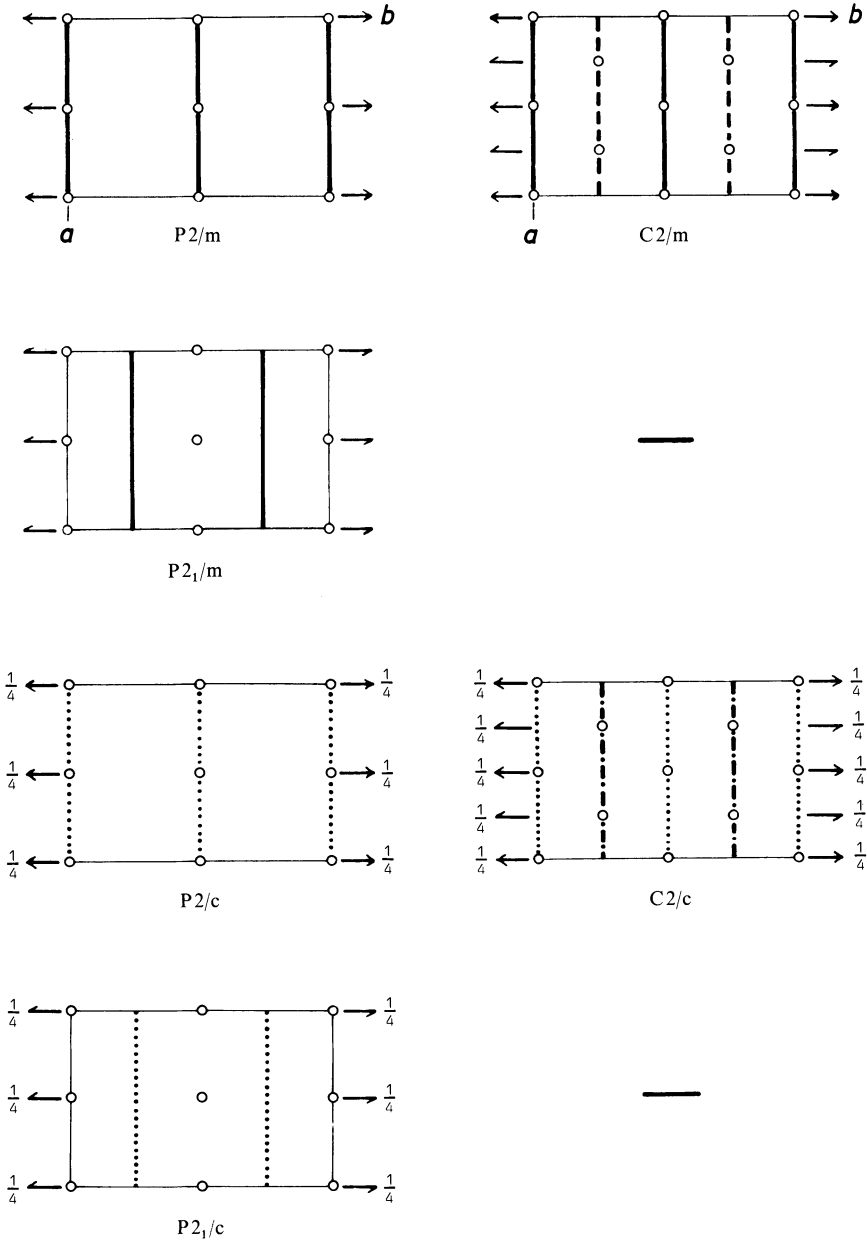
This is the main reason that Schönflies symbols are rarely used in crystallography.

9.3 Properties of Space Groups

It is certainly not necessary to study each of the 230 space groups individually, but a general knowledge of how space groups differ from one another is useful. For this reason, the properties of a few space groups will be explored in detail.

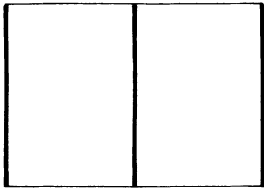
Figure 9.11 gives the symmetry elements for the space group Pmm2. The application of the symmetry operations to a point x, y, z will generate the points $x, \bar{y}, z; \bar{x}, y, z$ and \bar{x}, \bar{y}, z , as well as equivalent points such as $x, 1 - y, z; 1 - x, y, z$ and $1 - x, 1 - y, z$.

The number of equivalent points in the unit cell is called its multiplicity.

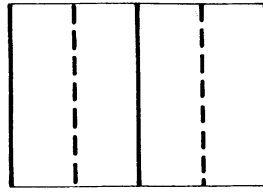


a Space groups of point group $2/m$

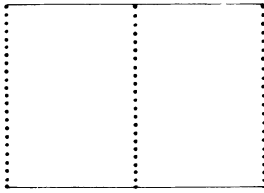
Fig. 9.9a-c. The monoclinic space groups projected on $x, y, 0$. The c -axis is not normal to the plane of projection, but is tilted such that $\beta > 90^\circ$.



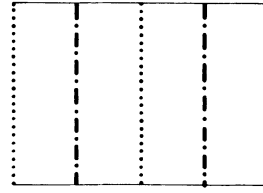
Pm



Cm

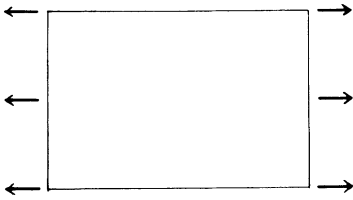


Pc

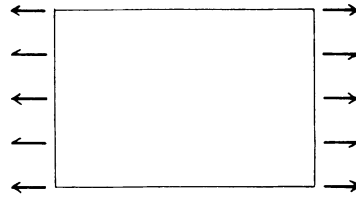


Cc

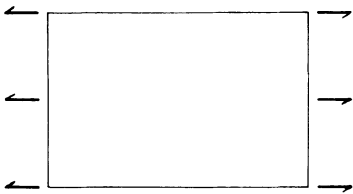
b Space groups of point group *m*



P2



C2



P2₁



c Space groups of point group 2

Fig. 9.9b,c

Table 9.1. The point and space groups of the monoclinic crystal system

Point groups	Space groups	
2/m	P2/m P2 ₁ /m P2/c P2 ₁ /c	C2/m - ^a C2/c - ^b
m	Pm Pc	Cm Cc
2	P2 P2 ₁	C2 - ^c

^a C2₁/m ≡ C2/m, ^b C2₁/c ≡ C2/c, ^c C2₁ ≡ C2

Table 9.2. The 230 Space groups

Crystal system	Point group	Space groups			
triclinic	1 $\bar{1}$	P1 P $\bar{1}$			
monoclinic	2 m 2/m	P2 Pm P2/m P2 ₁ /c	P2 ₁ Pc P2 ₁ /m C2/c	C2 Cm C2/m	Cc P2/c
orthorhombic	222 mm2 mmm	P222 C222 ₁ I2 ₁ 2 ₁ 2 ₁ Pmm2 Pca2 ₁ Pna2 ₁ Ccc2 Aba2 Iba2 Pmmm Pmma Pbam Pmmn Cmcm Cmma Immm	P222 ₁ C222 Pmc2 ₁ Pnc2 Pnn2 Amm2 Fmm2 Ima2 Pnnn Pnna Pccn Pbcn Cmca Ccca Ibam	P2 ₁ 2 ₁ 2 F222 Pcc2 Pmn2 ₁ Cmm2 Abm2 Fdd2 Pccm Pmna Pbcm Pbca Cmmm Fmmm Ibca	P2 ₁ 2 ₁ 2 ₁ I222 Pma2 Pba2 Cmc2 ₁ Ama2 Imm2 Pban Pcca Pnnm Pnma Cccm Fddd Imma

tetragonal	4	P4	P4 ₁	P4 ₂	P4 ₃
	$\bar{4}$	I4	I4 ₁		
	4/m	P $\bar{4}$	I $\bar{4}$	P4/n	P4 ₂ /n
	422	P4/m	P4 ₂ m		
		I4/m	I4 ₁ /a		
		P422	P4 ₂ 1 ₂	P4 ₁ 22	P4 ₁ 2 ₁ 2
	4mm	P4 ₂ 22	P4 ₂ 2 ₁ 2	P4 ₃ 22	P4 ₃ 2 ₁ 2
		I422	I4 ₁ 22		
		P4mm	P4bm	P4 ₂ cm	P4 ₂ nm
		P4cc	P4nc	P4 ₂ mc	P4 ₂ bc
	$\bar{4}2m$	I4mm	I4cm	I4 ₁ md	I4 ₁ cd
		P $\bar{4}2m$	P $\bar{4}2c$	P $\bar{4}2_1m$	P $\bar{4}2_1c$
		P $\bar{4}m2$	P $\bar{4}c2$	P $\bar{4}b2$	P $\bar{4}n2$
		I $\bar{4}m2$	I $\bar{4}c2$	I $\bar{4}2m$	I $\bar{4}2d$
4/mmm	P4/mmm	P4/mcc	P4/nbm	P4/nnc	
	P4/mbm	P4/mnc	P4/nmm	P4/ncc	
	P4 ₂ /mmc	P4 ₂ /mcm	P4 ₂ /nbc	P4 ₂ /nmm	
	P4 ₂ /mbc	P4 ₂ /mnm	P4 ₂ /nmc	P4 ₂ /ncm	
	I4/mmm	I4/mcm	I4 ₁ /amd	I4 ₁ /acd	
trigonal	3	P3	P3 ₁	P3 ₂	R3
	$\bar{3}$	P $\bar{3}$	R $\bar{3}$		
	32	P312	P321	P3 ₁ 12	P3 ₁ 21
		P3 ₂ 12	P3 ₂ 21	R32	
	3m	P3m1	P31m	P3c1	P31c
		R3m	R3c		
$\bar{3}m$	P $\bar{3}1m$	P $\bar{3}1c$	P $\bar{3}m1$	P $\bar{3}c1$	
	R $\bar{3}m$	R $\bar{3}c$			
hexagonal	6	P6	P6 ₁	P6 ₅	P6 ₂
	$\bar{6}$	P6 ₄	P6 ₃		
	6/m	P $\bar{6}$			
		P6/m	P6 ₃ /m		
	622	P622	P6 ₁ 22	P6 ₅ 22	P6 ₂ 22
		P6 ₄ 22	P6 ₃ 22		
	6mm	P6mm	P6cc	P6 ₃ cm	P6 ₃ mc
$\bar{6}m2$	P $\bar{6}m2$	P $\bar{6}c2$	P $\bar{6}2m$	P $\bar{6}2c$	
6/mmm	P6/mmm	P6/mcc	P6 ₃ /mcm	P6 ₃ /mmc	
cubic	23	P23	F23	I23	P2 ₁ 3
	m $\bar{3}$	I2 ₁ 3			
		Pm $\bar{3}$	Pn $\bar{3}$	Fm $\bar{3}$	Fd $\bar{3}$
	432	Im $\bar{3}$	Pa $\bar{3}$	Ia $\bar{3}$	
		P432	P4 ₃ 32	F432	F4 ₁ 32
		I432	P4 ₃ 32	P4 ₁ 32	I4 ₁ 32
	$\bar{4}3m$	P $\bar{4}3m$	F $\bar{4}3m$	I $\bar{4}3m$	P43n
		F $\bar{4}3c$	I $\bar{4}3d$		
	m $\bar{3}m$	Pm $\bar{3}m$	Pn $\bar{3}n$	Pm $\bar{3}n$	Pn $\bar{3}m$
		Fm $\bar{3}m$	Fm $\bar{3}c$	Fd $\bar{3}m$	Fd $\bar{3}c$
Im $\bar{3}m$		Ia $\bar{3}d$			

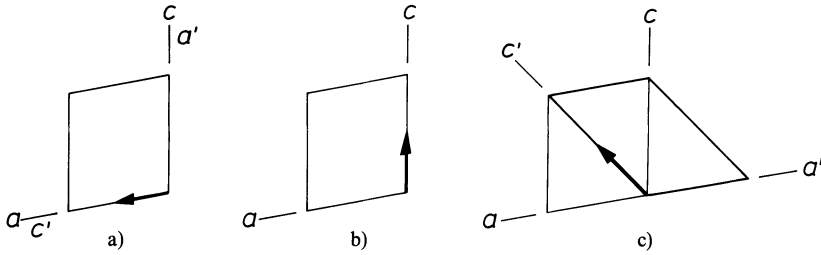


Fig. 9.10a-c. In the monoclinic system, a-, c-, and n-glide planes parallel to (010) are all possible. These are shown in a, b and c respectively. Suitable alteration of the choice of axes will convert a- and n- into c-glides

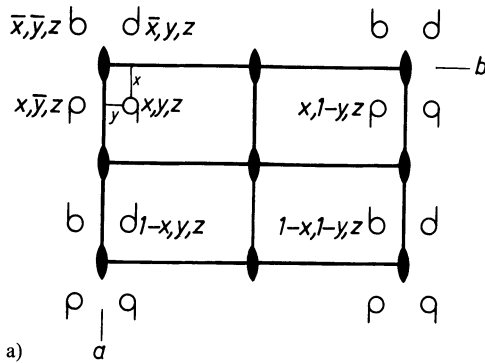
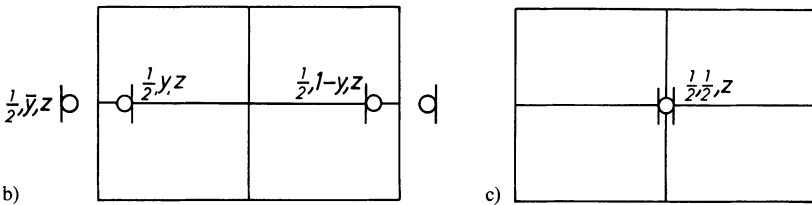


Fig. 9.11 a-c. Symmetry elements of space group Pmm2 in projection on $x, y, 0$. **a** The general position x, y, z . **b** the special position $\frac{1}{2}, y, z$. **c** The special position $\frac{1}{2}, \frac{1}{2}, z$



In Fig. 9.11a, the position is “4-fold”, or said to have a multiplicity of 4. This position has no restrictions on its movement; it has three degrees of freedom, and, as long as it does not move onto a point symmetry element, it continues to have a multiplicity of 4. Such a position is called a *general position*.

A general position is a set of equivalent points with point symmetry (site symmetry) 1.

It is asymmetric, and this is indicated in Fig. 9.11 by the tail on the circle. The figure is, of course, not really asymmetric, as it is unchanged on reflection in the plane of the paper, but it is sufficiently unsymmetrical for our present purpose!

If the point in the general site x, y, z is moved on to the mirror plane at $\frac{1}{2}, y, z$, the point $1 - x, y, z$ comes into coincidence with it; the two points coalesce

Table 9.3. Positions of the space group Pmm2

Position	Degrees of freedom	Multiplicity	Site symmetry	Coordinates of equivalent points	Fig.
general	3	4	1	$x, y, z; \bar{x}, \bar{y}, z;$ $x, \bar{y}, z; \bar{x}, y, z$	9.11 a
special	2	2	m	$\frac{1}{2}, y, z; \frac{1}{2}, \bar{y}, z$	9.11 b
		2	m	$0, y, z; 0, \bar{y}, z$	
		2	m	$x, \frac{1}{2}, z; \bar{x}, \frac{1}{2}, z$	
		2	m	$x, 0, z; \bar{x}, 0, z$	
	1	1	mm2	$\frac{1}{2}, \frac{1}{2}, z$	9.11 c
		1	mm2	$\frac{1}{2}, 0, z$	
		1	mm2	$0, \frac{1}{2}, z$	
		1	mm2	$0, 0, z$	

at the mirror plane to a single point $\frac{1}{2}, y, z$. At the same time, the points $x, 1 - y, z$ and $1 - x, 1 - y, z$ coalesce to the single point $\frac{1}{2}, 1 - y, z$ (Fig. 9.11a, b). From the 4-fold general position, we have obtained a 2-fold *special position*. The multiplicity of a special position is always an integral factor of the multiplicity 4 position. Special positions are not asymmetric; they possess site symmetry higher than 1, and in Fig. 9.11b, the site symmetry is m.

A special position is a set of equivalent points with point symmetry (site symmetry) higher than 1.

This particular special position has two degrees of freedom. As long as the point remains on the mirror plane, its multiplicity is unchanged. Other similar special positions arise from the mirror planes at $x, 0, z$; $x, \frac{1}{2}, z$ and $0, y, z$. A special position arises from the merging of equivalent positions.

If a point on $\frac{1}{2}, y, z$ moves onto the 2-fold axis at $\frac{1}{2}, \frac{1}{2}, z$ the two points $\frac{1}{2}, y, z$ and $\frac{1}{2}, 1 - y, z$ coalesce to $\frac{1}{2}, \frac{1}{2}, z$. This special position retains only a single degree of freedom. The point symmetry of the position rises to mm2, and the multiplicity falls to 1. The positions $0, 0, z$; $\frac{1}{2}, 0, z$ and $0, \frac{1}{2}, z$ are similar to $\frac{1}{2}, \frac{1}{2}, z$. Some space groups have special positions with no degrees of freedom, an important case of this being a point on an inversion centre (see Table 9.4).

The general and special positions in space group Pmm2 are set out in Table 9.3.

Another space group in point group mm2 is Pna₂₁, shown in Fig. 9.12. The space group symbol indicates that the unit cell is orthorhombic, with n-glide

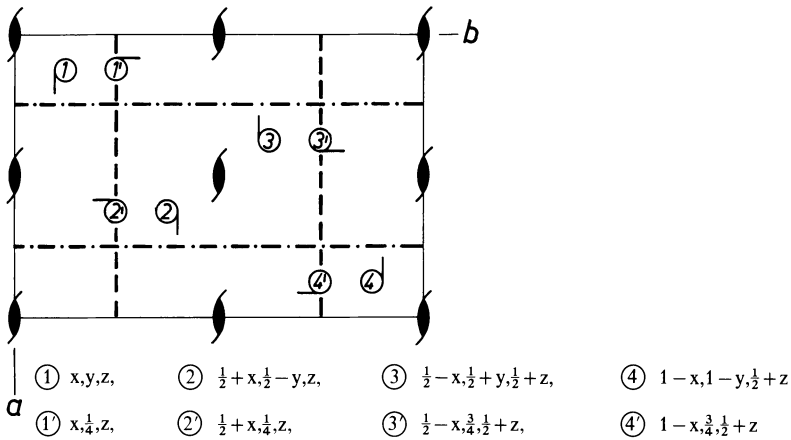


Fig. 9.12. Symmetry elements of the space group $Pna2_1$ in projection on $x, y, 0$ showing the general position x, y, z (1). Even if a point lies on the a -glide plane at $x, \frac{1}{4}, z$ (1'), this does not reduce its multiplicity. Glide planes and screw axes, unlike point-symmetry elements, do not reduce the multiplicity of a position which lies on them

planes normal to the a -axis with a glide component $\frac{1}{2}|\vec{b} + \vec{c}|$, a -glides normal to the b -axis, and 2_1 -screw axes parallel to the c -axis. The general position, x, y, z , as shown in Fig. 9.12, is again 4-fold. When, however, the point moves onto the a -glide at $x, \frac{1}{4}, z$, the multiplicity is unchanged. A special position does not arise, since glide planes and screw axes do not alter the multiplicity of a point. As a result, the space group $Pna2_1$ has no special positions.

Figure 9.13 shows the projection of the space group $P2/m$ on $x, y, 0$. In addition to the general position, there are special positions with m , 2 and $2/m$ site symmetry. Table 9.4 shows these points, and gives the degrees of freedom, the multiplicities, and the site symmetries of each type of position. Note that as the site symmetry rises, the multiplicity falls.

The asymmetric unit of a space group is the smallest part of the unit cell from which the whole cell may be filled exactly by the operation of all the symmetry operations. Its volume is given by:

$$V_{\text{asym. unit}} = \frac{V_{\text{unit cell}}}{\text{multiplicity of the general position}}$$

and it has the property that no two points within it are related to one another by a symmetry operation, cf. the asymmetric face unit of a point group in Chapter 8.2.1.

An asymmetric unit contains all the information necessary for the complete description of a crystal structure.

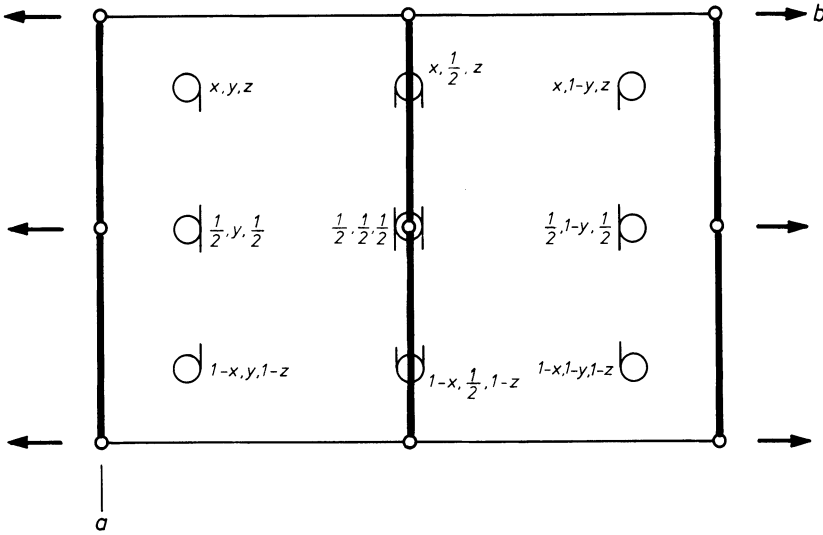


Fig. 9.13. Space group P2/m shown in projection on $x, y, 0$ with the general position x, y, z and the special positions on $m, 2$ and $2/m$

Table 9.4. Positions of the space group P2/m

Position	Degrees of freedom	Multiplicity	Site symmetry	Coordinates of equivalent points
general	3	4	1	x, y, z $x, 1-y, z$ $1-x, y, 1-z$ $1-x, 1-y, 1-z$
special	2	2	m	$x, \frac{1}{2}, z$ $1-x, \frac{1}{2}, 1-z$
	1	2	2	$\frac{1}{2}, y, \frac{1}{2}$ $\frac{1}{2}, 1-y, \frac{1}{2}$
	0	1	$2/m$	$\frac{1}{2}, \frac{1}{2}, \frac{1}{2}$

An asymmetric unit of the space group P2/m is the volume limited by $0 \leq x \leq \frac{1}{2}; 0 \leq y \leq \frac{1}{2}; 0 \leq z \leq 1$. Its volume is one quarter of that of the unit cell, so the equation above is fulfilled, as the multiplicity of the general position is 4.

The tetragonal space group $P4_2/mnm$ will be described in Section 9.4. The general position in the hexagonal space group $P6_1$ is illustrated in Fig. 9.14. Fig. 9.14a shows the operation of a 6_1 -axis at $0, 0, z$ on an asymmetrical point x, y, z . The coordinate for each generated equivalent point are easily determined. With different z -values, these x - and y -coordinates will also arise from

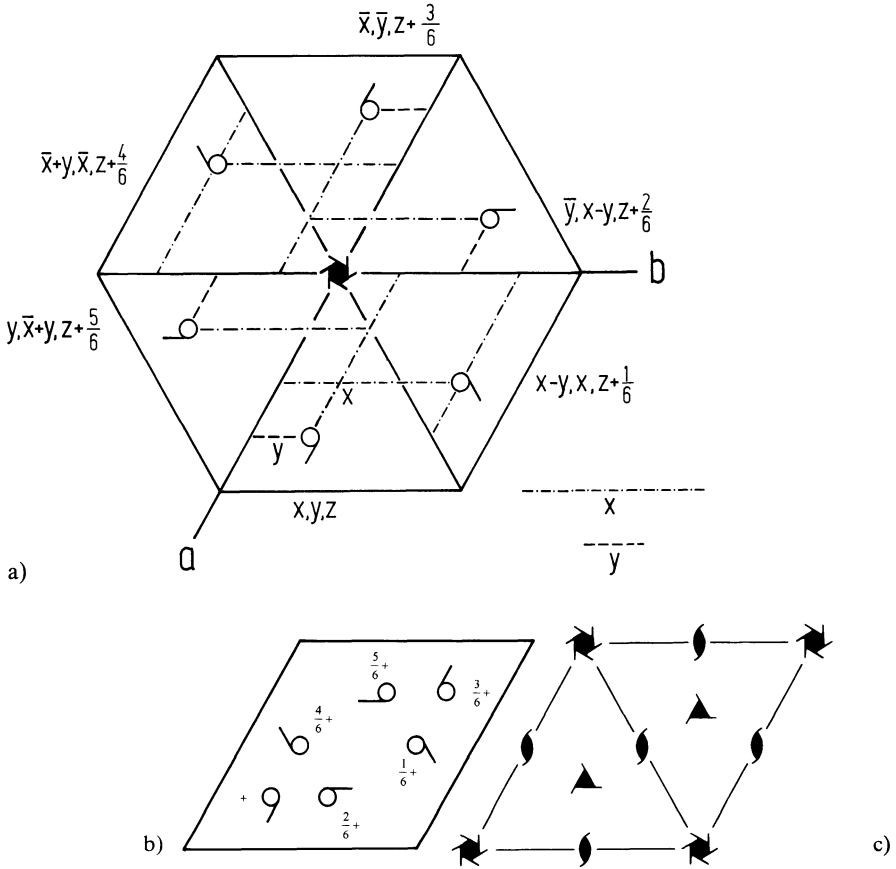


Fig. 9.14. a Operation of a 6_1 -screw axis at $0,0,z$ on a point in a general site x,y,z . b Displacement of the points originated in a by lattice translation into the unit cell (general position). c Space group $P6_1$

$6, \bar{6}, 6_2, 6_3, 6_4, 6_5, 3, \bar{3}, 3_1, 3_2$ -operations. In Fig. 9.14b, the equivalent points of a have been shifted to a single unit cell by lattice translations. From this arrangement of the points, the 2_1 at $\frac{1}{2}, \frac{1}{2}, z$ and the 3_1 at $\frac{2}{3}, \frac{1}{3}, z$ and $\frac{1}{3}, \frac{2}{3}, z$ are clearly shown. The symmetry elements of $P6_1$ are given in c.

We shall now consider, as an example of the cubic system, the space group $P4/m \bar{3} 2/m$. This is the space group of the cubic P-lattice, which has already been introduced in Fig. 6.13d. That diagram of the space group $P4/m \bar{3} 2/m$ is incomplete. It was, however, adequate for the introduction of symmetry relationships, and is also entirely suitable for the application of this space group, as we shall see later. M. J. Buerger [6] developed projections of the cubic space groups which have been included in the third edition of the *International Tables* [14]. Figure 9.15 shows such a projection on $x,y,0$ of the space group $P4/m \bar{3} 2/m$. In order to include those symmetry elements which are parallel to $\langle 110 \rangle$ and $\langle 111 \rangle$ in the diagram, Buerger used an orthographic

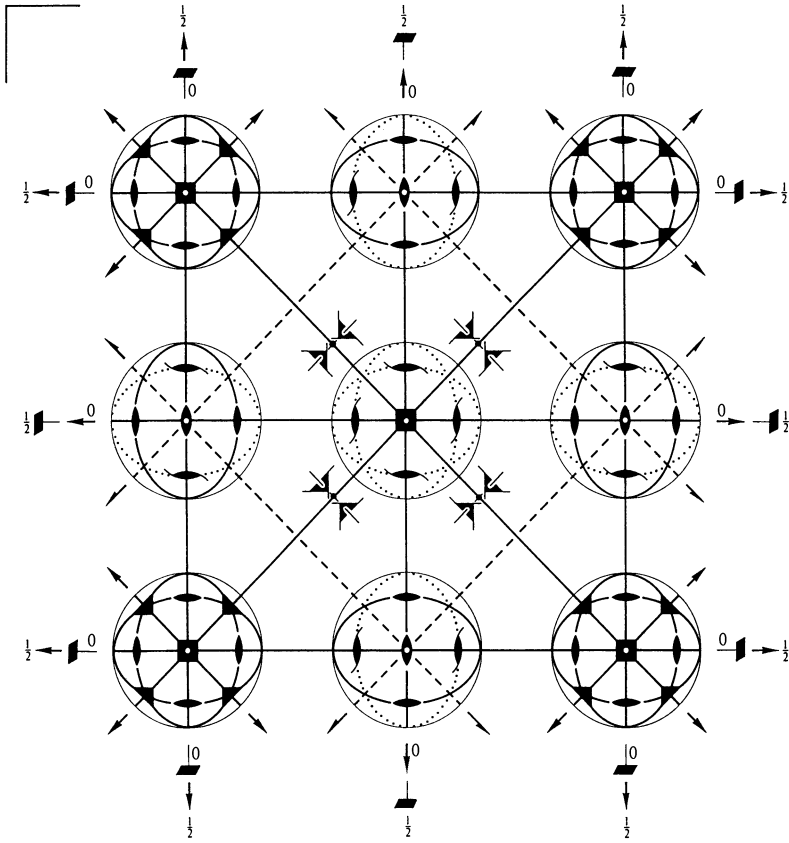


Fig. 9.15. Space group $P4/m \bar{3} 2/m$ [6], [14] projection on $x, y, 0$

projection¹, and representations of the oblique rotation- and screw-axes. In order to understand the relationship of the various symmetry elements, it is useful to study Fig. 9.15 and Fig. 6.13d, to see that they are representations of the same thing.

Even for so complex a space group as $P4/m \bar{3} 2/m$, it is relatively easy to describe a general position. Figure 9.16a shows a section of a cubic unit cell. A 3-fold rotation axis lies along the body-diagonal of the unit cell x, x, x , but it is not shown here. Starting from a point x, y, z ($x=0.3, y=0.2, z=0.1$), the operation of the 3-fold axis generates the points z, x, y and y, z, x (Fig. 9.16a). Figure 9.16b shows the projection of these three points on $x, y, 0$. The application of the mirror plane at x, x, z to these points converts them to a set of six points in a planar ring (Fig. 9.16c). The further application of the 4-fold axis at $0, 0, z$ converts this ring to a set of four rings (Fig. 9.16d). Finally, the mirror plane at $x, y, 0$ reflects these rings downwards and produces the full set of points for this 48-fold position. The coordinates of all 48 of these points are

¹ See section 4.8.

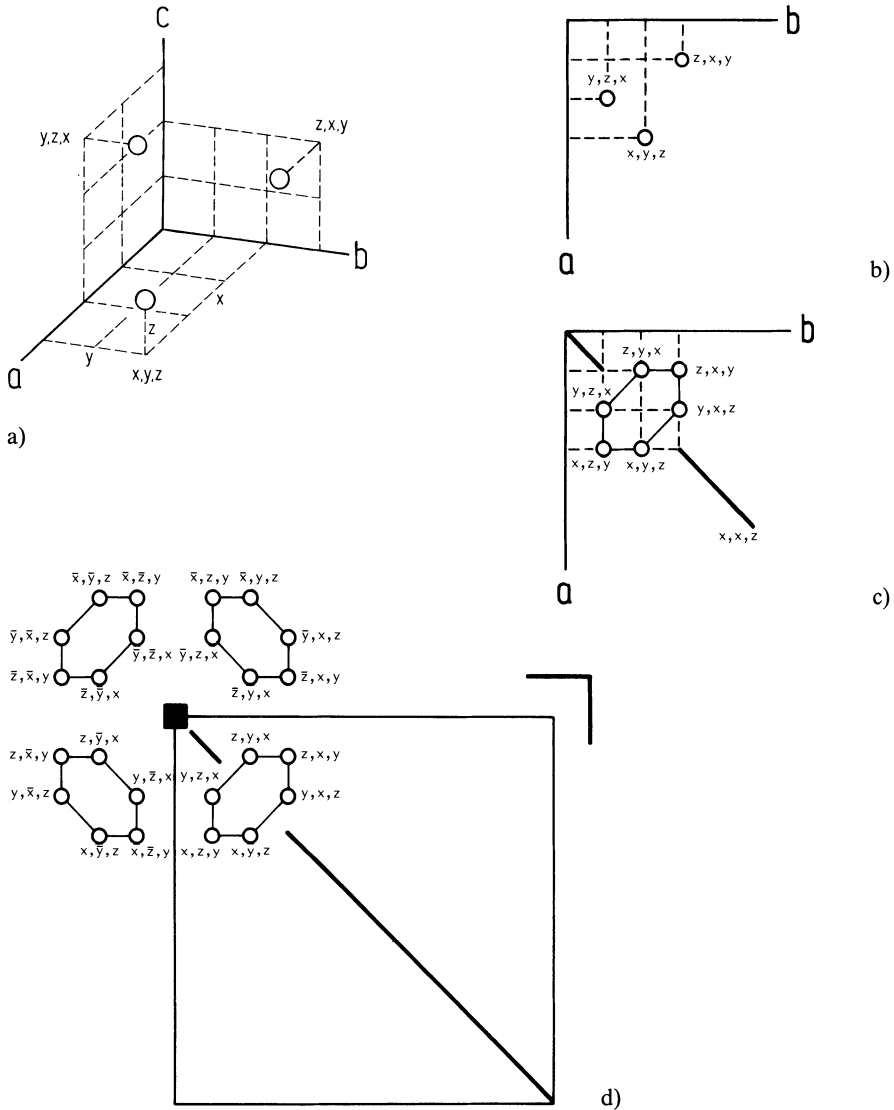


Fig. 9.16 a-d. The 48-fold general position of space group $P4/m \bar{3} 2/m$. **a** Section of a unit cell showing the operation of the 3-fold rotation axis at x, x, x (not drawn) on a general point x, y, z with $x = 0.3, y = 0.2, z = 0.1$. **b** Projection of the equivalent points in **a** on $x, y, 0$. **c** The operation of the mirror plane at x, x, z on the points in **b** generates six equivalent points in a planar, 6-membered ring. **d** The operations of the 4-fold axis at $0, 0, z$ and the mirror plane at $x, y, 0$ on the points in **c** complete the full set of 48 equivalent points of the general position. Only those points lying above the plane of the paper are shown. The rest may be generated by giving a minus sign to the third co-ordinate of each triple

given in Fig. 9.16d, if each triple is taken to imply one with a minus sign on the third co-ordinate as well. These 48 equivalent points are generated entirely by the symmetry of $4/m \bar{3} m$!

There is a simple relationship between the number of faces in the general form of a crystal of a particular point group and the multiplicity of the general position of a space group in that point group (cf. Table 9.2). For space groups with a P-lattice, the multiplicity of the general position is equal to the number of faces in the general form for the point group. For space groups with C-, A- and I-lattices, the multiplicity of the general position is twice as great as the number of faces, and for those with an F-lattice four times. The general form of the point group $mm2$ is the rhombic pyramid (cf. Exercise 8.15(5)) with four faces. The multiplicity of the general position in $Pmm2$ (Fig. 9.11a) or $Pna2_1$ (Fig. 9.12) is 4, while for $Cmm2$, $Aba2$, $Imm2$ or $Ima2$ it is 8, and for $Fmm2$, it is 16.

If the point group includes an inversion centre, all the corresponding space groups will be centrosymmetric, cf the monoclinic space groups in Fig. 9.9.

Consider now the space group $P4_2/n 2_1/c 2/m$. Removing the lattice symbol and converting all glide planes and screw axes to the corresponding point symmetry elements ($4_2 \rightarrow 4$; $2_1 \rightarrow 2$; $n, c \rightarrow m$) gives the point group of this space group: $4/m 2/m 2/m$.

9.4 International Tables for Crystallography

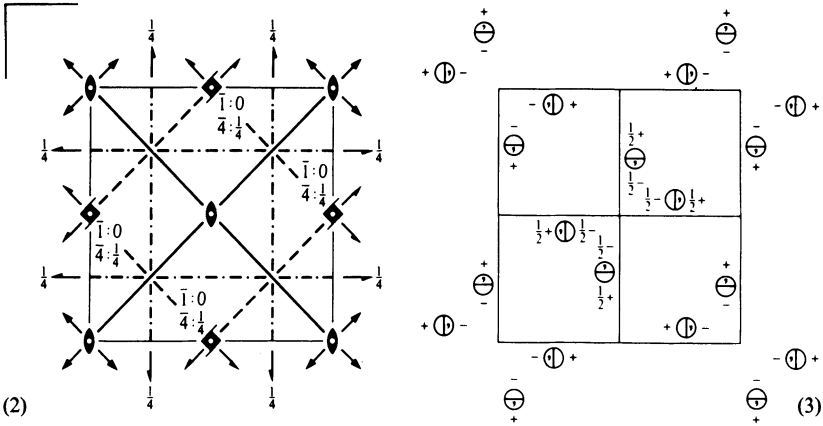
Many of the most important properties of the 230 space groups are collected in *International Tables for Crystallography*, Vol A. [18], [17], [14]. These tables are very useful. The information they contain may be illustrated with respect to the space group $P4_2/mnm$ (Fig. 9.17).

- (1) Short space group symbol, Schönflies symbol, point group, crystal system, number of the space group, full space group symbol.
- (2) Projection of the symmetry elements of the space group on $x, y, 0$; a points down the page, b across to the right, and the origin is in the upper left corner.
- (3) Projection of a general position on $x, y, 0$; the axial directions are as in (2), \circ represents a point, \oplus a point projecting on top of another, while \ominus implies that one of the points is derived from the other by a reflection or rotoinversion operation. The z-coordinate is indicated.
- (4) Information about the choice of origin, here at an inversion centre at the intersection of three mutually perpendicular mirror planes. Since this is a tetragonal space group, the symbols $2/m 1 2/m$ imply the symmetry directions, c, $\langle a \rangle$, $\langle 110 \rangle$.
- (5) The asymmetric unit:

$$V_{\text{asym. unit}} = \frac{V_{\text{unit cell}}}{\text{multiplicity of the general position}}$$

- (6) The symmetry operations of the space group.

(1) $P 4_2/m n m$ D_{4h}^{14} $4/m m m$ Tetragonal
 No. 136 $P 4_2/m 2_1/n 2/m$



(2) **Origin at centre (mmm) at 2/m 12/m**

(3) **Asymmetric unit** $0 \leq x \leq \frac{1}{2}; 0 \leq y \leq \frac{1}{2}; 0 \leq z \leq \frac{1}{2}; x \leq y$

(4) **Symmetry operations**

- | | | | |
|---|--|---|---|
| (1) 1 | (2) 2 0,0,z | (3) 4+(0,0, $\frac{1}{2}$) 0, $\frac{1}{2}$,z | (4) 4-(0,0, $\frac{1}{2}$) $\frac{1}{2}$,0,z |
| (5) 2(0, $\frac{1}{2}$,0) $\frac{1}{2}$,y, $\frac{1}{2}$ | (6) 2($\frac{1}{2}$,0,0) x, $\frac{1}{2}$, $\frac{1}{2}$ | (7) 2 x,x,0 | (8) 2 x, \bar{x} ,0 |
| (9) $\bar{1}$ 0,0,0 | (10) m x,y,0 | (11) 4+ $\frac{1}{2}$,0,z; $\frac{1}{2}$,0, $\frac{1}{2}$ | (12) 4- 0, $\frac{1}{2}$,z; 0, $\frac{1}{2}$, $\frac{1}{2}$ |
| (13) n($\frac{1}{2}$,0, $\frac{1}{2}$) x, $\frac{1}{2}$,z | (14) n(0, $\frac{1}{2}$, $\frac{1}{2}$) $\frac{1}{2}$,y,z | (15) m x, \bar{x} ,z | (16) m x,x,z |

(7) **Positions**

	Multiplicity, Wyckoff letter, Site symmetry	Coordinates
16	k 1	(1) x,y,z (2) \bar{x},\bar{y},z (3) $\bar{y}+\frac{1}{2},x+\frac{1}{2},z+\frac{1}{2}$ (4) $y+\frac{1}{2},\bar{x}+\frac{1}{2},z+\frac{1}{2}$ (5) $\bar{x}+\frac{1}{2},y+\frac{1}{2},z+\frac{1}{2}$ (6) $x+\frac{1}{2},\bar{y}+\frac{1}{2},z+\frac{1}{2}$ (7) y,x,z (8) \bar{y},\bar{x},z (9) \bar{x},\bar{y},z (10) x,y,z (11) $y+\frac{1}{2},\bar{x}+\frac{1}{2},z+\frac{1}{2}$ (12) $\bar{y}+\frac{1}{2},x+\frac{1}{2},z+\frac{1}{2}$ (13) $x+\frac{1}{2},\bar{y}+\frac{1}{2},z+\frac{1}{2}$ (14) $\bar{x}+\frac{1}{2},y+\frac{1}{2},z+\frac{1}{2}$ (15) \bar{y},x,z (16) y,x,z
8	j ..m	x,x,z \bar{x},\bar{x},z $\bar{x}+\frac{1}{2},x+\frac{1}{2},z+\frac{1}{2}$ $x+\frac{1}{2},\bar{x}+\frac{1}{2},z+\frac{1}{2}$ $\bar{x}+\frac{1}{2},x+\frac{1}{2},z+\frac{1}{2}$ $x+\frac{1}{2},\bar{x}+\frac{1}{2},z+\frac{1}{2}$ x,x,z \bar{x},\bar{x},z
8	i m..	x,y,0 $\bar{x},\bar{y},0$ $\bar{y}+\frac{1}{2},x+\frac{1}{2},\frac{1}{2}$ $y+\frac{1}{2},\bar{x}+\frac{1}{2},\frac{1}{2}$ $\bar{x}+\frac{1}{2},y+\frac{1}{2},\frac{1}{2}$ $x+\frac{1}{2},\bar{y}+\frac{1}{2},\frac{1}{2}$ y,x,0 $\bar{y},\bar{x},0$
8	h 2..	0, $\frac{1}{2}$,z 0, $\frac{1}{2}$,z+ $\frac{1}{2}$ $\frac{1}{2}$,0,z+ $\frac{1}{2}$ $\frac{1}{2}$,0,z 0, $\frac{1}{2}$,z 0, $\frac{1}{2}$,z+ $\frac{1}{2}$ $\frac{1}{2}$,0,z+ $\frac{1}{2}$ $\frac{1}{2}$,0,z
4	g m.2m	x, \bar{x} ,0 $\bar{x},x,0$ $x+\frac{1}{2},x+\frac{1}{2},\frac{1}{2}$ $\bar{x}+\frac{1}{2},\bar{x}+\frac{1}{2},\frac{1}{2}$
4	f m.2m	x,x,0 $\bar{x},\bar{x},0$ $\bar{x}+\frac{1}{2},x+\frac{1}{2},\frac{1}{2}$ $x+\frac{1}{2},\bar{x}+\frac{1}{2},\frac{1}{2}$
4	e 2.mm	0,0,z $\frac{1}{2},\frac{1}{2},z+\frac{1}{2}$ $\frac{1}{2},\frac{1}{2},z+\frac{1}{2}$ 0,0,z
4	d $\bar{4}$..	0, $\frac{1}{2}$, $\frac{1}{2}$ 0, $\frac{1}{2}$, $\frac{1}{2}$ $\frac{1}{2}$,0, $\frac{1}{2}$ $\frac{1}{2}$,0, $\frac{1}{2}$
4	c 2/m..	0, $\frac{1}{2}$,0 0, $\frac{1}{2}$, $\frac{1}{2}$ $\frac{1}{2}$,0, $\frac{1}{2}$ $\frac{1}{2}$,0,0
2	b m.mm	0,0, $\frac{1}{2}$ $\frac{1}{2}$, $\frac{1}{2}$,0
2	a m.mm	0,0,0 $\frac{1}{2}$, $\frac{1}{2}$, $\frac{1}{2}$

Fig. 9.17. Space group $P4_2/mnm$, from *International Tables for Crystallography*, Vol. A. [14]

(7) General and special positions.

Col. 1: the multiplicity of the position.

Col. 2: the Wyckoff letter assigned to this position; the letter furthest down the alphabet, here k, represents the general position.

Col. 3: the site symmetry (point symmetry of the position), in the order c, $\langle a \rangle$, $\langle 110 \rangle$.

Col. 4: the coordinates of equivalent points in the position.

9.5 Space Group and Crystal Structure

In Chapter 3, we defined a *crystal structure as lattice + basis*. It is thus possible to describe it as a geometrical arrangement of atoms. Table 9.5A gives the lattice and the basis for the rutile (TiO_2) structure. The perspective drawing and the projection on $x, y, 0$ in Fig. 9.18 are derived from these data.

Every crystal structure can be similarly described by its *space group and the occupation of general or special positions by atoms*. The crystal structure of rutile

Table 9.5. Description of the crystal structure of rutile TiO_2

A		B	
Lattice	Basis	Space group	Positions of the atoms
tetragonal P	Ti: 0, 0, 0 $\frac{1}{2}, \frac{1}{2}, \frac{1}{2}$	P $4_2/mnm$	a Ti: 0, 0, 0 $\frac{1}{2}, \frac{1}{2}, \frac{1}{2}$
$a_0 = 4.59 \text{ \AA}$ $c_0 = 2.96 \text{ \AA}$	O: 0.3, 0.3, 0 0.8, 0.2, $\frac{1}{2}$ 0.2, 0.8, $\frac{1}{2}$ 0.7, 0.7, 0	$a_0 = 4.59 \text{ \AA}$ $c_0 = 2.96 \text{ \AA}$	f O: $x, x, 0$ $\frac{1}{2} + x, \frac{1}{2} - x, \frac{1}{2}$ $\frac{1}{2} - x, \frac{1}{2} + x, \frac{1}{2}$ $\bar{x}, \bar{x}, 0$ $x = 0.3$

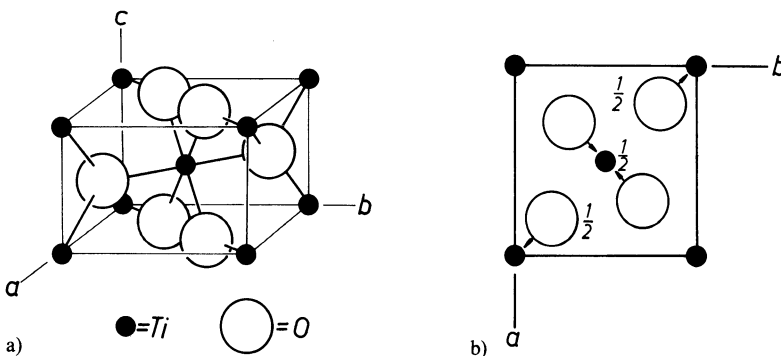


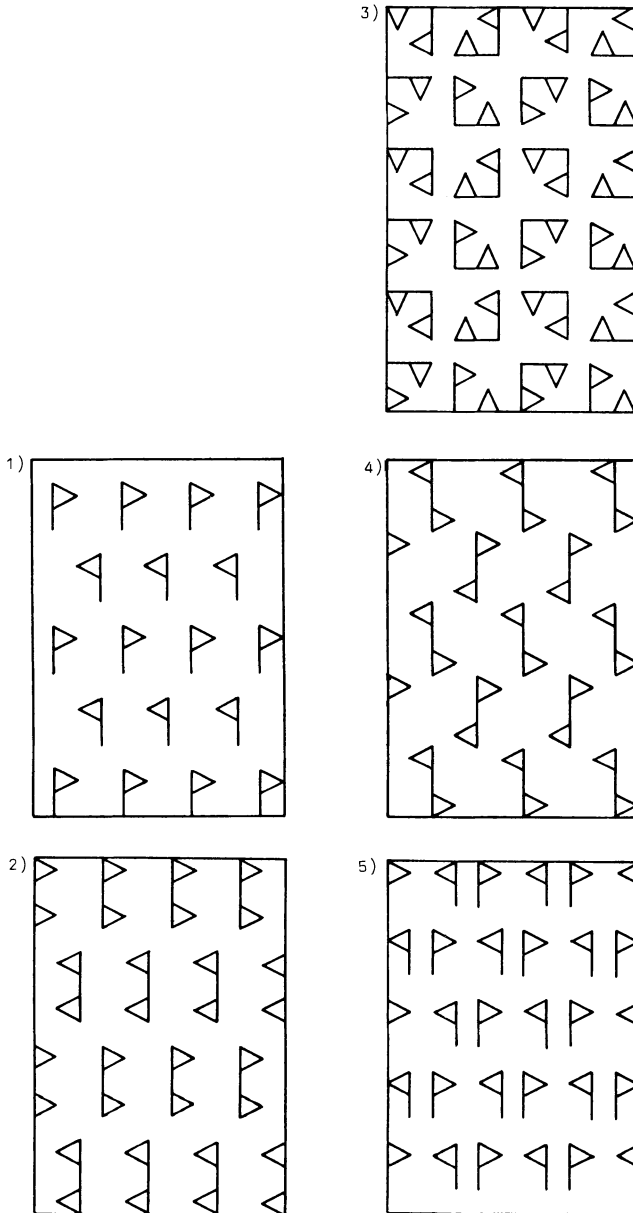
Fig. 9.18a, b. The crystal structure of rutile, TiO_2 , shown: **a** in a perspective drawing, **b** in projection on $x, y, 0$

is in space group $P4_2/mnm$. The titanium atoms occupy the position a, and the oxygen atoms the position f with $x=0.3$ (cf. the page of *International Tables* in Fig. 9.17). The special position a is 2-fold, implying $0,0,0$ and $\frac{1}{2}, \frac{1}{2}, \frac{1}{2}$; f is 4-fold: $x, x, 0$; $\frac{1}{2} + x, \frac{1}{2} - x, \frac{1}{2}$; $\frac{1}{2} - x, \frac{1}{2} + x, \frac{1}{2}$ and $\bar{x}, \bar{x}, 0$ (Table 9.5B). $0, 0, 0$ and $x, x, 0$ ($x=0.3$) lie in a single asymmetric unit of space group $P4_2/mnm$, cf. Fig. 9.17. Substituting 0.3 for x in the coordinates for the O-atoms gives the specific coordinates listed for the basis in Table 9.5A. The description of a crystal structure in terms of the space group is much simpler than that in terms of the basis when positions of high multiplicity are involved. In addition, the space group shows clearly which atoms are related to one another by the symmetry elements of the space group. This relationship is particularly important for positions with one or more degrees of freedom. Any movement in x (cf. position f in Fig. 9.17) alters the relationship of all the related atoms; for example, an increase of x results in the movement of the O-atoms indicated by the arrows in Fig. 9.18b.

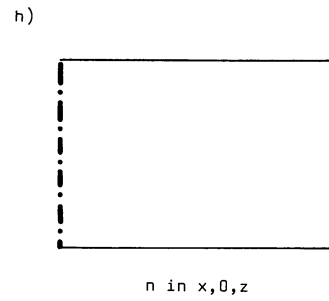
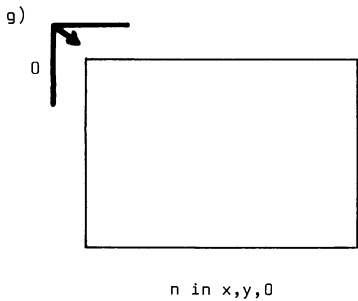
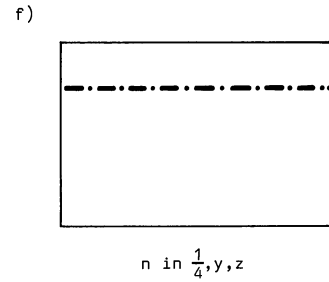
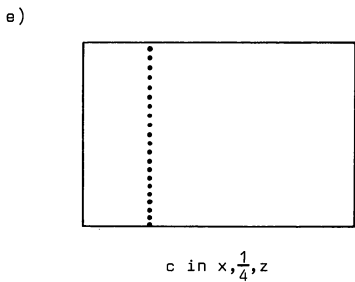
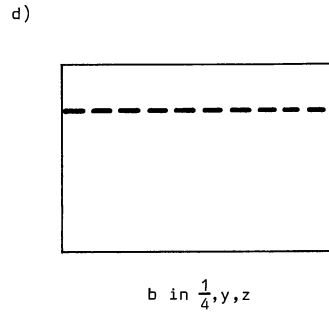
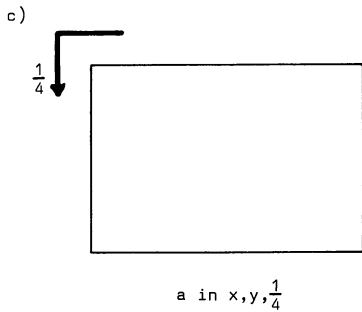
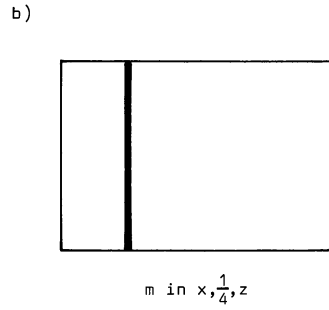
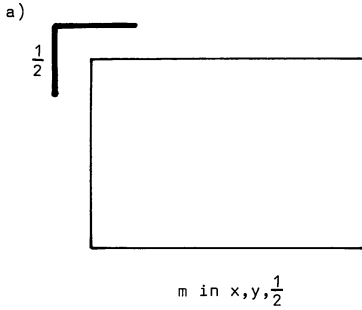
EXERCISES

Exercise 9.1. For the two-dimensional “Knockel” structures given below, indicate:

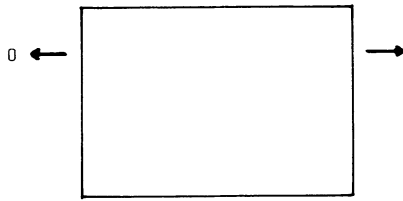
- The unit mesh.
- The symmetry elements, paying particular attention to glide planes.



Exercise 9.2. Glide planes and screw axes. In the projections below of a unit cell onto $x, y, 0$, only a single symmetry element is given. Allow this symmetry element to operate on an asymmetric point (in a general site) at x, y, z and give the coordinates of the equivalent point(s) generated.

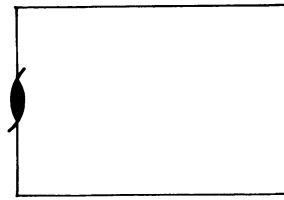


i)



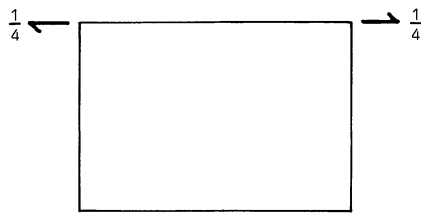
$$2 \text{ in } \frac{1}{4}, y, 0$$

j)



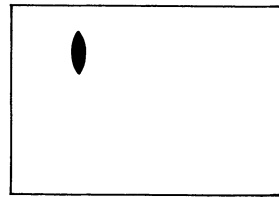
$$2_1 \text{ in } \frac{1}{2}, 0, z$$

k)



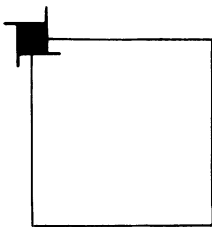
$$2_1 \text{ in } 0, y, \frac{1}{4}$$

l)



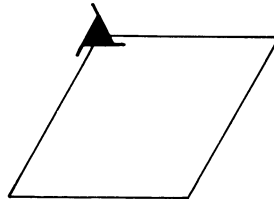
$$2 \text{ in } \frac{1}{4}, \frac{1}{4}, z$$

m)



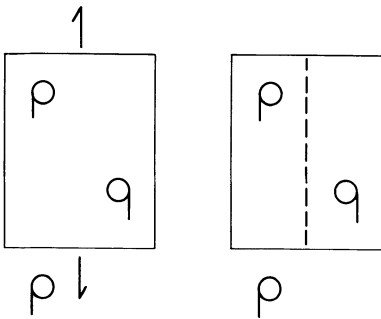
$$4_1 \text{ in } 0, 0, z$$

n)



$$3_1 \text{ in } 0, 0, z$$

Exercise 9.3. The figures show the operation of a glide plane and a 2_1 -axis on a point. The arrangement of the points appears to be the same in the two diagrams. Discuss this apparent contradiction.



Exercise 9.4. Show that (a) $C_{21}/c \equiv C_2/c$, (b) $C_{21}/m \equiv C_2/m$, and (c) $C_{21} \equiv C_2$.

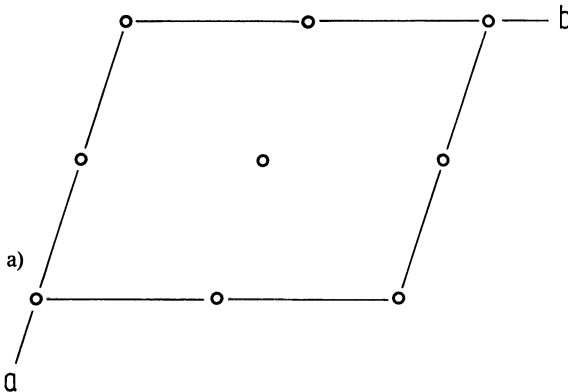
Start from the projections of the space groups (a) $P2_1/c$, (b) $P2_1/m$ and (c) $P2_1$ as given in Fig. 9.9. Place a point at x, y, z and another at $\frac{1}{2} + x, \frac{1}{2} + y, z$ (C-centring), and allow the symmetry elements to operate on them. This will give the general positions for: (a) C_{21}/c , (b) C_{21}/m and (c) C_{21} . Using these general positions, the complete symmetry of the space groups can be determined. Using Fig. 9.9, show the correspondence of (a) C_{21}/c with C_2/c , (b) C_{21}/m with C_2/m , and (c) C_{21} with C_2 , moving the origin of the diagram as necessary.

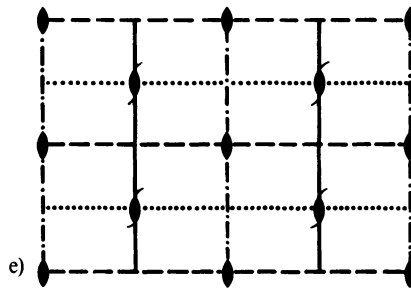
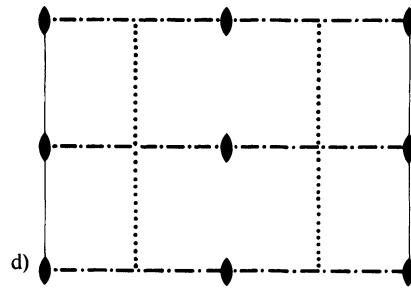
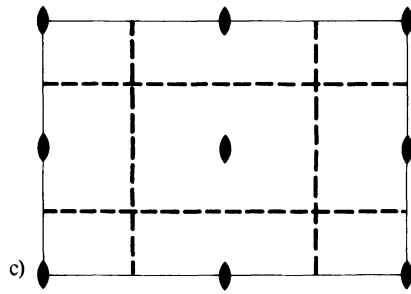
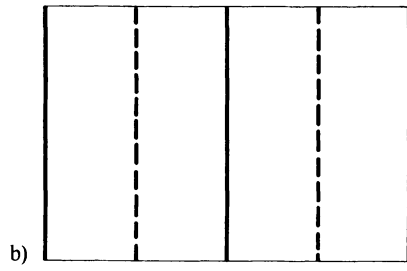
Exercise 9.5. Determine the symmetry of the orthorhombic C- and I-lattices. Indicate the symmetry elements on a projection of the lattice onto $x, y, 0$, and give the space group symbol.

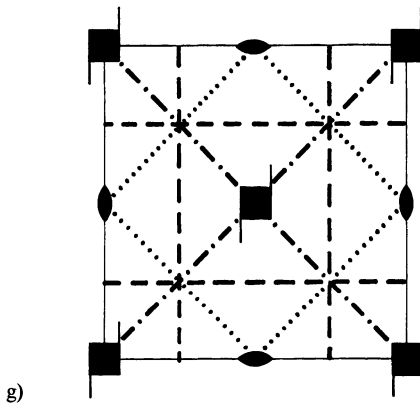
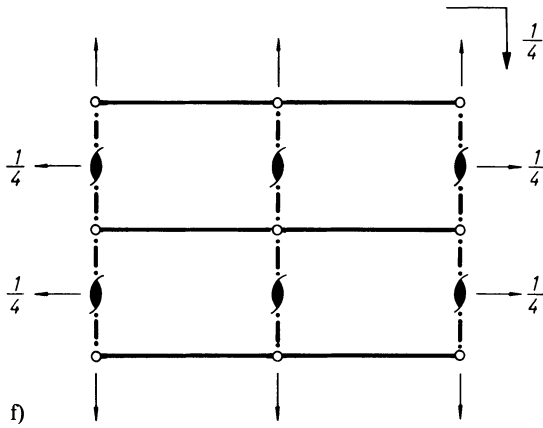
Exercise 9.6. Draw the symmetry diagram of space group $Pmm2$ on a piece of graph paper. Enter points in the general positions $0.1, 0.1, 0.1$; $0.1, 0.4, 0.1$; $0.25, 0.25, 0.1$; and $0.4, 0.4, 0.1$ and those points resulting from the operation of the symmetry elements on them.

Exercise 9.7. The symmetry diagrams for seven space groups are given below as projections on $x, y, 0$.

- Enter on each diagram a point in a general site x, y, z , and allow the symmetry to operate on it.
- Give the coordinates of the points equivalent to x, y, z .
- What is the multiplicity of the general position?
- Work out the space group symbol. (The graphical symbols for symmetry elements are given in Chap. 14.2).
- Indicate a special position – if there are any – and give its multiplicity.







Exercise 9.8. Make a tracing of the projection of a hexagonal unit cell on $x, y, 0$ (Fig. 9.14) and place at $0, 0, z$ (a) a 6_2 -axis, (b) a 6_3 -axis.

1. Allow the symmetry elements to operate on a point in a general site, and give the coordinates of the resulting equivalent points.
2. Draw in the other symmetry elements of the space group in the unit cell.
3. Which symmetry elements are contained within 6_2 and 6_3 ?

Exercise 9.9. Consider the space group $P4/m \bar{3} 2/m$ (Figs. 9.15 and 9.16). In a projection on $x, y, 0$, draw in the special positions (a) x, x, z , (b) x, x, x , (c) $x, 0, 0$.

Give the coordinates of the equivalent points and the multiplicities and site symmetry of the positions.

Exercise 9.10. Draw a projection of the symmetry diagram for the space groups $P2_1/c$, $Pna2_1$, $Pmna$, $Pbca$, and $P422$.

Exercise 9.11. Criticise the symbol $Pabc$.

10 The Interrelationship of Point Groups and Space Groups

When point groups and space groups are compared and contrasted with one another, various relationships between them become clear. Table 9.2 shows the 230 space groups arranged according to the corresponding point groups. Table 10.1 contains a comparative summary of properties of point groups and space groups.

The only forms which can occur on a crystal are those which belong to the point group resulting from the space group of the crystal structure. The rutile structure, for example (Fig. 9.18) has the space group $P4_2/mnm$, and consequently point group $4/mmm$. Point group $4/mmm$ includes only those forms given in Fig. 8.7. Of these, the crystal in Table 8.11.15 has developed only $\{111\}$, $\{110\}$ and $\{100\}$.

Molecules are also characterised by point groups. What is the role of molecular symmetry when equal molecules associate with one another in a crystal? Hexamethylenetetramine molecules belong to point group $\bar{4}3m$ (Fig. 10.1 a). These molecules form crystals with space group $I\bar{4}3m$ (Fig. 10.1 b), in which the molecules occupy positions with the site symmetry $\bar{4}3m$. Unfortunately, this correspondence is far from common!

Ethylene molecules (point group $2/m\ 2/m\ 2/m$ (mmm) Fig. 10.2a), give crystals with space group $P2_1/n\ 2_1/n\ 2/m$ ($Pnmm$) in which they occupy positions with site symmetry $2/m$ only (Fig. 10.2b).

Similarly, benzene molecules, which have the very high point symmetry of $6/mmm$, give orthorhombic crystals (space group $Pbca$) in which they occupy positions with site symmetry $\bar{1}$ only (Fig. 10.3). Here the symmetry of the free molecule is higher than that of the crystal structure.

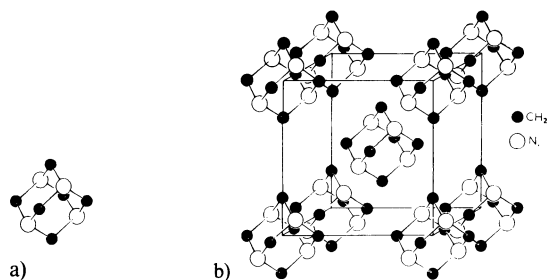


Fig. 10.1 a, b. Symmetry of hexamethylenetetramine ($C_6H_{12}N_4$). a molecule: $\bar{4}3m$. b crystal structure: $I\bar{4}3m$. (After [2])

Table 10.1. Comparison of point groups and space groups

Point group	Space group												
A group of point symmetry operations whose operation leaves at least one point unmoved. Any operation involving lattice translations is excluded.	A group of symmetry operations including lattice translations												
$1 \bar{1}$ $2 m$ $3 \bar{3}$ $4 \bar{4}$ $6 \bar{6}$	$1 \bar{1}$ $2 m$ 2_1 ; a, b, c, n, d $3 \bar{3}$ $3_1, 3_2$ $4 \bar{4}$ $4_1, 4_2, 4_3$ $6 \bar{6}$ $6_1, 6_2, 6_3, 6_4, 6_5$ lattice translations												
a, b, c α, β, γ	a_0, b_0, c_0 α, β, γ												
Order of the symmetry directions e.g. $4/m \ 2/m \ 2/m$ <table style="margin-left: auto; margin-right: auto; border-collapse: collapse;"> <tr> <td style="border: none; padding: 0 5px;"> </td> <td style="border: none; padding: 0 5px;"> </td> <td style="border: none; padding: 0 5px;"> </td> </tr> <tr> <td style="border: none; padding: 0 5px;">c</td> <td style="border: none; padding: 0 5px;">⟨a⟩</td> <td style="border: none; padding: 0 5px;">⟨110⟩</td> </tr> </table>				c	⟨a⟩	⟨110⟩	Order of the symmetry directions e.g. $P4_2/m \ 2_1/n \ 2/m$ <table style="margin-left: auto; margin-right: auto; border-collapse: collapse;"> <tr> <td style="border: none; padding: 0 5px;"> </td> <td style="border: none; padding: 0 5px;"> </td> <td style="border: none; padding: 0 5px;"> </td> </tr> <tr> <td style="border: none; padding: 0 5px;">c</td> <td style="border: none; padding: 0 5px;">⟨a⟩</td> <td style="border: none; padding: 0 5px;">⟨110⟩</td> </tr> </table>				c	⟨a⟩	⟨110⟩
c	⟨a⟩	⟨110⟩											
c	⟨a⟩	⟨110⟩											
General form Set of equivalent faces with face symmetry 1	General position Set of equivalent points with site symmetry 1												
$f_{\text{asym. face unit}} = \frac{f_{\text{surface area of the sphere}}}{\text{number of faces in the general form}}$	$V_{\text{asym. unit}} = \frac{V_{\text{unit cell}}}{\text{multiplicity of the general position}}$												
Number of faces in the general form of a point group	Multiplicity of the general position for all space groups with P-lattice, belonging to the point group												
Special form Set of equivalent faces with face symmetry > 1	Special position Set of equivalent points with site symmetry > 1												

Molecules C_{60} have the non-crystallographic point group $2/m \bar{3}5$ (Fig. 11.6). These molecules associate to give cubic crystals, with a ccp structure (space group $F4/m\bar{3}2/m$).

There is no simple relationship between molecular and crystal symmetry. The crystal structure that is adopted depends on many factors, including the type of chemical bonding, the shape and the packing possibilities of the molecules.

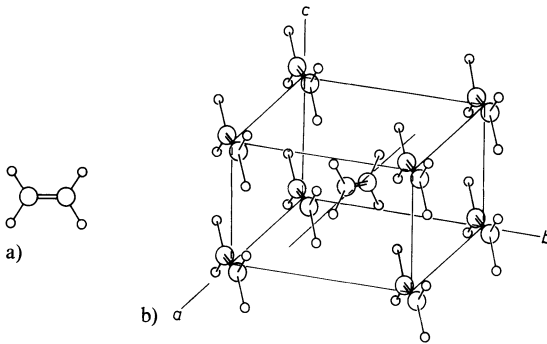


Fig. 10.2a, b. Symmetry of ethylene (C_2H_4). **a** Molecule: $2/m\ 2/m\ 2/m$ **b** Crystal structure $P2_1/n\ 2_1/n\ 2/m$

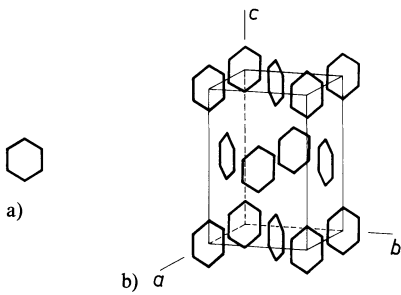


Fig. 10.3a, b. Symmetry of benzene (C_6H_6). **a** Molecule: $6/mmm$. **b** Crystal structure: $Pbca$

EXERCISES

Exercise 10.1. In each of the space groups $P\bar{1}$ (Fig. 6.7d), Pm and $P2/m$ (Fig. 9.9) and $P2/m\ 2/m\ 2/m$ (Fig. 6.9d), place an atom A at the origin $(0, 0, 0)$ and a different atom B at a general position x, y, z ($x, y, z < \frac{1}{4}$).

- What is the chemical formula of this structure?
- What is the value of Z , the number of formula units per cell?
- Describe the shape of the resulting molecule.
- Give the point group of the molecule.
- What is the site symmetry of the molecule in the crystal structure?

11 Fundamentals of Crystal Chemistry

Crystal chemistry is concerned with the crystal structure of the elements and of chemical compounds. It attempts to explain why particular types of crystal structures arise under specific conditions. It is, however, still only possible to understand how relatively simple crystal structures arise from the atoms that make them up.

A fundamental concept in crystal structures is the *idea of sphere packing*. In this approach, the atoms or ions of which the structure is composed are regarded as hard spheres which pack with one another. Goldschmidt and Laves summarised this approach in three principles:

1. *The Principle of Closest Packing*. Atoms in a crystal structure attempt to arrange themselves in a manner which fills space most efficiently.
2. *The Symmetry Principle*. Atoms in a crystal structure attempt to achieve an environment of the highest possible symmetry.
3. *The Interaction Principle*. Atoms in a crystal structure attempt to achieve the highest coordination (Sect. 11.1), i.e. the maximum possible number of nearest neighbours with which they can interact.

Chemical bonding is a very important factor in crystal chemistry, as it is concerned with the forces holding the atoms together in the structure. The atoms of a structure are held together in a characteristic order by the chemical bonding. This bonding arises from interaction of the electron shells of the atoms, and is conventionally divided into:

- a) *metallic bonding*
- b) *van der Waals bonding*
- c) *ionic or heteropolar bonding and*
- d) *covalent or homopolar bonding.*

They are illustrated schematically in Fig. 11.1. Actual compounds rarely correspond exactly to one of these types. In most cases, the bonding is a mixture of two or more types, which should be regarded only as limiting cases.

It is beyond the scope of this book to discuss the theory of chemical bonding. We shall restrict ourselves here, so far as bonding theory is concerned, to a small number of principles on which further study may be based.

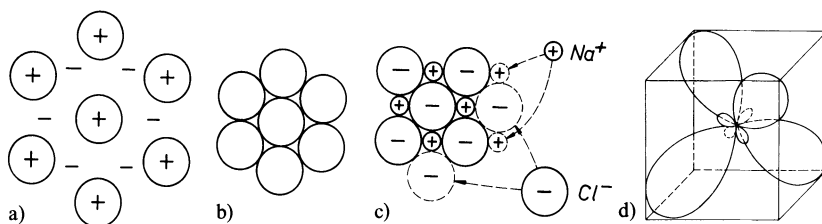


Fig. 11.1 a-d. Schematic summary of bonding types in crystals.

a Metallic bonding. Valence electrons of the metal atoms are delocalised in an “electron cloud”. This negatively charged cloud encloses the positively charged atom cores and holds them together.

b Van der Waals bonding. This arises from random variations in the charge distributions of the atoms and is very weak. The atoms and molecules tend toward a closest packing.

c Ionic bonding. In an ionic crystal, the positively and negatively charged ions are held together by electrostatic forces.

d Covalent bonding. This represents the four sp^3 -orbitals of a carbon atom in the diamond structure

The principles stated above work well in rationalising the structures of metallic and ionic materials. They also have some application to molecular crystals, those held together by van der Waals forces. For covalent structures, the principles of closest packing and of high coordination are rarely fulfilled. This results from the fact that covalent bonding is *directional* in nature.

11.1 Coordination

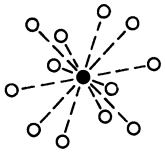
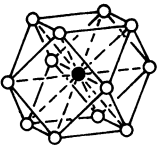
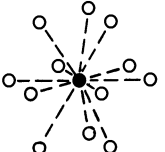
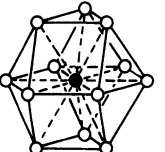
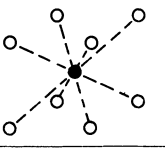
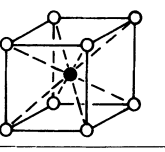
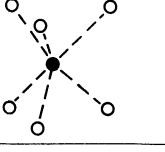
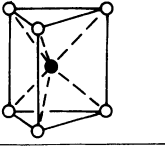
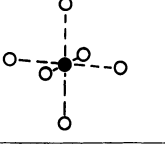
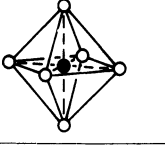
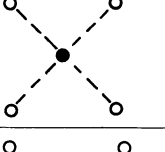
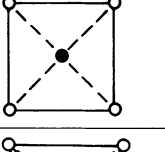
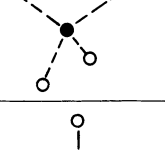
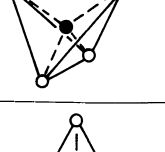
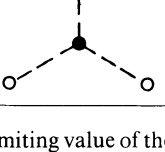
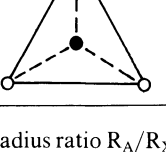
In crystal chemistry, the immediate neighbourhood of each atom and the forces which bind it to its neighbours play a leading role in the explanation of the overall geometry of the crystal.

The number of nearest neighbours of a central atom or ion is called its coordination number, and the polyhedron formed when the nearest neighbours are connected by lines is called its coordination polyhedron.

Some important coordination polyhedra are given in Table 11.1 along with actual examples. The coordination number, in square brackets, can be inserted in the chemical formula as a superscript, and thus add significant crystal-chemical information to the formula.

Ideally, coordination polyhedra have a high point symmetry. However, a coordination polyhedron is nothing like so sharply defined as a crystal form (Chap. 8.2.1). Even atoms of the same element coordinated to the same central atom are not necessarily equivalent. Strictly speaking, cubic ($m\bar{3}m$), octahedral ($m\bar{3}m$) and tetrahedral ($\bar{4}3m$) symmetries can only arise in the cubic system. Coordination polyhedra are often more or less distorted. The cubic coordi-

Table 11.1. Important coordination polyhedra

		Coordination		R_A/R_X^a	Examples
	Configuration	Polyhedron or polygon			
a)			Cuboctahedron	1	Cubic closest packing of spheres (Cu, Ne, etc.)
b)			Disheptahedron		
c)	[8] 		Cube	0,73	$\text{Cs}^{[8]}\text{Cl}$ $\text{Ca}^{[8]}\text{F}_2$
d)	[6] 		Trigonal prism	0,53	$\text{AlB}_2^{[6]b}$
e)			Octahedron	0,41	$\text{Na}^{[6]}\text{Cl}$ $\text{Ti}^{[6]}\text{O}_2$ $\text{Pt}^{[6]}\text{Cl}_6^-$
f)	[4] 		Square		
g)			Tetrahedron	0,23	$\text{Zn}^{[4]}\text{S}$ $\text{Si}^{[4]}\text{O}_2$ $\text{S}^{[4]}\text{O}_4^{2-}$
h)	[3] 		Equilateral triangle	0,15	$\text{C}^{[3]}\text{O}_3^{2-}$ $\text{N}^{[3]}\text{O}_3^-$

^a The limiting value of the radius ratio R_A/R_X is that at which spherical coordinating atoms X just touch one another, and the central atom A fits precisely into the resultant hole.

^b Cf. exercise 3.2.

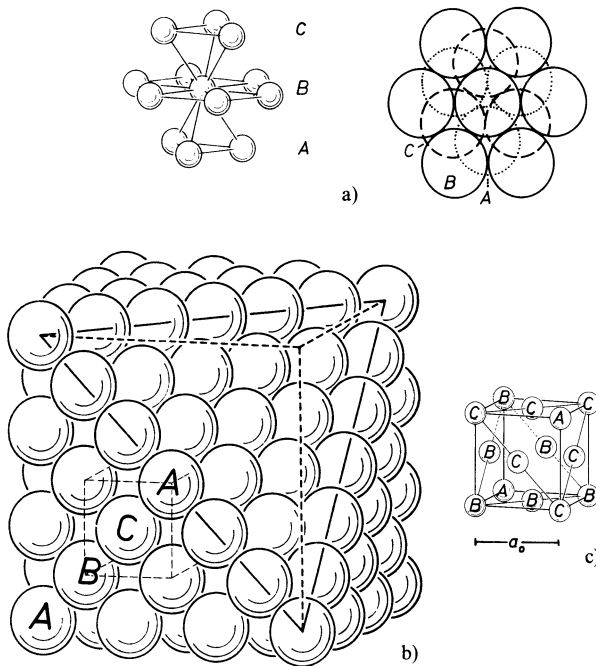


Fig. 11.2a-c. Cubic closest packing of spheres (Cu-type). **a** Coordination polyhedron [12] (cuboctahedron) as a perspective representation, using spheres reduced in size, and as a projection of the spheres on a close-packed layer. **b** The crystal structure. One of the layers parallel to (111) is shown together with the layer sequence ABCA. **c** A unit cell (cubic F-lattice). The spheres are reduced in size, and their correspondence to the stacked layers is indicated. The unit cell is also sketched in **b**

nation in cubic CsI (Fig. 3.4) and the octahedral coordination in NaCl (Fig. 11.17) are strictly regular, while the octahedral coordination in tetragonal rutile (Fig. 9.18) is distorted, cf. Exercise 11.10.

11.2 Metal Structures

A simple picture of metallic bonding is that the valence electrons of the metal atoms are delocalised in an “electron cloud” (Fig. 11.1 a). This negatively charged cloud encloses the positively charged atom cores (not ions) and shields them from one another. The bonding forces are not directional; they are equal in all directions.

In a metal, one can consider the atoms as spheres. Each atom attempts to associate itself with the maximum number of similar atoms. This can be achieved for 12 nearest neighbours in two different arrangements (coordination polyhedra), shown in Figs. 11.2a and 11.3a, and also Table 11.1 a and b. Starting from these coordination polyhedra as nuclei, crystal growth will result in the formation of two distinct crystal structures. These structures can be described as

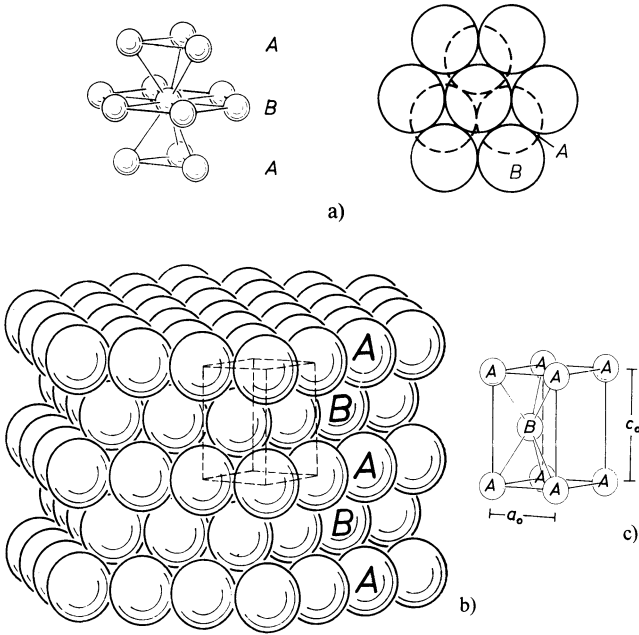
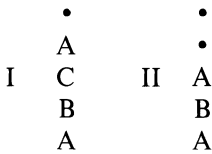


Fig. 11.3a–c. Hexagonal closest packing of spheres (Mg-type). **a** Coordination polyhedron [12] (disheptahedron) as a perspective representation, using spheres reduced in size, and as a projection of the spheres on a close-packed layer. **b** The crystal structure. One of the layers parallel to (0001) is shown together with the layer sequence ABA. **c** A unit cell. The spheres are reduced in size, and their correspondence to the stacked layers is indicated. The unit cell is also sketched in **b**

stackings of closest packed layers of spheres, and they differ in the layer sequence.



Structure I may be described by a cubic unit cell, with a cubic F-lattice, and is called the *Cu-type*, while structure II has a hexagonal unit cell, and is called the *Mg-type*. The two structures are thus called *cubic and hexagonal closest packing* respectively, abbreviated to *ccp* and *hcp*. Examples of each structure are given in Table 11.2. Some metals occur with both structure types, e.g. Ni.

The atoms of the Cu or ccp structure are all related by simple lattice translations, and are thus identical. In the Mg or hcp structure, atoms in the A-layers are all identical, as are atoms in the B-layers. The A- and B-atoms are, however, equivalent but not identical to one another. This is shown by the positions given in Table 11.2.

If the lattice constant is known, the radius of a sphere (the atomic radius) may be calculated. Figure 11.2b, c shows the diagonal of a (100) face of the cubic

Table 11.2. Data for the three most important metal structure types, Cu, Mg and W, and for α -Po

	Cu ccp	Mg hcp	W bcc	α -Po sc
Lattice + basis	Cubic F	Hexagonal P	Cubic I	Cubic P
	0, 0, 0	0, 0, 0; $\frac{2}{3}, \frac{1}{3}, \frac{1}{2}$	0, 0, 0	0, 0, 0
Space group + Positions occupied	F $4/m \bar{3} 2/m$	P $6_3/m 2/m 2/c$	I $4/m \bar{3} 2/m$	P $4/m \bar{3} 2/m$
	(a) 0, 0, 0	(c) 0, 0, 0; $\frac{2}{3}, \frac{1}{3}, \frac{1}{2}$	(a) 0, 0, 0	(a) 0, 0, 0
Coordination number	[12]		[8]	[6]
Atomic radii	$\frac{1}{4} a_0 \sqrt{2}$	$\frac{1}{2} a_0$	$\frac{1}{4} a_0 \sqrt{3}$	$\frac{1}{2} a_0$
Packing efficiency	0.74		0.68	0.52
Further examples	Ag, Au Ni, Al Pt, Ir Pb, Rh	Mg (1.62) Ni (1.63) Ti (1.59) Zr (1.59) Be (1.56) Zn (1.86)	Mo, V Ba, Na Zr, Fe	-

unit cell of the ccp-structure. Its length is equal to four sphere radii (B-2C-A). Thus $R = \frac{1}{4} a_0 \sqrt{2}$. In the hcp-structure, $R = \frac{1}{2} a_0$ (cf. Fig. 11.3b, c). Radii of metal atoms are given in Table 11.3.

It is possible to fill spaces completely by packing equal cubes, or, indeed, equal general parallelepipeds. This is not possible with spheres. In both types of closest sphere packings, there are interstices remaining of specific coordination; these are usually called "holes". These may be bounded by four spheres (*tetrahedral holes*) or by six (*octahedral holes*), (Fig. 11.4) and are examples of tetrahedral and octahedral coordination (Table 11.1).

The packing efficiency is defined as the ratio of the sum of the volumes of the spheres making up a unit cell to the volume of the unit cell. If the spheres are equal in size, it is given by

$$\frac{Z \cdot \frac{4}{3} \pi R^3}{V_{\text{unit cell}}}$$

As we have seen, in the ccp structure, $R = \frac{1}{4} a_0 \sqrt{2}$. Thus $a_0 = \frac{4R}{\sqrt{2}}$ and $V = a_0^3 = 16R^3 \sqrt{2}$. Since $Z = 4$, the packing efficiency is thus $\frac{\pi}{6} \sqrt{2} = 0.74$. The corresponding calculation for the hcp structure gives the same result.

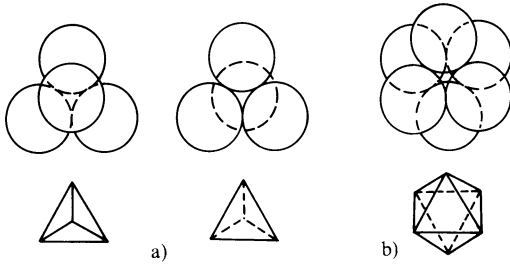


Fig. 11.4. a Tetrahedral [4] holes. b Octahedral [6] hole in closest packed arrays of spheres

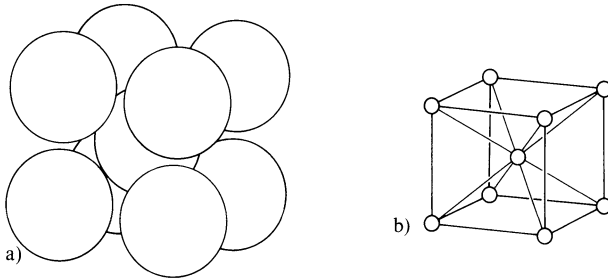


Fig. 11.5a, b. Crystal structure of tungsten. a With atomic radii shown to scale. b Showing only the centres of gravity of the atoms

For the hcp structure, the *ideal* $\frac{c_0}{a_0}$ ratio may be calculated, since c_0 is the height of two coordination tetrahedra of edge $2R = a_0$, sharing a common vertex (cf. Fig. 11.3c). This gives a value for $\frac{c_0}{a_0}$ of $\frac{2}{3} \cdot \sqrt{6} = 1.63$. In Table 11.2, the $\frac{c_0}{a_0}$ values for several metals are given; they tend to lie between 1.56 and 1.63. The value for Zn is considerably larger.

In addition to the two types of closest packing, a further structure adopted by some metals is the *W-type*, with a cubic I-lattice, usually simply called *body-centred cubic*, and abbreviated *bcc* (Fig. 11.5). In this structure, the body-diagonal of the unit cell consists of four sphere radii, i.e. $R = \frac{1}{4} a_0 \sqrt{3}$.

The packing efficiency of this structure is $\frac{\pi}{8} \sqrt{3} = 0.68$. The coordination number is [8], and the coordination polyhedron is a cube.

An arrangement of metal atoms in a cubic P-lattice occurs only for α -polonium (Fig. 2.1, Table 11.2). It has a packing efficiency of 0.52, a coordination number of [6] and an octahedron as its coordination polyhedron.

Considering the above data for the hcp and ccp structures, the Goldschmidt and Laves principles are very well fulfilled:

1. The packing efficiency is 0.74, the highest possible for the packing of equal spheres.
2. $F4/m \bar{3} 2/m$ is one of the highest symmetry space groups of the cubic system, and $P6_3/m 2/m 2/c$ is one of the highest symmetry space groups of the hexagonal system.
3. [12] is the highest possible coordination number for spheres of equal size.

The W-type or bcc structure has a packing efficiency of only 0.68 and its coordination number, [8], is smaller than that of the closest packed structures, but its symmetry, $I4/m \bar{3} 2/m$ is also high.

The α -Po structure also has a high symmetry ($P4/m \bar{3} 2/m$), but its packing efficiency and coordination of 0.52 and [6] respectively are very small. This is certainly the reason for α -Po being the sole example of this structure.

Metals attempt to achieve a high symmetry and a high packing efficiency. The great majority of metals crystallise in one of the first three given structure types.

Metals have many characteristic properties which are related to their structure and bonding:

a) *Electrical and Thermal Conductivity.* Metals are good conductors of both heat and electricity. These properties arise from the fact that the electron clouds between the atom cores can move freely.

b) *Plastic Deformation.* Plastic deformation in a metal is a shearing parallel to closest packed layers. This property is most prominent for metals with cubic closest packing in which four equivalent (111)-planes can undergo shear efficiently. These metals are generally soft, malleable and ductile. Gold, for example, can be beaten to a thin foil that weakly transmits green light. Crystals with hexagonal closest packing of the atoms are less malleable, since they have only one shear plane, parallel to (0001). Body-centred cubic metals are yet more brittle.

11.3 Structures of Noble Gases and Molecules

In *noble gas* and *molecular structures*, the atoms or molecules are held together by *van der Waals forces*. These forces are very weak. This is apparent from the very low melting points of such crystals, e.g. neon: -247.7°C , ethylene: -170°C , benzene: 5.5°C and phenyl salicylate 43°C .

Noble gas atoms can also pack together as spheres, having a noble gas electron configuration. The bonding forces, like those in metals are non-directional, and the same sphere packings occur:

- a) *cubic closest packing* (cf. Fig. 11.2): Ne, Ar, Kr, Xe, Rn.
- b) *hexagonal closest packing* (cf. Fig. 11.3): He.

Molecular structures are characterised by the fact that the energy holding the atoms in the molecules together (covalent bonding) is large, while that holding one molecule to another is very weak. Most molecular compounds are organic, inorganic examples include sulphur (cf. the S_8 molecule in Table 8.11.36) and C_{60} , see below.

Three molecular structures were introduced in Figs.10.1–10.3 (hexamethylenetetramine, ethylene and benzene). As was made clear in Chapter 10, there is no simple relationship between crystal symmetry and molecular symmetry. Although molecules are not spherical in shape, they do attempt to

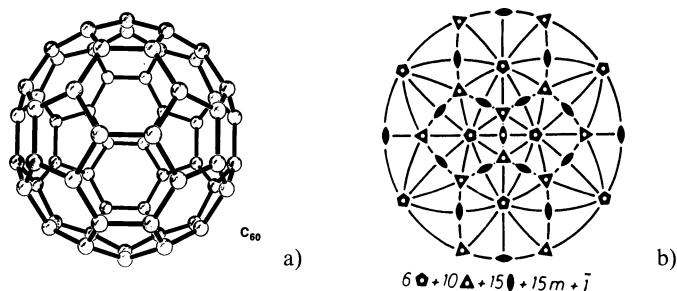


Fig. 11.6 a, b. The C_{60} -molecule forms an almost spherical cage with 20 six-membered rings and 12 five-membered rings (a) ([41]). The non-crystallographic point group $2/m\bar{3}5 (I_h)$ of the molecule (b) ([14])

pack as closely as possible in crystals. The hexamethylenetetramine structure (Fig. 10.1), for example, has a packing efficiency of 0.72. In the crystal structure of CO_2 , the C-atoms occupy the positions of a cubic closest packing, the linear molecules being parallel to $\langle 111 \rangle$.

Since the forces holding the molecules together are weak, it follows that the lattice energies of organic compounds are, in general, low. Nonetheless, the great majority of organic compounds can be crystallised. Even “giant” molecules with very large unit cell dimensions have been crystallised, for example:

1. vitamin B_{12} : $C_{63}H_{88}N_{14}O_{14}PCo$, $P2_12_12_1$, $a_0 = 25.33 \text{ \AA}$, $b_0 = 22.32 \text{ \AA}$, $c_0 = 15.92 \text{ \AA}$, $Z = 4$ (cf. Fig. 1.1 b)
2. pepsin: $M \approx 40000$, $P6_122$, $a_0 = 67 \text{ \AA}$, $c_0 = 154 \text{ \AA}$, $Z = 12$.

A recent discovery is a new series of molecules containing only carbon, the main one of which has the molecular formula C_{60} . In this molecule, the atoms form an almost spherical cage, made up of 20 six-membered rings and 12 five-membered rings. The structure is that of a soccer ball (Fig. 11.6a). The molecule has the non-crystallographic symmetry $2/m\bar{3}5 (I_h)$ (Fig. 11.6b), and for this reason, all atoms are equivalent.

C_{60} molecules have been crystallised with a ccp structure ($a_0 = 14.17 \text{ \AA}$).

11.4 Ionic Structures

Ionic crystals are built from positively and negatively charged ions, and the bonding energy is *Coulombic forces*, which are non-directional and equal in all directions. The strength of a bond is related to the charge on the ions, e , and the distance, d , between them:

$$\text{Coulomb's Law: } K = \frac{e_1 \cdot e_2}{d^2}$$

Each cation seeks to maximise the number of neighbouring anions, while each anion equally seeks to maximise its neighbourhood of cations (Fig. 11.1c). The formation of ionic structures is thus another packing problem, but now the spheres are ions of opposite charge which generally are also different in size. The relative sizes of the radius of the cation, R_A , and that of the anion, R_X , the *radius ratio* R_A/R_X , can suggest the appropriate coordination polyhedron and thus the crystal structure (Sect. 11.4.2–11.4.4).

11.4.1 Ionic Radii

Table 11.3 gives ionic radii as a function of atomic number.

The size of an ion, considering an ion as a sphere, depends on the charge on the nucleus and on the number of electrons.

a) Within a column of the periodic table, the ionic radius generally rises with the increasing nuclear charge.

$\text{Li}^+ = 0.70 \text{ \AA}$	$\text{F}^- = 1.33 \text{ \AA}$
$\text{Na}^+ = 0.98 \text{ \AA}$	$\text{Cl}^- = 1.81 \text{ \AA}$
$\text{K}^+ = 1.33 \text{ \AA}$	$\text{Br}^- = 1.96 \text{ \AA}$
$\text{Rb}^+ = 1.52 \text{ \AA}$	$\text{I}^- = 2.20 \text{ \AA}$
$\text{Cs}^+ = 1.70 \text{ \AA}$	

b) For isoelectronic ions, an increase in the nuclear charge results in a lowering of the ionic radius.

Na^+	Mg^{2+}	Al^{3+}	Si^{4+}	P^{5+}	S^{6+}	Cl^{7+}
0.98 Å	0.65 Å	0.57 Å	0.39 Å	0.34 Å	0.29 Å	0.26 Å

c) For a particular element, the ionic radius falls as the positive charge rises: Cf. S(16) or Mn(25) in Table 11.3.

11.4.2 Octahedral Coordination [6]

The octahedron as a coordination polyhedron is illustrated in Table 11.1e. The limiting value for the radius ratio R_A/R_X for this coordination may be determined by considering an octahedron composed of spherical anions which touch one another, and placing a cation precisely in the hole in its centre. Figure 11.7 shows a section through such an octahedron. It can be seen that $R_A + R_X = R_X \sqrt{2}$, or $R_A/R_X = \sqrt{2} - 1 = 0.41$. Octahedral coordination is only stable if R_A/R_X is greater than or equal to 0.41 (Fig. 11.8a, b). A section through an unstable octahedron is shown in Fig. 11.8c.

Octahedral coordination occurs in the $\text{Na}^{[6]}\text{Cl}$ (Figs. 11.9 and 11.17) and rutile $\text{Ti}^{[6]}\text{O}_2$ (Fig. 9.18) structure types. The NaCl structure type can be considered as a cubic closest packing of anions with cations in the octahedral holes. For LiCl ($R_A/R_X = 0.43$), the ideal radius ratio for octahedral coordi-

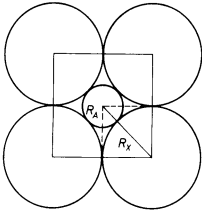
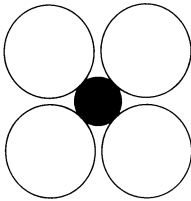
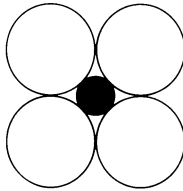


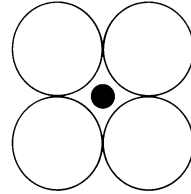
Fig. 11.7. Cross-section through a coordination octahedron ([6])



a) 0.54



b) 0.41



c) 0.25

Fig. 11.8a-c. Section through a coordination octahedron, with the corresponding radius ratio, R_A/R_X . The arrangements in (a) and (b) are stable; that in (b) shows the limiting case with $R_A/R_X=0.41$, and that in (c) is unstable

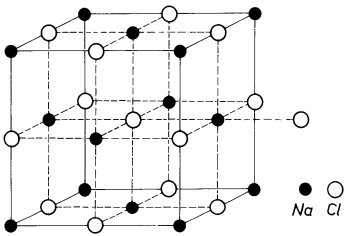


Fig. 11.9. $\text{Na}^{[6]}\text{Cl}$ structure, $Fm\bar{3}m$
Lattice: cubic F
Basis: Na^+ at $0,0,0$; Cl^- at $\frac{1}{2},0,0$

nation is almost achieved. By contrast, NaCl itself has a radius ratio of 0.54 (Fig. 11.8a).

The spinel structure $\text{Mg}^{[4]}\text{Al}_2^{[6]}\text{O}_4$ is based on a cubic closest packed array of oxide ions. The Mg^{2+} ions occupy tetrahedral holes and the Al^{3+} ions octahedral holes. Let us consider how many of the octahedral and tetrahedral holes are occupied.

Considering the NaCl structure as a cubic closest packing of Cl^- ions (Fig. 11.9), it will be noted that all octahedral holes are occupied by Na^+ ions. In NaCl, the ratio $\text{Cl}^- : \text{Na}^+$ is 1:1, thus each sphere in a ccp array (Cl^-) corresponds to an octahedral hole (Na^+). Figure 11.11 shows the “antifluorite” structure. The sulphide ions are in a ccp array (Fig. 11.11a), and the Li^+ ions occupy all tetrahedral holes. In Li_2S , the ratio $\text{Li}^+ : \text{S}^{2-} = 2:1$, so each sphere in a ccp array (S^{2-}) corresponds to two tetrahedral holes (Li^+). The relation 2[4], 1[6] per sphere applies equally to both closest packings.

Table 11.3. Atomic and ionic radii as a function of atomic number. (After Ramdohr and Strunz [37])

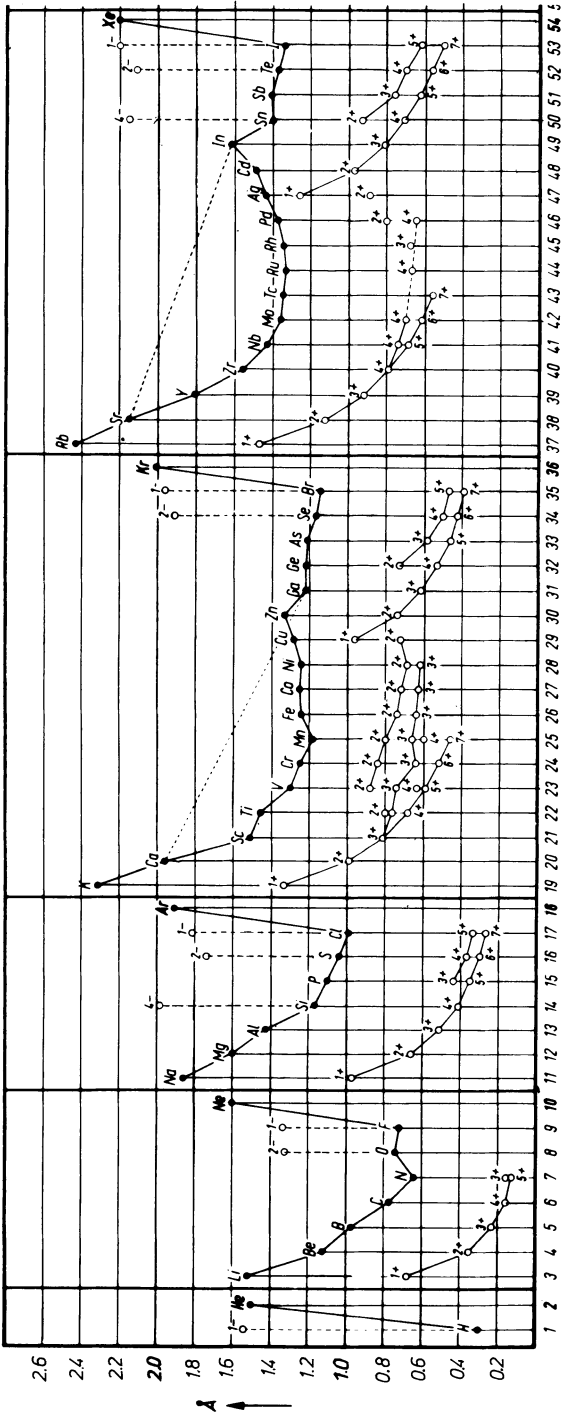
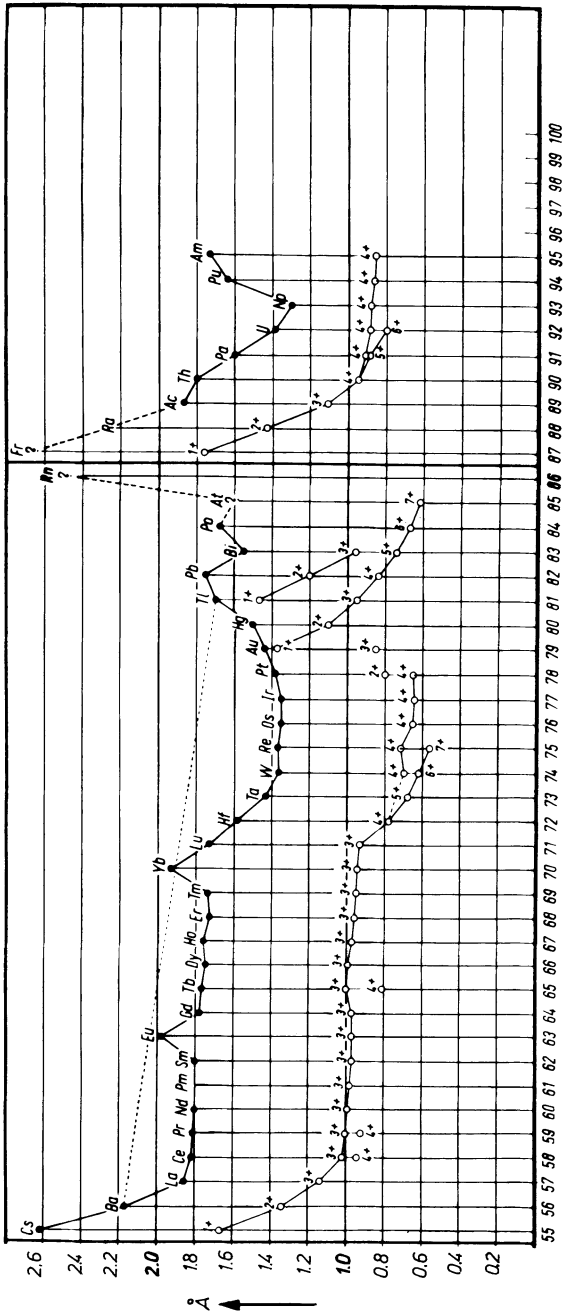


Table 11.3 (continued)



Returning now to the spinel structure, $\text{Mg}^{[4]}\text{Al}_2^{[6]}\text{O}_4$, we can see that $\frac{1}{8}$ of the tetrahedral holes are occupied by Mg^{2+} and $\frac{1}{2}$ of the octahedral holes by Al^{3+} .

In the $\text{Ni}^{[6]}\text{As}$ (niccolite) structure ($\text{P6}_3/\text{mmc}$), the As atoms are arranged as a hexagonal closest packing and the Ni atoms occupy all of the octahedral holes ($\text{Ni}:\text{As}=1:1$, Fig. 11.18). The O^{2-} -ions of the corundum, $\text{Al}_2^{[6]}\text{O}_3$, similarly form a hexagonal closest packing. The Al^{3+} ions are in octahedral holes. From the above relationship, $\frac{2}{3}$ of the octahedral holes are occupied. In corundum, every third octahedral hole is vacant, but in the ideal structure, all holes are equivalent. This results in a lowering of the space group symmetry to $\text{R}\bar{3}\text{c}$. Thus, corundum is trigonal, while in NiAs, the symmetry of the hexagonal closest packing ($\text{P6}_3/\text{mmc}$) is retained.

The O^{2-} -ions in forsterite, $\text{Mg}_2^{[6]}\text{Si}^{[4]}\text{O}_4$, also are arranged as a hexagonal closest packing. The Si^{4+} ions occupy $\frac{1}{8}$ of the tetrahedral holes, and the Mg^{2+} ions half of the octahedral holes. The symmetry is lowered to Pnma .

The atoms or ions in tetrahedral or octahedral holes are not statistically disordered. In most cases, they are ordered in the structure.

11.4.3 Cubic Coordination [8]

As the radius ratio increases, there should be a range in which the trigonal prism, with limiting $R_A/R_X=0.53$, is stable (cf. Table 11.1 d). In fact, for ionic structures, the stable structure becomes *cubic [8]-coordination*, cf. Table 11.1c. Making use of Fig. 11.10, which shows a section through a cube parallel to (110) (cf. Fig. 3.4), the limiting value for R_A/R_X for cubic coordination can be calculated: $R_A + R_X = R_X \cdot \sqrt{3}$, so $R_A/R_X = \sqrt{3} - 1 = 0.73$.

This implies that octahedral coordination is stable for the range $0.41 < R_A/R_X < 0.73$, while cubic coordination is preferred for $R_A/R_X > 0.73$.

Cubic coordination is found in structures of the $\text{Cs}^{[8]}\text{Cl}$ -type, and for the fluorite or $\text{Ca}^{[8]}\text{F}_2$ -type (Fig. 11.11). $\text{Cs}^{[8]}\text{I}$ (Fig. 3.4) has the $\text{Cs}^{[8]}\text{Cl}$ structure with an almost ideal radius ratio of 0.75.

In Fig. 11.11 b the CaF_2 structure has been drawn with an F^- -ion at 0,0,0. This makes the cubic coordination of the Ca^{2+} more evident. Ca^{2+} ions occupy every second cubic hole. The Cl^- ions have the same arrangement in the CsCl structure; in that case, every cubic hole is occupied by Cs^+ . The fluorite structure is found for SrF_2 , BaF_2 , SrCl_2 , UO_2 etc., and also for a number of alkali metal sulphides, e.g. Li_2S , Na_2S , K_2S etc. As is indicated by the chemical formulae, in

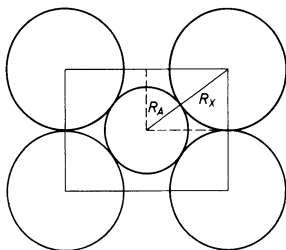


Fig. 11.10. Section parallel to (110) through a coordination cube [8] (cf. Fig. 3.4a)

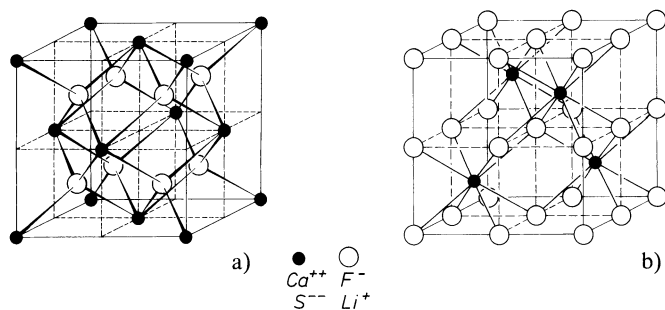


Fig. 11.11 a, b. The fluorite or $\text{Ca}^{[8]}\text{F}_2$ structure, and the “antifluorite” structure (e.g. Li_2S), space group $\text{Fm}\bar{3}\text{m}$

Lattice: cubic F

Basis: Ca^{2+} or S^{2-} at $0, 0, 0$;

F^- or Li^+ at $\frac{1}{4}, \frac{1}{4}, \frac{1}{4}$; $\frac{3}{4}, \frac{3}{4}, \frac{3}{4}$ (**a**)

Structure drawn with F^- at $0, 0, 0$ in order to emphasise the cubic coordination (**b**)

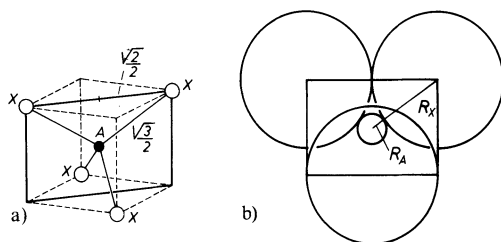


Fig. 11.12 a, b. Coordination tetrahedron $\text{A}^{[4]}\text{X}_4$, inscribed in a cube (**a**); (110)-section through a coordination tetrahedron derived from sphere packing (**b**)

these sulphides, the positions of the cations and the anions must be reversed, i.e. S^{2-} ions occupy the Ca^{2+} positions and the alkali metal cations occupy the F^- positions. This structure is called the “antifluorite” structure. In it, the S^{2-} ions form a ccp array, and the cations occupy all of the tetrahedral holes.

In Table 11.4, a number of AX and AX_2 compounds are listed, arranged according to structure type. The radius ratio values are also given. The agreement between theory and experiment is reasonable, considering that the use of radius ratios makes the assumption that ions are hard spheres.

11.4.4 Tetrahedral Coordination [4]

Table 11.1g shows the tetrahedron as a coordination polyhedron. A suitable radius ratio can also be calculated for *tetrahedral [4]-coordination*. In Fig. 11.12a, a coordination tetrahedron is shown inscribed in a cube. Figure 11.12b shows a section through the cube and tetrahedron parallel to (110), with the radii of ions drawn to scale. Since $R_A + R_X$ is half the body diagonal of the cube ($\frac{1}{2}\sqrt{3}$) and R_X is half of the face diagonal ($\frac{1}{2}\sqrt{2}$), $(R_A + R_X)/R_X = \sqrt{3}/\sqrt{2}$, and $R_A/R_X = \sqrt{\frac{3}{2}} - 1 = 0.225$.

Table 11.4. Structures and radius ratios for some AX and AX₂ compounds

R _A /R _X	AX		AX ₂	
	Cs ^[8] Cl-type	Na ^[6] Cl-type	Fluorite-type Ca ^[8] F ₂	Rutile-type Ti ^[6] O ₂
	> 0.73	0.73-0.41	> 0.73	0.73-0.41
	CsCl 0.91 CsBr 0.84 CsI 0.75	KF 1.00 SrO 0.96 BaO 1/0.94 RbF 0.89 RbCl 0.82 BaS 0.82 CaO 0.80 CsF 1/0.80 RbBr 0.76 BaSe 0.75 NaF 0.74	KCl 0.73 SrS 0.73 RbI 0.68 KBr 0.68 SrSe 0.66 CaS 0.61 KI 0.60 ScTe 0.60 MgO 0.59 LiF 0.59 CaSe 0.56 NaCl 0.54 NaBr 0.50 CaTe 0.50 MgS 0.49 NaI 0.44 LiCl 0.43	MgSe 0.41 LiBr 0.40 LiI 0.35
			BaF ₂ 1.05 PbF ₂ 0.99 SrF ₂ 0.95 HgF ₂ 0.84 ThO ₂ 0.83 CaF ₂ 0.80 UO ₂ 0.79 CeO ₂ 0.77 PrO ₂ 0.76 CdF ₂ 0.74	ZrO ₂ 0.67 HfO ₂ 0.67
				MnF ₂ 0.66 PbO ₂ 0.64 FeF ₂ 0.62 CoF ₂ 0.62 ZnF ₂ 0.62 NiF ₂ 0.59 MgF ₂ 0.58 SnO ₂ 0.56 NbO ₂ 0.52 MoO ₂ 0.52 WO ₂ 0.52 OsO ₂ 0.51 IrO ₂ 0.50 RuO ₂ 0.49 TiO ₂ 0.48 VO ₂ 0.46

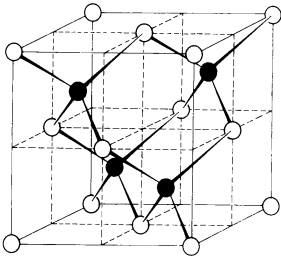


Fig. 11.13. $\text{Zn}^{[4]}\text{S}$ -structure (sphalerite or zinc blende). Space group $F\bar{4}3m$
Lattice: cubic F
Basis: S at $0, 0, 0$; Zn at $\frac{1}{4}, \frac{1}{4}, \frac{1}{4}$

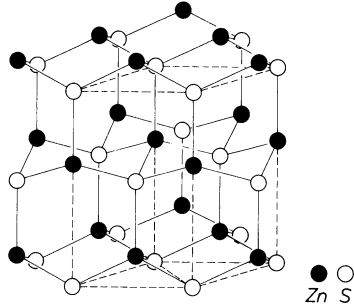


Fig. 11.14. $\text{Zn}^{[4]}\text{S}$ -structure (wurtzite). Space group $P6_3mc$
Lattice: hexagonal P
Basis: S at $0, 0, 0$; $\frac{2}{3}, \frac{1}{3}, \frac{1}{2}$;
Zn at $0, 0, \frac{1}{2} + z$; $\frac{2}{3}, \frac{1}{3}, z$ ($z \approx \frac{1}{8}$)

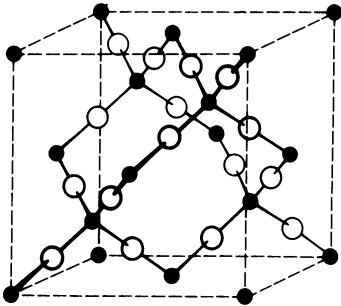


Fig. 11.15. Structure of high cristobalite, $\text{Si}^{[4]}\text{O}_2$, $Fd\bar{3}m$

This implies that tetrahedral coordination will have a range of stability for $0.225 < R_A/R_X < 0.41$. Important examples of this coordination are the sphalerite or zinc blende ($\text{Zn}^{[4]}\text{S}$) structure (Fig. 11.13), the wurtzite ($\text{Zn}^{[4]}\text{S}$) structure (Fig. 11.14) and all modifications of SiO_2 except stishovite. Figures 11.15 and 11.24 show the structures of different modifications of $\text{Si}^{[4]}\text{O}_2$. The SiO_4 tetrahedra build a framework structure through the sharing of vertices. The radius ratio for SiO_2 is 0.29.

The bonding in both $\text{Zn}^{[4]}\text{S}$ structures is, in fact, largely covalent in nature. If, however, the geometry alone is considered, the S-atoms in the sphalerite structure occupy the positions of a cubic closest packing, and in the wurtzite structure those of a hexagonal closest packing. In both structures, the Zn-atoms occupy half of the tetrahedral holes.

How, then, do the basic principles for the formation of ionic structures work out in practice?

1. In general, ionic structures have space groups of high symmetry, e.g. CsCl: $P4/m\bar{3}2/m$; NaCl and CaF_2 : $F4/m\bar{3}2/m$. Structures based on the closest packing of anions retain the space groups of those arrangements when

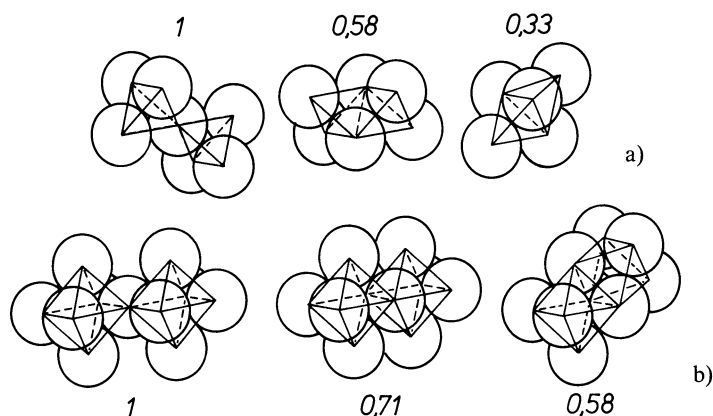


Fig. 11.16 a, b. Linking of pairs of tetrahedra (a) and octahedra (b) through a vertex, an edge and a face. The *numbers* give the relative distances apart of the two coordinated cations, after [35]

the interstices of a particular type are completely filled, e.g. $\text{Na}^{[6]}\text{Cl}$: $F4/m\bar{3}2/m$ (Fig. 11.9). When the interstices are only partly filled, the symmetry may be lowered, e.g. $\text{Al}_2^{[6]}\text{O}_3$: $R\bar{3}c$.

2. The packing efficiency of ionic structures is usually high: for the ideal CsCl type, with $R_A/R_X = 0.73$, it is 0.73; for the NaCl type with $R_A/R_X = 0.41$, it is 0.79. As the radius ratio increases for a particular structure type, the packing efficiency decreases. For the structure of the NaCl type, for example, with $R_A/R_X = 0.54$ (cf. Fig. 11.8a) it is 0.66.
3. In ionic structures, the commonly occurring coordination numbers, [8], [6], and [4], are dependent on radius ratio and are relatively small. A better correlation is obtained if only the coordinations of the anions are considered, e.g. NaCl and Al_2O_3 : Coordination number [12].

Finally, the linking of coordination polyhedra in ionic compounds should be considered. Linking by shared vertices is favourable. The sharing of edges, and in particular the sharing of faces lowers the stability of a crystal structure. This effect is greatest when a cation has a high charge or a low coordination number: *Pauling's third rule*. In Fig 11.16, the linking of pairs of tetrahedra and octahedra through a vertex, an edge and a face is shown. Taking the distance between cations in the vertex-sharing polyhedra to be 1, the values in Fig. 11.16 show the decrease in cation-cation distance in the edge- and face-sharing cases. Note that it is more severe for the linked tetrahedra (0.55, 0.38) than for the linked octahedra (0.71, 0.58). The closer the cations come to one another, the greater is the Coulombic repulsion, and the lower the stability of the structure. The effect is greater when the cations have higher charge.

The SiO_4^{4-} tetrahedra of numerous silicate structures, and of SiO_2 structures, share vertices (cf. the $\text{Si}^{[4]}\text{O}_2$ structures in Figs. 11.15 and 11.24). There are a few exceptions; stishovite, $\text{Si}^{[6]}\text{O}_2$, for example, has the rutile structure. In the fluorite structure (Fig. 11.11 b), the coordination cubes share edges.

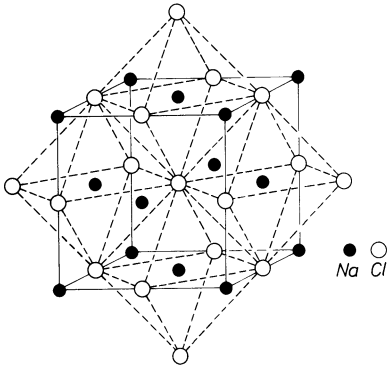
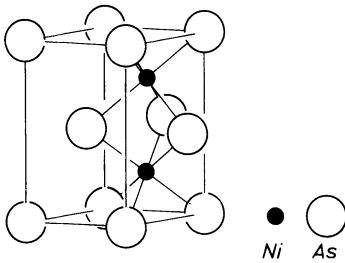
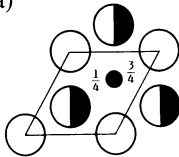


Fig. 11.17. The NaCl structure, showing the edge-sharing coordination octahedra. Every edge is shared by two octahedra



a)



b)

Fig. 11.18 a, b. Ni^[6]As structure, P6₃/mmc

Lattice: hexagonal P

Basis: As 0,0,0; $\frac{2}{3}, \frac{1}{3}, \frac{1}{2}$

Ni $\frac{1}{3}, \frac{2}{3}, \frac{1}{4}$; $\frac{1}{3}, \frac{2}{3}, \frac{3}{4}$

a Perspective drawing. **b** As projection on (0001).

The As-octahedra are face-sharing

In the NaCl and NiAs structures, the cations have octahedral coordination. This coordination is indicated on the structures in Figs. 11.17 and 11.18. In NaCl, the octahedra share edges, in NiAs, they share faces.

Comparison in this respect of the Na^[6]Cl and Cs^[8]Cl structures favours the NaCl structure, since the Cs⁺ ions have a cubic coordination in which all cube faces are shared.

The coordination octahedron of the rutile structure (Fig. 9.18) shares two edges. This becomes clear when the unit cells above and below that shown are considered. Two other forms of TiO₂, brookite and anatase, have coordination octahedra which share three and four edges respectively. The rutile structure is thus the most stable form of TiO₂, and, unlike brookite and anatase, its structure is adopted by many compounds.

11.5 Covalent Structures

Covalent or homopolar bonding, will be illustrated by the diamond structure, which consists entirely of carbon atoms. The outer shell of a carbon atom in free space is occupied by $2s^2 2p^2$ -electrons. We may consider one electron promoted to give $2s^1 2p^3$ and the resulting set mixed to form a set of four sp^3 orbitals, pointing to the corners of a tetrahedron (Fig. 11.1 d). Each C-atom can form bonds with a maximum of four other C-atoms. This results in the formation of a crystal structure, based on tetrahedra (Fig. 11.19), which has the same overall ordering of atoms as the sphalerite type in Fig. 11.13. Each C-atom is surrounded by a tetrahedron of four other C-atoms.

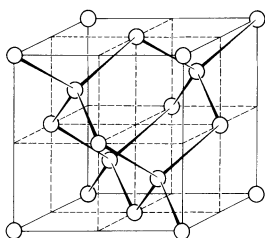


Fig. 11.19. Diamond structure, $Fd\bar{3}m$
 Lattice: cubic F
 Basis: C at $0, 0, 0$ and $\frac{1}{4}, \frac{1}{4}, \frac{1}{4}$

In this case, the picture of bonding as sphere-packing is inapplicable as the main forces are due to the directional bonding of overlapping atomic orbitals. The packing efficiency of the C-atoms in diamond is not high. The bonding in diamond is exceptionally strong, resulting in its great hardness.

11.6 Isotypes, Solid Solutions and Isomorphism

Crystals which have the same crystal structure are said to belong to a structure type or to be *isotypes*. Isotypes are generally characterised by having the same space group, analogous chemical formulae, and the same coordination polyhedra occupying the same sites. Neither the absolute size of the atoms nor the type of chemical bonding is important; ionic NaCl and metallic PbS crystals are isotypes, as are metallic Cu and van der Waals Ar crystals.

The relationship between isotypic structures becomes closer if atoms in one structure can replace those in the other. The following experiment will illustrate this. Two single crystals of the isotypic structures Au and Ag are pressed together as the temperature is raised, but kept below the melting point of either crystal. By diffusion, silver atoms pass into the gold crystal and occupy the places vacanted by gold atoms, while gold atoms similarly diffuse into the silver crystal. This diffusion can proceed to such an extent that eventually, in some parts of the mass, an atomic ratio Au:Ag of 1:1 is reached. The single crystal nature of the starting materials is apparently lost. In some

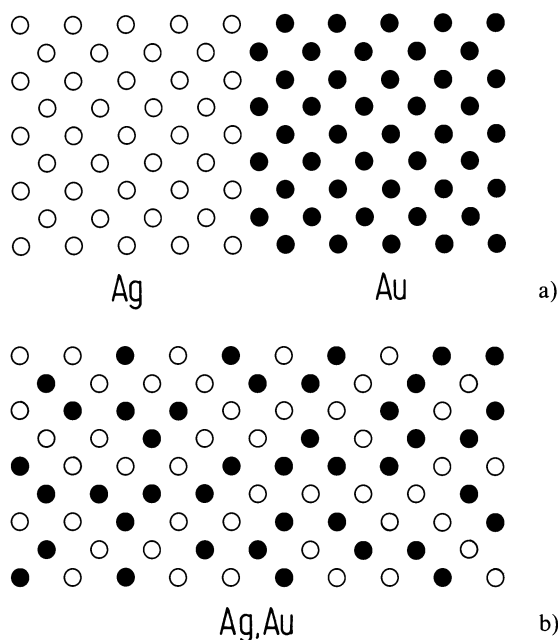


Fig. 11.20. **a** Single crystals of Ag and Au pressed against one another. **b** The resultant solid solution Ag,Au resulting from diffusion of one metal into the other. Only a single layer at $x, y, 0$ is shown

regions, arrangements of atoms like that in Fig. 11.20 will occur. Figure 11.20a shows the initial situation, with separate crystals of Ag and Au, while Fig 11.20b gives the situation after the diffusion process. The diffusion process has distributed the Au and Ag atoms statistically over the sites of the crystal structure.

Crystals in which one or more positions are occupied by a statistical distribution of two or more different atom types are called mixed crystals or solid solutions.

The reciprocal exchange of atoms in crystals is referred to as *diadochy* or replacement. Solid solutions in which one atom directly replaces another are called *substitutional solid solutions*.

The chemical formula is also an indication that a crystal structure is actually a solid solution. Interchangeable atoms are written together in a chemical formula, separated by a comma. The solid solution described above would be written as Ag,Au. $K(Cl, Br)$ describes a solid solution in which Cl^- and Br^- replace one another. In olivine, $(Mg, Fe)_2SiO_4$, the oxide ions form an hep array. The Mg^{2+} and Fe^{2+} ions are statistically distributed over specific octahedral holes.

Solid solutions form most commonly when the replaceable atoms or groups of atoms are most similar in chemical properties and size. A rule of

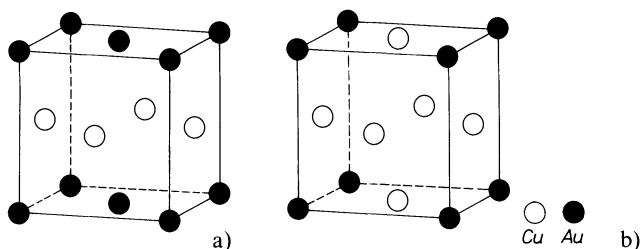


Fig. 11.21. **a** The CuAu structure. **b** The Cu_3Au structure as superstructures of the Cu, Au solid solution

thumb for solid solution formation is that the radii of the interchangeable atoms should differ by no more than 15%. Silver and gold are miscible in all proportions ($R_{\text{Ag}} = 1.44 \text{ \AA}$, $R_{\text{Au}} = 1.44 \text{ \AA}$, difference $\Delta \sim 0.0\%$). Ag, Au solid solutions are generally formed by slow cooling of a mixture of melts of the two components.

Copper and gold are only miscible in all proportions at high temperatures ($R_{\text{Cu}} = 1.28 \text{ \AA}$, $\Delta = 11\%$). During slow cooling the (Cu, Au) solid solution is converted to ordered structures, called *superstructures*. The superstructures with composition Cu_3Au and CuAu are given in Fig. 11.21. Note that CuAu is tetragonal, and no longer cubic.

Gold and nickel ($\Delta = 14\%$) are also miscible at high temperature. At lower temperature, the solution separates into Ni-rich and Au-rich solid solutions. The separation can be essentially complete, so that only pure Ni and Au domains remain.

Plagioclases are solid solutions whose limiting compositions are $\text{NaAlSi}_3\text{O}_8$ and $\text{CaAl}_2\text{Si}_2\text{O}_8$. Here, the formation of a solid solution occurs through the simultaneous substitution of Ca for Na and Al for Si, or vice versa. In order to keep the charges balanced $\text{Na}^+ + \text{Si}^{4+} = \text{Ca}^{2+} + \text{Al}^{3+}$.

When crystals of the same structure type (isotypic crystals) form solid solutions with one another, the structures are said to be *isomorphous*. As the following examples will show, however, solid solution formation is no criterion for isotypes.

$\text{Zn}^{[4]}\text{S}$ (sphalerite-type, Fig. 11.13) and FeS ($\text{Ni}^{[6]}\text{As}$ -type, Fig. 11.18) are clearly not isotypic. In sphalerite, however, a (Zn, Fe) substitution up to about 20% is possible. Fe^{2+} and Zn^{2+} are bivalent ions with almost equal radii of 0.74 \AA . A substitution (Fe, Zn) in FeS does not occur. The occurrence of substitution is thus not only dependent on the size of the atoms but also on the properties of the crystal structures.

$\text{Ag}^{[6]}\text{Br}$ (NaCl-type) and $\text{Ag}^{[4]}\text{I}$ (sphalerite-type) show limited solid solution formation. In AgBr, a (Br/I) substitution of up to 70% I⁻ is possible, while in AgI, substitution of Br⁻ occurs only very slightly.

$\text{Li}^{[6]}\text{Cl}$ (NaCl-type) and MgCl_2 (CdCl_2 -type, a layer structure) have not only different crystal structures, but also different chemical formulae. In both cases, the Cl⁻ ions form ccp arrays, and Li⁺ and Mg²⁺ occupy octahedral holes in these arrays. All octahedral holes are occupied in LiCl, while in MgCl_2 , only

every second hole is occupied. When solid solutions are formed, a Mg^{2+} ion occupies one Li^+ site in LiCl , and causes another Li^+ site to be vacant. Similarly, when a Li^+ ion occupies a Mg^{2+} site, another Li^+ ion will occupy one of the empty octahedral holes in MgCl_2 .

11.7 Polymorphism

Under different conditions, many solid substances can produce different crystal structures of the same chemical constitution. This phenomenon is known as *polymorphism*.

Nickel crystallises in both the $\text{Cu}^{[12]}$ -type (ccp) and the $\text{Mg}^{[12]}$ -type (hcp), zirconium in both the $\text{Mg}^{[12]}$ -type (hcp) and the $\text{W}^{[8]}$ -type (bcc), and $\text{Zn}^{[4]}\text{S}$ in both the sphalerite and wurtzite types. CaCO_3 can give crystals of both the calcite-type ($\text{Ca}^{[6]}\text{CO}_3$) and the aragonite-type ($\text{Ca}^{[9]}\text{CO}_3$). These CaCO_3 structures naturally produce different morphologies (cf. Table 8.11.8 and 20).

The interconversion of polymorphs, also called structure transformations, can proceed in a variety of ways. Buerger [5] distinguished the following types of transformation:

1. Transformations of First Coordination

The transformation alters the coordination numbers, and thus the arrangement of nearest neighbours. The new structure thus has new coordination numbers.

a) *Dilatational Transformations.* $\text{Cs}^{[8]}\text{Cl}$ is converted, above 445°C to the $\text{Na}^{[6]}\text{Cl}$ type. The CsCl structure (Fig. 11.22a) is converted to the NaCl structure by a dilatation along a body diagonal of the cube (Fig. 11.22b). From the cubic arrangement of the Cl^- ions (a cube is a special rhombohedron with a 90° angle) arises a rhombohedral arrangement with a 60° angle. A rhombo-

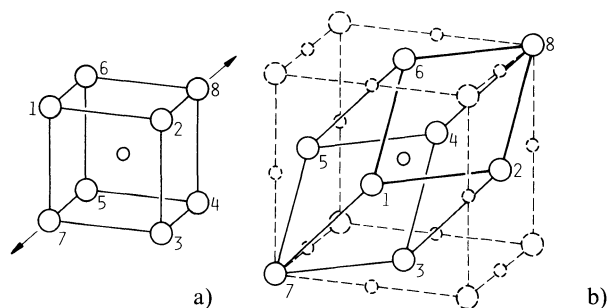


Fig. 11.22a, b. Dilatational transformation in the first coordination. The $\text{Cs}^{[8]}\text{Cl}$ structure (a) is converted by means of a dilatation along the body diagonal of the cube into the $\text{Na}^{[6]}\text{Cl}$ structure (b). (After [5])

Table 11.5. The occurrence of the calcite and aragonite structures as a function of cation radius.

Structure type	Formula	Cation radius (Å)	Coordination number
Calcite	MgCO ₃	0.66	[6]
	FeCO ₃	0.74	
	ZnCO ₃	0.74	
	MnCO ₃	0.80	
	CdCO ₃	0.97	
	CaCO ₃	0.99	
Aragonite	CaCO ₃	0.99	[9]
	SrCO ₃	1.12	
	PbCO ₃	1.20	
	BaCO ₃	1.34	

hedral P-cell with $\alpha = 60^\circ$ is a cubic F-lattice (cf. Chap. 6.4). The movement of the Cl^- ions causes the Cs^+ ions to lose two neighbours, and the cubic coordination is transformed to octahedral. Dilatational transformations are rapid.

b) *Reconstructive Transformations.* $\text{Ca}^{[9]}\text{CO}_3$ (aragonite) is converted about 400°C to $\text{Ca}^{[6]}\text{CO}_3$ (calcite). The coordination number falls from [9] to [6]. The bonds between Ca^{2+} and CO_3^{2-} are broken and reformed. Another example of this type of transformation is the conversion of Zr from the $\text{Mg}^{[12]}$ -type (hcp) to the $\text{W}^{[8]}$ -type (bcc). Reconstructive transformations are very slow.

In Table 11.5, examples are given of compounds crystallising in the calcite and aragonite structure types, with the radii of the cations. $R_{\text{Ca}^{2+}} = 0.99 \text{ \AA}$ is the limiting radius for the two types. Smaller cations fit well into the [6]-holes of the calcite structure, while larger ones fit better into the [9]-holes of the aragonite structure. Ca^{2+} ions can form both structures. Raising the temperature favours the conversion of $\text{Ca}^{[9]}\text{CO}_3$ (aragonite) to $\text{Ca}^{[6]}\text{CO}_3$ (calcite), while raising the pressure converts calcite to aragonite. These observations may be summarised by the rules: *higher temperatures favour lower coordination numbers; higher pressures favour higher coordination numbers.*

2. Transformations in Secondary Coordination

In these cases, the arrangement of nearest neighbours, i.e. the coordination, is unchanged. The arrangement of next-nearest neighbours is changed. Figure 11.23 shows such a change diagrammatically. The three structures are all made up of planar AB_4 "polyhedra" which are interconnected in different ways.

a) *Displacive Transformations.* These involve a direct conversion of (a) into (b) (Fig. 11.23). The polyhedra undergo rotation only, and no bonds are broken. An angle A-B-A which is less than 180° in (a) becomes equal to 180° in (b). The density falls and the symmetry rises.

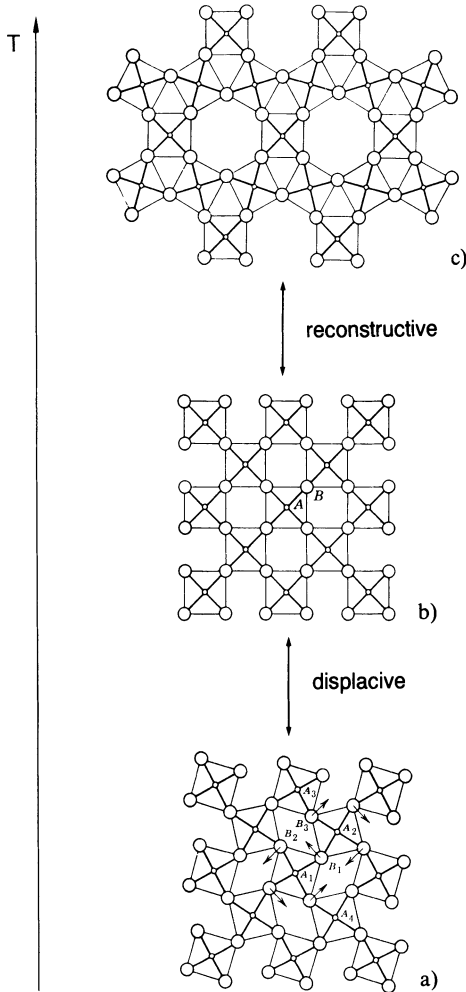


Fig. 11.23 a-c. Transformations in the secondary coordination sphere for structures based on square AB₄ coordination. **a** ↔ **b** is displacive, **b** ↔ **c** is reconstructive. (After [5])

Low- and high-quartz structures, Si^[4]O₂ are three-dimensional networks of SiO₄ tetrahedra, which share vertices with one another. In right-handed low-quartz (P3₂2) (cf. Table 8.11.24), these tetrahedra form a helix about a 3₂-screw axis, parallel to the c-axis. In right-handed high-quartz (P6₂22), this becomes a 6₂-screw axis. Figure 11.24 gives a projection of both structures onto (0001). At 573°C, a displacive transformation between low- and high-quartz occurs. The two structures are very similar; only a small rotation of one tetrahedron relative to another has occurred. The conversion of low- to high-quartz lowers the density from 2.65 to 2.53 g cm⁻³.

b) Reconstructive Transformations. Consider the conversion of (b) to (c) in Fig. 11.23. For this to occur, the bonds in b must be broken, so that the 4-membered rings of (b) may be rebuilt into the 6-membered rings of (c).

When high-quartz is heated above 870°C, it undergoes a reconstructive transformation to high-tridymite (P6₃/mmc, Fig. 11.24c). The tridymite struc-

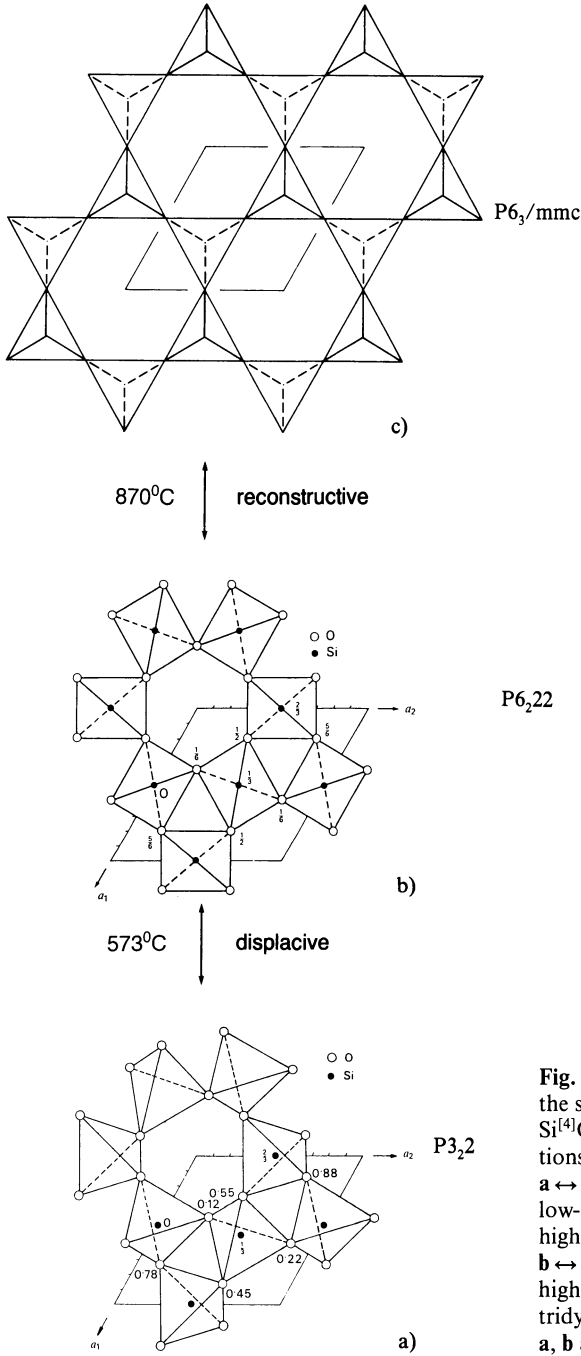


Fig. 11.24a-c. Transformations in the secondary coordination of Si^[4]O₂ structures shown as projections on (0001).
a ↔ b Displacive: right-handed low-quartz (P3₂2) ↔ right-handed high-quartz (P6₂22).
b ↔ c Reconstructive: right-handed high-quartz (P6₂22) ↔ high-tridymite (P6₃/mmc).
a, b after [39]

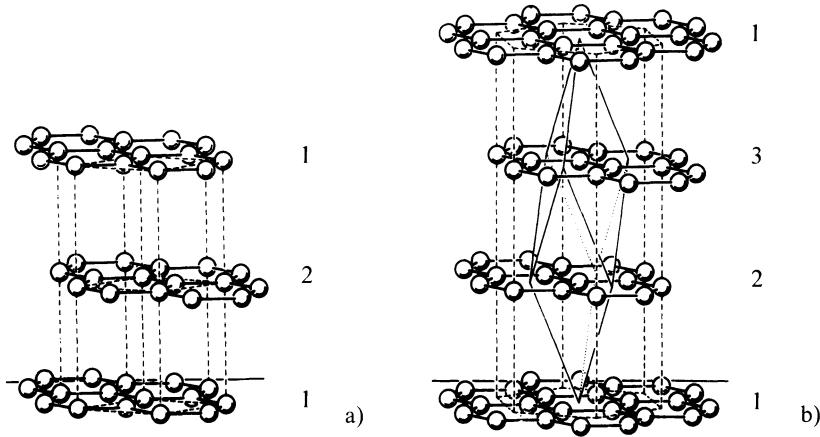


Fig. 11.25a, b. Polytypes of graphite structure. a 2H; b 3R. After [37]

ture consists of 6-membered rings of SiO_4 tetrahedra, which are packed above one another, normal to the c -axis.

The transformation between sphalerite and wurtzite is also reconstructive.

Displacive transformations require little energy and are relatively rapid; reconstructive ones require more energy and are very slow.

3. Order-Disorder Transformations

Copper and gold are miscible in all properties at high temperatures. In the (Cu, Au)-solid solution, the Cu and Au atoms are statistically distributed over the sites of the ccp crystal structure (*disorder*). On cooling, there is an *ordering* through the formation of the CuAu and Cu_3Au superstructures (Figs. 11.20 and 11.21, cf. Sect. 11.6)

4. Transformations Involving Changes in Type of Bonding

Carbon occurs as diamond (Fig. 11.19), graphite (Fig. 11.25) and the various fullerenes (e.g. C_{60} , Fig. 11.6a). In diamond, the bonding throughout the crystal is covalent. In graphite and in the fullerenes, covalent bonds hold the atoms in the layers or molecules while van der Waals forces hold layers and molecules together. Transformations of this sort are very slow.

In the graphite structure, the carbon atoms are ordered in 6-membered rings in the layers. The coordination “polyhedron” in this case is an equilateral triangle [3] (Table 11.1 h). The layer stacking can repeat itself at intervals of either two or three layers (Fig. 11.25). Both of these structures have been observed. This special form of polymorphism is called *polytypism*. In these

polytypic structures, (a) gives a hexagonal unit cell and (b) a rhombohedral. The structures are thus labelled as the 2H- and the 3R-polytypes of graphite, respectively.

11.8 Literature on Crystal Structures

Further information about specific crystal structures is obtainable from many sources. The following references are particularly recommended: [29], [43]–[45], [51].

EXERCISES

Exercise 11.1. Calculate the ideal radius ratio R_A/R_X for the coordination polyhedra: trigonal prism [6] and equilateral triangle [3] (cf. Table 11.1).

Exercise 11.2. Give a description of the following structures in terms of lattice + basis:

- α -Polonium (cubic P-lattice), cf. Fig. 2.1.
- Tungsten (cubic I-lattice), cf. Fig. 11.5.
- Magnesium (hexagonal closest packing) cf. Fig. 11.3.
- Copper (cubic closest packing) cf. Fig. 11.2.
- Draw four unit cells of the Mg-structure in projection on (0001). Find those symmetry elements which characterise the structure as hexagonal.

Exercise 11.3. Calculate the radii of the atoms in the structures in Exercise 11.2, using the following lattice parameters:

- α -Po: $a_0 = 3.35 \text{ \AA}$.
- W: $a_0 = 3.16 \text{ \AA}$.
- Mg: $a_0 = 3.21 \text{ \AA}$, $c_0 = 5.21 \text{ \AA}$.
- Cu: $a_0 = 3.61 \text{ \AA}$.

Compare these values with those given in Table 11.3.

Exercise 11.4. Calculate the ideal c_0/a_0 ratio for hexagonal closest packing.

Exercise 11.5. The packing efficiency is the ratio of the sum of the volumes of the atoms making up a unit cell to the volume of the cell itself. Calculate the packing efficiencies of:

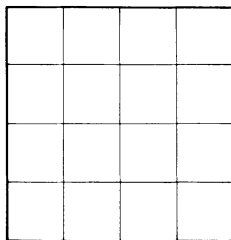
- α -Polonium (cubic P-lattice).
- Tungsten (cubic I-lattice).
- A hexagonal closest packing.
- A cubic closest packing.

Exercise 11.6. The diamond structure has:


lattice: cubic F, $a_0 = 3.57 \text{ \AA}$


basis: C: $0, 0, 0; \frac{1}{4}, \frac{1}{4}, \frac{1}{4}$


- Draw a projection of the structure on $x, y, 0$. Sketch tapered C–C bonds with colours indicating the height (use green for $0 < z < \frac{1}{2}$ and red for $\frac{1}{2} < z < 1$)




Atoms with

 $z = 0$

 $z = \frac{1}{4}$

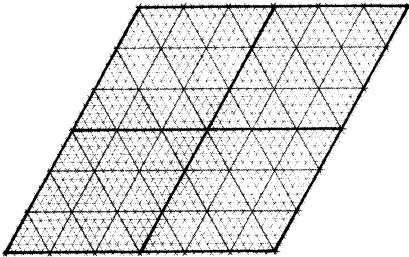
 $z = \frac{1}{2}$

 $z = \frac{3}{4}$

- Calculate the length of a C–C bond.
- What is the value of Z ?
- Describe the structure.
- Compare the diamond structure with that of sphalerite (Fig. 11.13).

Exercise 11.7. The graphite (2H) structure has
 lattice: hexagonal P: $a_0 = 2.46 \text{ \AA}$; $c_0 = 6.70 \text{ \AA}$.
 basis: C: $0, 0, 0$; $0, 0, \frac{1}{2}$; $\frac{1}{3}, \frac{2}{3}, 0$; $\frac{2}{3}, \frac{1}{3}, \frac{1}{2}$.

- a) Draw a projection on four unit cells on $x, y, 0$. Join each C-atom to its three nearest neighbours with the same z -coordinate with coloured lines ($z=0$ green, $z=\frac{1}{2}$ red).



- b) Calculate the length of a C–C bond.
 c) What is the value of Z ?
 d) Describe the structure. How large is the inter-layer spacing?
 e) Calculate the densities of diamond and graphite and comment on the difference.

Exercise 11.8. LiCl (NaCl-type; $a_0 = 5.13 \text{ \AA}$) has an arrangement of Cl^- ions which is cubic closest packed ($R_X/R_A = 0.43$). Calculate the ionic radii of Cl^- and Li^+ and the packing efficiency of the LiCl structure.

Exercise 11.9. Draw the ions on the $x, y, 0$ -plane of the NaCl ($a_0 = 5.64 \text{ \AA}$), LiCl ($a_0 = 5.13 \text{ \AA}$) and RbF ($a_0 = 5.64 \text{ \AA}$). The ionic radii can be taken from Table 11.3.

Exercise 11.10. Calculate the Ti–O distance in the coordination octahedron of the rutile structure (cf. Table 9.5). Which distances are equivalent by symmetry, and hence required to be equal?

Exercise 11.11. The pyrites structure (FeS_2) has:

- a) Space group $\text{Pa}\bar{3}$ ($\text{P2}_1/\text{a}\bar{3}$)

Fe: $4 a \bar{3} \quad 0, 0, 0$; $0, \frac{1}{2}, \frac{1}{2}$; $\frac{1}{2}, \frac{1}{2}, 0$; $\frac{1}{2}, 0, \frac{1}{2}$.

S: $8 c 3 \quad x, x, x$; $\frac{1}{2} + x, \frac{1}{2} - x, \bar{x}$; $\bar{x}, \frac{1}{2} + x, \frac{1}{2} - x$; $\frac{1}{2} - x, \bar{x}, \frac{1}{2} + x$;
 $\bar{x}, \bar{x}, \bar{x}$; $\frac{1}{2} - x, \frac{1}{2} + x, x$; $x, \frac{1}{2} - x, \frac{1}{2} + x$; $\frac{1}{2} + x, x, \frac{1}{2} - x$.

($x = 0.386$).

- b) Lattice constant: $a_0 = 5.41 \text{ \AA}$.

1. Draw the structure as a projection on $x, y, 0$ (let $a_0 = 10 \text{ cm}$).
2. Describe the structure.
3. What is the value of Z ?
4. Calculate the shortest Fe–S and S–S distances.
5. Draw the symmetry elements on the projection.

Exercise 11.12. A compound of $\text{NH}_4/\text{Hg}/\text{Cl}$ has:

- a) Space group $P4/\text{mmm}$.
 b) Lattice constants: $a_0 = 4.19 \text{ \AA}$, $c_0 = 7.94 \text{ \AA}$.
 c) Positions: Hg: $0, 0, 0$
 NH_4 : $\frac{1}{2}, \frac{1}{2}, \frac{1}{2}$
 Cl(1): $\frac{1}{2}, \frac{1}{2}, 0$
 Cl(2): $\pm(0, 0, z)$ $z = 0.3$

1. Draw a projection of the structure on $0, y, z$ ($1 \text{ \AA} = 1 \text{ cm}$).
2. Give the chemical formula of the compound, and the value of Z .
3. Describe the coordination of Hg and NH_4 , giving the coordination number and the coordination polyhedron.
4. Calculate the shortest Hg–Cl and NH_4 –Cl distances.

Exercise 11.13. The crystal structure of BaSO_4 has:

- a) Space group Pnma with special and general positions:
 (4c) $\pm(x, \frac{1}{4}, z; \frac{1}{2} + x, \frac{1}{4}, \frac{1}{2} - z)$
 (8d) $\pm(x, y, z; \bar{x}, \frac{1}{2} + y, \bar{z}; \frac{1}{2} - x, \frac{1}{2} - y, \frac{1}{2} - z; \frac{1}{2} - x, \bar{y}, \frac{1}{2} + z)$
 b) Lattice constants: $a_0 = 8.87 \text{ \AA}$, $b_0 = 5.45 \text{ \AA}$, $c_0 = 7.15 \text{ \AA}$.
 c) Occupation of positions:

	Position multiplicity and Wyckoff letter	x	y	z
Ba	(4c)	0.18	$\frac{1}{4}$	0.16
S	(4c)	0.06	$\frac{1}{4}$	0.70
O(1)	(4c)	-0.09	$\frac{1}{4}$	0.61
O(2)	(4c)	0.19	$\frac{1}{4}$	0.54
O(3)	(8d)	0.08	0.03	0.81

1. Draw a projection of the structure on $x, 0, z$.
2. What is the value of Z ?
3. Determine the coordination of O atoms around S.

12 Studies of Crystals by X-Ray Diffraction

Since the wavelengths of X-rays and the lattice parameters of crystals are of the same order of magnitude, X-rays are diffracted by crystal lattices. It was from the discovery of this effect in 1912 by *Max von Laue* that we may date the beginning of modern crystallography. Only then did it become possible to determine the structures of crystals.

We shall only describe here one X-ray method, the *Debye-Scherrer technique*, in detail, because it is a very important research tool for the scientist. Also, a brief description will be given of how a crystal structure may be determined.

For a fuller description of X-rays and their properties, the reader is referred to textbooks of physics.

12.1 The Bragg Equation

The diffraction of X-rays by crystals can be formally described as a reflection of X-rays from sets of lattice planes. Assume that a parallel, monochromatic beam of X-rays (i.e. one characterised by a single wavelength λ) falls on a set of lattice planes with a spacing of d , making a glancing angle of θ with them (Fig. 12.1). The waves I and II will be reflected at A_1 and B, and will

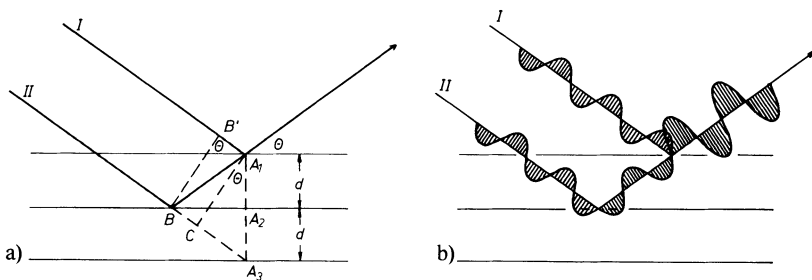


Fig. 12.1. a Diffraction (“reflection”) of an X-ray beam by a set of lattice planes. b Interference of waves reflected by a set of lattice planes ($\Gamma = 1\lambda$)

thus undergo interference. At the point A_1 , the waves will have had a path difference $\Gamma = BA_1 - A_1B' = BA_3 - BC = CA_3$, since $BA_1 = BA_3$ and $B'A_1 = BC$. Thus,

$$\sin \theta = \frac{\Gamma}{2d}$$

An interference maximum will be observed when Γ is an integral multiple n of λ , or $\Gamma = n\lambda$, where n is the order of the interference. This gives rise to the *Bragg equation*:

$$n\lambda = 2d \sin \theta.$$

12.2 The Debye-Scherrer Method

In the Debye-Scherrer method, a fine powder of a crystalline substance is irradiated with monochromatic X-rays. According to the Bragg equation, a set of parallel planes (hkl) will reflect X-rays with certain characteristic glancing angles θ (Fig. 12.2a). Since the crystallites are randomly arranged in a fine powder, there will always be a large number of crystals orientated in such a way that a given set of planes (hkl), which make an angle θ with the X-ray beam can cause reflection to occur. These planes are tangent to the surface of a cone with a cone-angle of 2θ . The beams reflected by these planes lie on the surface of a cone with a cone angle of 4θ (Fig. 12.2b). Figure 12.2c shows the reflection cones of a few different sets of planes.

In the Debye-Scherrer method, a cylindrical camera is used with the powdered specimen, contained in a thin tube mounted along the cylinder axis. The cones of reflection intersect the film in *Debye-Scherrer lines* (Fig. 12.2c,d). The angle between pairs of lines originating from the same cone is 4θ . Thus

$$\frac{S}{2\pi R} = \frac{4\theta}{360^\circ}$$

where R is the radius of the camera. For $R = 28.65$ mm ($2\pi R = 180$ mm), the measured value of S in mm is thus equal to the value of 2θ in degrees.

In order to obtain information from X-ray photographs, it is necessary to index the reflections, i.e. to determine which set of lattice planes gave rise to the observed interference. Since the value of θ is easy to read from the photograph and λ is known, the Bragg equation allows d , the spacing of the lattice planes, to be calculated.

How are these d -spacings related to (hkl)? The plane lying next to the one which passes through the origin in Fig. 12.3 intercepts the orthorhombic axes at the point $m00$ (a-axis), $0n0$ (b-axis) and 00∞ (c-axis), cf. Chapter 2.4.3.

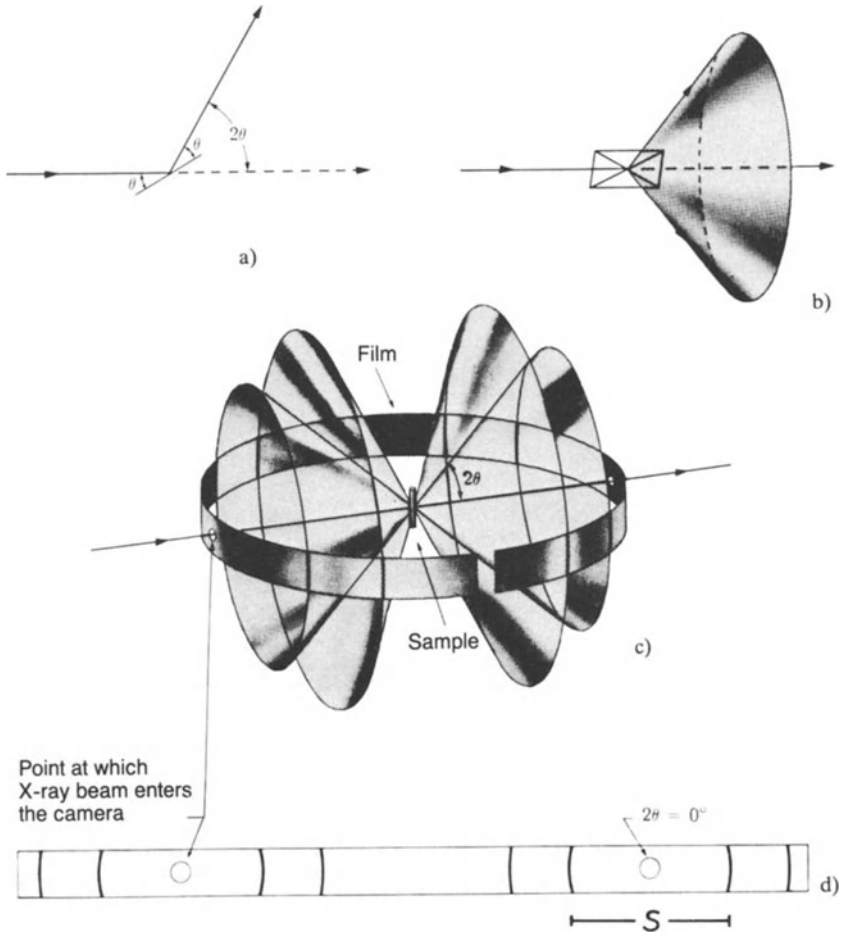


Fig. 12.2. **a** Relationship between the primary beam and a ray diffracted by the lattice planes (hkl). **b** Possible orientations of the set of planes (hkl) in a crystalline powder. The result of the random orientation of the planes giving a glancing angle of θ is a cone with a generating angle of 4θ . **c, d** The rays diffracted from the various lattice planes lie on concentric cones about the primary beam. Their intersections with the film give rise to the “lines” of the powder diagram. (After [11])

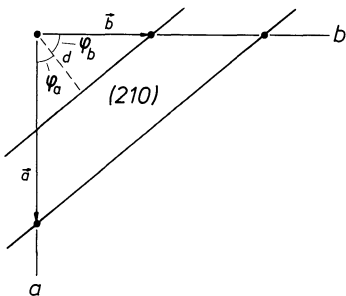


Fig. 12.3. Relationship between the Miller indices of a set of lattice planes and the spacing of the planes d for an orthorhombic crystal

For a set of planes (hkl):

$$\cos \varphi_a = \frac{d}{m \cdot a_0} = d \cdot \frac{h}{a_0}$$

$$\cos \varphi_b = \frac{d}{n \cdot b_0} = d \cdot \frac{k}{b_0}$$

$$\cos \varphi_c = \frac{d}{p \cdot c_0} = d \cdot \frac{l}{c_0}$$

Squaring these and adding them together gives:

$$\cos^2 \varphi_a + \cos^2 \varphi_b + \cos^2 \varphi_c = d^2 \cdot \left(\frac{h^2}{a_0^2} + \frac{k^2}{b_0^2} + \frac{l^2}{c_0^2} \right) = 1$$

$$d_{hkl} = \frac{1}{\sqrt{\frac{h^2}{a_0^2} + \frac{k^2}{b_0^2} + \frac{l^2}{c_0^2}}}$$

this relationship applies to the orthorhombic system. In the cubic system, it simplifies to

$$d_{hkl} = \frac{a_0}{\sqrt{h^2 + k^2 + l^2}}$$

Substituting this equation for the d-spacing into the Bragg equation and squaring gives:

$$\sin^2 \theta = \frac{\lambda^2}{4a_0^2} \cdot (h^2 + k^2 + l^2).$$

The right-hand side of this equation is the product of a constant factor $\lambda^2/4a_0^2$ and an integer ($h^2 + k^2 + l^2$). The values of $\sin^2 \theta$ for individual reflections are thus related to one another as integers.

The powder pattern for tungsten in Fig. 12.4 was taken with CuK_α radiation, $\lambda = 1.54 \text{ \AA}$. Table 12.1 shows the calculations for this photograph. Note that this table includes the reflections 200, 220 and 400, which contravene the definition of Miller indices as they do not represent the smallest integral multiples of the reciprocals of intercepts on the axes. In fact, they are Miller indices multiplied by the factor n, the order of diffraction. In other words, 200 may be

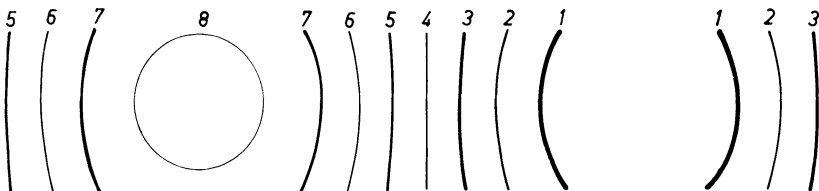


Fig. 12.4. Powder diagram of tungsten (reduced to 0.65 of original size)

regarded as the second order of diffraction from the (100) planes. These hkl triples, written without brackets, are called *Laue symbols*, and their use makes the factor n of the Bragg equation unnecessary.

From the constant factor $\lambda^2/4a_0^2 = 0.0592$, the lattice parameter $a_0 = 3.16 \text{ \AA}$ may be determined. Z , the number of formula units per unit cell, can also be determined (cf. Chap. 3)

$$Z = \frac{\rho \cdot V \cdot N_A}{M}$$

$$Z = \frac{19.3 \cdot 3.16^3 \cdot 10^{-24} \cdot 6.023 \cdot 10^{23}}{183.86}$$

$$Z \sim 2.$$

A cubic structure of an element with $Z = 2$ can only occur if the substance has a cubic I-lattice, cf. Fig. 11.5.

In Table 12.1, 100, 111 and 210 do not occur. Such absences occur in structures which have centred lattices or contain glide planes or screw axes.

The absent reflections are said to be *extinct*. Those reflections which do occur in Table 12.1 obey the rule $h + k + l = 2n$, where n is an integer, and this is characteristic for all structures with an I-lattice.

The number of reflections which can be observed on an X-ray photograph is limited. In the Bragg equation $\sin \theta = \frac{\lambda}{2d}$, $-1 \leq \sin \theta \leq +1$. Thus $\frac{\lambda}{2d} \leq +1$ and $d \geq \frac{\lambda}{2}$. Diffraction can only arise from those sets of lattice planes for which $d \geq \frac{\lambda}{2}$. For $\text{CuK}\alpha$ radiation, $\lambda = 1.54 \text{ \AA}$, the limiting value for d is

Table 12.1. Interpretation of the powder pattern of tungsten

No of reflection	S mm	θ degree	$\sin^2 \theta = \frac{\lambda^2}{4a_0^2} \cdot (h^2 + k^2 + l^2)$	hkl	$d_{\text{hkl}} \text{ \AA}$
1	40.3	20.15	$0.1187 = 0.0594 \cdot 2$	110	2.24
2	58.3	29.15	$0.2373 = 0.0593 \cdot 4$	200	1.58
3	73.2	36.60	$0.3555 = 0.0592 \cdot 6$	211	1.29
4	87.1	43.55	$0.4744 = 0.0593 \cdot 8$	220	1.12
5	100.8	50.40	$0.5937 = 0.0594 \cdot 10$	310	1.00
6	115.0	57.50	$0.7113 = 0.0592 \cdot 12$	222	0.91
7	131.2	65.60	$0.8294 = 0.0592 \cdot 14$	321	0.85
8	154.2	77.10	$0.9502 = 0.0592 \cdot 16$	400	0.79

4-806 JCPDS-ICDD Copyright © 1991 Quality:*

				d Å	Int.	h	k	l
W				2.238	100	1	1	0
Tungsten				1.582	15	2	0	0
				1.292	23	2	1	1
				1.1188	8	2	2	0
				1.0008	11	3	1	0
Rad: CuKα1	Lambda: 1.5405	Filter: Ni	dsp:	0.9137	4	2	2	2
Cutoff:	Int: Diffractometer	I/Icor: 18.00		0.8459	18	3	2	1
Ref: Swanson, Tatge, Natl. Bur. Stand. (U.S.), Circ. 539, 1 28 (1953)				0.7912	2	4	0	0
Sys: Cubic	S.G.: Im3m (229)							
a: 3.1648	b:	c:	A:	C:				
A:	B:	C:	Z: 2	mp:				
Ref: Ibid.								
Dx: 19.262	Dm:	SS/FOM: F8 = 108 (.009.8)						
ea:	nwB:	ey:	Sign:	2V:				
Ref:								
Color: Steel-gray to tin-white Pattern at 26°C. Sample prepared at Westinghouse Electric Corp. CAS no.: 7440-33-7. Analysis of sample shows SiO ₂ 0.04%, K 0.05%, Mo, Al ₂ O ₃ and 0.01% each. Merck Index, 8th Ed., p. 1087. W type. Also called: wolfram. PSC: cIz. Mwt: 183.85. Volume [CD]: 31.70.								

Strong lines: 2.24/X 1.29/2 1.58/2 0.85/2 1.00/1 1.12/1 0.91/1 0.79/1

Fig. 12.5. PDF (formerly ASTM) index “card” for tungsten, as a computer printout

thus 0.77 \AA . The pattern for tungsten contains no reflections with a d-value $\leq \frac{\lambda}{2} = 0.77 \text{ \AA}$.

The greatest use of the Debye-Scherrer method is in the identification of crystalline substances. Every sort of crystal produces a pattern of lines with characteristic positions and intensities. The intensity is roughly proportional to the blackness of a photograph. The American Society for Testing Materials published an index (the ASTM index) containing data for all crystalline inorganic and organic substances which have been studied by X-ray diffraction. This index is now administered by the Joint Committee for Powder Diffraction Standards (JCPDS) at the International Center for Diffraction Data in Swarthmore, USA. Every substance has an index card which contains the d-values and the relative intensities for individual reflections, as well as many other crystallographic data. The PDF-card for tungsten is given in Fig. 12.5. For the identification of an unknown substance, use is made of the lines with the strongest intensities, which are given in tabular form. Naturally, the file is now normally accessed by computer.

12.3 The Reciprocal Lattice

Crystals are three-dimensional systems. A stereographic projection, which gives a useful summary of the arrangements of the crystal faces with respect to one another, can be derived simply from a consideration of the morphology

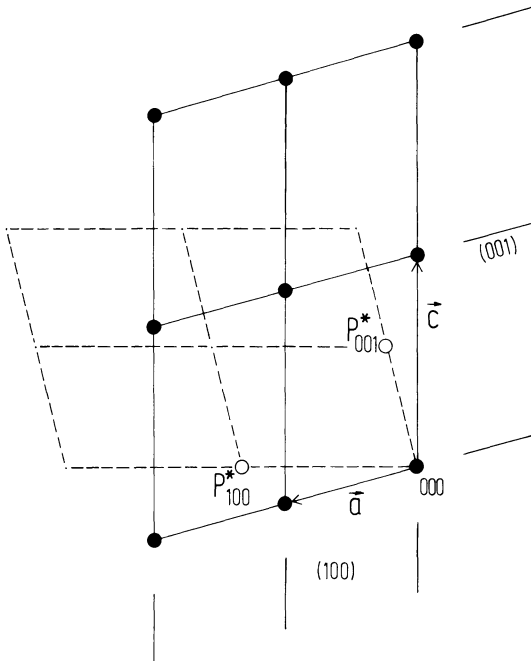


Fig. 12.6. Monoclinic P-lattice as a projection on (010) with the points P^*_{001} and P^*_{100} . P^*_{000} , P^*_{001} and P^*_{100} define a lattice, the reciprocal lattice

of a crystal. As described in Chapter 4.4, the normals to the crystal faces are used for this purpose.

An alternative system for representing the lattice planes was proposed by *P. P. Ewald* to discuss the scattering of X-rays by the crystal lattice. Since, as is described in section 12.1, the diffraction of X-rays can be interpreted as the reflection of the rays by sets of parallel lattice planes, it was important to devise an aid to illustrate both the orientations of the lattice planes and their diffraction. This aid is the “reciprocal lattice”. Each set of lattice planes in the crystal is represented by a point in the reciprocal lattice. The construction of a “reciprocal lattice” from the corresponding “direct lattice” may be performed as follows:

For each set of lattice planes (hkl) , the normal is drawn from the origin with a length $d^ = \frac{C}{d_{hkl}}$, where d is the lattice spacing and C is a proportionality constant.*

The construction of the reciprocal lattice corresponding to the projection on (010) of a direct monoclinic P-lattice is shown in Fig. 12.6. The normal to the set of lattice planes (001) is drawn from the origin and assigned a length

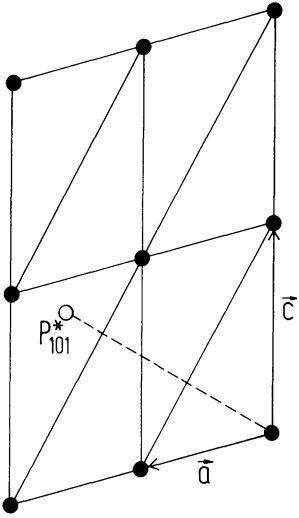


Fig. 12.7

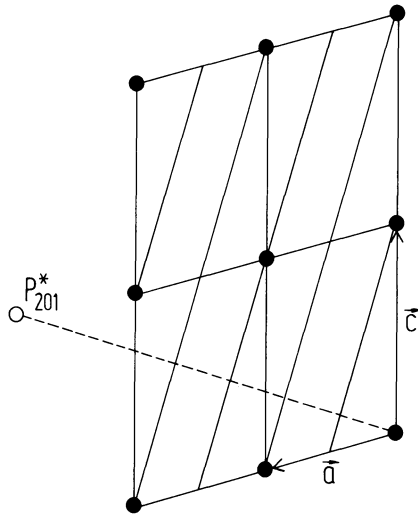


Fig. 12.8

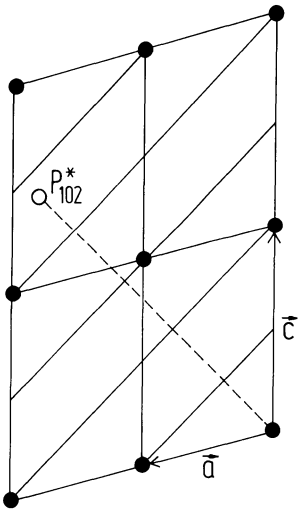


Fig. 12.9

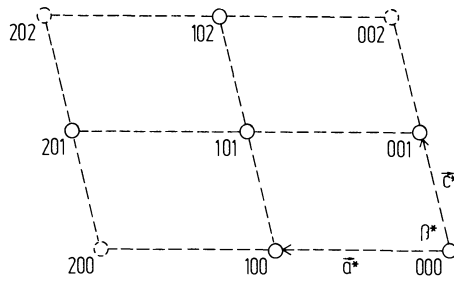


Fig. 12.10

Fig. 12.7. Monoclinic P-lattice as a projection on (010) with the traces of the lattice planes (101) and the point P_{101}^* of the reciprocal lattice

Fig. 12.8. Monoclinic P-lattice as a projection on (010) with the traces of the lattice planes (201) and the point P_{201}^* of the reciprocal lattice

Fig. 12.9. Monoclinic P-lattice as a projection on (010) with the traces of the lattice planes (102) and the point P_{102}^* of the reciprocal lattice

Fig. 12.10. Reciprocal lattice (a^*c^* -plane) corresponding to the monoclinic P-lattice of Fig. 12.6

$d^* = \frac{C}{d_{001}}$. The resulting point is called P_{001}^* . A similar construction for the set of (100) planes gives the point P_{100}^* . The points P_{001}^* and P_{100}^* represent the relative orientations of the (001) and (100) lattice planes.

Making use of the three points P_{000}^* , P_{100}^* and P_{001}^* , a two-dimensional lattice can be constructed. This reciprocal lattice plane is indicated by dashed lines in Fig. 12.6. It must now be shown that the reciprocal lattice points corresponding to all sets of lattice planes with indices (h0l) fall on this same plane. Figures 12.7–12.9 show the relevant constructions for the sets of (101), (201) and (102) planes. When all relevant points are added to the drawing, its lattice-like nature is apparent (Fig. 12.10). This construction does not, however, lead to all of the points required by the reciprocal lattice. For example, P_{002}^* , P_{200}^* and P_{202}^* are missing since lattice planes with indices such as (002), (200) and (202) contravene the definition of Miller indices given in Chapter 2.4.3. It is, of course, possible to define a set of “lattice planes” (002) with a spacing $d = \frac{d_{001}}{2}$. In these “lattice planes”, only half of the planes intersect points of the direct lattice. Furthermore, the Bragg equation (Sect. 2.1) can be written in the form $\lambda = 2 \frac{d}{n} \sin \theta$. If this is done, every n-th order diffraction with a plane spacing of d can be replaced by a first-order diffraction from planes with a spacing of $\frac{d}{n}$. P_{002}^* describes in the same way a second-order diffraction from the planes (001), P_{003}^* a third order, and so on. The same sort of reasoning applies to the points P_{200}^* , P_{202}^* , etc. (see also Sect. 12.2).

The rule for constructing the reciprocal lattice given above (p. 255) is thus incomplete and should read: ... with a length $d^ = \frac{C}{d_{hkl}}$, and all integral multiples thereof, where d is the lattice spacing*

The reciprocal lattice, like the direct lattice, is defined by six lattice parameters:

$$|\vec{a}^*| = a_0^* = \frac{1}{d_{(100)}} = \frac{b_0 c_0 \sin \alpha}{V}$$

$$|\vec{b}^*| = b_0^* = \frac{1}{d_{(010)}} = \frac{a_0 c_0 \sin \beta}{V}$$

$$|\vec{c}^*| = c_0^* = \frac{1}{d_{(001)}} = \frac{a_0 b_0 \sin \gamma}{V}$$

$$V = a_0 b_0 c_0 \cdot \sqrt{1 - \cos^2 \alpha - \cos^2 \beta - \cos^2 \gamma + 2 \cos \alpha \cos \beta \cos \gamma}$$

(Volume of the unit cell)

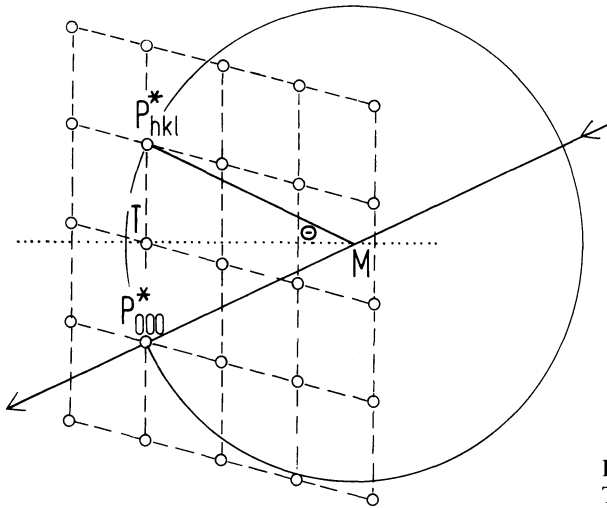


Fig. 12.11.
The Ewald construction

$$\alpha^* = \vec{b}^* \wedge \vec{c}^*; \quad \cos \alpha^* = \frac{\cos \beta \cos \gamma - \cos \alpha}{\sin \beta \sin \gamma}$$

$$\beta^* = \vec{a}^* \wedge \vec{c}^*; \quad \cos \beta^* = \frac{\cos \alpha \cos \gamma - \cos \beta}{\sin \alpha \sin \gamma}$$

$$\gamma^* = \vec{a}^* \wedge \vec{b}^*; \quad \cos \gamma^* = \frac{\cos \alpha \cos \beta - \cos \gamma}{\sin \alpha \sin \beta}$$

The use of the reciprocal lattice allows an elegant discussion of the application of the Bragg equation to the diffraction of X-rays by a lattice. Figure 12.11 shows a section through a reciprocal lattice. The direction of the primary beam is indicated by a straight line through the point P_{000}^* . A sphere (which in Fig. 12.11 becomes a circle) with a radius of $\frac{C}{\lambda}$ and a centre at the point M on the line is then constructed so that the surface of the sphere intersects the origin of the reciprocal lattice, P_{000}^* . This sphere is known as the sphere of reflection. In general, no point of the reciprocal lattice other than P_{000}^* lies on the surface of the sphere. By choosing the direction of the primary beam appropriately, however, it may be possible to cause another point P_{hkl}^* to lie on the surface of the sphere of reflection, as in Fig. 12.11. In this case, the condition for the Bragg equation $n\lambda = 2d \sin \theta$ is fulfilled precisely for the set of planes (hkl). Diffraction occurs, and the diffracted beam has the direction MP_{hkl}^* . The orientation of the planes (hkl) is shown in Fig. 12.11 by a dotted line. It is obvious that the diffracted beam with a glancing angle equal to θ can equally well be described as a reflection from the lattice planes (hkl).

It will be noticed that for the triangle P_{hkl}^*MT , $\sin \theta = \frac{1}{\frac{2d}{1}} = \frac{\lambda}{2d}$, fulfilling

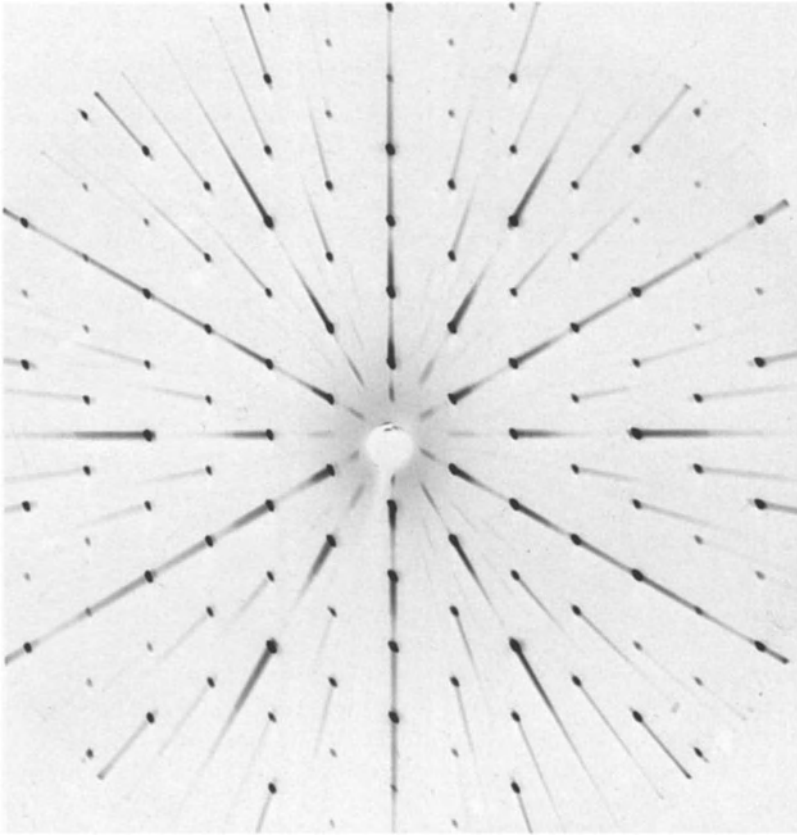


Fig. 12.12. Precession photograph of β -eucryptite, LiAlSiO_4 (space group $P6_422$): a^*b^* -plane (Photograph A. Breit)

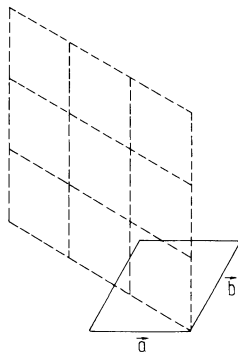


Fig. 12.13. a^*b^* -plane of a hexagonal reciprocal lattice, cf. Fig. 12.12

the Bragg condition. This geometrical construction is known as the *Ewald construction*.

If a single crystal is rotated about an axis which is perpendicular both to the primary beam and to a selected plane of the reciprocal lattice, then the reciprocal lattice itself rotates about an axis through P_{000}^* . During this rotation, other points of the reciprocal lattice will pass through the surface of the sphere of reflection, and the corresponding lattice planes will come into the diffracting position. These relationships are the basis of rotating crystal methods.

The precession method of *M. Buerger* produces an undistorted representation of the reciprocal lattice. In this technique, an axis of the crystal precesses about the primary beam. The resulting picture is of the reciprocal lattice plane perpendicular to this axis. A precession photograph of β -eucryptite, LiAlSiO_4 (space group $P6_422$) is shown in Fig. 12.12. It represents the a^*b^* -plane. The reciprocal lattice of a hexagonal lattice is itself hexagonal, as is shown in Fig. 12.13 which should be compared with Fig. 12.12.

12.4 Laue Groups

In general, the intensity of an X-ray beam diffracted from one side of a set of lattice planes is equal to that diffracted from the other. A diffraction pattern is thus centrosymmetric. It follows that instead of 32 point groups only the 11 which contain an inversion centre can characterise a diffraction pattern. These 11 point groups are known as Laue groups (cf. Table 8.10).

As an example, the Laue groups of the tetragonal system will be explained. An inversion centre is added to each point group:

Laue group $4/m$

$4 + \bar{1} \rightarrow 4/m$ (Symmetry rule I)

$\bar{4} + \bar{1} \rightarrow 4/m$ (cf. Fig. 5.13) The operation of an inversion centre on the $\bar{4}$ array in (a) results in the $4/m$ array in (b).

Laue group $4/m\ 2/m\ 2/m$ ($4/mmm$)

$422 + \bar{1} \rightarrow 4/m\ 2/m\ 2/m$ (Symmetry rule I)

$4mm + \bar{1} \rightarrow 4/m\ 2/m\ 2/m$ (Symmetry rule I)

$\bar{4}2m + \bar{1} \rightarrow 4/m\ 2/m\ 2/m$ ($\bar{4} + \bar{1} \equiv 4/m$ as above and symmetry rule I).

Consideration of the first Symmetry rule together with the relationships $3 + \bar{1} \equiv \bar{3}$ and $\bar{6} + \bar{1} \equiv 6/m$ will allow the Laue groups of the other crystal systems to be derived from each point group (cf. Table 8.10).

12.5 The Determination of a Crystal Structure

Powder diffraction patterns allow the determination only of relatively simple structures. Techniques have been developed which make use of measurements of the intensities of the reflections of sets of lattice planes from single crystals. Study of relationships among intensities and “systematic absences” in the diffraction pattern can lead to the determination of the space group. Measurement of the density of the crystals gives Z (cf. Sect. 12.2), the number of formula units in the unit cell. The intensity of the individual reflections depends on the extent to which the sets of lattice planes are occupied by atoms. Since different sets of lattice planes will vary greatly in both the number of atoms occupying them and the “heaviness” (in terms of electrons) of those atoms, the intensities of a very large number of reflections can allow the determination of the arrangement of atoms in the unit cell.

For simple crystal structures, it is possible to make useful structural conclusions from only a small amount of data. This may be illustrated by the structure of SnO_2 , cassiterite, for which the following data have been determined:

1. Lattice constants: $a_0 = 4.74 \text{ \AA}$, $c_0 = 3.19 \text{ \AA}$.
2. Space group: $P4_2/mnm$
3. Density: 6.96 g cm^{-3} .

The value of Z (the number of chemical formula units per unit cell) may be directly calculated (cf. the formulae on p. 24):

$$Z = \frac{\rho \cdot N_A \cdot V}{M} = \frac{6.96 \cdot 6.023 \cdot 10^{23} \cdot 4.74^2 \cdot 3.19 \cdot 10^{-24}}{150.69} = 1.99 \approx 2.$$

Thus, there must be two formula units of SnO_2 or two tin and four oxide ions per unit cell. The Sn^{4+} ions must then occupy a set of 2-fold positions in the unit cell, and the O^{2-} ions a set of 4-fold positions, or (less likely) two sets of 2-fold positions. The space group, $P4_2/mnm$, (Fig. 9.17) has two sets of 2-fold positions (a and b), and five sets of 4-fold positions (c to g). Let us see whether the ionic radii ($R(\text{Sn}^{4+}) = 0.71 \text{ \AA}$, $R(\text{O}^{2-}) = 1.32 \text{ \AA}$) can help to select the sites which are actually occupied. In the following illustrations, the lattice constants and the ionic radii have been drawn to the same scale.

First, consider the possible 4-fold positions for the O^{2-} ions.

1) Positions (c): These comprise the fixed point $0, \frac{1}{2}, 0$ and $0, \frac{1}{2}, \frac{1}{2}$ (Fig. 9.17). These are shown as points on the line $0, \frac{1}{2}, z$ in Fig. 12.14c, in which the lattice repeat is scaled to the actual length c_0 . When the O^{2-} ions are then drawn in to scale, it is clear that they overlap badly.

2) Positions (d): These also comprise fixed point $0, \frac{1}{2}, \frac{1}{4}$ and $0, \frac{1}{2}, \frac{3}{4}$ which are shown as points on the line $0, \frac{1}{2}, z$ in Fig. 12.14d. When the O^{2-} ions are then drawn in to scale, the overlap is the same as in (1).

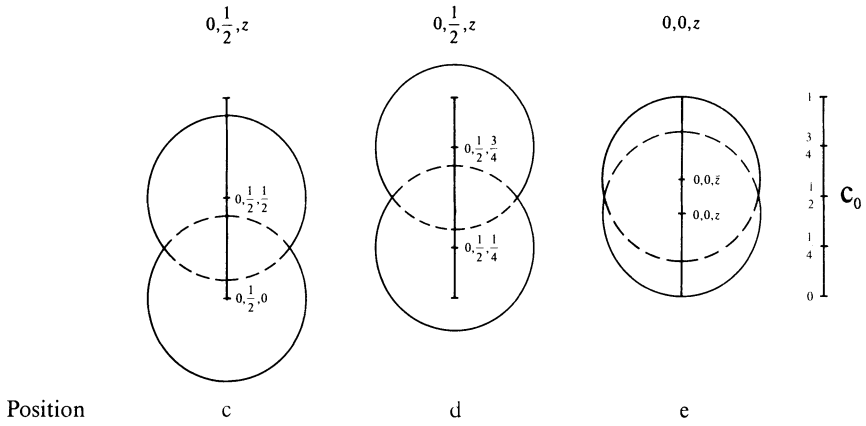


Fig. 12.14c, d, e. Investigation of the structure of SnO_2 . The O^{2-} ions cannot lie in the given places as required by the positions c to e of space group $P4_2/m\bar{m}$

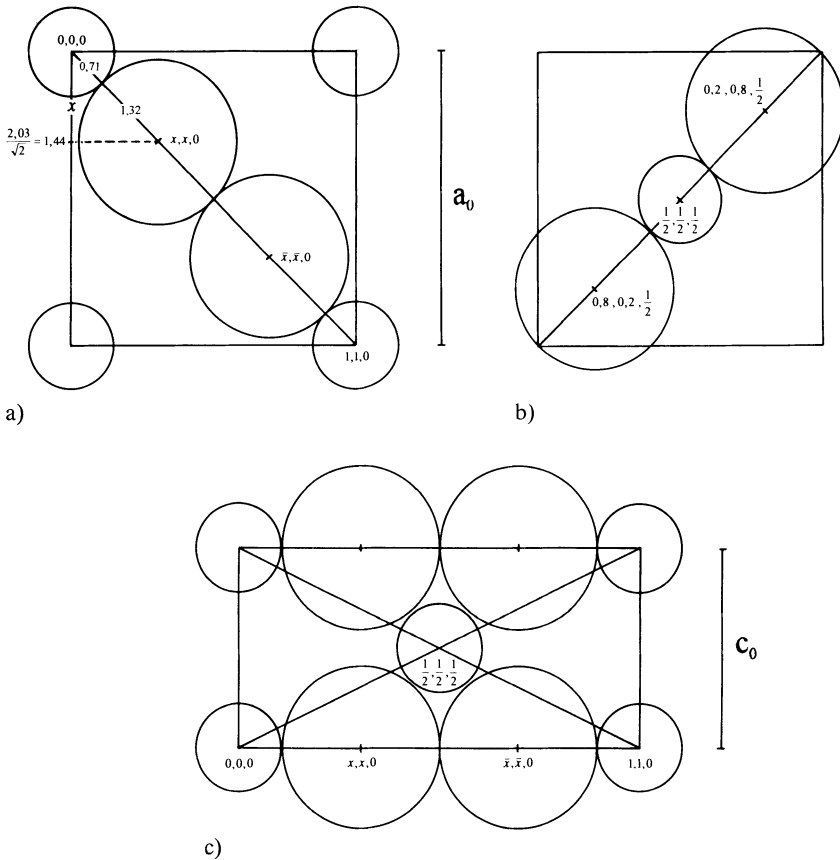


Fig. 12.15a, b, c. Structure of SnO_2 . Placing the Sn^{4+} ions on positions a and the O^{2-} ions on f leads to an acceptable arrangement. a) the $x, y, 0$ plane. b) the $x, y, \frac{1}{2}$ plane. c) the x, x, z plane

3) Positions (e): Here, there is one degree of freedom to be considered. A pair of points $0, 0, z$ and $0, 0, \bar{z}$ must both lie within the range of the lattice constant c_0 (Fig. 11.14e). Whatever value is chosen for z , the overlap will be at least as bad as that in (1) and (2).

Clearly, these three sets of positions are not possible for the SnO_2 structure.

4) Positions (f): Again, there is one degree of freedom to be considered. In order to limit the possibilities for the O^{2-} ions somewhat, the Sn^{4+} ions have been inserted at $0, 0, 0$ (positions (a)) in a scale drawing of the $x, y, 0$ -plane (Fig. 12.15a). It is then possible to draw in the O^{2-} ions at $x, x, 0$ and $\bar{x}, \bar{x}, 0$ along the diagonal between the Sn^{4+} ions at $0, 0, 0$ and $1, 1, 0$. In fact, the ions fill the gaps precisely! It is possible to estimate a value for x :

$$R(\text{Sn}^{4+}) + R(\text{O}^{2-}) = 0.71 + 1.32 = 2.03 \text{ \AA};$$

$$2.03 \text{ \AA} / \sqrt{2} = 1.44 \text{ \AA}; 1.44 \text{ \AA} / c_0 = 0.304 = x.$$

Substituting the value $x = 0.3(04)$ in the positions (f) gives $0.2, 0.8, \frac{1}{2}$ and $0.8, 0.2, \frac{1}{2}$ for ions 3 and 4. These are shown along with the Sn^{4+} ion at $\frac{1}{2}, \frac{1}{2}, \frac{1}{2}$ in Fig. 12.15b. Fig. 12.15c shows the x, x, z section through Figs. 12.15a and b. Each Sn^{4+} ion occupies an octahedral hole formed by six O^{2-} ions.

The structural results may then be summarised thus: Space group $P4_2/mnm$ (Fig. 9.17). Sn^{4+} in $2a$ m. mm and O^{2-} in $4f$ m. 2m with $x = 0.304$. The currently accepted value for x is 0.3053 . SnO_2 has the same structure type as rutile (Fig. 9.18).

5) The positions (g) have not yet been considered. In fact, placing the O^{2-} ions in these positions leads to an alternative description of the same structure.

The following are a few still simpler examples; the calculation of Z will be omitted.

I) CsI : $Z = 1$. The space group is $P4/m \bar{3}2/m$, which has only two 1-fold positions:

$$1b \text{ m}\bar{3}m \frac{1}{2}, \frac{1}{2}, \frac{1}{2} \quad \text{and} \quad 1a \text{ m}\bar{3}m 0, 0, 0$$

Thus, the Cs^+ may be placed at $0, 0, 0$ and the I^- at $\frac{1}{2}, \frac{1}{2}, \frac{1}{2}$ or vice-versa (cf. Fig. 3.4).

Table 12.2. Coordinates for some of the positions of space group $F4/m \bar{3}2/m$, from [14].

			$(0, 0, 0)^+$	$(0, \frac{1}{2}, \frac{1}{2})^+$	$(\frac{1}{2}, 0, \frac{1}{2})^+$	$(\frac{1}{2}, \frac{1}{2}, 0)^+$
24	d	m. mm	$0, \frac{1}{4}, \frac{1}{4}$	$0, \frac{3}{4}, \frac{1}{4}$	$\frac{1}{4}, 0, \frac{1}{4}$	$\frac{1}{4}, 0, \frac{3}{4}$
8	c	$\bar{4}3m$	$\frac{1}{4}, \frac{1}{4}, \frac{1}{4}$	$\frac{1}{4}, \frac{1}{4}, \frac{3}{4}$	$\frac{1}{4}, \frac{1}{4}, 0$	$\frac{3}{4}, \frac{1}{4}, 0$
4	b	$m\bar{3}3m$	$\frac{1}{2}, \frac{1}{2}, \frac{1}{2}$			
4	a	$m\bar{3}m$	$0, 0, 0$			

II) NaCl: $Z=4$. The space group is $F4/m\bar{3}2/m$. Table 12.2 gives the coordinates of the positions a to d for this space group. There are two 4-fold sets of positions, so Na^+ may be placed on a and Cl^- on b or vice-versa, cf. Fig. 11.9. In Fig. 11.9, $\frac{1}{2}, 0, 0$ is given instead of the equivalent $\frac{1}{2}, \frac{1}{2}, \frac{1}{2}$.

III) CaF_2 : $Z=4$. Space group $F4/m\bar{3}2/m$ (Table 12.2). The F^- ions occupy the 8-fold positions c, while the Ca^{2+} ions may be placed either on a (0, 0, 0 etc.) or on b ($\frac{1}{2}, \frac{1}{2}, \frac{1}{2}$ etc.). Either choice leads to the same structure.

EXERCISES

Exercise 12.1. Draw the (100)- and the (001)-lattice planes of the rutile structure (cf. Fig. 9.18 and Table 9.5). Using the introduction in Section 12.3, construct the a^*c^* - and the a^*b^* -planes of the reciprocal lattice.

Exercise 12.2. For the crystal structure of thallium, the lattice parameters are $a_0 = b_0 = c_0 = 3.88 \text{ \AA}$, $\alpha = \beta = \gamma = 90^\circ$, and the density is 11.85 g cm^{-3} . Determine the crystal structure, and draw it, projected on $x, y, 0$.

Exercise 12.3. Derive the cubic Laue groups.

Exercise 12.4. A powder photograph has been taken of the cube-shaped crystals of KI, using $\text{Cu K}\alpha$ radiation ($\lambda = 1.54 \text{ \AA}$). The first nine lines, measured from the position of the direct beam, give the following 2θ -values:

21.80; 25.20; 36.00; 42.50; 44.45; 51.75; 56.80; 58.45; 64.65.

1. Index these powder lines and calculate their d-values.
2. Determine the lattice constant a_0 .
3. What is the value of Z ? (The density of KI is 3.13 g cm^{-3})
4. Suggest the structure type of KI.

13 Crystal Defects

A crystal with a volume of 1cm^3 will contain about 10^{23} atoms. Lattice theory requires in principle that all of these atoms occupy a regular lattice. The array of atoms must conform to one of the 230 space groups. The equivalent points of a position of a space group must be fully occupied by atoms of the same type. This theoretical model is only achieved conceptually, by an *ideal crystal*.

The observation of a large number of crystals will show that they in fact have cracks and fissures, and that crystal faces are often not really flat. At cleavage surfaces, crystalline domains are often displaced with respect to one another. Inclusions occur in crystals, which may themselves be crystalline, liquid or gas. In practice, a *real crystal* deviates considerably from the ideal model described above.

All deviations from ideal crystalline behaviour are described as *crystal defects*. Many important properties of crystals derive from defects, including luminescence, diffusion, mechanical properties, etc. Nevertheless, the ideal crystal structure is the starting point for all studies of crystals.

Individual defects make themselves apparent in many ways. They can be categorised in terms of their dimensionality (Table 13.1).

Table 13.1. Types of crystal defects

13.1 Point defects	13.2 Line defects	13.3 Plane defects
a) Substitution defects b) Solid solutions c) Schottky and Frenkel defects	a) Edge dislocations b) Screw dislocations	a) Small angle grain boundaries b) Stacking faults c) Twin boundaries

13.1 Point Defects

Point defects are concerned with atomic dislocations.

a) *Substitution Defects.* An ideal crystal must consist entirely of the substance to which its formula refers, and this situation never occurs. As there are about 10^{23} atoms in 1cm^3 of a crystal, even a purity of 99.99999% implies the presence of some 10^{16} foreign atoms! These foreign atoms will in general be larger or smaller than the atoms they replace. Furthermore, the foreign atoms may have different bonding capacities. This can result in the propagation of further irregularities in the crystal which may no longer be of the point-defect type.

In some cases, crystals with specific impurities are actually required. It is such impurities which control the electrical conductivity of many semiconductors.

b) *Solid Solutions.* The statistical distribution of atoms in solid solutions (cf. Chap. 11.6) are also point defects.

c) *Schottky- and Frenkel Defects.* Every crystal contains voids. These are places in a crystal where the expected atoms do not occur. If these missing atoms have “wandered” to a surface of the crystal, the result is called a Schottky defect, while if they have moved to places between other atoms (interstitial sites), the result is called a Frenkel defect. Both of these types are illustrated for an ionic crystal in Fig. 13.1. The concentration of faults in a crystal is in thermal equilibrium, and increases with rising temperature. The type of fault which occurs depends on the structure itself, its geometry and its bonding type. In alkali halides, Schottky defects predominate, while Frenkel defects predominate in silver halides. Measurement of the density of a crystal gives an indication of the defect type, since Schottky defects decrease the density (more volume for the same mass) while Frenkel defects leave the volume and hence the density unchanged.

Wuestite (NaCl-structure type) does not have the ideal stoichiometry FeO , because the Fe^{2+} ions in some places are replaced by Fe^{3+} . This unbalanced charge results in a corresponding number of cation vacancies, giving a formula Fe_{1-x}O .

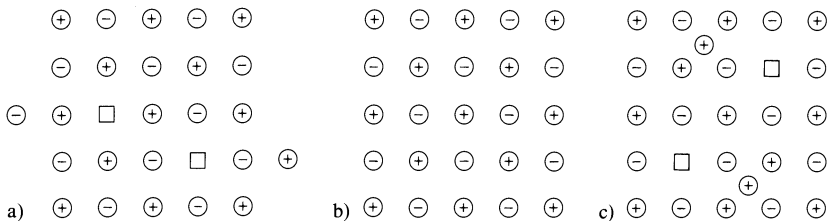


Fig. 13.1 a–c. Schottky defects (a) and Frenkel defects (c) in an ionic crystal (\square void); (b) the ideal crystal

The occurrence of these faults gives rise to a number of properties. The defects make possible the diffusion of ions through the crystal. If a gold crystal and a silver crystal are pressed firmly against one another as the temperature is raised, Ag-atoms diffuse into the gold crystal, and Au-atoms into the silver, forming solid solutions (cf. Fig. 11.20). At sufficiently high temperatures, ionic crystals, such as NaCl, show a small electrical conductivity. This does not result from electronic conduction, as in metals, but is brought about by ionic movement. Without crystal defects, this would not occur.

Solid-state reactions are almost always propagated by crystal defects. The heating of a mixture of finely powdered ZnO and Fe₂O₃ crystals to a temperature well under their melting points brings about a reaction yielding crystals of the spinel zinc ferrite, ZnFe₂O₄. The rates of solid-state reactions are much less than those taking place in the gas or liquid phase. They do, however, rise with temperature as the concentration of crystal faults and the rates of diffusion rise.

13.2 Line Defects

This type of defect forms along a line, the line of dislocation.

a) *Edge Dislocations*. The upper portion of the crystal in Fig. 13.2a has been displaced by the vector $BC (= B'C')$ in the plane $ABA'B'$ relative to the lower portion in such a way that the line AA' (the line of dislocation) marks the limit of the displacement. Figure 13.2b shows the structure of a plane normal to the line of dislocation AA' . The displacement vector, which amounts to a displacement $(= BC)$ is known as the Burgers vector \vec{b} , and is normal to the line of dislocation AA' .

b) *Screw Dislocations*. The crystal in Fig. 13.3 contains a screw dislocation which arises from a displacement in the plane ABCD with the line of dislocation AD. In the region of the line of dislocation, the crystal does not consist of neatly stacked lattice planes, but of an arrangement of atoms which repeat through the

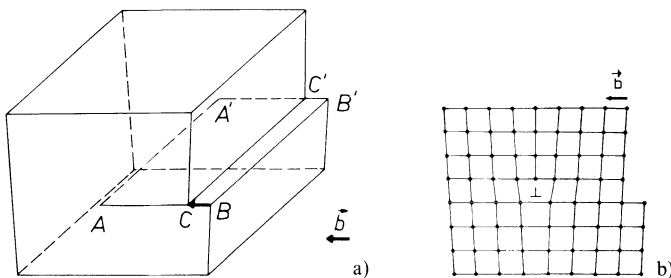


Fig. 13.2a, b. Edge dislocation; pictorial (a), structural representation (b) (\perp end of the line of dislocation)

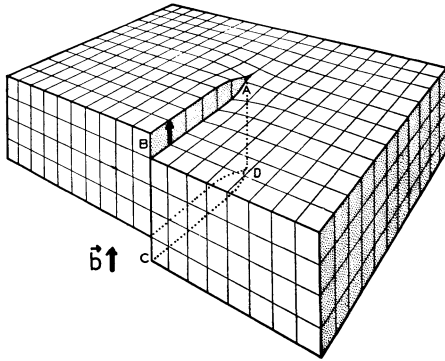


Fig. 13.3. Screw dislocation ([38])

structure in a helical manner (screw dislocation). In this case, the Burgers vector \vec{b} is parallel to the line of dislocation.

Edge- and screw dislocations, as described here, are only limiting cases; intermediates also occur. Dislocations are important in the plastic deformation of metals (Chap. 11.2) (movement of dislocations).

Screw dislocations also play an important role in crystal growth. The deposition of atoms on a step of the helix is always energetically favourable, and these steps persist during the growth of the crystal, permanently.

Dislocations are active regions in crystal faces, and etching gives rise there to characteristic etch-figures (cf. Table 8.11.21). By etching, the concentration of dislocations per cm^2 can be estimated. This varies from virtually zero in the most perfect single crystals of germanium (semiconductor) to 10^{12} per cm^2 in the most strongly deformed metals.

“Whiskers”, or ultrathin, needle crystals, often form with the screw dislocation parallel to the needle axis. They display remarkable mechanical properties. For example, the breaking strength of a NaCl-whisker of $1\ \mu\text{m}$ diameter is as much as $110\ \text{kP mm}^{-2}$.

13.3 Plane Defects

a) *Small Angle Grain Boundaries*. It frequently occurs that different domains of a single crystal are tilted by a small angle with respect to each other. Their boundary faces are small angle grain boundaries, and are built up by a series of dislocations. A small angle grain boundary, consisting entirely of step dislocations, is illustrated in Fig. 13.4. The inclination angle θ which the crystal domains make with each other, may be calculated from the Burgers vector \vec{b} and the separation of the displacements D , since

$$\theta = \frac{\vec{b}}{D}.$$

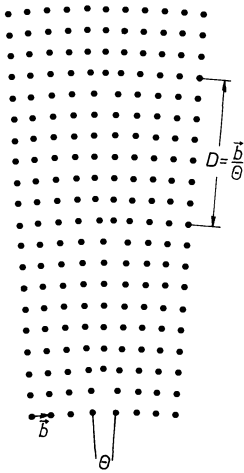


Fig. 13.4. Small angle grain boundary formed from edge dislocations (θ = inclination angle)

b) *Stacking Faults*. Stacking faults are disturbances of the normal layer sequence in the building of a structure. They are most frequently observed in metals (ccp and hcp, Figs. 11.2 and 11.3) and in some layer structures (e.g. graphite, Fig. 11.25). Cobalt crystallises with both cubic and hexagonal closest packing, and it also occurs that both stacking sequences (ABCA... and ABA...) may alternate irregularly. Such an array is only periodic in two dimensions and thus does not qualify to be called a crystal.

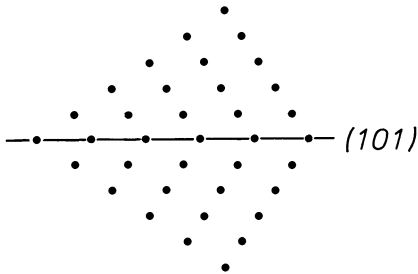


Fig. 13.5. Twin with twin-plane (101)

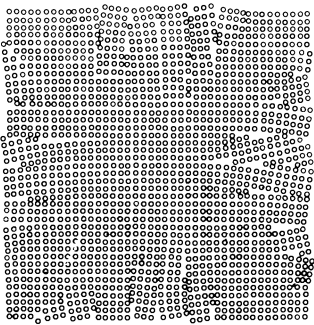


Fig. 13.6. Plane of a real crystal with mosaic blocks. ([1])

c) *Twin Boundaries*. A twin is the regular growing together of crystals of the same sort. The crystals lie in a symmetric relationship to one another. The commonest twinning symmetry elements are 2 and m . Twins can arise during crystal growth (growth twins) or through mechanical stress (deformation twins). In Fig. 13.5, the twin element is a mirror plane parallel to (101).

In general, because of the occurrence of small angle grain boundaries, a crystal may be thought of as being built up of small mosaic blocks, which are only slightly displaced relative to one another. Figure 13.6 shows such a mosaic formation, with the inclination angles grossly exaggerated.

14 Appendix

14.1 Symbols for Crystallographic Items

a, b, c	Crystallographic axes	
$a_1, a_2; a_1, a_2, a_3$	Symmetrically equivalent crystallographic axes	
$\langle a \rangle$	Set of symmetrically equivalent crystallographic axes ($a_1, a_2; a_1, a_2, a_3$)	
$\frac{a}{b} : 1 : \frac{c}{b}$	Morphological axial ratio	
$\vec{a}, \vec{b}, \vec{c}$	Lattice vectors of the unit cell	
$\left. \begin{array}{l} \vec{a} = a_0 \\ \vec{b} = b_0 \\ \vec{c} = c_0 \end{array} \right\}$	$\left. \begin{array}{l} \text{Lengths of vectors} \\ \text{Lengths of cell edges} \end{array} \right\} \text{Lattice parameters}$	
$\left. \begin{array}{l} \alpha = \vec{b} \wedge \vec{c} \\ \beta = \vec{a} \wedge \vec{c} \\ \gamma = \vec{a} \wedge \vec{b} \end{array} \right\}$		$\left. \begin{array}{l} \text{Interaxial angles} \end{array} \right\}$
$\frac{a_0}{b_0} : 1 : \frac{c_0}{b_0}$	Structural axial ratio	




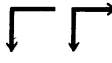



Crystallographic “triples”

x, y, z	Coordinates of the vector $\vec{r} = x\vec{a} + y\vec{b} + z\vec{c}$ Coordinates of a point in the unit cell, $0 \leq x, y, z < 1$
uvw	Coordinates of the lattice translation vector $\vec{r} = u\vec{a} + v\vec{b} + w\vec{c}$ Coordinates of a lattice point, integers and integers + $\frac{1}{2}; \frac{1}{3}, \frac{2}{3}$
$[uvw]$	Indices of a set of parallel lattice lines. Indices of a zone axis or parallel crystal edges
$\langle uvw \rangle$	Indices of a set of symmetrically equivalent lattice lines or directions

- (hkl) Miller indices: Indices of a crystal face or of a set of parallel lattice planes
 - (hkil) Bravais-Miller indices: indices of a crystal face, or of a set of parallel lattice planes, for the hexagonal axes a_1, a_2, a_3, c
 - {hkl} Indices of a set of symmetrically equivalent crystal faces (crystal form) or lattice planes
 - {hkil} Indices of a set of symmetrically equivalent crystal faces (crystal form) or lattice planes, for the hexagonal axes a_1, a_2, a_3, c
 - hkl Laue symbol (indices): indices of a X-ray reflection from a set of parallel lattice planes (hkl)
 - $\vec{a}^*, \vec{b}^*, \vec{c}^*$ Vectors of the unit cell in the reciprocal lattice
- | | | |
|---|--------------------|--|
| $\left. \begin{aligned} \vec{a}^* &= a_0^* \\ \vec{b}^* &= b_0^* \\ \vec{c}^* &= c_0^* \end{aligned} \right\}$ | Lengths of vectors | } Parameters of the reciprocal lattice |
| $\left. \begin{aligned} \alpha^* &= \vec{b}^* \wedge \vec{c}^* \\ \beta^* &= \vec{a}^* \wedge \vec{c}^* \\ \gamma^* &= \vec{a}^* \wedge \vec{b}^* \end{aligned} \right\}$ | Interaxial angles | |

14.2 Symmetry Elements

a) Symmetry elements (planes)

Symmetry element	Glide component $ \vec{g} $	Symbol	Graphical symbol	
			\perp Plane of projection	\parallel Plane of projection ^a
Mirror plane Plane of symmetry	–	m		
Glide plane with axial glide component	$\frac{\vec{a}}{2}$	a		
	$\frac{\vec{b}}{2}$	b		
	$\frac{\vec{c}}{2}$	c		

^a If the z-coordinate is not 0 or $\frac{1}{2}$, its value is given.


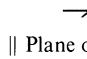









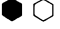






^b In tetragonal and cubic systems only.

Symmetry element	Glide component $ \vec{g} $	Symbol	Graphical symbol	
			\perp Plane of projection	\parallel Plane of projection ^a
Glide plane with diagonal glide component	$\frac{\vec{a} + \vec{b}}{2}$	n		
	$\frac{\vec{a} + \vec{c}}{2}$			
	$\frac{\vec{b} + \vec{c}}{2}$		-----	
	$\frac{\vec{a} + \vec{b} + \vec{c}^b}{2}$			
"Diamond" glide plane	$\frac{\vec{a} + \vec{b}}{4}$	d		
	$\frac{\vec{a} + \vec{c}}{4}$			
	$\frac{\vec{b} + \vec{c}}{4}$		←----- -----→	
	$\frac{\vec{a} + \vec{b} + \vec{c}^b}{4}$			

b) Symmetry elements (axes)

Symmetry element	Screw component $ \vec{s} $	Symbol	Graphical symbol
Onefold rotation axis \equiv identity	-	1	
Inversion centre Centre of symmetry	-	$\bar{1}$	\circ^a
Twofold rotation axis	-	2	 \perp Plane of projection
			 \parallel Plane of projection ^a

Symmetry elements (axes) (continued)

Symmetry element	Screw component $ \bar{s} $	Symbol	Graphical symbol
Twofold screw axis	$\frac{1}{2} \bar{\tau} $	2_1	 ⊥ Plane of projection
			 Plane of projection ^a
Threefold rotation axis	-	3	
Threefold rotoinversion axis	-	$\bar{3}$	
Threefold screw axes	$\frac{1}{3} \bar{\tau} $	3_1	
	$\frac{2}{3} \bar{\tau} $	3_2	
Fourfold rotation axis	-	4	
Fourfold rotoinversion axis	-	$\bar{4}$	
Fourfold screw axes	$\frac{1}{4} \bar{\tau} $	4_1	
	$\frac{2}{4} \bar{\tau} $	4_2	
	$\frac{3}{4} \bar{\tau} $	4_3	
Sixfold rotation axis	-	6	
Sixfold rotoinversion axis	-	$\bar{6}$	
Sixfold screw axes	$\frac{1}{6}c_0$	6_1	
	$\frac{2}{6}c_0$	6_2	
	$\frac{3}{6}c_0$	6_3	
	$\frac{4}{6}c_0$	6_4	
	$\frac{5}{6}c_0$	6_5	

c) Symmetry directions in the seven crystal systems, cf. Table 7.2.

d) Characteristic symmetry elements in the seven crystal systems, cf. Table 8.9.

14.3 Calculation of Interatomic Distances and Angles in Crystal Structures

Specific interatomic distances (e.g. bond lengths) and the angles between the corresponding vectors (bond angles) are often of great interest.

Interatomic Distances. The distance l between atoms A (x_1, y_1, z_1) and B (x_2, y_2, z_2) may be calculated by use of the following formulae:

Crystal system	l
Triclinic	$\{(\Delta x)^2 a_0^2 + (\Delta y)^2 b_0^2 + (\Delta z)^2 c_0^2 + 2\Delta x \Delta y a_0 b_0 \cos \gamma + 2\Delta x \Delta z a_0 c_0 \cos \beta + 2\Delta y \Delta z b_0 c_0 \cos \alpha\}^{1/2}$
Monoclinic	$\{(\Delta x)^2 a_0^2 + (\Delta y)^2 b_0^2 + (\Delta z)^2 c_0^2 + 2\Delta x \Delta z a_0 c_0 \cos \beta\}^{1/2}$
Orthorhombic	$\{(\Delta x)^2 a_0^2 + (\Delta y)^2 b_0^2 + (\Delta z)^2 c_0^2\}^{1/2}$
Tetragonal	$\{(\Delta x)^2 + (\Delta y)^2 + (\Delta z)^2\}^{1/2}$
Trigonal or hexagonal	$\{(\Delta x)^2 + (\Delta y)^2 - \Delta x \Delta y + (\Delta z)^2\}^{1/2}$
Cubic	$\{(\Delta x)^2 + (\Delta y)^2 + (\Delta z)^2\}^{1/2}$

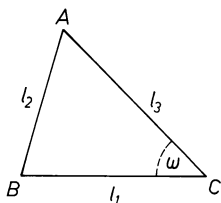


Fig. 14.1. The triangle formed by atoms, A, B and C

Angles. The angle ω , relating the atoms A, B and C (Fig. 14.1) may be readily calculated by calculating the lengths of the three edges, l_1 , l_2 and l_3 of the triangle ABC and applying the cosine rule:

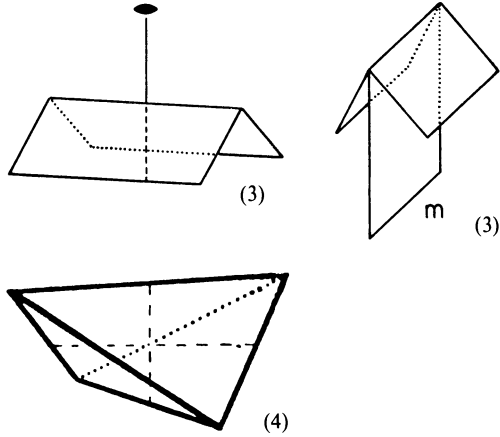
$$\cos \omega = \frac{l_1^2 - l_2^2 + l_3^2}{2l_1 l_3}.$$

14.4 Crystal Forms (Table 14.1)

Table 14.1. The 47 crystal forms

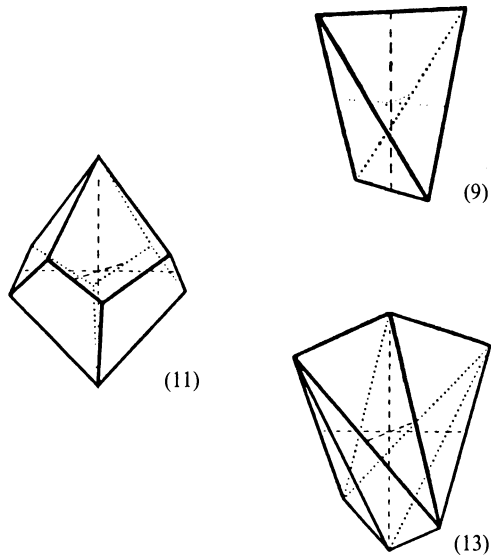
14.1.1 Triclinic, monoclinic and orthorhombic systems

1. Pedion
(Monohedron)
2. Pinacoid
(Parallelohedron), Fig. 8.7g
3. Dihedron
(Sphenoid (2), Dome (m))
4. Rhombic disphenoid
5. Rhombic pyramid,
Exercise 8.15(5)
6. Rhombic prism,
Exercise 8.15(1)
7. Rhombic dipyramid,
Exercise 8.15(9)



14.1.2 The tetragonal system

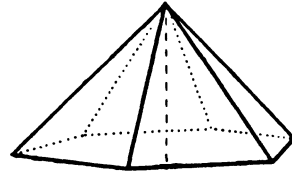
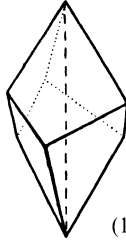
8. Tetragonal pyramid,
Fig. 8.10b, c
 9. Tetragonal disphenoid
 10. Tetragonal prism,
Fig. 8.7e, f
 11. Tetragonal
trapezohedron
 12. Ditetragonal pyramid,
Fig. 8.10a
 13. Tetragonal
scalenoedron
 14. Tetragonal dipyramid,
Fig. 8.7c, d
 15. Ditetragonal prism,
Fig. 8.7b
 16. Ditetragonal dipyramid,
Fig. 8.7a
- 1 Pedion
2 Pinacoid



Some crystal forms after Niggli [32]

14.1.3 The hexagonal (trigonal) system

17. Trigonal pyramid,
Exercise 8.15(7)



18. Trigonal prism,
Exercise 8.15(3)

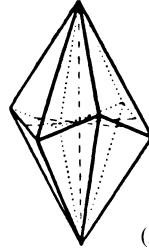
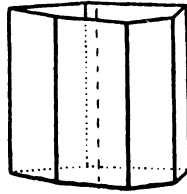
(19)

(20)

19. Trigonal trapezohedron

20. Ditrigonal pyramid

21. Rhombohedron,
Exercise 8.15(16)



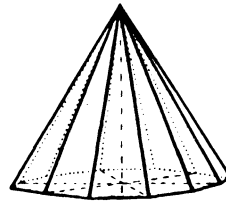
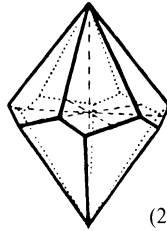
(22)

(26)

22. Ditrigonal prism

23. Hexagonal pyramid,
Exercise 8.15(8)

24. Trigonal dipyramid,
Exercise 8.15(11)



(27)

(28)

25. Hexagonal prism,
Exercise 8.15(4)

26. Ditrigonal scalenohedron

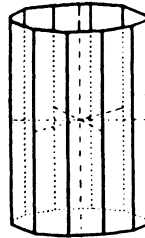
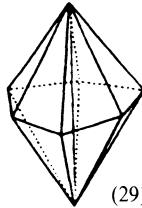
27. Hexagonal trapezohedron

28. Dihexagonal pyramid

29. Ditrigonal dipyramid

30. Dihexagonal prism

31. Hexagonal dipyramid,
Exercise 8.15(12)

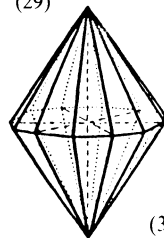


(29)

(30)

32. Dihexagonal dipyramid

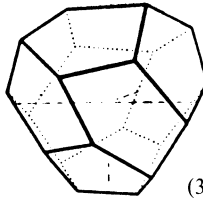
- 1 Pedion
- 2 Pinacoid



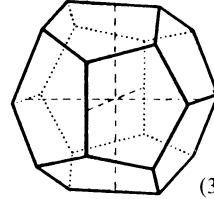
(32)

14.1.4 The cubic system

33. Tetrahedron,
Exercise 8.15(15)



(36)

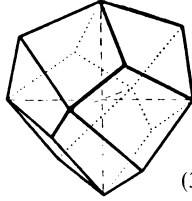


(37)

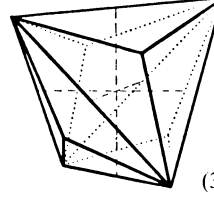
34. Hexahedron (cube),
Exercise 8.15(13)

35. Octahedron,
Exercise 8.15(14)

36. Tetartoid (Tetrahedral
pentagon-dodecahedron)



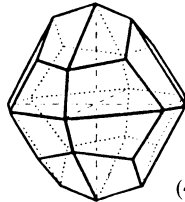
(38)



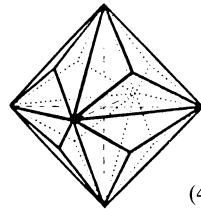
(39)

37. Pyritohedron
(pentagon-dodecahedron)

38. Deltoid-dodecahedron
(deltohedron)



(41)

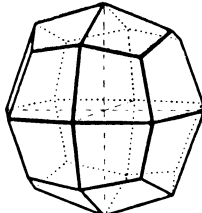


(42)

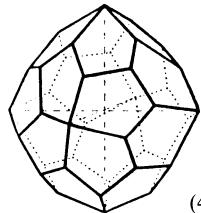
39. Tristetrahedron

40. Rhomb-dodecahedron,
Fig. 1.1 a

41. Diploid
(disdodecahedron)



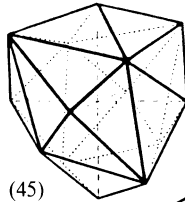
(43)



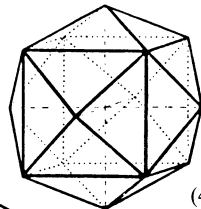
(44)

42. Trisoctahedron

43. Trapezohedron
(deltoid-icositetrahedron)



(45)

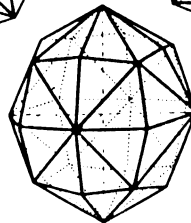


(46)

44. Gyroid

45. Hexatetrahedron
(hexakistetrahedron)

46. Tetrahexahedron
(tetrakisshexahedron)



(47)

47. Hexaoctahedron
(hexakisshoctahedron)

15 Solutions to the Exercises

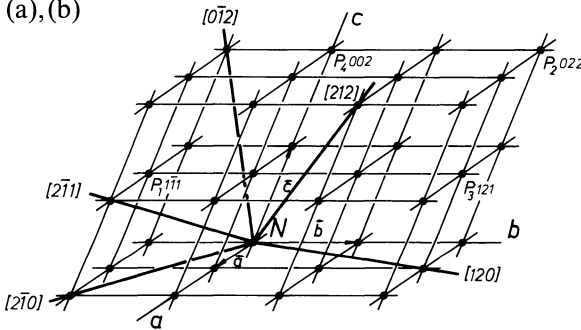
The solutions to a few exercises are incomplete, as the drawings would require too much space.

Chapter 1

- 1.1 $22.41 \text{ (the molar volume)}/6.023 \times 10^{23} \text{ (the Avogadro number, } N_A) = 37191 \text{ \AA}^3$, which corresponds to a cube with an edge of 33.4 \AA .
- 1.2 0.046% .
- 1.3 No glass can be a crystal, nor any crystal a glass!

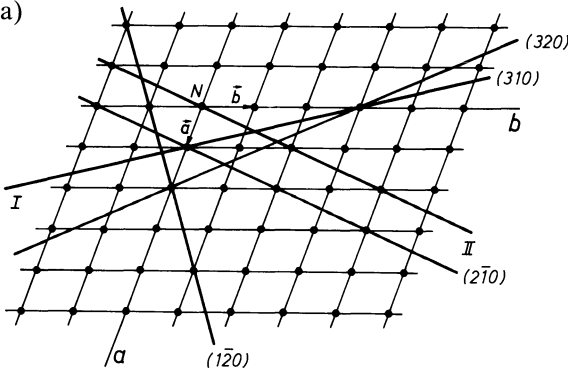
Chapter 2

- 2.2 (a), (b)



- (c) $(1\bar{1}2)$.

- 2.3 (a)



- (b) $[001]$.

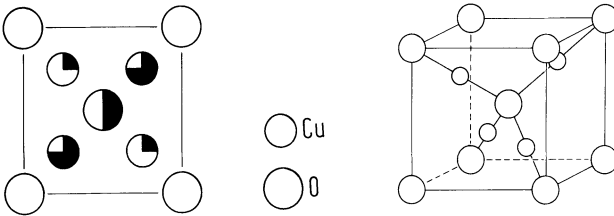
2.4 $(\bar{1}\bar{1}1)$, (102) , $(\bar{1}\bar{2}0)$, $(\bar{1}\bar{1}\bar{1})$
 $[\bar{1}\bar{1}1]$, $[10\bar{1}]$, $[\bar{2}10]$, $[01\bar{2}]$.

2.5 a) $\beta = \gamma = 90^\circ$
 b) $a_0 = b_0$; $\alpha = \beta = 90^\circ$
 c) $a_0 = b_0 = c_0$; $\alpha = \beta = \gamma$

2.6 (hkl) and $(\bar{h}\bar{k}\bar{l})$ belong to the same set of parallel planes; $[uvw]$ and $[\bar{u}\bar{v}\bar{w}]$ are opposite directions.

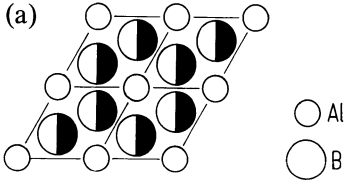
Chapter 3

3.1 (a)



(b) Cu_2O , $Z = 2$, (c) $\frac{a_0}{4}\sqrt{3} = 1.85 \text{ \AA}$, (d) 6.1 g/cm^3 .

3.2 (a)



(b) 2.37 \AA (c) 3.20 g/cm^3

3.3 All combinations of $0, \frac{1}{2}$, and 1 from $0, 0, 0$, to $1, 1, 1$. Figure 2.5 includes a partial solution; see also p. 91

3.4 $x, 0, 0$; $0, y, 0$; $0, 0, z$
 $x, 1, 0$; $1, y, 0$; $1, 0, z$
 $x, 0, 1$; $0, y, 1$; $0, 1, z$
 $x, 1, 1$; $1, y, 1$; $1, 1, z$

3.5 $x, y, 0$; $x, 0, z$; $0, y, z$
 $x, y, 1$; $x, 1, z$; $1, y, z$

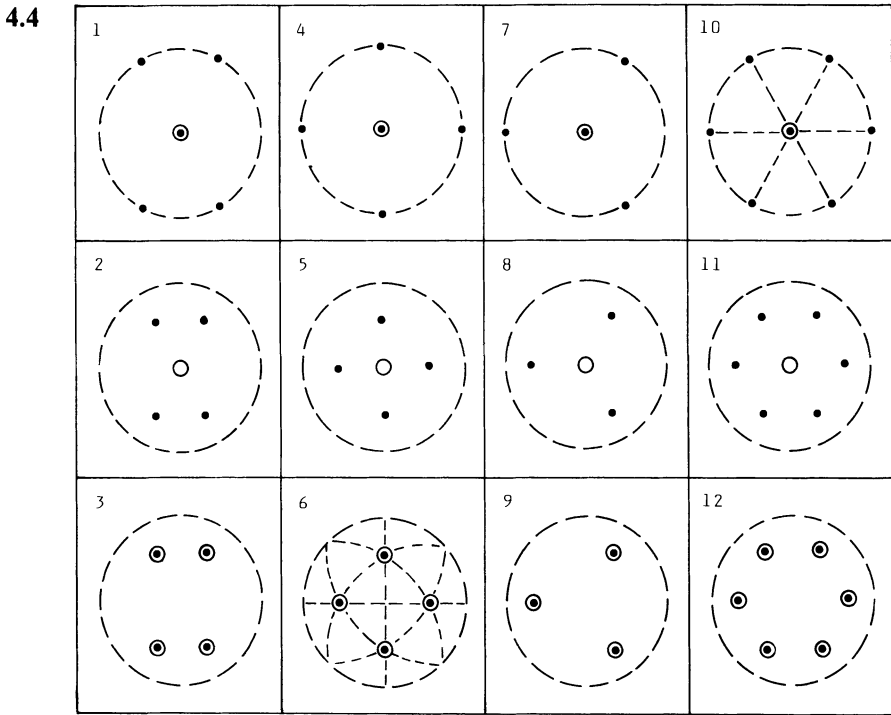
3.6 $x, y, \frac{1}{4}$; $x, \frac{1}{2}, z$; $x, \frac{1}{2}, \frac{1}{4}$.

Chapter 4

4.2 (1) + (2) = Fig. 4.11 a (lower part).



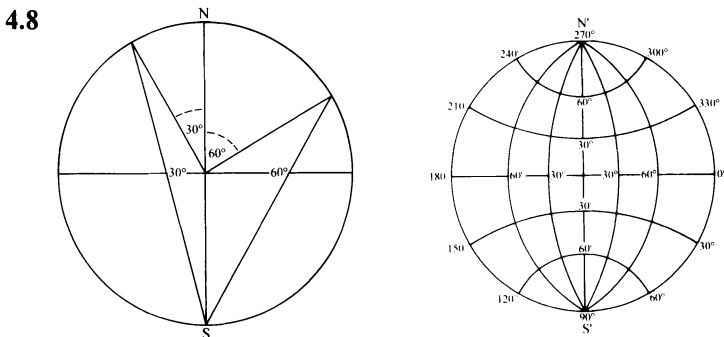
4.3 (1) = Exercise 4.4 (4) (2) = Exercise 4.4 (10).



4.5 Cf. Exercise 4.4 (6) and (10).

- 4.6
1. Trigonal pyramid and pedion.
 2. Tetragonal dipyramid.
 3. Hexahedron, tetragonal prism and pinacoid, rectangular box, orthogonal axes.
 4. Hexagonal prism and pinacoid, hexagonal axes.

4.7 Cf. Fig. 4.18.



- 4.9
- a) $60^\circ/229^\circ$; 58°
 - b) $46^\circ/260^\circ$; 30°
 - c) $44^\circ/32^\circ$; 69°

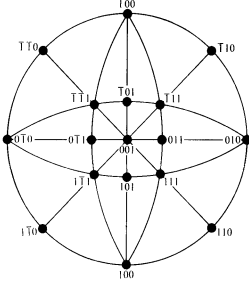
4.10 100° ; 44° und 280° ; -44° , parallel

4.11 They lie in a plane, perpendicular to the zone axis.

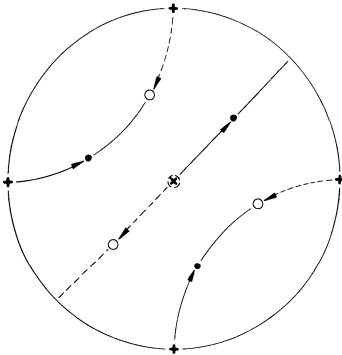
4.12 Cf. Fig. 6.13f (432).

4.13 Cf. Fig. 4.11. The stereograms in Exercises 4.12 and 4.13 are geometrically equivalent.

4.14

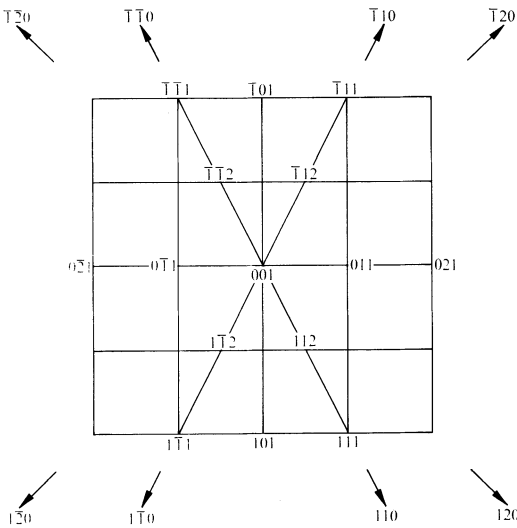



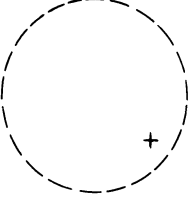
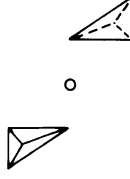
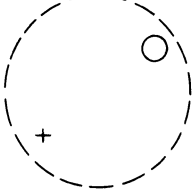
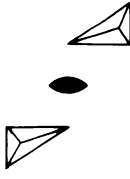
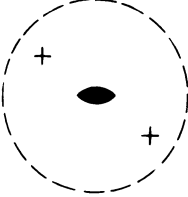

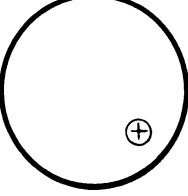
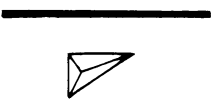
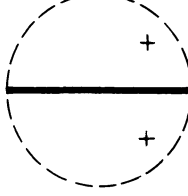
4.15 Hexahedron $1 + \circ$; Hexahedron $2 \cdot \circ$



4.16 Cf. Orthographic projection in 0, 0, 0 of Fig. 9.15

4.17



X	1	a		b		a		b		\bar{X}	T
2					$\bar{Z} = m$						

to 5.1

\bar{X}	$\bar{3}$	$\bar{4}$	$\bar{6}$
b			
a			
b			
a			
X	3	4	6

to 5.1

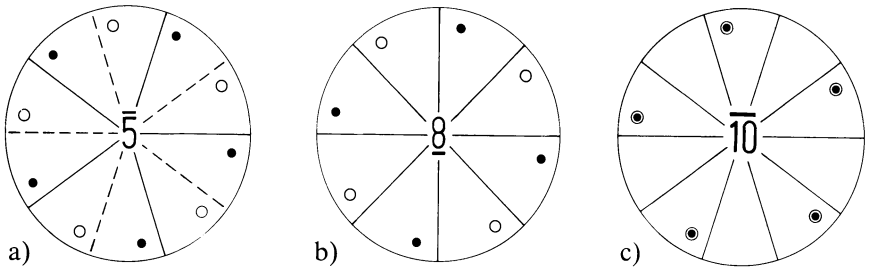
Chapter 5

5.1 Cf. pp. 283 and 284.

5.2

5.3 Parallel.

5.4



5.5 $\bar{1} \equiv$ Inversion centre, $\bar{2} \equiv m$, $\bar{3} \equiv 3 + \bar{1}$, $\bar{5} \equiv 5 + \bar{1}$,
 $\bar{6} \equiv 3 \perp m$, $\bar{10} \equiv 5 \perp m$.

5.6 \bar{X} (odd): $\bar{1}$, $\bar{3}$, $\bar{5} \dots$

5.7 Trigonal, tetragonal, hexagonal pyramid; trigonal dipyramid.

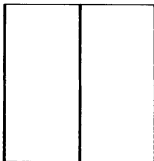
5.8 Rhombus¹, equilateral triangle, square, regular hexagon.

5.9 Cf. Fig. 4.21.

Chapter 6

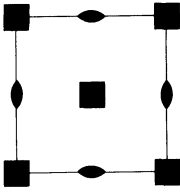
6.1 Cf. Figs. 6.6 and 5.5b.

6.2 (1) (2) Cf. Fig. 6.6a, (3) Cf. Fig. 6.6c,



¹ Solids with rectangular or parallelogram cross-sections are not prisms in the crystallographic sense as their faces are not all equivalent (cf. Chapter 8.2.1).

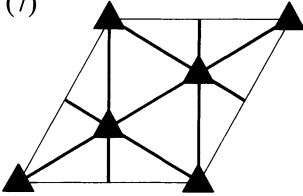
(4)



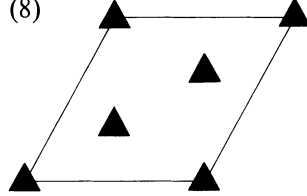
(5) Cf. Fig. 6.6d,

(6) Cf. Fig. 5.5b,

(7)

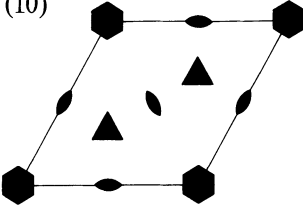


(8)

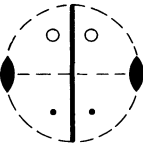


(9) No symmetry except lattice translation.

(10)



6.3 (a)



(b)

- (1) 2 in $x, \frac{1}{2}, 0$,
- (2) m in $x, y, \frac{1}{2}$,
- (3) $\bar{1}$ in $\frac{1}{2}, 0, \frac{1}{2}$,
- (4) m in $x, y, 0$,
- (5) $\bar{1}$ in $\frac{1}{2}, \frac{1}{2}, \frac{1}{2}$,
- (6) 2 in $\frac{1}{2}, y, \frac{1}{2}$,
- (7) 2 in $0, \frac{1}{2}, z$.

6.4 (a) Cf. Fig. 6.9f (right) and Fig. 8.11.7

- (b) (1) 2 in $x, \frac{1}{2}, \frac{1}{2}$,
- (2) m in $x, y, \frac{1}{2}$,
- (3) 2 in $\frac{1}{2}, \frac{1}{2}, z$,
- (4) m in $x, 0, z$.

6.5 (a) cubic P, (b) monoclinic P, (c) triclinic P, (d) orthorhombic P, (e) tetragonal P, (f) hexagonal P.

6.6 (a) Cf. Fig. 6.7a–6.12a,
 (b) Cf. Fig. 6.7d–6.12d,
 (c) and (d) Cf. Figs. 6.18–6.23.

6.7 (A), (B), C, I, F.

6.8 I.

Chapter 8

8.1a The directions parallel and antiparallel to a polar axis have distinct physical properties.

8.1b (1) $\bar{1}$, (2) $m \perp X$, (3) $2 \perp X$ [also valid for 4 and 6].

8.2 No. Rotoinversion implies rotation through an angle followed by inversion. The two ends of the axis remain equivalent.

8.3 $\bar{1}$, $2/m$, $\bar{3}$, $4/m$, $6/m$.

8.4

622	6mm	$\bar{6}m2$	$6/m\ 2/m\ 2/m$
422	4mm	$\bar{4}2m$	$4/m\ 2/m\ 2/m$
32	3m	$\bar{3}\ 2/m$	$\bar{3}\ 2/m$
222	mm2	mm2	$2/m\ 2/m\ 2/m$

Cf. also Figs. 6.9e, f–6.12e, f.

8.5

23	$\bar{4}3m$	432
$2/m\ \bar{3}$	$4/m\ \bar{3}\ 2/m$	$4/m\ \bar{3}\ 2/m$

Cf. also Fig. 6.13e, f.

8.6 $3m$, 32 , $\bar{3}$, 3 .

8.7 Cf. Table 8.4.

8.8 Cf. p. 145.

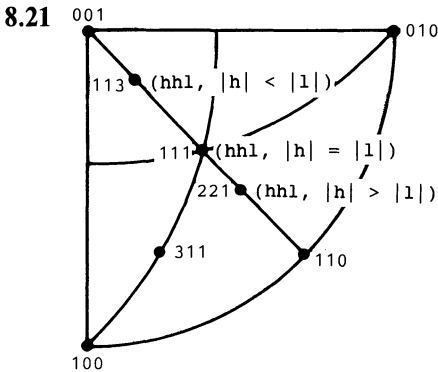
8.9 (1) $\bar{4}2m$, (2) m , (3) 32 , (4) $6mm$, (5) $mm2$, (6) $\bar{4}3m$.

8.10 Cf. Figs. 6.8e, f–6.13e, f.

8.11 (1) $6/m\ 2/m\ 2/m$, (2)–(4) $mm2$, (5) $2/m\ 2/m\ 2/m$, (6) $mm2$, (7) m , (8) $\bar{6}m2$, (9) $4/m\ \bar{3}\ 2/m$, (10) $4mm$, (11) $4/m\ 2/m\ 2/m$, (12) $mm2$, (13) $3m$, (14) $mm2$, (15) $\bar{4}3m$, (16) $3m$, (17) $mm2$, (18) = (16), (19) = (15), (20) $3m$, (21) + (22) $\bar{6}m2$, (23) m , (24) $mm2$, (25) m , (26) 2 , (27) 2 , (28) $3m$, (29) m , (30) + (31) 1 , (32) $\bar{3}\ 2/m$, (33) $mm2$, (34) 2 , (35) $mm2$, (36) $4/m\ 2/m\ 2/m$, (37) $4mm$, (38) $\bar{4}2m$, (39) $2/m\ 2/m\ 2/m$, (40) $mm2$, (41) $2/m$, (42) + (43) m , (44) + (45) 2 , (46)–(49) 1
 (a) Enantiomers: (26)–(27), (30)–(31), (44)–(45), (46)–(47), (48)–(49).
 (b) Polar molecules: (2)–(4), (7), (8), (10), (12), (14), (16)–(18), (20), (23)–(31), (33)–(35), (37), (40), (42)–(49)

8.12 (1) Bent, (2) pyramidal, (3) Table 8.11.14, (4) Fig. 8.9.

- 8.13** $mm2$ (0°); 2 ($0^\circ < \varphi < 180^\circ$);
 $2/m$ (180°); 2 ($180^\circ < \varphi < 360^\circ$).
- 8.14** Yes; $mm2(+)$; $2/m(0)$.
- 8.15** (1) $2/m\ 2/m\ 2/m$, (2) $4/m\ 2/m\ 2/m$, (3) $\bar{6}\ m2$, (4) $6/m\ 2/m\ 2/m$,
 (5) $mm2$, (6) $4mm$, (7) $3m$, (8) $6mm$, (9) $2/m\ 2/m\ 2/m$,
 (10) $4/m\ 2/m\ 2/m$, (11) $\bar{6}\ m2$, (12) $6/m\ 2/m\ 2/m$, (13) + (14) $4/m\ \bar{3}\ 2/m$,
 (15) $\bar{4}\ 3m$, (16) $\bar{3}\ 2/m$.
- 8.16** (3), (5), (6), (7), (8), (11), (15).
- 8.17** Faces + vertices = edges + 2 (Euler).
- 8.18** a) Cf. Fig. 8.8.
 b) Ditetragonal dipyramid; from $(hk0)$ arise (hkl) and $(hk\bar{l})$ etc., or from (210) arise, for example, (211) and $(21\bar{1})$ etc.
- 8.19** a) Cf. Fig. 8.12a.
 b) Hexagonal dipyramid; from $(hki0)$ arise $(hkil)$ and $(hki\bar{l})$ etc. or from $(21\bar{3}0)$ arise, for example, $(21\bar{3}1)$ and $(21\bar{3}\bar{1})$.
- 8.20** (1), (2): Table 8.4; (3), (4): Table 8.7;
 (5), (6), (7): Table 8.5; (8), (9): Table 8.6.



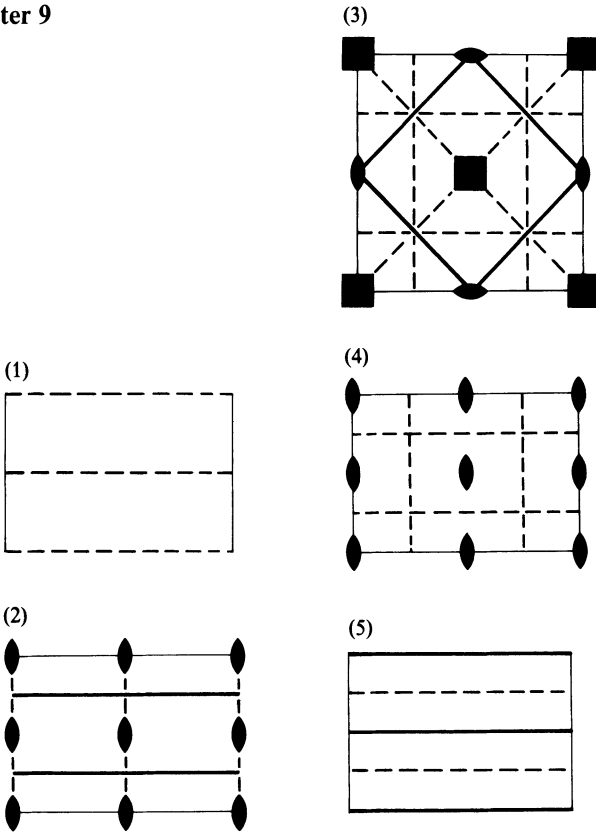
(Part of Fig. 8.15)

The pole (113) corresponds to the crystal form trapezohedron or deltoic icositetrahedron $\{311\}$ or $\{hkk\}$. (311) lies in the asymmetric face unit.

- 8.22** $\bar{6}m2$: ($m..$); ditrigonal prism $\{hki0\}$; hexagonal prism $\{11\bar{2}0\}$
 $\bar{3}\ 2/m$: ($.m.$); rhombohedron $\{h0\bar{h}1\}$; hexagonal prism $\{10\bar{1}0\}$
 $6mm$: ($.m.$); hexagonal pyramid $\{h0\bar{h}1\}$; hexagonal prism $\{10\bar{1}0\}$
 ($.m.$; hexagonal pyramid $\{hh\bar{2}\bar{h}1\}$; hexagonal prism $\{11\bar{2}0\}$
 $3m$: ($.m.$), trigonal pyramid $\{h0\bar{h}1\}$; trigonal prism $\{10\bar{1}0\}$.

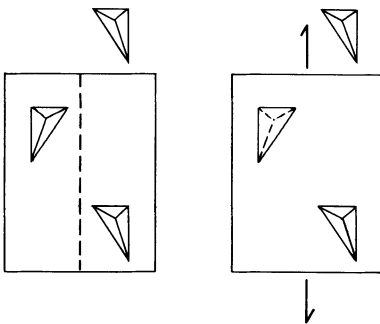
Chapter 9

9.1

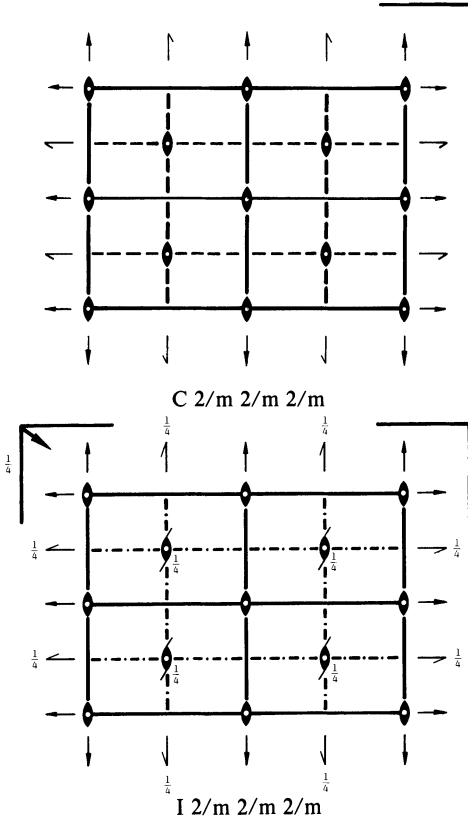


- 9.2 (a) $x, y, 1-z$, (b) $x, \frac{1}{2}-y, z$, (c) $\frac{1}{2}+x, y, \frac{1}{2}-z$, (d) $\frac{1}{2}-x, \frac{1}{2}+y, z$,
 (e) $x, \frac{1}{2}-y, \frac{1}{2}+z$, (f) $\frac{1}{2}-x, \frac{1}{2}+y, \frac{1}{2}+z$, (g) $\frac{1}{2}+x, \frac{1}{2}+y, \bar{z}$,
 (h) $\frac{1}{2}+x, \bar{y}, \frac{1}{2}+z$, (i) $\frac{1}{2}-x, y, \bar{z}$, (j) $1-x, \bar{y}, \frac{1}{2}+z$, (k) $\bar{x}, \frac{1}{2}+y, \frac{1}{2}-z$,
 (l) $\frac{1}{2}-x, \frac{1}{2}-y, z$, (m) $\bar{y}, x, \frac{1}{4}+z; \bar{x}, \bar{y}, \frac{1}{2}+z; y, \bar{x}, \frac{3}{4}+z$, (n) $\bar{y}, x-y, \frac{1}{3}+z;$
 $\bar{x}+y, \bar{x}, \frac{2}{3}+z$.

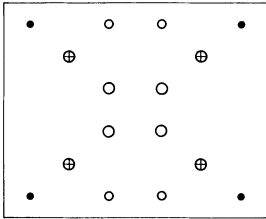
9.3 The difference between the operation of a glide plane and a 2_1 is only evident when a “fully asymmetric point” is considered. An example is the asymmetric pyramid in the following figure.



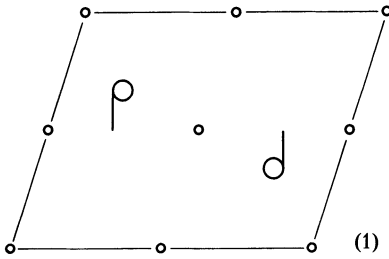
9.5



9.6

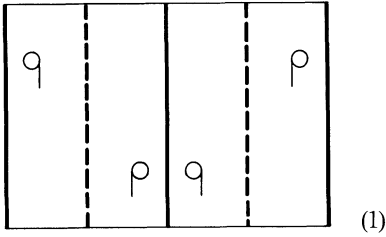


9.7

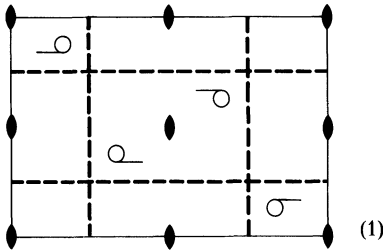


(a) (2) $x, y, z; \bar{x}, \bar{y}, \bar{z}$,² (3) 2, (4) $P\bar{1}$, (5) on all $\bar{1}$, one-fold.

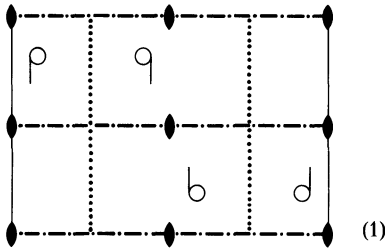
² Coordinates are given as in *International Tables* [18] [17] [14], i.e. instead of $1-x, 1-y, 1-z$ is written $\bar{x}, \bar{y}, \bar{z}$.



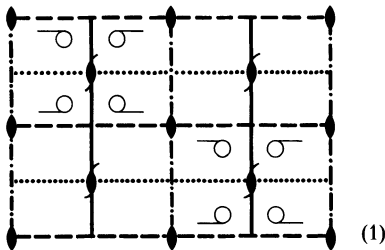
- (b) (2) $x, y, z; x, \bar{y}, z; \frac{1}{2} + x, \frac{1}{2} - y, z; \frac{1}{2} + x, \frac{1}{2} + y, z$, (3) 4, (4) C_m , (5) on m , 2-fold.



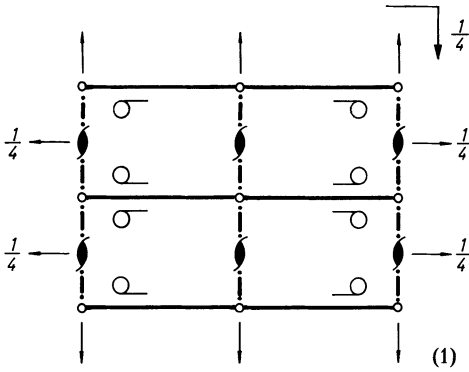
- (c) (2) $x, y, z; \frac{1}{2} + x, \frac{1}{2} - y, z; \frac{1}{2} - x, \frac{1}{2} + y, z; \bar{x}, \bar{y}, z$, (3) 4, (4) Pba_2 , (5) on 2, 2-fold.



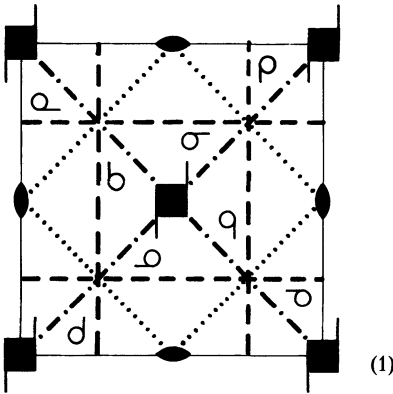
- (d) (2) $x, y, z; x, \frac{1}{2} - y, \frac{1}{2} + z; \bar{x}, \frac{1}{2} + y, \frac{1}{2} + z; \bar{x}, \bar{y}, z$, (3) 4, (4) Pnc_2 , (5) on 2, 2-fold.



- (e) (2) $x, y, z; x, \frac{1}{2} - y, z; \frac{1}{2} - x, y, \frac{1}{2} + z; \frac{1}{2} - x, \frac{1}{2} - y, \frac{1}{2} + z; \frac{1}{2} + x, \frac{1}{2} + y, \frac{1}{2} + z; \frac{1}{2} + x, \bar{y}, \frac{1}{2} + z; \bar{x}, \frac{1}{2} + y, z; \bar{x}, \bar{y}, z$. (3) 8, (4) Ibm_2 , (5) on 2, 4-fold.



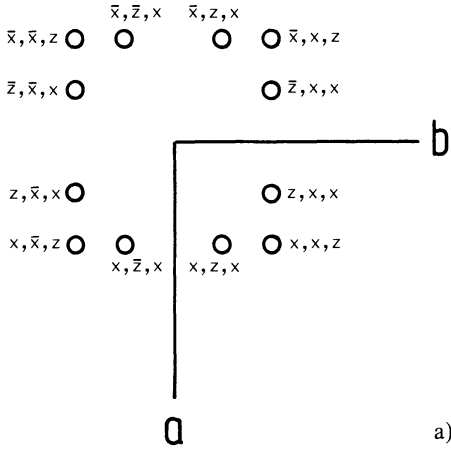
- (f) (2) $x, y, z; \frac{1}{2} - x, \frac{1}{2} - z; \frac{1}{2} + x, y, \frac{1}{2} - z; \bar{x}, y, z; x, \bar{y}, \bar{z}; \frac{1}{2} - x, \bar{y}, \frac{1}{2} + z;$
 $\frac{1}{2} + x, \bar{y}, \frac{1}{2} + z; \bar{x}, \bar{y}, \bar{z},$ (3) 8, (4) $P 2/m 2/n 2_1/a,$ (5) on m and 2, 4-fold, on $\bar{1},$ 2-fold.



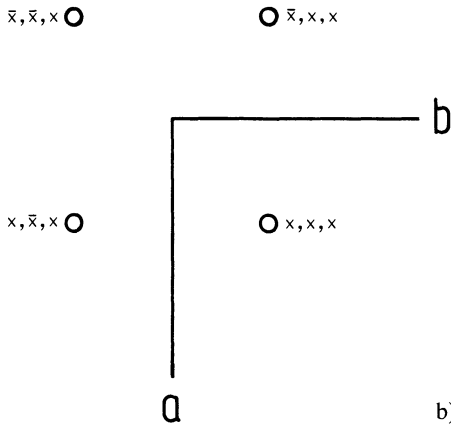
- (g) (2) $x, y, z; \bar{x}, \bar{y}, z; \bar{y}, x, \frac{1}{2} + z; y, \bar{x}, \frac{1}{2} + z; \frac{1}{2} + x, \frac{1}{2} - y, z; \frac{1}{2} - x, \frac{1}{2} + y, z;$
 $\frac{1}{2} - y, \frac{1}{2} - x, \frac{1}{2} + z; \frac{1}{2} + y, \frac{1}{2} + x, \frac{1}{2} + z.$ (3) 8, (4) $P4_2bc,$ (5) on 2, 4-fold.

- 9.8 a) 1. $x, y, z; \bar{x}, \bar{y}, z; x - y, x, z + \frac{1}{3}; \bar{x} + y, \bar{x}, z + \frac{1}{3};$
 $\bar{y}, x - y, z + \frac{2}{3}; y, \bar{x} + y, z + \frac{2}{3}$
 2. 2 in $\frac{1}{2}, 0, z; \frac{1}{2}, \frac{1}{2}, z; 0, \frac{1}{2}, z; 3_2$ in $\frac{2}{3}, \frac{1}{3}, z; \frac{1}{3}, \frac{2}{3}, z$
 3. $3_2, 2$
 b) 1. $x, y, z; \bar{y}, x - y, z; \bar{x} + y, \bar{x}, z; x - y, x, z + \frac{1}{2};$
 $\bar{x}, \bar{y}, z + \frac{1}{2}; y, \bar{x} + y, z + \frac{1}{2}$
 2. 2_1 in $\frac{1}{2}, 0, z; \frac{1}{2}, \frac{1}{2}, z; 0, \frac{1}{2}, z; 3$ in $\frac{2}{3}, \frac{1}{3}, z; \frac{1}{3}, \frac{2}{3}, z$
 3. $3, 2_1$

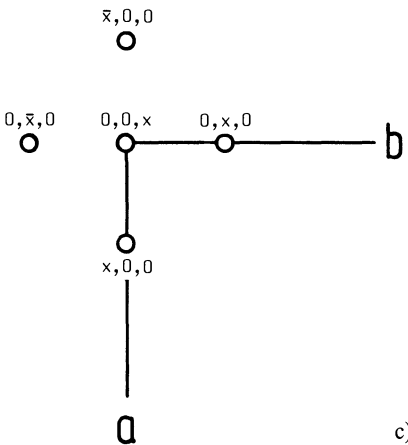
9.9



24
..m



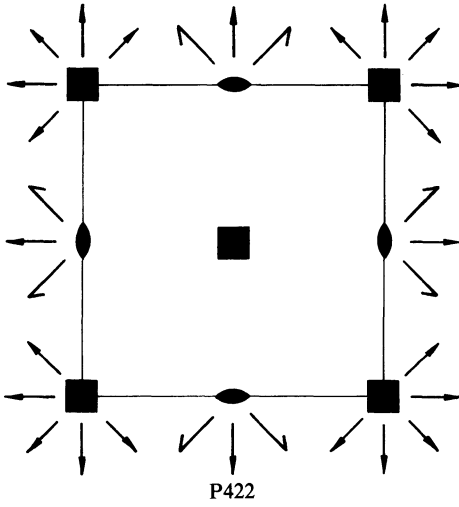
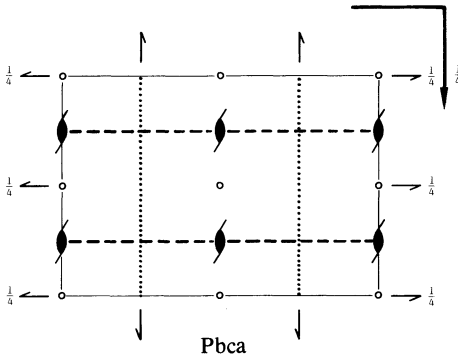
8
.3m



6
4m . m

Coordinates are not given for those points which are reflected by m to locations below the plane $x, y, 0$. The third coordinate of each triple must be taken to have both a plus and a minus sign.

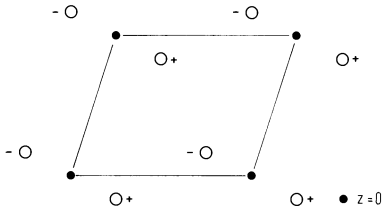
9.10 $P2_1/c$ (Fig. 9.9a), $Pna2_1$ (Fig. 9.12), $Pmna$ (Exercise 9.6f).



9.11 This is absurd: an a -glide plane cannot be normal to the a -axis ...

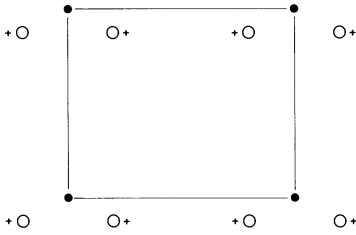
Chapter 10

10.1 $P\bar{1}$:



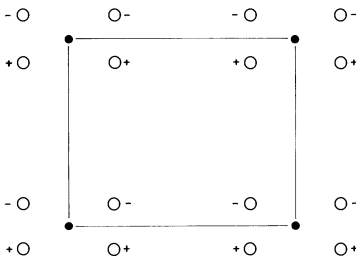
- (a) AB_2 , (b) $Z=1$, (c) linear,
(d) $\infty/m\bar{m}$, (e) $\bar{1}$.

Pm :



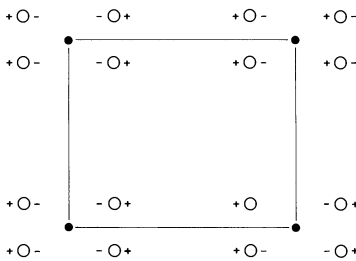
- (a) AB_2 , (b) $Z=1$,
(c) bent, (d) $mm2$, (e) m .

$P 2/m$:



- (a) AB_4 , (b) $Z=1$, (c) planar
[4]-coordination
(rectangular),
(d) $2/m 2/m 2/m$, (e) $2/m$.

$P 2/m 2/m 2/m$:



- (a) AB_8 , (b) $Z=1$,
(c) [8]-coordination
(rectangular parallelepiped),
(d) and (e) $2/m 2/m 2/m$.

Chapter 11

11.1 Cf. Table 11.1 d and h.

11.2 (a) cub. P; Po: 0, 0, 0

(b) cub. I; W: 0, 0, 0

(c) hex. P; Mg: 0, 0, 0; $\frac{2}{3}, \frac{1}{3}, \frac{1}{2}$

(d) cub. F; Cu: 0, 0, 0

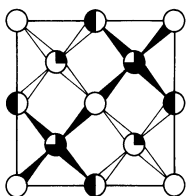
(e) 6_3 in $\frac{1}{3}, \frac{2}{3}, z$; $\bar{6}$ in 0, 0, z

11.3 (a) 1.675 Å, (b) 1.37 Å, (c) 1.605 Å, (d) 1.28 Å.

11.4 1.63.

11.5 (a) 0.52, (b) 0.68, (c) 0.74, (d) 0.74.

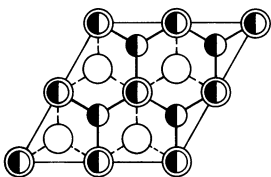
11.6 (a) Cf. Fig. 11.14



(b) 1.546 Å, (c) 8, (d) each C is tetrahedrally coordinated by 4C.

(e) The two structures have the same geometry.

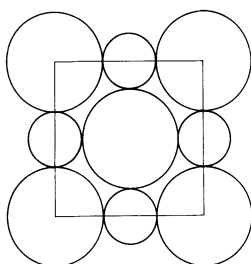
11.7 (a) Cf. 11.15a



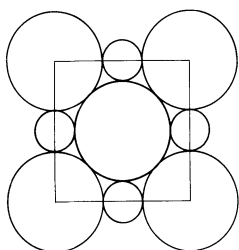
(b) 1.42 Å, (c) 4, (d) 3.35 Å, (d) $\rho_D = 3.50 \text{ g/cm}^3$;
 $\rho_G = 2.27 \text{ g/cm}^3$.

11.8 Li^+ : 0.76 Å; Cl^- : 1.81 Å; 0.79

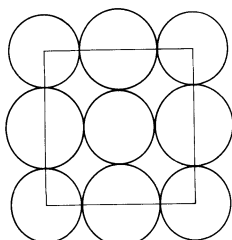
11.9



NaCl

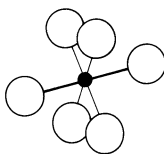


LiCl



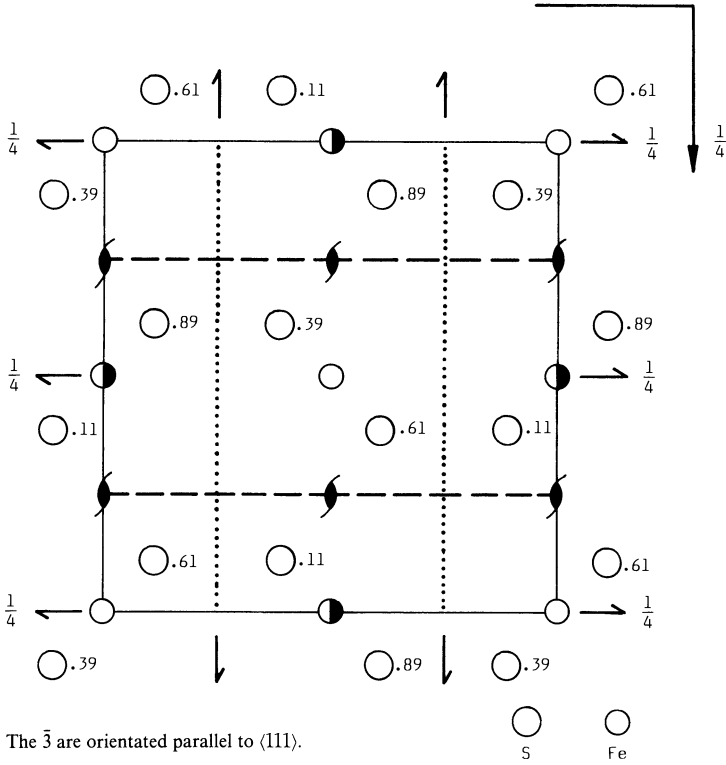
RbF

11.10



1.95 Å (distances indicated by thick lines), 1.97 Å (distances indicated by thin lines), cf. Fig. 9.18.

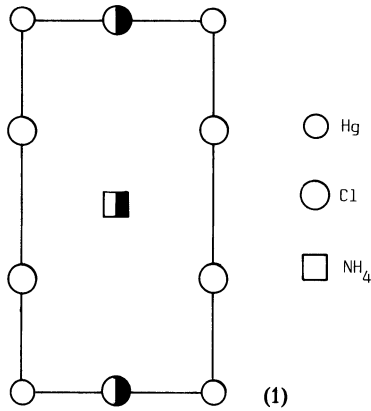
11.11



The $\bar{3}$ are orientated parallel to (111).

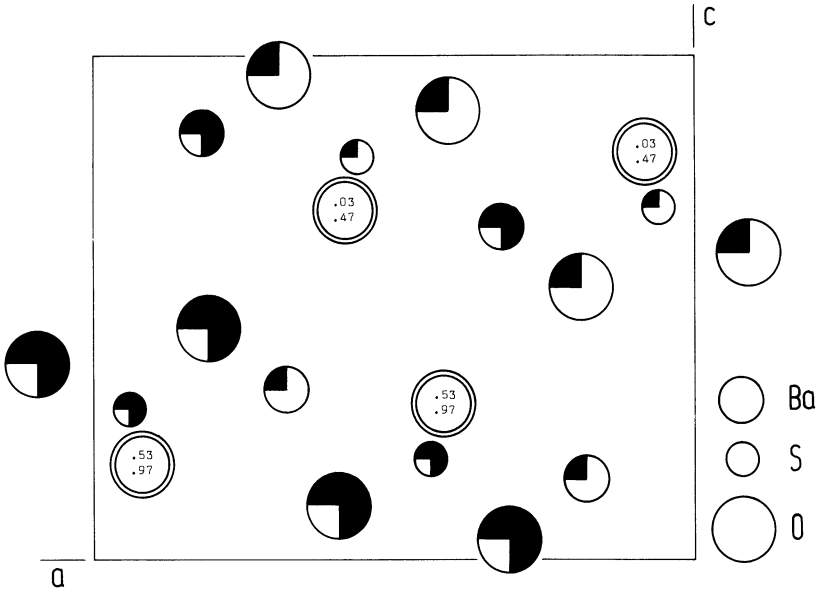
(3) 4, (4) Fe-S: 2.27 Å; S-S: 2.06 Å.

11.12



(2) HgNH₄Cl₃, Z=1, (3) Hg^[6] (octahedron), NH₄^[8] (cube),
 (4) Hg-Cl: 2.38 Å; 2.96 Å, NH₄-Cl: 3.36 Å.

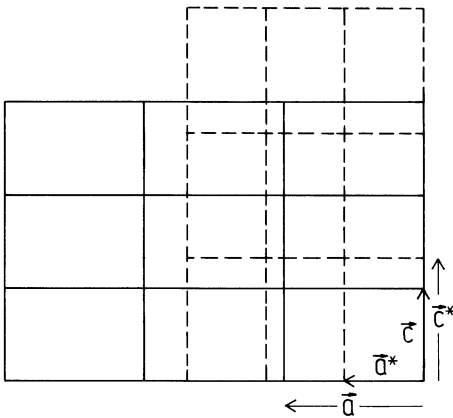
11.13

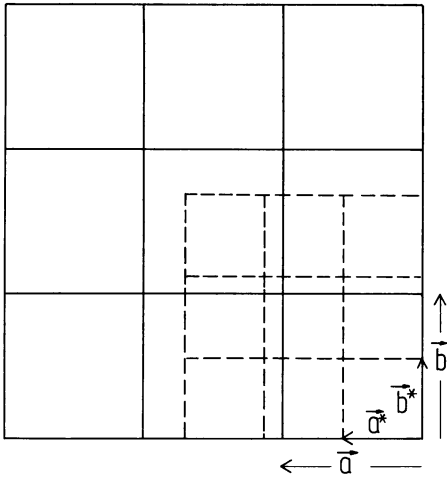


(2) 4, (3) S is tetrahedrally coordinated by 4O.

Chapter 12

12.1





12.2 $Z = 2$, W-type (Fig. 11.5).

$$\begin{array}{l}
 12.3 \quad \left. \begin{array}{l} 23 \quad 2 + \bar{1} = 2/m, 3 + \bar{1} = \bar{3} \\ 2/m\bar{3} \end{array} \right\} 2/m\bar{3} \\
 \left. \begin{array}{l} 432 \quad 4 + \bar{1} = 4/m, 3 + \bar{1} = \bar{3}, 2 + \bar{1} = 2/m \\ \bar{4}3m \quad \bar{4} + \bar{1} = 4/m, 3 + \bar{1} = \bar{3}, m + \bar{1} = 2/m \\ 4/m\bar{3}2/m \end{array} \right\} 4/m\bar{3}2/m
 \end{array}$$

- 12.4 (1) 111 4.077; 200 3.534; 220 2.495; 311 2.127; 222 2.038; 400 1.766; 331 1.621; 420 1.579; 422 1.442.
 (2) $a_0 = 7.06 \text{ \AA}$. (3) $Z = 4$. (4) Because $Z = 4$, so KI must have either the rock salt or the sphalerite structure. As R_A/R_X for KI is 0.61 (see Table 11.3) the structure should be the rock salt (NaCl) type.

References

This list makes no claim to completeness. It merely provides an indication of some textbooks, collections of tables and other publications which treat the subject in greater depth. Particular reference is made to those cited in the text.

1. Azaroff, L. V.: Elements of X-ray crystallography. New York: McGraw-Hill Book Company 1968.
2. Bijvoet, J. M., Kolkmeier, N. H., Macgillavry, C. H.: X-Ray analysis of crystals. London: Butterworths Scientific Publication 1951
3. Bloss, F. D.: Crystallography and crystal chemistry. New York: Holt, Rinehart and Winston 1971.
4. Borsdorf, R., Dietz, F., Leonhardt, G., Reinhold, J.: Einführung in die Molekülsymmetrie. Weinheim: Chemie Physik 1973.
5. Buerger, M. J.: Crystallographic aspects of phase transformations; in Smoluchowski, R.: Phase transformations in solids. New York: John Wiley; London: Chapman and Hall 1951.
6. Buerger, M. J.: Elementary crystallography. New York London Sydney: Wiley 1967.
7. Buerger, M. J.: Introduction to crystal geometry. New York: McGraw-Hill Book Company 1971.
8. Buerger, M. J.: Contemporary crystallography. New York: McGraw-Hill 1970.
9. Burzlaff, H., Zimmermann, H.: Kristallsymmetrie – Kristallstruktur. Erlangen: Merkel 1986.
10. Chernov, A. A.: Modern crystallography, Vol. III (Crystal Growth). Berlin Heidelberg New York Tokyo: Springer 1984.
11. Cullity, B. D.: Elements of X-ray diffraction. Reading Massachusetts London: Addison-Wesley Publishing Company Inc. 1956.
12. Evans, R. C.: Introduction to crystal chemistry. Cambridge: University Press 1964. Einführung in die Kristallchemie. Berlin New York: de Gruyter 1976.
13. Fischer, E.: Einführung in die mathematischen Hilfsmittel der Kristallographie. Freiberg: Bergakademie – Fernstudium 1966.
14. Hahn, T. (Editor): International Tables for Crystallography, Vol. A. Dordrecht Boston: Reidel Publishing Company 1992.
15. Harsch, G., Schmidt, R.: Kristallgeometrie. Frankfurt/M.: Moritz Diesterweg/Otto Salle 1981.
16. Haussühl, S.: Kristallgeometrie. Weinheim: Chemie Physik 1977.
17. Henry, N. F. M., Lonsdale, K. (Editors): International Tables for X-Ray Crystallography, Vol. 1, Birmingham: the Kynoch Press 1952.
18. Hermann, C. (Herausgeber): Internationale Tabellen zur Bestimmung von Kristallstrukturen, Bd. 1. Berlin: Gebrüder Borntraeger 1935.
19. Jaffe, H. H., Orchin, M.: Symmetry in chemistry. New York: John Wiley 1965.
20. Jagodzinski, H.: Kristallographie. In: Handbuch der Physik, Bd. VII, Teil 1. Berlin Göttingen Heidelberg: Springer 1955.
21. Johnsen, A.: Über den Unterschied von Mineralien und Lebewesen. Berlin: Gebrüder Borntraeger 1930
22. de Jong, W. F.: Kompendium der Kristallkunde. Wien: Springer 1959.
23. Kittel, Ch.: Introduction to solid state physics. New York: John Wiley 1986

24. Kirsch, H.: Applied mineralogy. London: Chapman & Hall and Science Paperback 1968.
25. Kitaigorodskii, A. I.: Organic chemical crystallography. New York: Consultants Bureau 1961.
26. Kleber, W.: Angewandte Gitterphysik. Berlin: de Gruyter 1960.
27. Kleber, W. (Bautsch, J., Bohm, J., Kleber, I.): Einführung in die Kristallographie. Berlin: Technik 1990.
28. Krebs, H.: Grundzüge der Anorganischen Kristallchemie. Stuttgart: Ferdinand Enke 1968.
29. Landolt-Börnstein: Kristallstrukturdaten anorganischer Verbindungen, Bd. 7. Berlin Heidelberg New York: Springer 1973–1986
30. McKie, D., McKie, C.: Essentials of crystallography. Oxford, London, Edinburgh, Boston, Melbourne: Blackwell Scientific Publications 1990.
31. Meyer, K.: Physikalisch-chemische Kristallographie. Leipzig: Deutscher Verlag für Grundstoffindustrie 1977.
32. Niggli, P.: Lehrbuch der Mineralogie und Kristallchemie. Berlin: Gebrüder Borntraeger 1941.
33. Paufler, P., Leuschner, D.: Kristallographische Grundbegriffe der Festkörperphysik. Berlin: Akademie 1975.
34. Paufler, P.: Physikalische Kristallographie. Weinheim: Chemie Physik 1986.
35. Pauling, L.: The nature of the chemical bond and the structure of molecules and crystals. Ithaca, New York: Cornell University Press 1960
36. Phillips, F. C.: An introduction to crystallography. Edinburgh: Oliver and Boyd 1971
37. Ramdohr, P., Strunz, H.: Lehrbuch der Mineralogie. Stuttgart: Ferdinand Enke 1978.
38. Read, W. T.: Dislocations in crystals. New York: McGraw-Hill Book Company 1953.
39. Schulz, H., Tscherry, V.: Acta Cryst. (1972) B 28, 2168.
40. Shuvalov, L. A. et al.: Modern crystallography IV (Physical Properties of Crystals). Berlin Heidelberg New York Tokyo: Springer 1988.
41. Stoddart, J. F.: Angew. Chem. (1991) 103, 71.
42. Stout, G. H., Jensen, L. H.: X-Ray Structure determination. London: The Macmillan Company Collier-Macmillan Limited 1989.
43. Strukturberichte, Leipzig: Akademische Verlagsgesellschaft 1913–1940.
44. Structure Reports, Utrecht: N. V. A. Oosthoek's Uitgevers Mij, since 1956.
45. Strunz, H.: Mineralogische Tabellen. Leipzig: Akademische Verlagsgesellschaft Geest & Portis KG 1977.
46. Vainshtein, B. K.: Modern crystallography, Vol. I (Symmetry of crystals. Methods of structural crystallography). Berlin Heidelberg New York Tokyo: Springer 1994.
47. Vainshtein, B. K., Fridkin, V. M., Indenbom, V. L.: Modern crystallography, Vol. II (Structure of crystals). Berlin Heidelberg New York Tokyo: Springer 1995.
48. Wells, A. F.: Structural inorganic chemistry, Oxford: Clarendon Press 1984.
49. Wilke, K.-Th., Bohm, J.: Kristallzüchtung. Berlin: Deutscher Verlag der Wissenschaften 1988.
50. Winkler, H. G. F.: Struktur und Eigenschaften der Kristalle. Berlin Göttingen Heidelberg: Springer 1955.
51. Wyckoff, R. W. G.: Crystal structures. New York London Sydney: John Wiley 1963 (Vol. 1) – 1971 (Vol. 6).
52. Zemann, J.: Kristallchemie. Berlin: de Gruyter (Sammlung Göschen) 1966.

Subject Index

- A-lattice 100
Acicular 29
Ag,Au 237
Aggregate 33
Allene 156
Amorphous 7
Angle between the normals 33
Ångström 6, 23
Anisotropic 4, 5
Antifluorite structure 227, 231
Apatite 159
Aragonite 155
Aragonite structure 240
Asymmetric 150
Asymmetric face unit 126–128, 131, 134–137, 139, 141, 214
Asymmetric unit 198, 203, 214
Atomic radii 228
Avogadro number 24
Axial ratio 46, 116, 117, 211
Axial system 77, 78, 80, 82, 86, 88, 115
Azimuthal angle 38
- B-lattice 101
Basis 22
bcc 223
Benzene 143, 160, 213, 224
Bragg equation 249, 250, 253
Bravais lattice 71, 103
Buerger 239, 260
Burgers vector 267, 268
- C-lattice 90, 100
C₆₀ 162, 214, 225
CaCO₃ structure 240
CaF₂ 161
CaF₂ structure 263
CaF₂-type 230
Calcite 158
Calcite structure 240
ccp 221, 223
Centre of symmetry 58
Centred lattice 97
Centrosymmetric 63
Characteristic symmetry elements 145
- Chemical bonding 217
Chiral 150
Cleavage 3
Combination of symmetry operations 64, 65, 89
Complication rule 43, 45
Compound symmetry operation 64, 65
Conformation 145
Continuous 6
Coordination 218
Coordination number 218, 240
Coordination polyhedron 218
Corderite 4
Coronene 143
Corundum structure 230
Coulomb's law 225
Coulombic force 225
Covalent bonding 236
Cristobalite 233
Crystal 5, 7, 21, 62
Crystal aggregate 33
Crystal chemistry 217
Crystal data – determination tables 116
Crystal defects 265
Crystal edge 28
Crystal face 28
Crystal form 28, 127, 133–137, 139, 141
Crystal growth 30
Crystal structure 21, 27, 59, 104, 115, 205, 244
– Cu-type 220, 222, 224
– Cubic closest packing 220, 222–224
– Mg-type 221–224
– Hexagonal closest packing 221–224
– W-type 223–224
– Ag,Au 237, 238
– CuAu 238
– Cu₃Au 238
– α -Polonium 9, 223, 224
– Diamond 236, 243, 245, 296
– Graphite 243, 246, 296
– CsCl-type 23, 230, 232
– NaCl-type 223, 228, 230–236, 238, 239, 297
– LiCl 297

- RbF 297
- ZnS 233, 238
- Sphalerite 233, 238
- Wurtzite 233
- NiAs-type 230, 235, 238
- CaF₂ 230–232, 234
- Fluorite 230–232, 234
- Antifluorite 231
- TiO₂ 205, 235, 297
- Rutile 205, 235, 297
- SiO₂ 233, 234, 241, 242
- Quartz (low) 241
- Quartz (high) 251
- Tridymite 242
- Cristobalite 233
- Cuprite 25, 280
- Cu₂O 25, 280
- AlB₂ 25, 280
- Pyrite 161, 246, 298
- Corundum-type 230, 234
- Al₂O₃ 234
- Spinel-type 227, 230
- Forsterite 230
- HgNH₄Cl₃ 247, 298
- BaSO₄ 247, 299
- Hexamethylenetetramine 213
- Ethylene 213
- Benzene 213
- Crystal system 115, 147
- Crystallographic axes 11, 271
- CsCl 230
- CsCl structure 239
- CsCl-type 232
- CsI 23
- CsI structure 263
- Cu-type 221
- Cubic 86, 138–140
- Cubic closest packing 221, 224
- Cubic coordination 230
- Cuprite structure 25, 280
- Cyclohexane 158

- Debye-Scherrer line 250
- Debye-Scherrer method 250
- Degree of freedom 125–129, 196–199
- Deltahedron 278
- Deltoid-dodecahedron 139, 278
- Deltoid-icositetrahedron 278
- Density 23
- Determinant 17
- Determination of point groups 145
- Diadochy 237
- Diamond structure 236
- Dihedron 141, 276
- Dihexagonal dipyramid 136/137, 277
- Dihexagonal prism 136/137, 277
- Dihexagonal pyramid 136/137, 277

- Dilatational transformation 239
- Diploid 139, 278
- Dipole moment 152
- Discontinuous 6
- Disdodecahedron 278
- Displacive transformation 240
- Dissymmetric 150
- Ditetragonal dipyramid 127, 134/135
- Ditetragonal prism 127, 134/135
- Ditetragonal pyramid 131, 134/135
- Ditrigonal dipyramid 136/137, 277
- Ditrigonal prism 136/137, 277
- Ditrigonal pyramid 136/137, 277
- Ditrigonal scalenohedron 136/137, 277
- Dolomite 157
- Dome 141, 276

- Edge dislocation 267
- Eigensymmetry 142
- Electrical conductivity 224
- Enantiomeric 150, 153
- Enantiomorphism 147–150, 189, 190
- Equant 29
- Equivalent 59
- Equivalent by translation 59
- Etch-figure 146, 268
- Ethane 144
- Ethylene 213, 224
- Ewald 255
- Ewald construction 258
- Extinct 253

- F-lattice 90, 101
- Face symmetry 125–127, 131, 134–137, 139, 141
- Fivefold rotation axis 61
- Fluorite structure 231, 234
- Fluorite-type 232
- Forsterite structure 230
- Fourfold rotation axis 61
- Frenkel defect 266
- Full symbol 121

- Galena 27, 33, 48, 50, 55, 124
- Garnet 3
- Gas 5, 6
- General form 125, 214
- General plane lattice 71, 76
- General position 196, 203, 214
- Generating symmetry 142
- Glancing angle 249
- Glass 8
- Glide component 184
- Glide plane 183–187
- Glide reflection 183, 184
- Gnomonic projection 47
- Goldschmidt 43

- Goniometer 37
 Graphite structure 243
 Great circle 33, 40
 Growth rate 31
 Gypsum 4, 57
 Gyroid 139, 278

 Habit 29
 Handedness 188
 Hardness 4
 hcp 221, 223
 Hermann 122
 Hermann-Mauguin symbol 147, 191
 Heteropolar bonding 217
 Hexagonal 86, 136–138
 Hexagonal closest packing 221, 224
 Hexagonal dipyrmaid 53, 136/137
 Hexagonal prism 53, 136/137
 Hexagonal pyramid 53, 136/137
 Hexagonal trapezohedron 136/137, 277
 Hexahedron 139, 179
 Hexakisoctahedron 278
 Hexakistetrahedron 278
 Hexamethylenetetramine 213, 224
 Hexaoctahedron 139, 278
 Hexatetrahedron 139, 278
 {hkil} 133, 272
 {hkil} 272
 hkl 253, 272
 (hkl) 14, 28, 125, 272
 {hkl} 125, 272
 Homogeneous 5–7
 Homopolar bonding 217

 I-lattice 90, 101
 Idea of sphere packing 217
 Ideal crystal 265
 Identical 59
 Identical points 10
 Indexing 41–45
 Interaction principle 217
 International symbol 123, 124, 147, 191
 International tables for crystallography 133, 203
 Interrelationship of point groups and space groups 213
 Inversion 58, 63
 Inversion centre 58, 63, 66
 Ionic bonding 217
 Ionic radii 226, 228
 Ionic structure 225
 Isometric 29
 Isomorphism 236
 Isotropic 5
 Isotypes 236

 JCPDS 254

 Kyanite 4

 Lattice 9, 21
 Lattice line 12
 Lattice parameter 10, 11, 253
 Lattice plane 13
 Lattice point 11
 Lattice translation 10, 71
 Laue 249
 Laue group 260
 Laue symbol 253
 Law constancy of the angle 31
 Limiting form 126
 Line defect 265, 267
 Line lattice 10
 Liquid 5, 7

 Magnesium 146
 Malonic acid 153
 Metal structure 220
 Metallic bonding 217
 Methane 146, 161
 Mg-type 221
 Miller indices 14, 42, 251
 Mirror plane 58, 62
 Mixed crystals 237
 Molecular dipole moment 152
 Molecular structure 224
 Molecular symmetry 143
 Monochromatic beam 249
 Monoclinic 79, 120
 Morphological axial ratio 46, 117, 271
 Morphology 27, 59, 115, 124
 Mosaic blocks 269
 Multiplicity 191, 197

 NaCl 161, 226, 3
 NaCl structure 235, 239, 263
 NaCl-type 232, 238
 Naphthalene 143
 Nepheline 159
 NiAs structure 230, 235
 NiAs-type 238
 Noble gas structure 224
 Non-crystallographic point group 143, 162
 Nucleation 30
 Nucleus 30
 Number of chemical formula units per unit cell 23, 253, 261

 Octahedral coordination 226
 Octahedral hole 222
 Octahedron 40, 139, 179
 Olivine structure 237
 One-circle reflection goniometer 37
 Optical activity 147–150

- Order-disorder transformation 243
 Orthographic projection 47
 Orthorhombic 80, 120, 140, 141
- P-lattice 12, 74, 76–78, 80, 82, 86, 88, 90–97
 Packing efficiency 222, 223
 Parallelohedron 276
 Pauling's third rule 234
 PDF index card 254
 Pentagon-dodecahedron 278
 Periodically homogeneous 5
 Phenanthrene 143
 Physical property 4, 71, 150
 Piezoelectricity 147–149, 151
 Pinakoid 28, 35, 127
 Plagioclase 238
 Planar 29
 Plane defect 265, 268
 Plane lattice 10
 Plastic deformation 224
 Pleochroism 3
 Point defect 265, 266
 Point group 77, 79, 81, 83, 85, 87, 89, 119, 120, 147
 Point lattice 9
 Point symmetry operation 120
 Point symmetry elements 67
 Points equivalent by translation 10
 Polar 146–149
 Polar axis 151
 Pole distance 38
 Pole of the face 33
 α -Polonium 9, 223
 Polymorphism 239
 Polytypism 243
 Powder diagram 251, 252
 Powder pattern 253
 Precession method 260
 Principle of closest packing 217
 Prismatic 29
 Pyrene 143
 Pyrite 161, 246, 298
 Pyritohedron 139, 278
 Pyroelectricity 147–149, 152
- Quartz 31, 151, 158
 Quartz structure 241
- R-lattice 84
 Radius ratio 219, 226, 227, 230–234
 Rate of crystal growth 31
 Real crystal 265
 Reciprocal lattice 255–259
 Reconstructive transformation 240, 241
 Reflection goniometer 36
 Reflection 58, 62
- Repetition operation 10, 57
 Rhomb-dodecahedron 3, 139
 Rhombic dipyramid 52, 141
 Rhombic disphenoid 141, 276
 Rhombic prism 52, 141
 Rhombic pyramid 52, 141
 Rhombohedral 84
 Rhombohedron 136/137, 179
 Rotation 58
 Rotation axis 58, 59
 Rotoinversion 65
 Rotoinversion axis 65
 Rotoreflexion 67
 Rotoreflexion axis 67
 Rutile 157, 205, 213, 226
 Rutile structure 232, 235
 Rutile-type 232
- Schönflies symbol 123, 124, 147, 191
 Schottky defect 266
 Screw axis 183, 187–189
 Screw component 187
 Screw dislocation 267
 Screw rotation 183, 187
 Short symbol 121
 Single crystal 33
 SiO₂ structure 234
 Site symmetry 196–199, 203
 Sixfold rotation axis 61
 Small angle grain boundaries 268
 Small circle 41
 SnO₂ structure 261
 Solid solution 236, 266
 Space group 77, 78, 80, 82, 84, 86, 88, 92, 183, 189, 194
 – P $\bar{1}$ 77, 92, 210, 290
 – P2 193
 – P2₁ 193
 – C2 193
 – Pm 193
 – Pc 193
 – Cm 193, 211, 291
 – Cc 193
 – P2/m 78, 92, 192, 198, 199
 – P2₁/m 192
 – C2/m 192
 – P2/c 192
 – P2₁/c 192
 – C2/c 192
 – Pmm2 106, 191
 – Pnc2 211, 291
 – Pba2 211, 291
 – Pna2₁ 197, 198
 – Ibm2 206, 211, 291
 – P2/m 2/m 2/m 80, 93, 94
 – P2/m 2/n 2₁/a 207, 212, 292
 – P2₁/b 2₁/c 2₁/a 294

- C2/m 2/m 2/m 290
- I2/m 2/m 2/m 290
- P4/m 2/m 2/m 82, 95, 96
- P4₂/m 2₁/n 2/m 204
- P4₂bc 212, 292
- P422 294
- R2/m 84, 103
- P6/m 2/m 2/m 86, 95, 98
- P6₁ 198–200
- P4/m 2/m 88, 97, 99, 199–202, 293
- P2₁/a 246, 298
- Space lattice 9, 10
- Special form 126, 214
- Special plane lattice 72–76
- Special position 197, 203, 214
- Sphalerite 161, 233
- Sphalerite-type 238
- Sphenoid 141, 276
- Spinel structure 227, 230
- Stacking faults 269
- Statistically homogeneous 5
- Steno 32
- Stereographic projection 33–36
- Structural axial ratio 47, 117, 271
- Substitution defect 266
- Substitutional solid solution 237
- Superstructure 238
- Symmetry 89
- Symmetry direction 92–97, 103, 117, 147
- Symmetry element 57, 59, 272–274
- Symmetry operation 57, 214
- Symmetry principle 217
- Symmetry rule 91

- Tabular 29
- Tartaric acid 153
- Tautozonal 29
- Tetartoid 139, 278
- Tetragonal 82, 130
- Tetragonal dipyramid 52, 127, 134/135
- Tetragonal disphenoid 131, 134/135, 276
- Tetragonal prism 35, 52, 127, 132, 134/135
- Tetragonal pyramid 35, 52, 131, 134/135
- Tetragonal scalenohedron 131, 134/135, 276
- Tetragonal trapezohedron 131, 134/135, 276
- Tetrahedral coordination 231
- Tetrahedral hole 222
- Tetrahedral pentagon-dodecahedron 278
- Tetrahedron 139, 179
- Tetrahexahedron 139, 278
- Tetrakisshexahedron 278
- Thermal conductivity 224
- Threefold rotation axis 60
- TiO₂ 157, 205, 226
- Topaz 42, 44
- Tourmaline 152, 158
- Transformation in secondary coordination 240
- Transformation involving changes in type of bonding 243
- Transformation of first coordination 239
- Trapezohedron 139, 278
- Triclinic 77, 120
- Tridymite structure 242
- Trigonal 84
- Trigonal dipyramid 53, 136/137
- Trigonal prism 53, 136/137
- Trigonal pyramid 53, 136/137
- Trigonal trapezohedron 136/137, 277
- Trisectahedron 139, 278
- Tristetrahedron 139, 278
- Two-circle reflection goniometer 37
- Twofold rotation axis 59

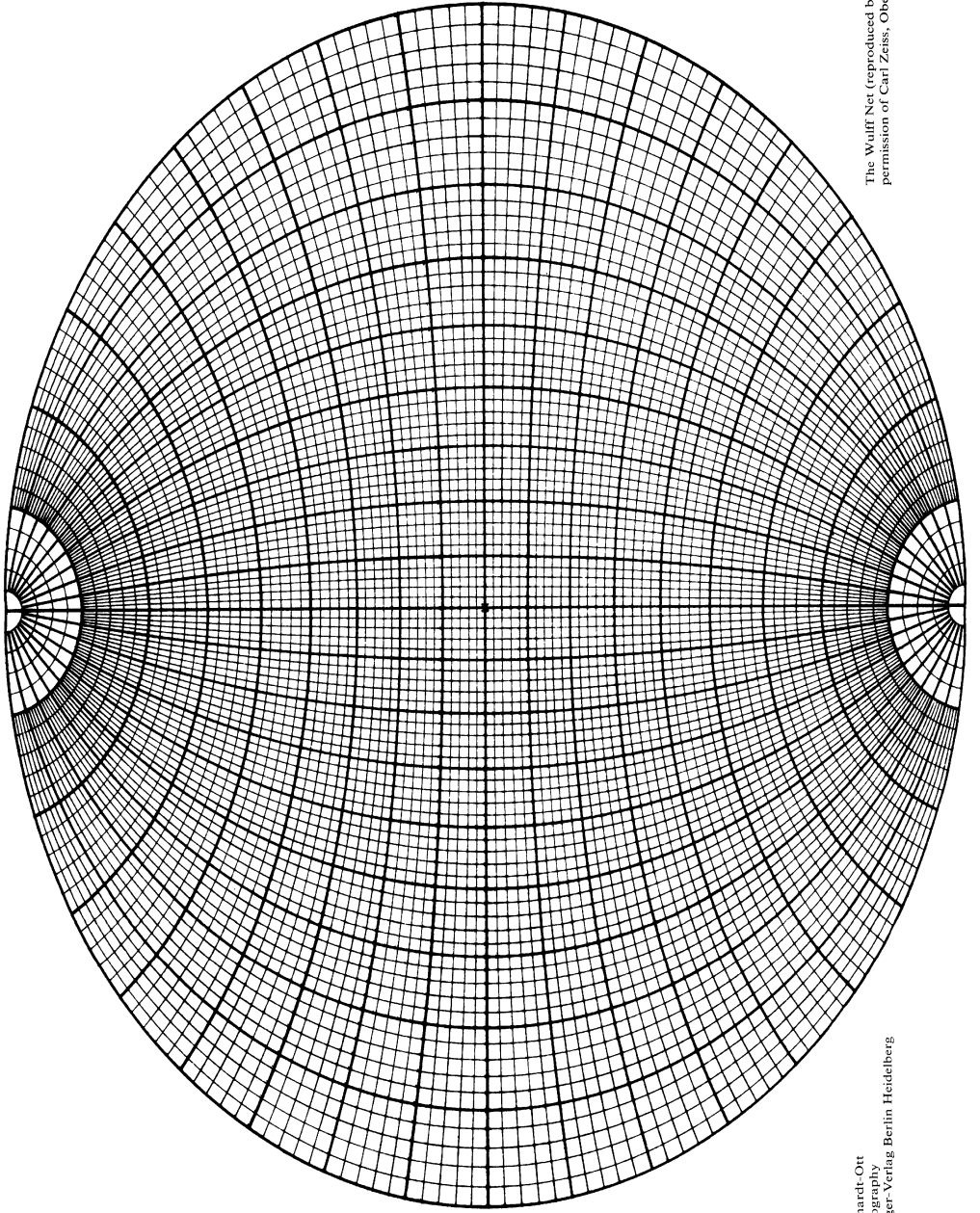
- Unit cell 11
- Unit length 46
- Unit mesh 10, 76
- uvw 11, 271
- [uvw] 12, 28, 125, 271
- (uvw) 93, 125, 271

- van der Waals bonding 217
- Vitamin B₁₂ 3, 225

- W-type 223
- Whisker 268
- Wulfenite 155
- Wulff net 37–41
- Wurtzite structure 233

- x,y,z 21–23, 271
- X-ray 8
- X-ray diffraction 249

- Zinc blende 233
- ZnS 233
- Zonal equation 16–19
- Zone 29, 33, 39
- Zone axis 29, 39
- Zone pole 39



W. Borchardt-Ott
Crystallography
© Springer-Verlag Berlin Heidelberg

The Wulff Net (reproduced by kind
permission of Carl Zeiss, Oberkochen)